Intra-tumoral holmium-166 therapy

Feasibility in head and neck cancer

Robbert Christiaan Bakker

PhD thesis, Utrecht University, the Netherlands

© R.C. Bakker, Utrecht 2020

robbert.c.bakker@gmail.com

All rights reserved. No part of this publication may be reproduced or transmitted in any form or by any means without permission in writing from the author. The copyright of the articles that have been published or have been accepted for publication has been transferred to the respective journal

Part of the research in this thesis was supported by a grant from the Dutch Cancer Society (KWF Kankerbestrijding)

ISBN: 978 90 361 0598 9

Cover: HAVEKA B.V. Alblasserdam, The Netherlands

Printed by: HAVEKA B.V. Alblasserdam, The Netherlands

Intra-tumoral holmium-166 therapy

Feasibility in head and neck cancer

Intra tumorale holmium-166 therapie

Toepasbaarheid in hoofdhals kanker

(met een samenvatting in het Nederlands)

Proefschrift

ter verkrijging van de graad van doctor aan de Universiteit Utrecht
op gezag van de rector magnificus, prof.dr. H.R.B.M. Kummeling,
ingevolge het besluit van het college voor promoties
in het openbaar te verdedigen op
woensdag 15 januari 2020 des middags te 2.30 uur

door

Robbert Christiaan Bakker

geboren op 5 maart 1987

te Bleskensgraaf

Promotoren: Prof. dr. M.G.E.H. Lam

Prof. dr. A.J.W.P. Rosenberg

Copromotoren: Dr. J.F.W. Nijsen

Dr. R.J.J. van Es

CONTENTS

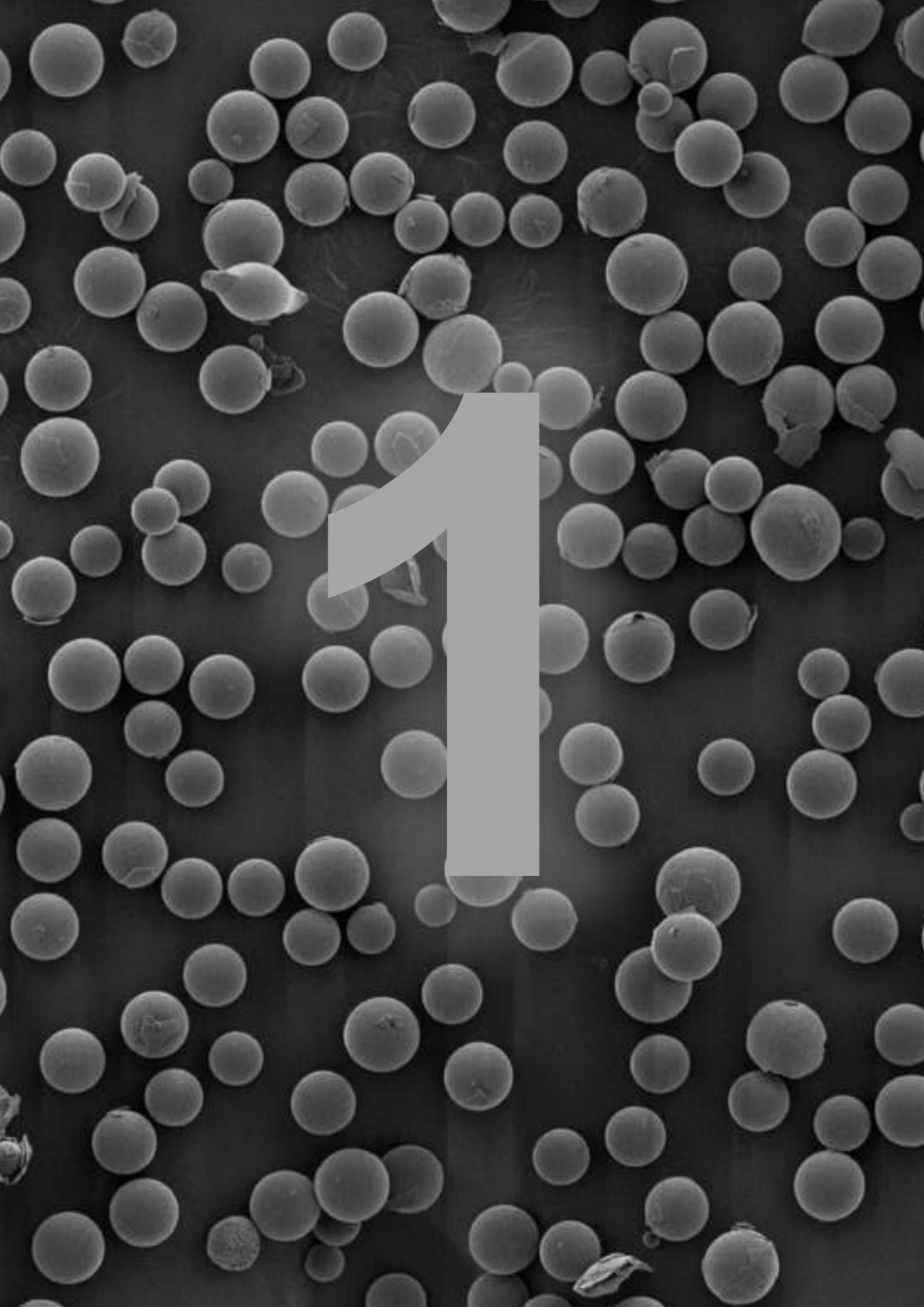
1

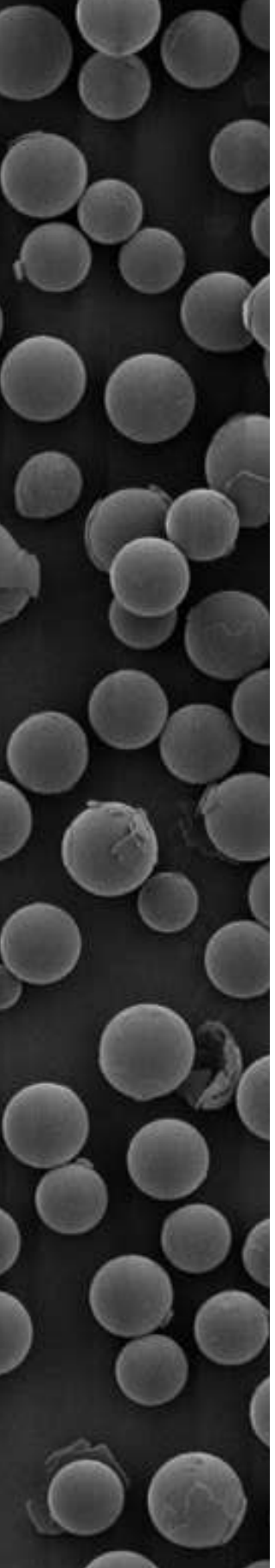

General introduction and outline of thesis

GENERAL INTRODUCTION

Epidemiology

Head and neck cancer (HNC) is the sixth most common cancer, with an annual incidence of 700,000 cases and 380,000 deaths worldwide.[1] Most head and neck cancers are squamous cell carcinomas and develop in the mucosal surfaces of the upper aerodigestive tract, which is often divided in 5 subsites: (Figure 1.1)

- The oral cavity (lips, buccal mucosa, anterior tongue, floor of the mouth, hard palate, and upper and lower gum);
- The pharynx (nasopharynx, oropharynx, and hypopharynx);
- The larynx (supraglottic, glottic, and subglottic regions);
- The nasal cavity and paranasal sinuses (maxillary, ethmoid, sphenoid, and frontal);
- The salivary glands (parotid, submandibular, sublingual, and the minor glands).

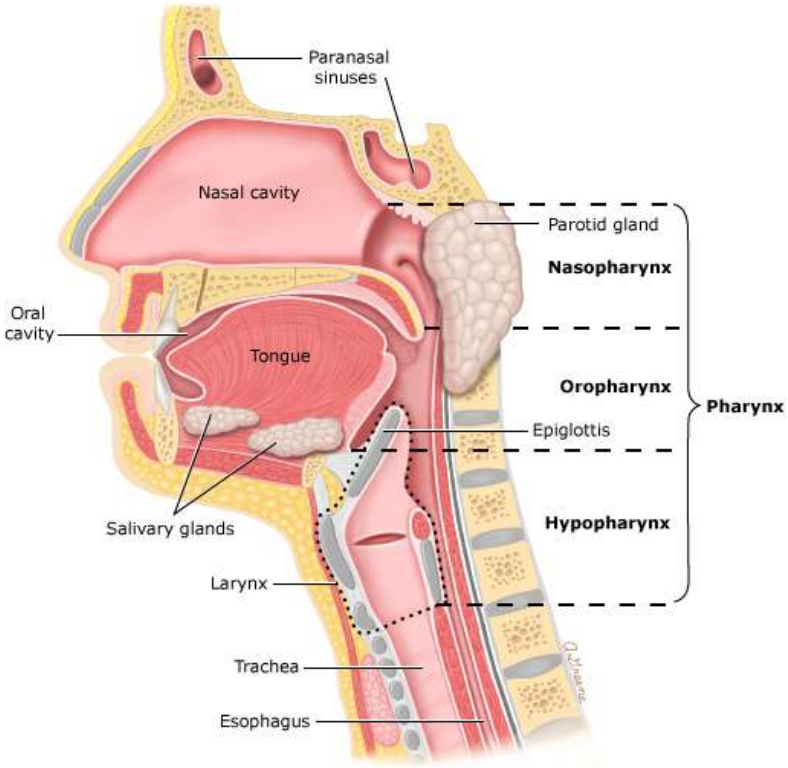

Figure 1.1. *Anatomy of the upper aerodigestive tract and the division in; oral cavity, pharynx, larynx, nasal cavity and paranasal sinuses, and salivary glands. Reproduced with permission from: Poon CS, Stenson KM. Overview of the diagnosis and staging of head and neck cancer. In: UpToDate, Post TW (Ed), UpToDate, Waltham, MA. (Accessed on 20 Aug 2019) Copyright © 2019 UpToDate, Inc. For more information visit www.uptodate.com.*

These head and neck squamous cell carcinomas (HNSCC) account for 3-4 percent of all malignancies.2,3 In addition to HNSCC, non-melanoma skin cancers (NMSC) (squamous cell and basal cell carcinomas) occur at an epidemic rate. The sun-exposed skin of the face is a frequent site for these cancers. Fortunately, local treatment is usually curative in patients with a cutaneous squamous cell carcinoma. However, 0.8% of all cancer deaths are caused by NMSC and 60% of these lesions arise from the head and neck region.

In the Netherlands between 1989 and 2011, 1500 males and 650 females developed HNSCC annually.4 The site with the highest incidence is the oral cavity and the incidence has increased during the past decades, with 0.7% and 1.8% per year in males and females, respectively. The majority is located on the tongue (40%) and floor of the mouth (28%), followed by the buccal mucosa (16%) and the lower and upper gum (10% and 3%, respectively).4

Risk factors

The primary risk factors associated with head and neck cancer are tobacco use and alcohol consumption. The chronic exposure to these carcinogenic substances can result in dysplastic or premalignant lesions in the oropharyngeal mucosa and ultimately result in cancer. In heavy smokers, there is a 7-fold increased risk for the development of head and neck cancer compared with nonsmokers.[5] In addition, the survival rate of patients who continued to smoke was 21% to 35% lower compared with patients who quit smoking.[6] Luckily, the proportion of male daily smokers has gradually declined from 37.5 to 21.7% during the past 20 years in the Netherlands and the cessation of smoking is associated with a decrease in risk of HNSCC.[7,8]

Alcohol consumption increases the risk of cancer in the oral cavity, although it is often difficult to separate the effects of smoking and alcohol. The risk of developing HNSCC appears to be dose dependent with a 5-fold increased risk for head and neck cancer with daily alcohol intake.[9]

Chewing Betel nut is a common practice in many parts of Asia and globally among Asian immigrants. In a meta-analysis, a strong relationship was found between oral/oropharyngeal cancer and chewing betel nut.[10,11] The relative risk for oral/oropharyngeal cancer was 2.56–10.98 and roughly half of oral cancers in these countries could be prevented if the chewing of betel nuts is abandoned.

The number of oral/oropharyngeal cancer cases among young individuals with no typical toxic habits, such as the previously mentioned tobacco and/or alcohol is also rising. Multiple viral infections have been associated with an increased risk of HNSCC, including Epstein-Barr virus (EBV), hepatitis C virus (HCV), human immunodeficiency virus (HIV) and human papilloma virus (HPV). Epidemiologic studies suggest a strong association between the infection by HPV, especially types 16 and 18, which have demonstrated their etiological role in anal and cervix cancer. Vaccine efficacy against persisting oral infections was 88% (2–98%), however the vaccine-induced protection against oral/oropharyngeal cancer is currently unknown.[12]

Immunodeficiency is also associated with an increased incidence of malignancies in the head and neck region. The main causes of immunodeficiency are HIV and organ transplantation. Patients infected with HIV have an increased incidence of a variety of non-AIDS-defining malignancies. For example, there is a 2 to 3-fold increase in the incidence of HNSCC.[13–15] Also patients who have undergone organ transplantation have an increased risk of cancer in the head and neck region. In a series of 2817 patients, 391 head and neck malignancies occurred in 175 patients of which the great majority were cutaneous malignancies.[16]

Radiation is one of the main treatment modalities of HNSCC but it is also known to induce malignancies in the head and neck.[17–19] However, the risk of radiation-induced malignancies (often adenocarcinoma or sarcoma) is low (0.7%), and the latency time is long (12.7–36.5 years) compared to the median survival of HNSCC patients.

There are several other risk factors for development of HNC, such as occupational exposure like sawdust and metal dust.[20,21] In addition, a tremendous number of genetic factors are discovered.[22] One well-known genetic disease is Fanconi anemia. Patients with this autosomal recessive disorder have a 28% chance of developing non-hematogenous malignancies, half of which are HNSCC.[22]

Treatment

The treatment of HNSCC depends on the tumor location, stage and patient characteristics. Approximately 30 to 40 percent of patients with HNSCC present with stage I or II (early stage) disease. In general, these patients are treated with primary surgery for the oral cavity and primary irradiation for the larynx.

HNSCC frequently metastasize to the cervical lymph nodes (Figure 1.2). Even if lymph node involvement is clinically occult, these metastases have significant impact on the prognosis. Therefore, treatment of the cervical neck nodes is part of the treatment strategy.

The detection of occult neck nodal disease is one of the most challenging items. Until now, the search for optimal biomarkers did not yield a holy grail.[23,24] Both genetics and proteomics have extensively been explored. Since several years also for oral cancers, the sentinel node procedure is performed in patients with early cancers and a clinically negative neck. During the combined procedure with the department of Nuclear Medicine, radioactive traces are injected around the tumor. Subsequently, the first echelon of draining lymph nodes is visualized and surgically removed.

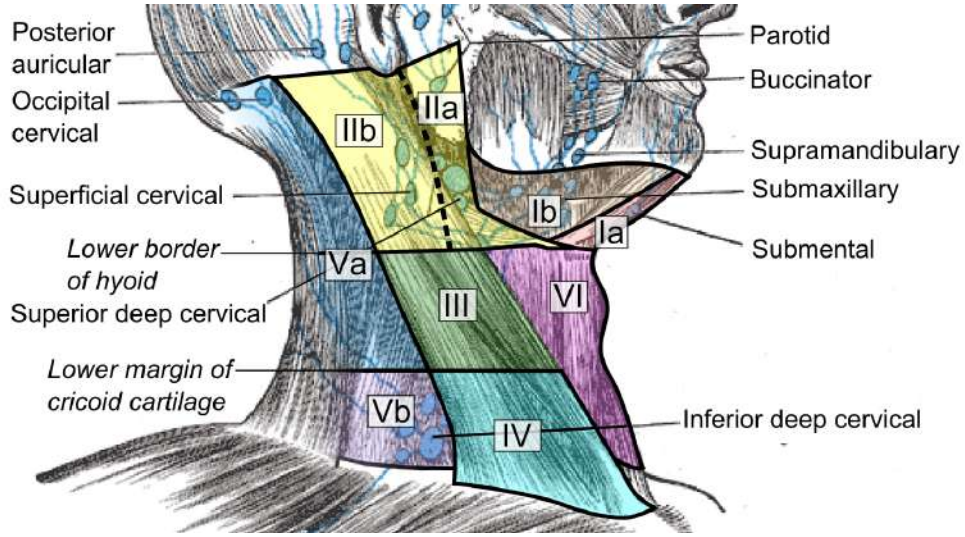

Figure 1.2. *Classification of the cervical lymph nodes divided in several levels based on anatomical location. The lymph nodes of level I and II are often the first echelon of lymph drainage in case of malignancies of the oral cavity. Häggström, M (2014). "Medical gallery of Mikael Häggström 2014". WikiJournal of Medicine 1 (2). ISSN 2002–4436. Creative Commons CC0 1.0 Universal Public Domain Dedication. Used with permission.*

Surgery is the preferred treatment option for locoregionally advanced oral cavity squamous cell carcinomas, especially in case the bony tissues of the jaws are involved, because chemo-radiation of jawbones bears the risk of osteoradionecrosis, with serious morbidity. In most cases simultaneous resection and reconstruction with acceptable functional outcomes can be accomplished.

Loco-regional tumors in the oral cavity behave aggressively. A combined treatment with or without postoperative radiotherapy and chemotherapy is frequently necessary. Therefore, the treatment of HNC requires a multidisciplinary team that includes surgeons, medical oncologists, and radiation oncologists, as well as dentists, nuclear medicine physicians, pathologists, speech/swallowing therapists, dieticians, and rehabilitation therapists.

Over the last decades, the overall 5-year survival remained poor, despite improvements like altered fractionation radiotherapy, integration of chemotherapy with radiotherapy, incorporation of intensity-modulated radiotherapy and the introduction of targeted biological therapy.

As a result, new alternative treatment options of HNSCC are welcomed. One of these could be the intra-tumoral injection of radioactive holmium microspheres, also called "holmium microbrachytherapy".

Holmium-166 microspheres

Several types of holmium-166 (^{166}Ho) microspheres have been developed in the nineties.[25,26] These microspheres were developed as an alternative to yttrium-90 (^{90}Y) radioembolization. Radioembolization is an intra-arterial treatment of liver malignancies. A catheter is placed in the hepatic artery via the femoral artery. Subsequently, millions of radioactive microspheres are injected into the hepatic artery, combining embolization with internal radiation therapy (Figure 1.3).

Radioembolization with ^{90}Y microspheres delays the progression of liver malignancies. In phase III studies, the addition of radioembolization to fluoropyrimidine-based chemotherapy in patients with metastatic colorectal cancer improved median progressive free survival in the liver by 7.9 months.[27] In hepatocellular carcinomas, radioembolization was better tolerated compared to targeted therapy with sorafenib.[28] However, an overall survival benefit could not be established yet.

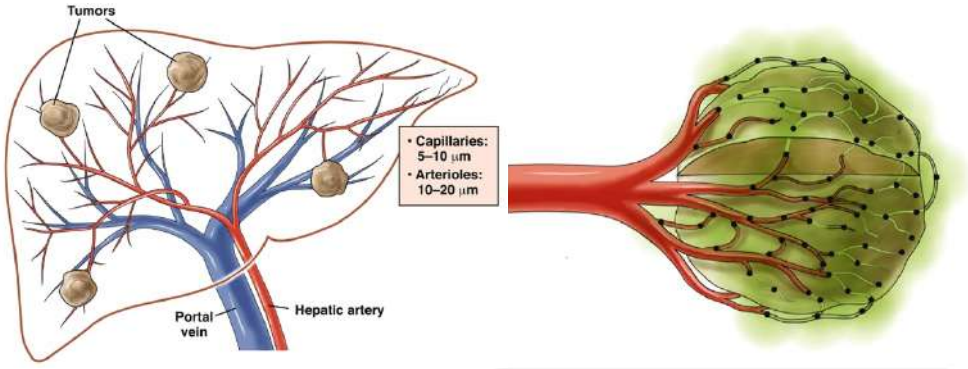

Figure 1.3. *The principle of radioembolization. Through a catheter placed in the hepatic artery via the femoral artery, millions of radioactive microspheres are injected into the liver. The particle lodge in the capillaries of the tumor combining embolization with internal radiation therapy. Reprinted from Chemoembolization and Radioembolization for Hepatocellular Carcinoma, 11 /6 number, Salem R, Lewandowski RJ. Clin Gastroenterol Hepatol. 2013 Jun;11(6):604–11. Copyright (2013), with permission from Elsevier.*

The preparation of [^{166}Ho]Ho-acetylacetonate-poly(L-lactic acid) microspheres (^{166}Ho-microspheres) was originally invented by Mumper et al.[25,29,30], and introduced for the first time in patients at the University Medical Center Utrecht in the HEPAR 1 study.[31] Using a solvent evaporation technique, ^{165}Ho-acetylacetonate can be incorporated into poly-L-lactic acid microspheres as previously described (Figure 1.4).[32] Today, these microspheres have received CE-mark for radioembolization. They are produced by Quirem Medical B.V. (QuiremSpheres®).

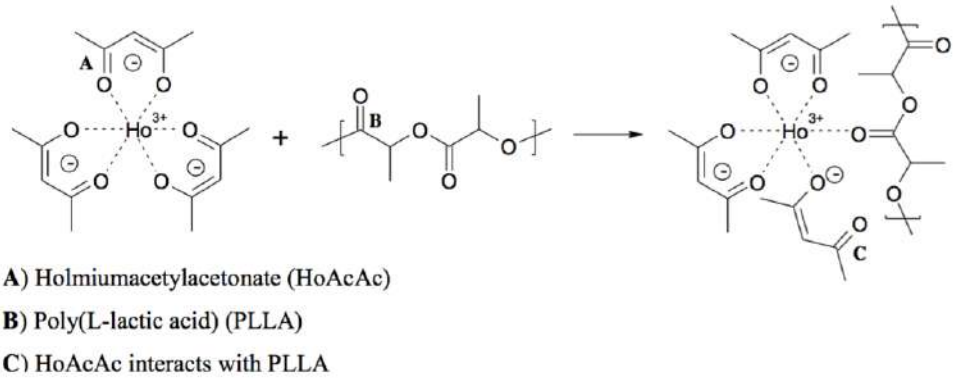

A) Holmiumacetylacetonate (HoAcAc)

B) Poly(L-lactic acid) (PLLA)

C) HoAcAc interacts with PLLA

Figure 1.4. *The supposed reactions in the preparation of holmium microspheres. Reprinted from: Characterization of poly(L-lactic acid) microspheres loaded with holmium acetylacetonate. Nijsen JFW et al. Biomaterials. 2001 Nov;22(22):3073–81. Copyright (2001), with permission from Elsevier.*

These microspheres contain 17–20% weight per volume of non-radioactive holmium-165 and are sized between 15 to 60 μm, with a mean diameter of 30 ± 5 μm (Figure 1.5).[32] Subsequently, the holmium microspheres are neutron irradiated, depending on the desired ^{166}Ho-activity.

The fraction of ^{166}Ho produced during activation ranges between 0 and 8 parts per million (ppm). This depends on the duration of irradiation and the neutron flux. A typical activated fraction is 1.5 ppm at the beginning of treatment. Relative to most radionuclides an activated fraction of only a few parts per million is very low. Activation of holmium microspheres towards higher activated fractions is hampered since it potentially causes loss of integrity of the poly (L lactic acid) microspheres.

The ^{166}Ho-microspheres emit β-radiation ($E_{\beta, max}$ = 1.84 MeV, $t_{1/2}$ = 26.8 hrs.) with a maximum tissue penetration of 8.7 mm. The short β penetration depth enables a high, tumor-ablative radiation dose, without causing extensive collateral damage in surrounding tissues.

Besides the high-energy β-radiation required for tumor destruction, ^{166}Ho also emits low-energy gamma radiation of 81 Kev, 6.7% yield[34], which can be used for quantitative SPECT/CT imaging.[35,36] Furthermore, the paramagnetic property and amount of holmium causes sufficient signal relaxation for quantitative analysis of holmium on magnetic resonance imaging (MRI).[37,38] In addition, holmium causes high attenuation on CT due to the high density of holmium (z = 67).[39]

^{166}Ho-microspheres are used in radioembolization of palliative patients with various liver malignancies. The safety and maximum tolerated average absorbed dose of 60 Gy of ^{166}Ho-microspheres were tested in the HEPAR I and II studies.[3,4] Disease control was obtained in 73% after three months in the HEPAR II study, with an overall survival of 15.3 months.[40]

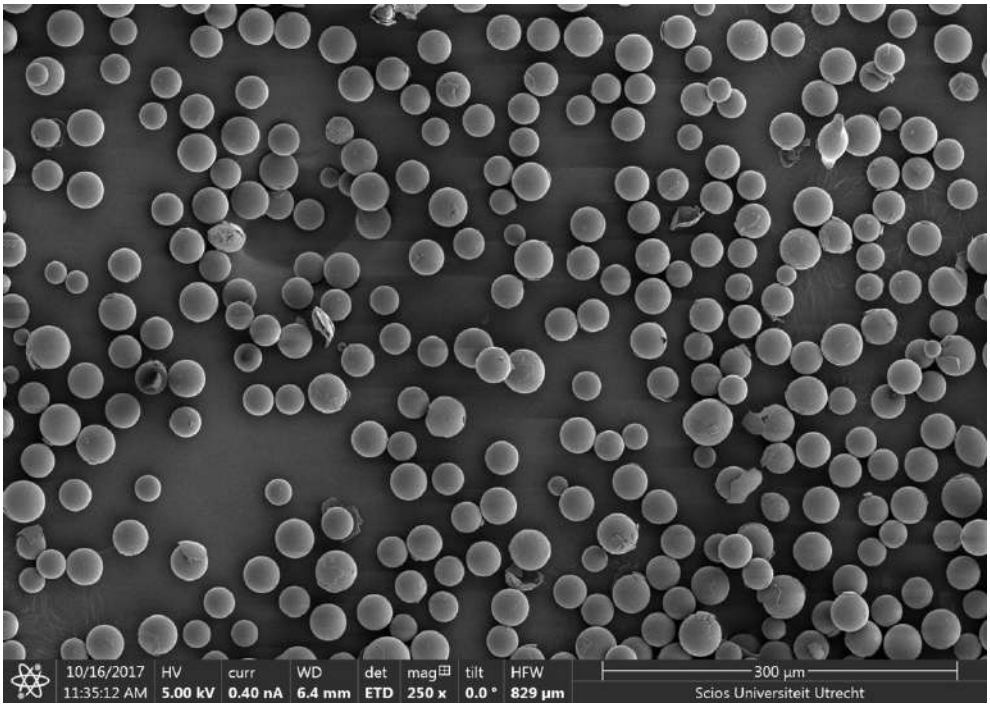

Figure 1.5. *Electron microscopy showing several non-irradiated holmium-acetylacetonate-poly(L-lactic-acid) microspheres.*

Intra-arterial treatment of head and neck cancer

Intra-arterial administration of chemotherapeutics combined with radiotherapy has shown promising results in head and neck tumors.[41–43] Subsequently, an animal model to investigate new locoregional treatment strategies against HNSCC was developed.[44] In this VX-2 carcinoma in the rabbit auricle model, intra-arterial embolization was performed.[45] The optimal size of embolization particles in this head and neck tumors was approximately between 40 and 70 µm. These particles are small enough to obtain a sufficient distribution throughout the tumor and large enough to prevent massive shunting to the lungs.[46] In rabbits with VX-2 carcinoma, embolization with ^{166}Ho-microspheres induced a complete remission of 79–86% of the rabbits.

However, the head and neck region has multiple and variable potentially dangerous anastomoses in the arterial anatomy. Failure to recognize such anastomoses can cause stroke, cranial nerve injury, blindness, as well as persistent hemorrhage in embolization.[46] Neurological complications were observed in several animals and described in humans.[47–49]

Intra-tumoral injections of holmium-166 microspheres

After the attempts to perform radioembolization of head and neck tumors, the concepts of an intra-tumoral approach with these microspheres were proposed. In rabbits with a VX-2 liver tumor, 0.1 mL with 5 mg of microspheres were injected in the tumor.[50] Approximately 80% of the intended dose was administered. In one animal, uptake was seen in the lung, corresponding to approximately 5% of the injected dose. Subsequently, ^{166}Ho-microspheres were intra-tumorally injected in a kidney tumor model in mice.[51] The tumor growth arrested in these animals and no ^{166}Ho related toxicity was seen. Furthermore, the potential of imaging ^{166}Ho on SPECT, MRI and CT imaging was shown. This generated potential for image guided therapy in the future. Finally, a feasibility study in three veterinary patients (cats) was performed with spontaneous liver cancer.[52] This study revealed that this radio-ablation technique was efficacious, with minimal side effects. These studies were the foundation to assess the feasibility of intra-tumoral injection of ^{166}Ho-microspheres in domestic animals and translate this therapy to human patients with HNSCC.

OUTLINE OF THIS THESIS

In this thesis, the feasibility of intra-tumoral injections of radioactive ^{166}Ho-microspheres for the use of HNSCC patients is explored. The work focuses on the technique of intra-tumoral injections with radioactive beta-emitting particles and the stability of the ^{166}Ho-microspheres. Additionally, the feasibility and translation of intra-tumoral injections of radioactive ^{166}Ho-microspheres from a pre-clinical setting to the first use in human patients is described. Finally, it explores technical possibilities for CT imaging, which could be used for future image guided treatment and robotic administration.

Technique and Material

Intra-tumoral treatments are often propagated to be superior to systemic therapies in relation to efficacy and side effects, however still not routinely used in clinical practice. In **Chapter 2** an extensive literature review is provided on the potential role of direct intra-tumoral treatment of solid malignant neoplasms with radioactive beta-emitting particles. It describes a large variety of isotopes, particles and injection techniques and furthermore, it describes the efficacy, and concerns with regard to safety. Based on this report additional recommendations for further investigations are formulated.

The UMC Utrecht developed and until recently produced radioactive ^{166}Ho-microspheres. The stability of these microspheres is described in **Chapter 3**. Both in-vitro samples, and blood and urine samples of patients treated with radioembolization in the HEPAR 1 and HEPAR 2 studies were analyzed. Effects of irradiation-time, re-suspension time and the changed composition of the resuspension medium are described.

Clinical feasibility

After investigation of the technique and possibilities, **Chapter 4** describes the results of intra-tumoral injection with radioactive ^{166}Ho-microspheres in veterinary HNSCC patients. In this pilot and subsequent dose reduction study, felines with spontaneous unrespectable squamous cell carcinoma of the oral cavity were treated. Clinical outcomes like safety and efficacy of the intra-tumoral treatment with radioactive ^{166}Ho-microspheres in feline patients.

Based on these results, the rationale and design of a "first-in-man" pilot study in HNSCC patients was made as described in **Chapter 5**. Unfortunately, the study was prematurely terminated as due to of low accrual. Probably, the result of the simultaneous introduction of the almost identical sentinel node procedure and the absence of a potential benefit.

However, for patients with previously irradiated and/or irresectable regional recurrent tumors, limited treatment options exist. In **Chapter 6** the feasibility and safety of intra-tumoral injections of direct intra-tumoral injection of radioactive ^{166}Ho-microspheres is investigated in palliative recurrent HNSCC patients.

Technical possibilities

Potential technical improvements related to intra-tumoral treatment with ^{166}Ho-microspheres are investigated in Chapter 7 and 8 where both CT quantification of ^{166}Ho-microspheres and newer dual energy CT material decomposition is evaluated. In **Chapter 7** a calibration curve of holmium on plain CT was made, and subsequently quantification of ^{166}Ho microsphere after intra-tumoral injection was performed in ex-vivo tissue, in laboratory animals and three human patients.

Chapter 8 The study assessed the feasibility of DECT-based quantification of holmium using dual X-ray spectra information and the spectral behavior with regard to the applied tube voltage and observing phantom-size dependent changes. Finally, the feasibility of quantification was assessed on three rabbit specimens with intra-tumoral ^{166}Ho-microspheres injections.

Finally, this thesis is summarized and future directions are outlined in **Chapter 9** and **Chapter 10**.

REFERENCES

1. Bray F, Ferlay J, Soerjomataram I, Siegel RL, Torre LA, Jemal A. Global cancer statistics 2018: GLOBOCAN estimates of incidence and mortality worldwide for 36 cancers in 185 countries. CA Cancer J Clin. 2018;68(6):394–424.
2. Gatta G, Botta L, Sánchez MJ, Anderson LA, Pierannunzio D, Licitra L. Prognoses and improvement for head and neck cancers diagnosed in Europe in early 2000s: The EUROCARE-5 population-based study. Eur J Cancer. 2015;51(15):2130–43.
3. Siegel RL, Miller KD, Jemal A. Cancer statistics, 2017. CA Cancer J Clin. 2017;67(1):7–30.
4. Braakhuis BJM, Leemans CR, Visser O. Incidence and survival trends of head and neck squamous cell carcinoma in the Netherlands between 1989 and 2011. Oral Oncol. 2014;50(7):670–5.
5. Wyss A, Hashibe M, Chuang SC, Lee YCA, Zhang ZF, Yu GP, et al. Cigarette, cigar, and pipe smoking and the risk of head and neck cancers: Pooled analysis in the international head and neck cancer epidemiology consortium. Am J Epidemiol. 2013;178(5):679–90.
6. van Imhoff LCR, Kranenburg GGJ, Macco S, Nijman NL, van Overbeeke EJ, Wegner I, et al. Prognostic value of continued smoking on survival and recurrence rates in patients with head and neck cancer: A systematic review. Head Neck. 2016 Apr;38(S1):E2214–20.
7. Marron M, Boffetta P, Zhang ZF, Zaridze D, Wunsch-Filho V, Winn DM, et al. Cessation of alcohol drinking, tobacco smoking and the reversal of head and neck cancer risk. Int J Epidemiol. 2010;39(1):182–96.
8. Leefstijlmonitor, Centraal Bureau voor de Statistiek +Rijksinstituut voor Volksgezondheid en Milieu.
9. Toporcov TN, Znaor A, Zhang Z-F, Yu G-P, Winn DM, Wei Q, et al. Risk factors for head and neck cancer in young adults: a pooled analysis in the INHANCE consortium. Int J Epidemiol. 2015;44(1):169–85.
10. Guha N, Warnakulasuriya S, Vlaanderen J, Straif K. Betel quid chewing and the risk of oral and oropharyngeal cancers: A meta-analysis with implications for cancer control. Int J Cancer. 2014;135(6):1433–43.
11. Jacob BJ, Straif K, Thomas G, Ramadas K, Mathew B, Zhang ZF, et al. Betel quid without tobacco as a risk factor for oral precancers. Oral Oncol. 2004;40(7):697–704.
12. Harder T, Wichmann O, Klug SJ, van der Sande MAB, Wiese-Posselt M. Efficacy, effectiveness and safety of vaccination against human papillomavirus in males: a systematic review. BMC Med. 2018;16(1):110.
13. Patel P, Hanson DL, Sullivan PS, Novak RM, Moorman AC. Incidence of Types of Cancer among HIV-Infected Persons Compared with the General Population in the United States , 1992–2003. Ann Intern Med. 2008;(Cdc):1992–2003.
14. Grulich AE, van Leeuwen MT, Falster MO, Vajdic CM. Incidence of cancers in people with HIV / AIDS compared with immunosuppressed transplant recipients: a meta-analysis. Lancet. 2007;370(9447):59–67.
15. Deeken JF, Tjen-A-Looi A, Rudek MA, Okuliar C, Young M, Little RF, et al. The rising challenge of non-AIDS-defining cancers in HIV-infected patients. Clin Infect Dis. 2012;55(9):1228–35.
16. Rabinovics N, Mizrachi A, Hadar T, Ad-El D, Feinmesser R, Guttman D, et al. Cancer of the head and neck region in solid organ transplant recipients. Head Neck. 2014 Feb;36(2):181–6.
17. van der Laan BF, Baris G, Gregor RT, Hilgers FJ, Balm AJ. Radiation-induced tumors of the head and neck. J Laryngol Otol. 1995;109(4):346–9.
18. Sale KA, Wallace DI, Girod DA, Tsue TT. Radiation-induced malignancy of the head and neck. Otolaryngol - Head Neck Surg. 2004;131(5):643–5.
19. Miyahara H, Sato T, Yoshino K. Radiation-induced cancers of the head and neck region. Acta Otolaryngol Suppl. 1998;533(June):60–4.
20. Hauptmann M, Lubin JH, Stewart PA, Hayes RB, Blair A. Mortality from solid cancers among workers in formaldehyde industries. Am J Epidemiol. 2004;159(12):1117–30.
21. Becher H, Ramroth H, Ahrens W, Risch A, Schmezer P, Dietz A. Occupation, exposure to polycyclic aromatic hydrocarbons and laryngeal cancer risk. Int J Cancer. 2005;116(3):451–7.
22. Lacko M, Braakhuis BJM, Sturgis EM, Boedeker CC, Suárez C, Rinaldo A, et al. Genetic susceptibility to head and neck squamous cell carcinoma. Int J Radiat Oncol Biol Phys. 2014;89(1):38–48.
23. Leusink KFJ. Molecular markers of lymph node metastasis in oral cancer. 2016.
24. Noorlag R. Prognostic biomarker in oral cancer towards more individualized treatment. 2016.
25. Mumper RJ, Ryo UY, Jay M. Neutron-activated holmium-166-Poly(L-lactic acid) microspheres: A potential agent for the internal radiation therapy of hepatic tumors. J Nucl Med. 1991;32(11):2139–43.
26. Turner JH, Claringbold PG, Klemp PF, Cameron PJ, Martindale AA, Glancy RJ, et al. 166Ho-microsphere liver radiotherapy: A preclinical SPECT dosimetry study in the pig. Nucl Med Commun. 1994 Jul;15(7):545–53.
27. van Hazel GA, Heinemann V, Sharma NK, Findlay MPN, Ricke J, Peeters M, et al. SIRFLOX: Randomized Phase III Trial Comparing First-Line mFOLFOX6 (Plus or Minus Bevacizumab) Versus mFOLFOX6 (Plus or Minus Bevacizumab) Plus Selective Internal Radiation Therapy in Patients With Metastatic Colorectal Cancer. J Clin Oncol. 2016 May 20;34(15):1723–31.

28. Vilgrain V, Bouattour M, Sibert A. Selective internal radiation therapy is better tolerated compared to sorafenib, but does not increase overall survival in patients with HCC. Int liver Congr GS0-12. 2017;6–8.
29. Mumper RJ, Ryo UY, Jay M. Acid) Microspheres : A Potential Agent for the Internal Radiation Therapy of Hepatic Tumors. J Nucl Med. 1991;32(11):2139–43.
30. Mumper RJ, Jay M. Poly(L-lactic acid) microspheres containing neutron-activatable holmium-165: a study of the physical characteristics of microspheres before and after irradiation in a nuclear reactor. Pharm Res. 1992 Jan;9(1):149–54.
31. Smits MLJ, Nijsen JFW, van den Bosch MAAJ, Lam MGEH, Vente MAD, Mali WPTM, et al. Holmium-166 radioembolisation in patients with unresectable, chemorefractory liver metastases (HEPAR trial): A phase 1, dose-escalation study. Lancet Oncol. 2012 Oct;13(10):1025–34.
32. Zielhuis SW, Nijsen JFW, De Roos R, Krijger GC, Van Rijk PP, Hennink WE, et al. Production of GMP-grade radioactive holmium loaded poly(L-lactic acid) microspheres for clinical application. Int J Pharm. 2006;311(1–2):69–74.
33. Nijsen JFW, Van Steenbergen MJ, Kooijman H, Talsma H, Kroon-Batenburg LMJ, Van De Weert M, et al. Characterization of poly(L-lactic acid) microspheres loaded with holmium acetylacetonate. Biomaterials. 2001;22(22):3073–81.
34. Elschot M, Smits MLJ, Nijsen JFW, Lam MGEH, Zonnenberg BA, van den Bosch MAAJ, et al. Quantitative Monte Carlo-based holmium-166 SPECT reconstruction. Med Phys. 2013;40(11):112502.
35. Wit TC de, Xiao J, Nijsen JFW, Schip FD van het, Staelens SG, Rijk PP van, et al. Hybrid scatter correction applied to quantitative holmium-166 SPECT. Phys Med Biol. 2006 Oct 7;51(19):4773–87.
36. Elschot M, Nijsen JFW, Dam AJ, de Jong HWAM. Quantitative evaluation of scintillation camera imaging characteristics of isotopes used in liver radioembolization. PLoS One. 2011;6(11).
37. Nijsen JFW, Seppenwoolde J-H, Havenith T, Bos C, Bakker CJG, van het Schip AD. Liver Tumors: MR Imaging of Radioactive Holmium Microspheres—Phantom and Rabbit Study. Radiology. 2004;231(2):491–9.
38. Seevinck PR, Van De Maat GH, De Wit TC, Vente MAD, Nijsen JFW, Bakker CJG. Magnetic resonance imaging-based radiation-absorbed dose estimation of 166Ho-microspheres in liver radioembolization. Int J Radiat Oncol Biol Phys. 2012;83(3):e437–44.
39. Seevinck P, Seppenwoolde J-H, de Wit T, W. Nijsen JFW Beekman F, van het Schip A, et al. Factors Affecting the Sensitivity and Detection Limits of MRI, CT, and SPECT for Multimodal Diagnostic and Therapeutic Agents. Anticancer Agents Med Chem. 2007 May 1;7(3):317–34.
40. Prince JF, van den Bosch MAAJ, Nijsen JFW, Smits MLJ, van den Hoven AF, Nikolakopoulos S, et al. Efficacy of radioembolization with holmium-166 microspheres in salvage patients with liver metastases: a phase 2 study. J Nucl Med. 2017;jnumed.117.197194.
41. Yu KH, Yu SCH, Hui EP, Kam MKM, Vlantis AC, Yuen E, et al. Accelerated fractionation radiotherapy and late intensification with 2 intra-arterial cisplatin infusions for locally advanced head and neck squamous cell carcinoma. Head Neck. 2009;36(10):NA-NA.
42. Balm AJM, Rasch CRN, Schornagel JH, Hilgers FJM, Keus RB, Schultze-Kool L, et al. High-dose superselective intra-arterial cisplatin and concomitant radiation (radplat) for advanced head and neck cancer. Head Neck. 2004;26(6):485–93.
43. Suzuki T, Sakashita T, Homma A, Hatakeyama H, Kano S, Mizumachi T, et al. Effectiveness of superselective intra-arterial chemoradiotherapy targeting retropharyngeal lymph node metastasis. Eur Arch Oto-Rhino-Laryngology. 2016;273(10):3331–6.
44. van Es RJJ. The rabbit Vx2 auricle carcinoma An animal model for development of new locoregional treatment strategies against squamous cell carcinoma of the head and neck. 2001.
45. van Es RJJ, Franssen O, Dullens HF, Bernsen MR, Bosman F, Hennink WE, et al. The VX2 carcinoma in the rabbit auricle as an experimental model for intra-arterial embolization of head and neck squamous cell carcinoma with dextran microspheres. Lab Anim. 1999;33:175–84.
46. van Es RJJ, Nijsen JFW, Dullens HF, Kicken M, van der Bilt A, Hennink W, et al. Tumor embolization of the Vx2 rabbit head and neck cancer model with Dextran hydrogel and Holmium-poly(L-lactic acid) microspheres: a radionuclide and histological pilot study. J Craniomaxillofac Surg. 2001;29(5):289–97.
47. Platzbecker H, Köhler K. Embolization in the head and neck region. Acta Radiol Suppl. 1991;377(212):25–6.
48. van Es RJJ, Nijsen JFW, van het Schip AD, Dullens HF, Slootweg PJ, Koole R. Intra-arterial embolization of head-and-neck cancer with radioactive holmium-166 poly(L-lactic acid) microspheres: an experimental study in rabbits. Int J Oral Maxillofac Surg. 2001;30(5):407–13.
49. Blanchard RJ, Lafave JW, Kim YS, Frye CS, Ritchie WP, Perry JF. Treatment of patients with advanced cancer utilizing Y90 microspheres. Cancer. 1965 Mar;18(3):375–80.
50. Bult W, De Leeuw H, Steinebach OM, Van Der Bom MJ, Wolterbeek HT, Heeren RMA, et al. Radioactive holmium acetylacetonate microspheres for interstitial microbrachytherapy: An in vitro and in vivo stability study. Pharm Res. 2012;29(3):827–36.

51. Bult W, Kroeze SGC, Elschot M, Seevinck PR, Beekman FJ, de Jong HWAM, et al. Intratumoral administration of holmium-166 acetylacetonate microspheres: antitumor efficacy and feasibility of multimodality imaging in renal cancer. PLoS One. 2013;8(1):e52178.
52. Bult W, Vente MADD, Vandermeulen E, Gielen I, Seevinck PR, Saunders J, et al. Microbrachytherapy using holmium-166 acetylacetonate microspheres: A pilot study in a spontaneous cancer animal model. Brachytherapy. 2013 Mar;12(2):171–7.


2

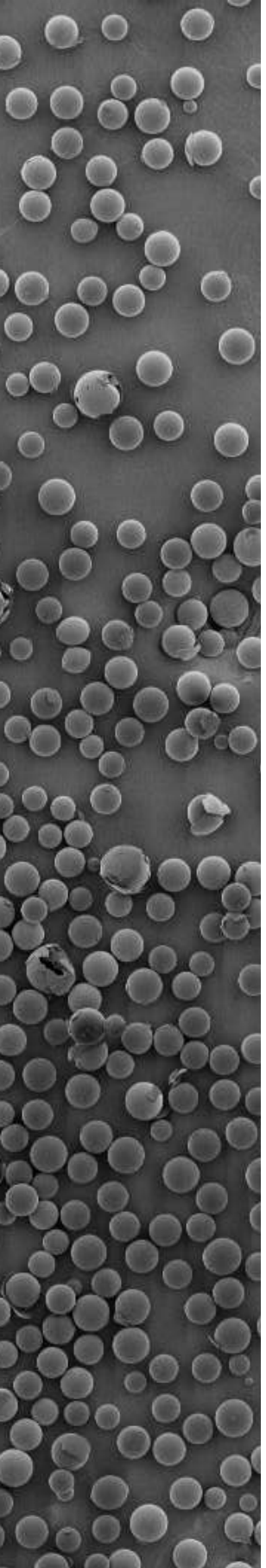

Intra-tumoral treatment with radioactive beta-emitting microparticles: a systematic review

R.C. Bakker

M.G.E.H. Lam

S.A. van Nimwegen

A.J.W.P. Rosenberg

R.J.J. van Es

J.F.W. Nijsen

Journal of Radiation Oncology 2017

Bakker RC, Lam MGEH, van Nimwegen SA, Rosenberg AJWP, van Es RJJ, Nijsen JFW. **Intratumoral treatment with radioactive beta-emitting microparticles: a systematic review.** J Radiat Oncol 2017;6:323–341.

ABSTRACT

Introduction

The purpose of this study was to review the role of radioactive microparticles (1–100 μm) for the treatment of solid tumors and provide a comprehensive overview of the feasibility, safety, and efficacy.

Methods

A systematic search was performed in MEDLINE, EMBASE, and The Cochrane Library (January 2017) by combining synonyms for the determinants "tumor," "injection," and "radionuclide." Data on injection technique, toxicity, tumor response, and survival were collected.

Results

The search yielded 7271 studies, and 37 were included for analysis. Twelve studies were performed in human patients and 25 animal studies. The studies were heterogeneous in patient population, tumors, follow-up time, and treatment characteristics. The direct intra-tumoral injection of radioactive microparticles resulted in a response rate of 71% in a variety of tumors and uncomplicated procedures with high cumulative doses of >19,000 Gy were reported.

Conclusion

The large variety of particles, techniques, and treated tumors in the studies provided an important insight into issues concerning efficacy, safety, particle and isotope choice, and other concepts for future research. Animal studies showed efficacy and a dose response. Most studies in humans concluded that intra-tumoral treatment with radioactive beta-emitting microparticles is relatively safe and effective. Conflicting evidence about safety and efficacy might be explained by the considerable variation in the treatment characteristics. Larger particles had a better retention which resulted in higher anti-tumor effect. Leakage seems to follow the path of least resistance depending on anatomical structures. Subsequently, a grid-like injection procedure with small volume depots is advised over a single large infusion. Controlled image-guided treatment is necessary because inadequate local delivery and inhomogeneous dose distribution result in reduced treatment efficacy and in potential complications.

INTRODUCTION

Interventional oncology is an emerging field in cancer care that has the potential to complement existing treatment modalities. Today, various image-guided interventions have an active role in the palliative cancer treatment setting.[1–3] Driven by technical innovation, new image-guided treatment solutions are continuously developing. Interventional oncology techniques, using microspheres or "microbrachytherapy," have potential benefits, including minimal invasive delivery, outpatient treatment, and improved (progression-free) survival and quality of life.[4,5] The high-absorbed dose of beta-radiation enables a local tumor-ablative effect while the limited penetration depth of maximum 2–11 mm (Table 2.1) minimizes side effects.

The aim of this literature study was to review the potential role of beta-emitting microparticles for intra-tumoral (IT) treatment of solid malignant neoplasms. A comprehensive overview of the technical aspects and the characteristics of commonly used radionuclides are provided. Finally, recommendations for further investigation are formulated.

METHODS

Protocol and registration

Methods of the analysis and inclusion criteria were specified in advance and documented in a protocol registered in an international prospective register of systematic reviews (PROSPERO).[6]

Eligibility criteria

Type of studies: There were no restrictions based on study design, setting, timing, and publication date or publication status. Only full-text articles reported in the English language were included. Studies that examined human or veterinary patients or animal models with solid tumors were included. There were no restrictions on tumor size, type, or location. The administration of the radioactive microparticles had to be performed directly into the tumor. Particles sized between 1 and 100 μm fulfilled our definition of microparticles (Figure 2.1), and the particles had to emit beta-radiation. Combined treatment regimens with external beam radiotherapy (EBRT) or chemotherapy were also included. Local treatments after incomplete tumor resections were excluded.

Endpoints included technical details (particle size, injection method, and the amount of injection fluid), biodistribution (retention, IT distribution, and leakage of activity), safety (local and systemic adverse events), and efficacy.

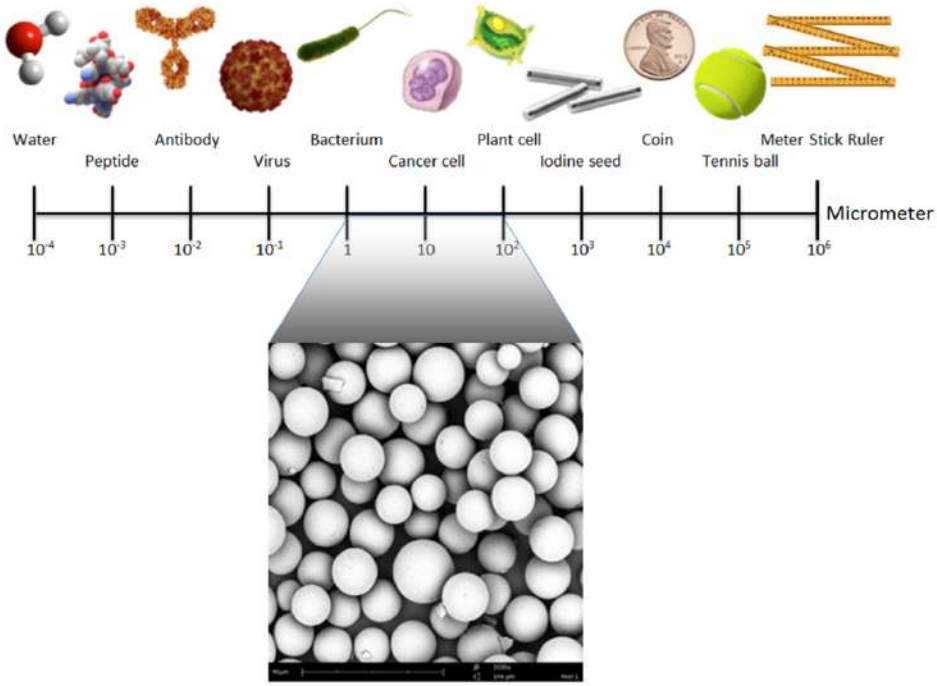

Figure 2.1. *Illustration of particle size. Particles sized between 1 and 100 µm fulfilled our definition of microparticles, as compared to smaller carriers like antibodies for radioimmunotherapy or nanoparticles, and larger particles or seeds for conventional brachytherapy.*

Search

For this review, the electronic databases MEDLINE, EMBASE, and Cochrane Library were searched from dates of inception until January 1, 2017. To ensure literature saturation, the reference lists and citing articles of included studies or relevant reviews identified through the search were scanned. The full search strategy is listed in the Appendix.

Study selection

The records derived from the search were assessed for eligibility by the author (R.B.) on the titles and abstracts. Full-text manuscripts were screened for all titles that met the inclusion criteria. The reasons for exclusion were recorded. The risk of bias was assessed according to the Newcastle-Ottawa scale to ascertain the validity of eligible trials.[7]

Data extraction

The data included (1) methodology, (2) participant details, (3) intervention details, and (4) treatment effect and side effects.

RESULTS

After the removal of duplicates, 7,271 records remained out of 10,247 initial records. Of these, 7,151 publications did not meet the criteria after reviewing the title and abstract. Subsequently, 22 of the 120 publications were discarded because full text was not available (n=2), not in the English language (n=9), or conference abstract or poster (n=11). The full texts of the remaining 98 studies revealed another 68 studies that did not meet the inclusion criteria. Two additional studies were excluded because of preliminary data and double publication. Cross-referencing identified nine additional studies that fulfilled the inclusion criteria. A total of 37 studies (performed between 1962 and 2014) were included in this review (Figure 2.2).

Characteristics and quality of included studies

Twelve studies described the use of beta-emitting microparticles in humans, 23 studies a single animal model, a single study two species, and a single study was performed in veterinary patients. In humans, only one randomized clinical trial was conducted, six cohort studies and five case series. In total, 183 human patients were treated, including a large variety of malignancies, all refractory to other treatments. The used animals in the tumor model studies were mice (13/24), rats (10/24), and rabbits (2/24). Microbrachytherapy in animals was performed in relatively small tumors (±1 cm), as larger tumors are considered not ethically feasible in small rodent models. The tumors were implanted subcutaneously (n=15) or in the organ of origin (orthotopically) (n=7), or were chemically induced (n=2).[8,9] Furthermore, a case series of three feline veterinary patients with a large spontaneous tumor in the liver were treated.[5] The quality of evidence was poor, primarily by design and number of participants. Furthermore, the large variety of microparticles, treatment methods, tumor type, and location made a proper systematic comparison impossible. Therefore, a more descriptive approach was necessary.

Type of microparticles

Microspheres (MS)[10–14] and chromic phosphate particles (CPP) were used in five and seven human studies, respectively[15–21] (Table 2.2). In the 25 animal studies including the study in veterinary patients, a similar division between MS[5,22–35] (n=15) and CPP[8,9,36–40] (n=7) was made, with some additional microparticles like ^{188}Re sulfide particles[41,42] (n=2) and labeled MAA particles[43] (Table 2.3).

The microspheres were initially made of inert materials such as ceramics/glass, acetylacetonate[5,31,32], resin[24,29], and plastics.[10–13] Nowadays, a large variety of biodegradable microspheres exists made of biosilicon[14,28] and gelatin.[33,34] The currently used microspheres are often chemically stable for at least the time that they remain radioactive, about 5–10 times the half-life of the incorporated isotope.[14] Thus, the minimum stability depends on the radioisotope; e.g., ^{90}Y microspheres with a half-life of 2.6 days must be stable for at least 13 days and ^{166}Ho with a half-life of 1.1 days at least 5.5 days. In most studies, stability was much longer than minimally required.[31,34]

The second group consisted of CPP with phosphorus-32 (^{32}P). These particles were mostly used in the treatment of hemophilic arthropathy or natural cavities with malignant effusion. The main reason for a direct IT approach with these particles was the inability to deliver sufficient absorbed doses with systemic radioimmunotherapy.[40] In addition to the ^{32}P CPP, ^{188}Re sulfide particles were fabricated, with the advantage of easier production by generator and the possibility of SPECT imaging of the gamma radiation.[42]

Particle size

In the included studies (see Tables 2.1 and 2.2), different particle sizes were used. Only one study investigated the preferred microparticle size for IT ablation.[41] In that study, two suspensions of ^{188}Re sulfide particles with a particle size distribution of 70.1% of 1–5 µm and 19.8% of 5–10 µm particles compared to 86.6 and 10.9%, respectively, were injected in a sarcoma model with a diameter of 1 cm in Kunming mice.[41] The IT retention was higher for the larger particles at various time points (Figure 2.3). A similar trend was observed in other studies that investigated the kinetics of IT injected microparticles compared to sub-micron[35], nanoparticles[9], or the effect of the addition of larger particles.[40]

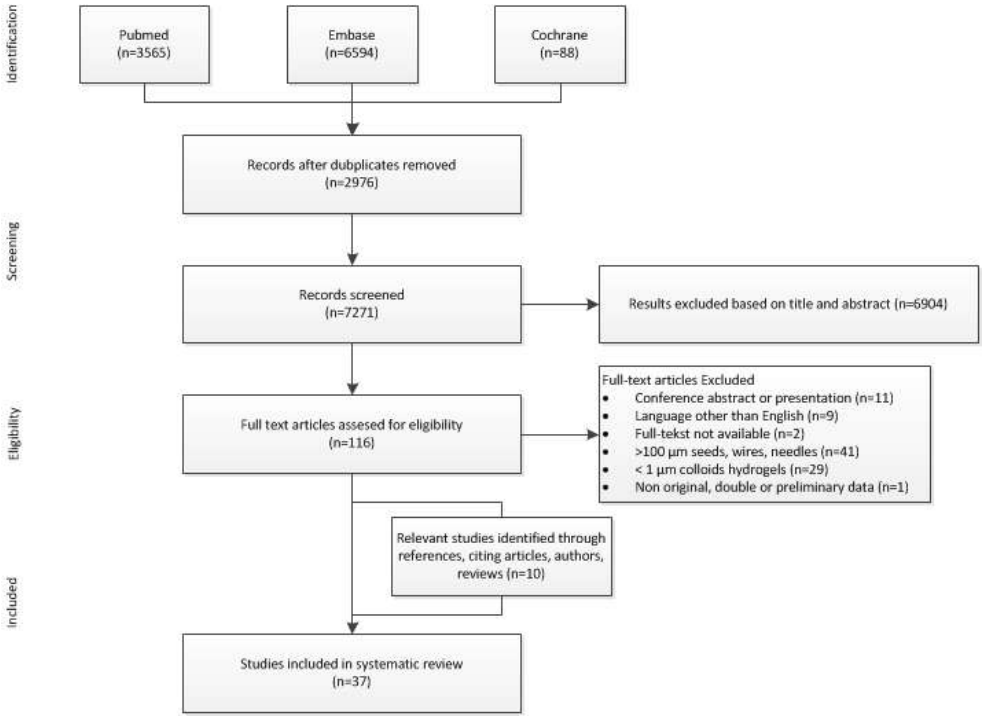

Figure 2.2. *Flow diagram of article selection.*

The effect of particle size on distribution, retention, elimination, and efficacy was clearly displayed in a study of five different sized phosphorus-32 compounds in 89 Sprague-Dawley rats with chemically induced breast tumors.[9] Thirty-two days after injection, an IT retention of radioactivity was found of 2.51 ± 0.39% for molecular ^{32}P sodium orthophosphate (<1 nm), while 10–30 nm CPP had a retention of 28.93 ± 1.30%. The retention further increased for 30–70 nm (49.82 ± 5.41%) and 0.6–1.3 µm (51.61 ± 5.82%) sized particles. Larger charcoal CPP of 2.5–4.0 µm had the best retention of 84.50 ± 2.50% after 32 days. The elimination was primarily through urine and feces and had an inverse relationship with particle size ranging from 85.90 to 12.70% of the injected dose, respectively. The anti-tumor efficacy improved with higher retention because the tumor size ratios (tumor diameter after 32 days/tumor diameter at the start) after 32 days were 4.9 in non-treated controls and 4.5, 1.4, 1.1, 0.9, and 0.6 for the treated tumors in increasing order of particle size.

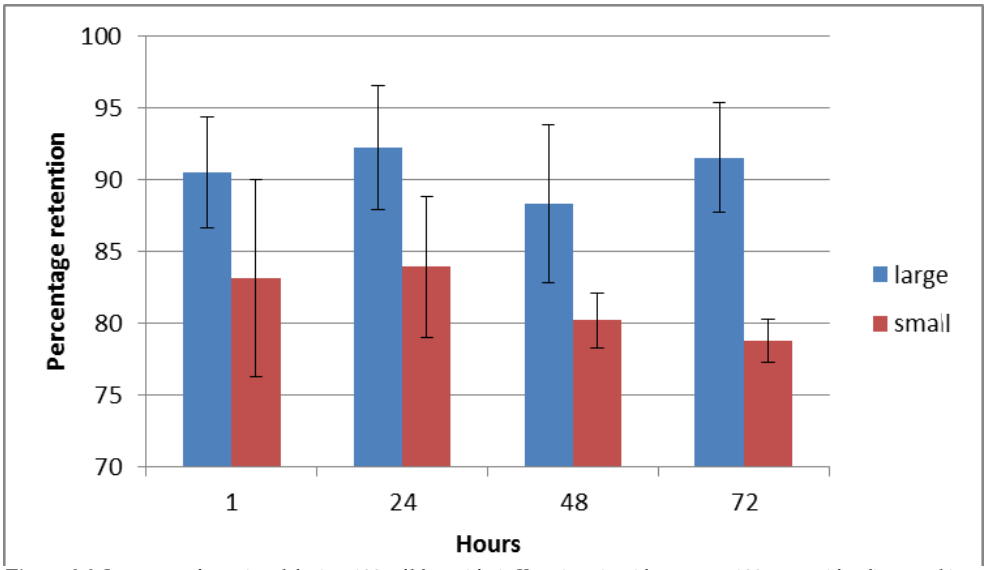

Figure 2.3. *Intra-tumoral retention of rhenium-188 sulfide particles in Kunming mice with a sarcoma-180 tumor with a diameter of 1 cm. The larger particles (mix, 70.1% 1–5 µm; 19.8% 5–10 µm) showed a larger retention compared to the smaller particles (mix, 86.6% 1–5 µm; 10.9% 5–10 µm).*[41]

Beta-emitting isotopes

Eight human studies used ^{32}P and four used ^{90}Y. These isotopes were often considered ideal by the authors because of their pure beta-emission. In animal studies, ^{131}I, ^{166}Ho, ^{186}Re, and ^{188}Re were used.[44] These isotopes also emit gamma radiation, which can be used for particle localization and quantitative imaging. None of the reviewed studies compared safety and efficacy between different radionuclides. Experience, production, biodistribution, imaging possibilities, pharmacokinetics, and clearance mostly defined preference.[33,42] Besides these differences, relatively small differences in the energy spectrum, penetration depth, and half-life time exist (Table 2.1).

Table 2.1. Characteristics of radionuclides in microparticles

Radionuclide	Half-life (days)	Beta energy (MeV)		Tissue penetration (mm)		Gamma energy		Production method
		Mean	Maximum	Mean	Maximum	keV	% Decay	
Phosphorus-32 (^{32}P)	14	0.695	1710.6	2.9	8	–	–	Reactor
Yttrium-90 (^{90}Y)	2.7	0.935	2280.1	3.9	11	–	–	Reactor or strontium-90 /yttrium-90 generator
Iodine-131 (^{131}I)	8.0	0.182	806.9	0.9	5	365	82%	Reactor
Holmium-166 (^{166}Ho)	1.1	0.666	1854.9	3.2	9	81	6.7%	Reactor
Rhenium-186 (^{186}Re)	3.8	0.362	1069.5	1.8	7	137	9.8%	Reactor
Rhenium-188 (^{188}Re)	0.71	0.764	2120.4	3.5	10	155	15.6%	Tungsten-188 /rhenium-188 generator

Characteristics of radionuclides in microparticles. MeV: Megaelectron Volt. keV: Kilo electron Volt

Technique

Due to the experimental nature of IT microbrachytherapy, no generally accepted standard administration method exists. Furthermore, most research was performed in small rodent tumor models, which are less informative for translation of the administration technique to the human situation. Therefore, the differences and similarities of the 12 reviewed human studies and the one treatment in veterinary patients will be described in the following paragraphs. These include differences in administration method, the amount of activity, the volume of injection, and imaging during and after administration.

Administration methods

The larger microspheres were most often injected using multiple manual injection locations (i.e., sub-milliliter volumes) in a grid-like pattern.[13,21] The smaller CPP were also administered through a single infusion technique in which a larger volume up to 4.5 mL of ^{32}P CPP was administered in the tumor center, assuming that the pressure force would distribute the particles throughout the tumor.[15] Empirically, 5 cm was the largest tissue diameter satisfactorily covered by microparticles after a single infusion. The specific characteristics of the needle used for IT injection were not frequently described. Needle sizes between 18 and 22G (outer diameter 1.2–0.7 mm) were commonly used percutaneously. In addition, an endoscopic ultrasound approach with a 22G needle was utilized in a published abstract[45] and unpublished trial (clinicaltrial.gov NCT00346281). Only a single study in eight humans with pancreatic tumors describes the use of a gel foam, which was injected through the 18G introducer needle to minimize back leakage and seal the needle tract.[14]

Volume of injection

No studies related the injected volume of fluid-suspended microparticles to the amount of leakage or distribution. The ideal amount of injected fluid to obtain the desired IT distribution is unknown. However, some suggested that larger fluid volumes might result in leakage of microparticles out of the tumor. With a higher amount of volume (i.e., 4.5 mL), high resistance with a sudden release of syringe pressure was often felt during infusion.[15] Subsequently, radioactivity was detected outside the tumor, presumably due to tissue destruction and leakage to surrounding tissues.[15]

The amount of injection volume varied from 7 to 25% of the tumor volume in the most recent studies in pancreatic cancer.[14,21] In liver tumors with a diameter of 2 to 8.8 cm, small (0.1–0.3 mL) volumes were used per location with a total maximum of 1.0–1.5 mL per treatment session.[13] Results obtained from non-particle intra-tumoral radionuclide therapies showed that larger volumes were associated with more side effects.[46,47] In prostate cancer, 20–50 mL (equal to the prostate volume) was injected, which resulted in 55 adverse events like strictures, fistulas, and ulcers in the first 100 patients. In the subsequent 87 patients, only 2–3 mL injection fluid was used, and only eight events occurred.[46]

Amount of activity/absorbed dose

The absorbed dose in tissue (Gray) varied from 120 to 19,300 Gy. A proper rationale for the injected activity or the desired absorbed dose was often missing. In a phase I study of ^{32}P CPP in 28 patients with unresectable pancreas tumors, a maximum of 1110 MBq for a single infusion was decided.[15] This empirically determined maximum was based on the expected limitation of the injection volume of 4.5 mL. This approach resulted in a maximum cumulative absorbed dose of 17,000 Gy. A more accurate dosing approach was applied in recent studies on pancreas cancer patients. However, the injected activity per gram (or cm^3) in the RCT with ^{32}P CPP and the cohort study with ^{32}P BioSilicon microspheres still varied with a factor of 4.6 (4 vs. 18.5 MBq/cm^3 tumor).[14,21]

Image-guided administration

The administration procedure was image guided in nine human studies. In most animal studies (n=22), no imaging was used during the administration. In the veterinary patients and rabbit studies with liver tumors, ultrasound guidance (n=2) was used, and a stereotactic frame was used in glioma-bearing rats. With CT or ultrasound, the tip of the needle was positioned at the desired location before administration. Some authors preferred ultrasound because this modality provided easy and real-time imaging during the actual injection.[13] During the injections of MS, echogenic spots were sometimes seen "flowing" in some narrow, vessel-like gaps and sometimes even out of the tumor boundaries, especially after a fast, forceful injection.[13] Subsequently, shaking of the vial before administration, resulting in air bubbles, was used to visualize any major unexpected leakage outside the tumor during the injection on ultrasound.[16]

Outcomes

The primary outcomes of IT microbrachytherapy were safety and efficacy. However, a more fundamental understanding of this treatment is necessary, especially because the outcomes of safety and efficacy probably mostly depend on the distribution of the activity. Therefore, distributional data will be described first.

Distribution

Insufficient retention of radioactive microparticles leads to an insufficiently absorbed dose and therefore an ineffective treatment. However, apart from total absorbed dose, the IT distribution of activity throughout the tumor is crucial, as "missed" parts of the tumor will result in residual vital tumor. Leakage of activity, on the other hand, may lead to an unintended absorbed dose to healthy tissue and could potentially result in side effects.

Leakage

Several potential routes of leakage were identified, and a distinction was made between external leakage and internal leakage. External leakage from the syringe occurred twice during treatment of pancreatic tumors with ^{32}P CPP infusion due to high resistance in the tumor.[16] The authors experienced with ^{166}Ho microsphere injections in ex vivo tissues, a needle disconnection from a Luer lock after exerting high pressure to overcome tissue resistance. Another possible route of external leakage is injection canal leakage. Injection canal leakage was not described in the human or animal studies. However, in the study of eight humans with pancreatic tumors, the authors describe the use of a gel foam pledget/slurry which was injected through the introducer needle to minimize back leakage and seal the needle tract.[14]

Internal leakage to non-target tissues was divided in hematogenous or intravenous and intraductal leakage. In the majority of human[13,15,16] and animal[8,9,24,35,39,43] studies, some degree of intravenous leakage or shunting of particles through the capillary bed was described. After the improved retention of CCP particles with an additional injection of larger 10–90 μm MAA particles, 56 vs. 90%, respectively, and the hypothesis of a vascular blockade, vascularity became an important variable for leakage. ^{32}P CCP 0.6–1.3 μm was injected in nude mice with human pigmented melanoma cell line (HBL) and a human squamous cell carcinoma cell line (SCC1); three to four times higher organ counting was found in SCC1.[39] This phenomenon is probably explained by the difference in vascularity between HBL and SCC1 tumors, which contained 5.7 vs. 21.4 blood vessels/mm^2, respectively.

In Wistar rats, ^{188}Re microspheres (25 μm) and small ^{186}Re sulfide particles (0.3 μm) were injected in hypervascularized Walker 256 carcinomas and hypovascularized Yoshida sarcomas. This study revealed a bi-phasic drainage of the injected particles out of the tumor. A fast wash-out phase, where the IT activity decreases to approximately 70% within 10 min, was followed by a slow decline in which IT activity falls to 60% of the initially injected activity at 48 hrs. The fast leakage was more pronounced in hypervascularized tumors with smaller particles, whereas the slow decline was independent of particle size and vascularity.[35]

In addition, the distribution of activity after IV leakage depends on the tumor location and particle size. In 33 liver cancer patients treated with ^{90}Y MS, a lung shunt of 9–20% of the injected activity was observed in six patients.[13] Similar shunts were observed after IT injections with ^{188}Re microspheres in rats with subcutaneous and liver tumors which resulted in trapped

microspheres in the pulmonary capillary bed.[24,35] Detected activity in the liver, after the treatment of the pancreas, was probably caused by venous shunting of CCP + MAA.[15,16] However, small particles such as CCP (±1 μm) and ^{186}Re-sulfide particles (0.3 μm) can probably also pass through the capillary bed of the tumor and phagocytized in the reticuloendothelial system and therefore detected in the liver.

During the treatment of malignancies in the pancreas and liver, intraductal leakage and activity in the gastrointestinal tract were described. In the 48 patients with ^{32}P CCP infusion in pancreatic cancer, accidental needle placement and injection into the pancreatic duct occurred. Forty-eight hours after injection, all intestinal activity was excreted without gastrointestinal toxicity.[15] During the treatment of 33 patients with liver malignancies with ^{90}Y MS, a similar leakage was found in the intestines in four patients that disappeared within 1– 2 days.[13]

Lymphatic drainage is an additional potential route which was however not observed in the reviewed studies. This well-known route of tumor drainage is commonly used in the sentinel node procedure. The microparticles were presumably too large for drainage of significant amounts of radioactivity to the draining lymph nodes.

Safety

The safety and toxicity were closely related to the distribution. The safety or clinical complications were divided into local and systemic side effects. The experimental treatment was often performed in progressively ill patients.[10] The probability of a causal relationship between an event and treatment was therefore often difficult to determine. However, in general, the authors of both animal and human studies concluded that the treatment was safe.

A safety concern, which was not described in the clinical studies, was needle tract metastasis. This complication might have occurred in one animal study. After three thallium-201 injections in eight Fischer 344 rats with an orthotopic glioma model, five metastases occurred of which three were along the needle tract.[48] Whether this was due to disruption of natural barriers or by dragging cells into the needle tract was ambiguous.

Table 2.2. Technical details of human studies

Study	Number of patients	Tumor type	Isotope	Particle	Particle size (µm)	Multiple injections/ Single infusion
Kim et al. 1962[10]	10	Breast, bladder, brain, prostate, lung, metastasis	^{90}Y	Ceramic MS	60 (5)	Multiple injections
Blanchard et al. 1965[11]	12	Bladder, prostate, breast, lung, metastasis	^{90}Y	Ceramic MS	40–60	Multiple injections
Ariel et al. 1978[12]	1	Rhabdomyosarcoma	^{90}Y	Ceramic MS	15 (10)	Multiple injections
Order et al. 1996 [15]	47	Pancreas Carcinoma	^{32}P	CPP + MAA	0.6–1.3 + 10–90	Single infusion
Tian et al. 199613	33	27 Hepatocellular carcinoma 6 liver metastasis	^{90}Y	Glass MS	0.6–1.3 + 10–90	Multiple injections
Westlin et al. 1997[16]	17	Pancreas Carcinoma	^{32}P	CPP + MAA	0.6–1.3 + 10–90	Single infusion
DeNittes et al. 1999[17]	5	Pancreas Carcinoma	^{32}P	CPP + MAA	0.6–1.3 + 10–90	Single infusion
Firusian et al. 1999[18]	17	Various solid malignancies	^{32}P	CPP	0.6–2	Single infusion
Montijo et al. 2003[19]	1	Pancreas carcinoma	^{32}P	CPP + MAA	0.6–1.3	Single infusion
Alimi et al. 2007[20]	14	Secondary resistant H&N tumors	^{32}P	CPP	0.6–1.3	Single infusion
Goh et al. 2007[14]	8	Hepatocellular carcinoma	^{32}P	BioSilicon MS	30	Multiple injections
Rosemurgery et al. 2008[21]	30 18 Tx 12 Co	Pancreas Carcinoma	^{32}P	CPP	0.6–1.3	Multiple Injections

^{90}Y: yttrium-90, ^{32}P: phosphorus-32, CPP: chromic phosphate particles, MAA: macroaggregated albumin, MS: microspheres, US: ultrasound, CT: computed tomography, MBq: megabecquerel, Gy: Gray, Tx: treated, Co: control

Local side effects

A reported local side effect in eight pancreatic tumor patients treated with ^{32}P BioSilicon microspheres was pain at the injection site (n=3) and the treated region (n=1) which resolved within 1 or 2 days.[14] Similar results were found with ^{32}P CPP in the pancreas. The injection of ^{90}Y microspheres in the liver was not painful, in contrast to ethanol injections.[13] Another mild effect that was observed twice was transient erythema after microbrachytherapy of superficial cervical lymph node metastasis of H&N tumors with ^{32}P CPP.[18] In the 23 patients from the three case series treated with ^{90}Y MS, the following four local complications were reported: a rectovesical fistula in prostate cancer, a lung abscess and localized radiation fibrosis in bronchial cancer, and a skin defect in a rhabdomyosarcoma of the nose.[10–12,14] In addition, after treatment of pancreas cancer with ^{32}P, some patients had increased serum amylase as a sign of local damage.[14,15,21]

Imaging	Needle gauge	Tumor size	Amount of fluid	Injected activity (MBq)/ absorbed dose (Gy)
				925–11,100 MBq
	20	2 cm^2	3 mL	185 MBq
CT	22	T1–T3	<4.5 mL	148–1,110 MBq
US	18	1.8–10.7 cm	0.1–0.3 mL Max 1.5 mL/session	370–4,440 MBq
US	19	13 cm^3 (3.1–37.5)	Max 25% tumor volume	1,390–9,000 Gy
US	22		3–4.5 mL	1110 MBq
US		10–290 cm^3	5–15 mL	<20 cm^3 74 MBq 20–40 cm^3 148 MBq 50–100 cm^3 222 MBq >100 cm^3 2–3 sessions 100–200 cm^3 370 MBq 200–300 cm^3 555 MBq
				544 MBq
US			5–15 mL	<20 cm^3 74 MBq 20–40 cm^3 148 MBq 41–50 cm^3 185 MBq 51–100 cm^3 296 MBq >100 cm^3 in 2–5 sessions >100 cm^3 444 MBq
US/CT	18 outer 22 inner		7% tumor volume	4 MBq/cm^3 of tumor
CT		19.7 (10.5) cm^2 24.1 (16.8) cm^2	25% tumor volume	18.5 MBq/g tissue, max 740 MBq Median dose 1255 Gy

In the randomized trial of 30 patients with pancreas carcinoma treated with a combination of 5FU, 60 Gy EBRT, and gemcitabine[21], 18 patients were additionally treated with ^{32}P therapy. A gastrointestinal bleeding was experienced in 15 patients of whom 13 were treated with ^{32}P. In eight patients, this complication seemed attributable to pancreatic tumor eroding into the duodenum. This complication was described in two other pancreas carcinoma patients treated with ^{32}P CPP.[16,19]

Table 2.3. Technical details of animal studies

Study	Number and type of animals	Tumor type	Location: Subcutaneous orthotopic spontaneous	Isotope
Nakhgevany et al. 1988[22]	150 Lewis Wistar rats	Rat mammary carcinoma: AC33	Subcutaneous	^{90}Y
Brown et al. 1991[23]	6 BALB/c mice	Human mammary carcinoma: BT-20	Subcutaneous	^{166}Ho
Order et al. 1994[40]	27 Male ACI rats	Rat hepatoma: $H4_2E$	Subcutaneous	^{32}P
Lee et al. 1997[38]	C3hf/sed mice Nude mice Rats	Murine fibrosarcoma: FsaII Human colon carcinoma: LS174t Rat hepatoma: $H4_2E$	Subcutaneous	^{32}P
Nguyen et al. 1997[39]	Nude mice	Human melanoma: HBL Human head and neck squamous cell carcinoma: SCC1	Subcutaneous	^{32}P
Watanabe et al. 1997[43]	Balb/c nude mice	Human neuroblastoma cell line: SK-N-MC	Subcutaneous	^{90}Y
Zubillaga et al. 1997[9]	89 SD rats	NMU-induced breast carcinoma	Orthotopic	^{32}P
Wang et al. 1998[24]	42 SD rats	Rat hepatoma: N1S1	Orthotopic	^{188}Re
Zubillaga et al. 1998[8]	70 SD rats	NMU-induced breast carcinoma	Orthotopic	^{32}P
Junfeng et al. 1999[41]	Kunming mice	Mice sarcoma: S180	Subcutaneous	^{188}Re
Lee et al. 1999[37]	Nude mice	Human pancreatic carcinoma: AsPC-1	Subcutaneous	^{32}P
Lee et al. 1999[36]	Nude mice	Human pancreatic carcinoma: AsPC-1 Human colon carcinoma: LS174t	Subcutaneous	^{32}P
Liu et al. 1999[25]	Balb/c mice	Human liver cancer: H-CS	Subcutaneous	^{32}P
Junfeng et al. 2000[42]	Athymic nude mice	Human liver cancer: SMMC 7721	Subcutaneous	^{188}Re
Lin et al. 2000[26]	SD rats	Rat hepatoma: N1S1	Orthotopic	^{90}Y
Chen et al. 2001[27]	SD rats	Rat hepatoma: N1S1	Orthotopic	^{90}Y
Lin et al. 2005[29]	NZW rabbits	Rabbit SCC: VX2	Orthotopic	^{188}Re
Zhang et al. 2005[28]	BALB/c mice	Human liver carcinoma: HepG2 human liver carcinoma: 2119	Subcutaneous	^{32}P
Hafeli et al. 2007[30]	SD rats	Rat gliosarcoma: 9L	Orthotopic	^{186}Re ^{188}Re
Lubolt et al. 2009[35]	Wistar rats	Rat mammary carcinoma: Walker carcinoma 256 Rat Yoshida sarcoma	Subcutaneous	^{186}Re ^{188}Re
Bult et al. 2012[31]	NZW rabbits	Rabbit SCC: VX2	Orthotopic	^{166}Ho
Bult et al. 2013[32]	24 Balb/C mice	Mice renal cell carcinoma	Orthotopic	^{166}Ho
Bult et al. 2013[5]	3 DS cats	Various	Spontaneous liver	^{166}Ho
Li et al. 2014[33]	Nude BABL/c mice	Human breast: MCF-7	Subcutaneous	^{131}I
Chi et al. 2014[34]	Nude BABL/c mice	Human HCC: HepG2	Subcutaneous	^{131}I

[a]Tumor size presented as TNM stage, mean (SD) or median (min–max), cm: diameter, cm²: tumor cross-sectional area, cm³: volume. SD rats: Sprague-Dawley rats, NZW rabbits New Zealand White rabbits, DS: domestic shorthair, SCC: squamous cell carcinoma, HCC: hepatocellular carcinoma, NMU: N-nitroso-N-methylurea, ^{90}Y: yttrium-90, ^{188}Re: Renium-188,^{32}P: phosphorus-32, ^{131}I: iodine-131,

Particle	Particle size (μm)	Number of injections	Needle (gauge)	Tumor size	Amount of fluid	Amount of activity (MBq)
MS	18	1		0.73	0.5 mL	37
Glass fragments	2–5 Irregular	1		19 (7–37) mm^3	0.04 mL	7.4
CPP + MAA	0.6–1.3 + 10–90	1		0.5–1.5 mm		3.7
CPP + MAA		1		FsaII /LS174t 0.5 cm^3 H4IIE 1.5 cm^3	0.01 mL HBSS/ MAA	3.7, 7.4, 14.8
CPP + MAA	0.6–1.3 + 10–90	1		1–1.5 cm^3	0.1 mL MAA/^{32}P	1.85
MAA		1	Fine	1.0 cm^3	0.05 mL	3.7
CPP	2.5–4	1			0.05 mL	18.5
Resin MS	15 ± 2	1		2 cm	0.1 mL	7.4, 37
CPP + charcoal	2.5–4	1			0.05 mL	18.5
Sulfide suspension	1–5	1		1 cm	0.1 mL	17.02 + 6 days 23.31
CPP + MAA	0.6–1.3 + 10–60	1		500 mm^3	0.1 mL	
CPP + MAA	0.6–4	1		500 mm^3	0.1 mL	
Glass MS	46–76	1		1.0 cm		183–7,320 Gy
Sulfide suspension	1–10	1		0.9– 1.2 cm	0.1 mL	HBSS, 0, 3.7, 7.4, 18.5, 29.6 Repeat day 6
Glass MS Therapheres™	20–30	1		2 cm	0.1 mL	37
Glass MS Therapheres™	20–30	1		2 cm	0.1 mL	7.4
Resin MS	15 ± 2	1	22	2–3 cm	2 mL	370
BioSilicon MS	20	1		65.3–88.9 mm^3	50 μL	0.5, 1, 2
Glass MS	25–35	1		Identical location	2 × 10 μL Fibrin glue	1.85 ^{188}Re/ ^{186}Re (ratio 3:1)
Colloids MS	0.3 25			10–15 mm		
AcAc MS	15	1	29	2 cm^3	0.1 mL	50
AcAc MS	10–15	1	29	5.6 ± 1.6 mm	0.01 mL	5
AcAc MS	8 ± 2	Multiple	22	94–648 cm^3		550–2170
Gelatin MS	30–50	1	27	0.83 cm^3	0.1 mL 25% glucose	14.8, 92.5
Gelatin MS	30–50	1	24	510 mm^3	0.1 mL 25% glucose	7.4, 37

^{166}Ho: holmium-166, AcAc: Acetylacetonate, MS: microspheres, CPP: chromic phosphate particles, MBq: megabecquerel, Gy: Gray, MAA: macroaggregated albumin, Tumor size: cm = diameter, cm^2 = tumor cross-sectional area, cm^3 = volume, Gy: Gray, HBBS: Hanks' Balanced Salt solution

Table 2.4. Outcomes of distribution, efficacy, and safety of human studies

Study	Number of Patients	Tumor type	Isotope	Retention
Kim et al. 1962[10]	10	Breast, bladder, brain prostate, lung, metastasis	^{90}Y	
Blanchard et al. 1965[11]	12	Bladder, prostate, breast, lung, and metastasis	^{90}Y	
Ariel et al. 1978[12]	1	Rhabdomyosarcoma	^{90}Y	
Order et al. 1996[15]	47	Pancreas carcinoma	^{32}P	Patients without metastasis Livershunting + (n=15) Mean 96% (range 86–100%) Livershunting – (n=12) Mean 52% (range 17–88) Patients with metastasis n=19 Mean 79% (range 22–100)
Tian et al. 1996[13]	33	27 Hepatocellular carcinoma 6 Liver metastases	^{90}Y	Biological $T^{1/2}$ = 57.6 ± 1.02 h Physical $T^{1/2}$ = 66 h
Westlin et al. 1997[16]	17	Pancreas carcinoma	^{32}P	
DeNittes et al. 1999[17]	5	Pancreas carcinoma	^{32}P	100%
Firusian et al. 1999[18]	17	Various solid malignancies	^{32}P	Biological $T^{1/2}$ = Physical $T^{1/2}$
Montijo et al. 2003[19]	1	Pancreas carcinoma	^{32}P	
Alimi et al. 2007[20]	14	Secondary resistant *head and neck cancer*	^{32}P	Biological $T^{1/2}$ = Physical $T^{1/2}$
Goh et al. 2007[14]	8	hepatocellular carcinoma	^{32}P	
Rosemurgery et al. 2008[21]	30 18 treated 12 control	Pancreas carcinoma	^{32}P	

^{90}Y: yttrium-90, ^{32}P: phosphorus-32, cm^2: $T^{1/2}$: half-life, tumor cross-sectional area, SAE: serious adverse events, Gr: grade, GI: gastrointestinal [a]n: number of lesions in 27/33 patients, Co: control

Leakage	Toxicity	Efficacy
	n=1 localized radiation fibrosis	n=4 regression n=2 no response n=3 no data n=1 died before evaluation
	n=1 lung abscess n=1 rectovesical fistula n=1 pancytopenia	n=1 marked regression n=2 regression n=2 no regression n=7 no data
	n=1 skin defect	n=1 complete response
Blood 1.85–3552 Bq/mL Shunting to the liver n=12	Without metastases n=2 Gr III leukopenia n=2 Gr IV thrombocytopenia n=1 Gr III amylase n=1 Gr IV amylase With metastases n=1 Gr III leukopenia n=1 Gr III thrombocytopenia n=2 Gr IV thrombocytopenia	n=7 complete response n=11 partial response
Liver outside tumor most patient's 3.1–11.6% Lung n=6 8.8–20.8% Intestines n=4	n=1 acute myocardial infarction day 0 of the 2nd treatment n=2 temp leukopenia after Combination with chemotherapy	Tumor shrinkage rates n=12 ≥50% or more n=12 25–50% n=5 ≤25% n=3 no change n=6 no data
Intestines n=2 Liver n=2	n=1 arterial bleeding n=2 slightly decreased blood counts	n=4 complete response n=5 partial response n=7 stable disease n=1 no data
	No significant toxicity	n=2 complete response n=3 stable disease
Blood <11 Bq/mL	n=1 Gr IV thrombocytopenia n=2 erythema of skin after superficial lymph node treatment	n=7 complete response n=5 partial response n=5 no response
	Arterial bleeding fistula	n=1 died before evaluation
	n=3 Gr I/II thrombocytopenia n=2 transient erythema	n=8 partial response n=6 no response
No detectable radioactivity in blood samples	n=3 injection site pain n=2 portal hypertension n=1 abdominal pain n=1 rigor n=1 vomiting n=1 Gr IV diabetes mellitus n=1 Gr III neutropenia n=1 Gr III pancytopenia	12 weeks n=2 complete response n=2 partial response n=4 stable disease 24 weeks n=2 complete response n=2 partial response n=1 progressive disease n=3 withdrawn
Intestines	^{32}P/Co	Survival
	SAEs 75/22	^{32}P 5.2 months
	Hospitalizations 34/10	Co 12.2 months
	GI bleedings 13/2	
	Pancytopenia 1/0	Tumor size
	Leukocytopenia 1/0	Pre → Post-treatment
	Anemia 5/4	^{32}P 16.1 → 13.3 cm^2
	Thrombocytopenia 5/0	Co 20.0 → 12.4 cm^2

Table 2.5. Main outcomes of animal studies

Study	Animal	Tumor type	Isotope	Retention		
Nakhgevany et al.1988[22]	150 Lewis Wistar	Rat mammary carcinoma: AC33	^{90}Y			
Brown et al. 1991[23]	6 BALB/c mice	Human mammary carcinoma: BT-2	^{166}Ho			
Order et al. 1994[40]	27 Male ACI rats	Rat hepatoma: $H4_2E$	^{32}P		MAA-	MAA+
				30min	32 ± 2%	90 ± 10%
				24h	56 ± 20%	90 ± 10%
				48h	44 ± 6%	73 ± 6%
Lee et al. 1997[38]	Rats	Rat hepatoma: $H4_2E$	^{32}P	18h	^{32}P	^{32}P + MAA
				100μCi	56%	26%
				200μCi	25%	36%
				400μCi	42%	42%
Nguyen et al. 1997[39]	Nude mice	Human melanoma: HBL (5.3 vessels mm^2)	^{32}P		MAA-	MAA+
				24h	65.2 ± 6.5%	60.2 ± 4.2%
				48h	50.6 ± 8.6%	56.1 ± 5.3%
				72h	60.6 ± 5.3%	58.0 ± 5.3%
	Nude mice	Human head and neck squamous cell carcinoma: SCC1 (20.5 vessels mm^2)	^{32}P		MAA-	MAA+
				24h	8.2 ± 2.2%	23.2 ± 4.3%
				48h	8.4 ± 4.6%	14.6 ± 3.18%
				72h	8.0 ± 5.2%	15.6 ± 3.84%
Watanabe et al. 1997[43]	Balb/c nude mice	Human Neuroblastoma Cell Line: SK-N-MC	^{90}Y		^{90}Y MAA	^{90}Y acetate
				3h	99.2 ± 0.56%	6.88 ± 2.52%
				24h	99.0 ± 0.98%	3.67 ± 1.32%
				72h	7.6 ± 0.96%	2.56 ± 2.21%
				120h	95.7 ± 1.56%	2.10 ± 2.25%
				168h	93.3 ± 1.75%	2.15 ± 2.57%
Zubbilaga et al. 1997[9]	89 SD rats	NMU-induced breast carcinoma	^{32}P			Retention at 32 days
				$Na^{32}P$		2.51 ± 0.39%
				10–30nm		28.93 ± 1.30%
				30–70nm		49.82 ± 5.41%
				Phosphocol (0.6–1.3 μm)		51.61 ± 5.82%
				Pirocarbotrat (2.5–4 μm)		84.50 ± 2.60%
Wang et al. 1998[24]	42 SD rats	Rat hepatoma: N1S1	^{188}Re	1h	21.16 ± 5.25%	
				24h	18.74 ± 3.17%	
				48h	17.16 ± 2.56%	
Zubbilaga et al. 1998[8]	70 SD rats	NMU-induced breast carcinoma	^{32}P			Retention at 32 days
				$Na^{32}P$ + charcoal (0.6μm)		6.60 ± 4.39
				CCP + charcoal (0.9μm)		80.50 ± 18.12
				Pirocarbotrat (2.5μm)		84.50 ± 2.60
Junfeng et al. 1999[41]	Kunming mice	Mice sarcoma: S180	^{32}P		70.1% (1–5μm)	86.6% (1–5μm)
				Time	19.8% (5–10 μm)	10.9% (5–10 μm)
				1h	90.5 ± 7.7%	83.1 ± 13.7%
				24h	92.2 ± 8.6%	83.9 ± 9.8%
				48h	88.3 ±10.9%	80.2 ± 3.8%
				72h	91.5 ± 7.6%	78.8 ± 3.0%
Lee et al.1999[37]	Nude mice	Human pancreatic carcinoma: AsPC-1	^{32}P	High adherence to the infused regions, and reduction in tumor blood flow.		

Toxicity	Efficacy			Survival		
No histological	Tumor volume (cm^3)				Control	Treated
evidence of		Control	Treated	23 days	44%	96%
radiation	Day 7:	0.72 (0.4–1.3)	0.74 (0.5–1.3)	27 days	0%	35%
damage of liver,	Day 11:	9.7 (1.9–2I.0)	1.3 (0.5–8.4)	Mean	17.4	30.8
bone marrow,	Day 15:	22.6 (4.1–43.6)	5.4 (0–25.1)			
kidney	Day 19:	48.7 (11.3–83.1)	13.1 (0–70.2)			
	Tumor volume (mm^3)					
		Control	Treated			
	Day 0:	18.0 ± 9.6	20.7 ± 14.6			
	Day 12:	117.7 ± 72.0	11.7 ± 5.9			

	MSR	% tumor regression
Control	4.9 ± 1.9	0.0
Na32P	4.5 ± 2.2	0.0
10–30nm	1.4 ± 0.3	0.0
30–70nm	1.1 ± 0.7	52.0
Phosphocol (0.6–1.3 μm)	0.9 ± 0.6	61.0
Pirocarbotrat (2.5–4 μm)	0.6 ± 0.3	78.3

	Survival 60 days
Treated	12/15 (80.0%)
Control	4/15 (26.7%)

	MSR	% tumor regression
$Na^{32}P$ + charcoal (0.6 μm)	3.1±2.0	0.0
CCP + charcoal (0.9 μm)	0.8±0.5	77.0
Pirocarbotrat (2.5 μm)	0.6±0.3	78.3

Tumor weight (mg) 13 days after treatment	
Saline	2885.3 ± 1241.3
Rhenium	2839.9 ± 1965.2
^{188}Re	98.4 ± 45.5

Table 2.5. Main outcomes of animal studies (Continued)

Study	Animal	Tumor type	Isotope	Retention		
Lee et al.1999[36]	Nude mice	Human pancreatic carcinoma: AsPC-1 Human colon carcinoma: LS174t	^{32}P	High adherence to the infused regions, and reduction in tumor blood flow.		
Liu et al.1999[25]	Balb/c	Human liver cancer: H-CS	^{32}P			
Junfeng et al. 2000[42]	Athymic nude mice	Human liver cancer: SMMC 7721	^{188}Re	Time 1h 24h 48h	%ID/g tumor 84.79 ± 2.53 125.20 ± 63.13 150.92 ± 38.48	
Lin et al. 2000[26]	SD rats	Rat hepatoma: N1S1	^{90}Y			
Li et al. 2014[33]	Nude BABL/c mice	Human breast: MCF-7	^{131}I	Time 1h 6h 24h 48h 72h 4d 8d 16d	^{131}I-MS 43.29 ± 5.27 29.28 ± 3.72 24.71 ± 7.28 19.93 ± 5.24	Na^{131}I 1.83 ± 0.46 0.60 ± 0.29 0.45 ± 0.07 0.14 ± 0.02 0.06 ± 0.01
Chi et al. 2014[34]	Nude BABL/c mice	Human Hepatocelular carcinoma HepG2	^{131}I	1d 4d 8d 16d 24d	39.06 ± 63.78 26.43 ± 60.24 23.28 ± 61.06 21.58 ± 63.64 19.55 ± 64.29	

SD rats: Sprague-Dawley rats, NZW rabbits New Zealand White rabbits, DS: domestic shorthair, SCC: squamous cell carcinoma, HCC: hepatocellular carcinoma, NMU: N-nitroso-N-methylurea, ^{90}Y: yttrium-90, ^{188}Re: Renium-188,^{32}P: phosphorus-32, ^{131}I: iodine-131, ^{166}Ho: holmium-166,

Systemic side effects

Hematological abnormalities were a frequently described side effect. This could result from treatment of blood-pooled organs, leaking of activity from microspheres, or disintegration of microspheres into smaller particles. Most of the used radioactive isotopes do have an increased accumulation in bone after leakage, which may result in bone marrow suppression. Pancytopenia was described in 1965 in a patient in whom 10% of the activity leaked from an inadequate batch of ^{90}Y MS. In the cohort of 48 pancreas carcinoma patients, grade III leukopenia and grade III/IV thrombocytopenia were observed in three and five patients, respectively.[15] Additionally, after treatment of the liver with ^{90}Y MS, leukopenia was observed in 2 out of 33 patients.[13] However, since the amounts of activity were low (venous samples <11 Bq/mL)[18], the leakage often did not result in clinical toxicity.

Toxicity	Efficacy			Survival		
	Time	Weight of tumor (g) Tx/Control	Tumor inhibiting rate (%)	Absorbed dose (Gy)	Tumor weight (g)	Tumor-inhibiting rate 14 days (%)
	3h	1.5/2.3	34.8	Control	6.25 ± 0.39	
	6h	1.7/3.2	46.9	183	2.43 ± 0.33	59.7
	13h	2.1/5.9	64.4	366	2.17 ± 0.26	65.3
	20h	1.6/6.7	76.1	1830	0.94 ± 0.10	84.8
	28h	1.0/6.8	85.3	3660	0.46 ± 0.08	92.5
				7320	0.40 ± 0.10	93.6
	Injected dose (MBq)	Absorbed dose (Gy)		Tumor-inhibiting rate at day 14 (%)		
	3.7 × 2	63.5		20.8%		
	7.4 × 2	126.9		39.3%		
	18.5 × 2	317.3		63.6%		
	29.6 × 2	507.6		89.0%		
		Tumor size decrease			Survival day 60	
		Treated	Control		Treated	Control
	IT	83.3% (10/12)	0/12	IT	83% (10/12)	25% (3/12)
	IA	58.3% (7/12)	0/12	IA	66% (8/12)	16.7% (2/12
		Tumor volume (cm^3)				
		Treated	Control			
	Start	0.87 ± 0.39	0.79 ± 0.06			
	21 days	0.63 ± 0.39	7.03 ± 0.95			
	Growth rate (cm^3/week)				Survival 64 days	
	Treated	0.037 ± 0.04		Treated	73.3% (11/15)	
	Control	0.68 ± 0.19		Control	13.3% (2/15)	

MS: microspheres. IA: intra-arterial, IT: intra tumorale: %ID/g: percentage injected dose/ gram, h: hours, d: days

Efficacy

The tumoricidal efficacy of intra-tumoral treatment with radioactive beta-emitting microparticles was shown in animal models. Forty nude mice with subcutaneous liver tumors were treated with ^{32}P glass MS. This study did not only show that ^{32}P glass microspheres were effective in the treatment of a subcutaneous liver tumor model; it additionally showed a dose-response relation.[25] The tumor-inhibiting rate improved from the lowest dose of 183 Gy to the highest dose of 7,320 Gy, from 59.7 to 93.6%, respectively. These results were confirmed in another liver carcinoma line in nude mice with ^{188}Re.[42]

The efficacy in the human studies was more difficult to interpret as 11/12 were non-comparative studies (Table 2.4). However, the results of eight patients with pancreas carcinomas treated with ^{32}P BioSilicon microspheres were promising, with two complete responses, two partial responses, and four patients with stable disease after 12 weeks.[14] Furthermore, a survival benefit

was found in the responders as compared to the non-responders for 14 head and neck cancer patients treated with ^{32}P CCP. On the other hand, a survival benefit was not found in the RCT in 30 pancreas cancer patients with a treatment history of 5-FU, EBRT, and gemcitabine. Patients receiving ^{32}P CCP in addition to standard therapy survived a median of 5.2 months, whereas patients receiving standard therapy alone survived 12.2 months, p=0.16. A decrease in radiologic tumor size was not detected on CT because cancer persisted along the periphery of the injection sites.[21]

DISCUSSION

In this study, all currently available literature on the potential role of beta-emitting microparticles for IT treatment of solid malignant neoplasms was reviewed. The results of 12 human and 25 animal studies were included. The large variety of particles, techniques, and treated tumors in the studies provided an important insight into issues concerning efficacy, safety, particle and isotope choice, and other concepts for future research.

Is microbrachytherapy effective? Based on the reviewed data, it can be concluded that beta-emitting microparticles seem to be an effective tumoricidal agent. The majority of the studies showed promising results in both humans and animals with complete responses and long-term survival.[14] However, a direct IT injection with tumoricidal particles does not automatically lead to an effective tumor treatment.[21] Obtaining a sufficient dose coverage of all tumor tissue requires the challenging design of an optimal treatment modality with regard to biological stability, injection techniques, dosimetry, biodistribution, etc.

Is microbrachytherapy safe? In the only performed randomized control trial, concerns were raised about the safety of additional IT treatment with small ^{32}P CPP in pancreas cancer patients treated with 5-fluorouracil, EBRT, and gemcitabine.[21] More patients experienced gastrointestinal bleeding compared to the standard therapy alone. Bleedings were not observed in studies with other particles and other tumors. Other local side effects included manageable discomfort at the injection site. Except for manageable hematological abnormalities, other systemic adverse events were not encountered. Therefore, apart from pancreas tumors, IT treatment seems to be a reasonably safe alternative.

Can we predict complications? Leakage appears to follow the path of least resistance. An easy route of leakage after IT administration is injection canal leakage. The use of a small needle can reduce this. However, care should be taken to prevent premature settling and clotting of microparticles inside the syringe and blocking the needle.[5,31,32] A 21G needle seems to be the preferred needle to use. Additional measures to reduce leakage may include slow injection and withdrawal of the needle with slight pressure or injection of obstructing pledget/foam. Other

routes of leakage (i.e., intravascular or intraductal) may be caused by injection position, excessive volume, or pressure. Increased permeability of tumor neovascularization may be considered a risk factor for hematogenous leakage. Leakage of an entire dose may happen when a single infusion technique is used.[15] A grid-like injection procedure with larger microspheres in small volume depots may, therefore, be preferred over the infusion of smaller particles.

How much fluid should be injected during microbrachytherapy? Theoretically, more fluid results in more propelling force and a more homogeneous distribution of microparticles in the target tissue. This should be balanced against the chances of more side effects.[46,47] The injected volume should probably range between 7 and 30% of the tumor volume[14,16] as excessive volume or pressure may result in leakage.[15,16] In addition, intra-tumoral pressure depends on tumor characteristics and location and should be taken into account.[36–38] A more viscous fluid may be used to obtain even more control.[6,12] For example, 25% glucose, fibrin glue, and other formulas were used to improve the injection procedure[14,30], or hydrogels such as chitosan.[49]

Which particles should be used? There is a relation between particle size and retention: the larger the particle, the higher the retention. Subsequently, preferences for the larger microspheres exist. On the other hand, particles must be small enough to distribute evenly throughout the tumor to deliver an adequate homogeneously absorbed dose. The optimal number of particles was not mentioned in the studies, but it is likely to influence biodistribution, safety, and efficacy too, and must be investigated to result in a better understanding of IT injection.

What are the ideal radionuclide characteristics? ^{90}Y is often considered the ideal isotope, with a high energy, pure beta-emitter for easy radiation protection, and an intermediate half-life of 64 hrs. However, because of the questions related to both IT distribution and retention of microparticles, isotopes with better imaging properties are more suitable for imaging-guided monitoring of IT particle distribution and dosimetry.

For leakage to other organs, low-resolution bremsstrahlung scintigraphy is sufficient. However, the resolution of this technique is insufficient for local tumor dose distribution monitoring. SPECT imaging can greatly improve particle distribution measurements for ^{186}Re, ^{188}Re, and ^{166}Ho because of the associated gamma-radiation of 80–200 keV. Furthermore, ^{166}Ho can be visualized and quantified with CT and MRI.[32] There are several developments in imaging of these isotopes. ^{90}Y PET/CT is also quantitative but requires long acquisition times due to the low number of positrons. Another relative new imaging opportunity is Cerenkov luminescence imaging (CLI).[50] CLI could provide quantitative high-resolution imaging and image-based dosimetry for a large variety of isotopes.[50–52] The main limitation of CLI is the limited penetration depth of light of approximately 10 mm into tissue, however very promising, in small animal models.[51,53]

In addition to imaging characteristics, half-life and beta energy should be considered in relation to efficacy and safety, but also logistics, like production and cost. In this respect, a generator like the tungsten-188/rhenium-188 generator may be beneficial. In theory, a high dose rate (i.e., short half-life) will prevent the recovery of radiation damaged tumor cells and may lead to higher efficacy. In terms of logistics, a short half-life may lead to production and logistic challenges on the one hand, but a shorter hospital stay with fewer restrictions after discharge on the other hand.

IT injections can be performed in a variety of tumor types and organs. Based on the postulated methods of leakage, potential risks of side effects, and more challenging administration, the pancreas seems to be a difficult-to-treat organ. Superficial tumors, such as lymph node metastases of the head and neck region, and liver tumors are better accessible, show minimal leakage, and have minimal side effects. With increasing knowledge, microbrachytherapy may be adjusted to tumor characteristics, for example, the addition of a vasoconstrictive drug in hypervascular tumors.

CONCLUSION

Intra-tumoral treatment with radioactive beta-emitting microparticles, microbrachytherapy, in solid malignant neoplasms may have additional value for patients with tumors at various locations. The uncomplicated treatments with high cumulative doses of up to 19,000 Gy suggest that microbrachytherapy is relatively safe. Larger particles resulted in a higher retention and tumor-inhibiting efficacy of >90% with an intra-tumoral absorbed dose of 7,320 Gy. A small injected volume of 7–30% of the tumor volume divided in small volume depots, 0.1–0.3 mL, administered in a grid-like injection procedure is preferred. With accurate administration and high-resolution imaging, the efficacy may be improved while the risk of side effects will be reduced. Particles that emit a small amount of gamma-radiation and can be visualized with high-resolution imaging are preferred at this stage. Experiments should be performed in larger tumor models to obtain better clinical relevant data on the IT distribution. Subsequently, the threshold absorbed dose to successfully treat the tumor should be investigated. Furthermore, accurate administration requires skilled physicians and controlled injection, and will be time consuming. In the near future, with advanced technologies such as controllable needle placement and injection systems, the procedure could be performed easily, quickly, and safely for patients and personnel.

FUNDING

The work was supported by the Department of Radiology and Nuclear Medicine, University Medical Center Utrecht, Utrecht, The Netherlands.

Author R.C. Bakker is funded by the Dutch Cancer Society research grant 2014-6620.

CONFLICT OF INTEREST

Author R.C. Bakker declares that he has no conflict of interest.

Author M.G.E.H. Lam is consultant for Sirtex, BTG, Mirada, and Bayer Healthcare.

Author S.A. van Nimwegen declares that he has no conflict of interest.

Author A.J.W.P. Rosenberg declares that he has no conflict of interest.

Author R.J.J. van Es declares that he has no conflict of interest.

Author J.F.W. Nijsen is co-founder and scientific director of Quirem Medical and has a minority share in the company Quirem Medical. Furthermore, J.F.W. Nijsen is inventor on the patents related to the ^{166}Ho-PLLA-microspheres that are assigned to University Medical Center Utrecht Holding B.V. (patent numbers WO2012060707 A1 and US 2005/0201940 A1).

The Department of Radiology and Nuclear Medicine of the UMC Utrecht receives royalties from Quirem Medical B.V.

ETHICAL APPROVAL

This article does not contain any studies with human participants or animals performed by any of the authors.

INFORMED CONSENT

For this type of study, formal consent is not required.

APPENDIX SEARCH STRATEGY

Medline

#1. Humans [Mesh]
#2. Animals [Mesh]
#3. Animal [Title/Abstract]
#4. Human [Title/Abstract]
#5. #1 OR #2 OR #3 OR #4
#6. Neoplasms [Mesh]
#7. Tumor*[Title/Abstract]
#8. Tumor*[Title/Abstract]
#9. Cancer*[Title/Abstract]
#10. #6 OR #7 OR #8 OR #9
#11. Intratumor*[Title/Abstract]
#12. Intra-tumor*[Title/Abstract]
#13. Intratumor*[Title/Abstract]
#14. Intra-tumor*[Title/Abstract]
#15. Intralesion*[Title/Abstract]
#16. Intra-lesion*[Title/Abstract]
#17. Interstitial*[Title/Abstract]
#18. #10 OR #11 OR #12 OR #13 OR #14 OR #15 OR #16 OR 17#
#19. Radiotherapy [Mesh Terms]
#20. Radiotherapy [Title/Abstract]
#21. Radioisotopes [Mesh]
#22. Isotopes [MeSH]
#23. Gold [Mesh]
#24. Gold [Title/Abstract]
#25. Lutetium [Mesh]
#26. Lutetium [Title/Abstract]
#27. Rhenium [Mesh]
#28. Rhenium [Title/Abstract]
#29. Holmium [Mesh]
#30. Holmium [Title/Abstract]
#31. Iodine [Mesh]
#32. Iodine [Title/Abstract]
#33. Yttrium [Mesh]
#34. Yttrium [Title/Abstract]
#35. Phosphorus [Mesh]
#36. Phosphorus [Title/Abstract]
#37. 32P[Title/Abstract]
#38. P32 [Title/Abstract]
#39. 32-P [Title/Abstract]
#40. P-32 [Title/Abstract]
#41. #19 OR #20 OR #21 OR #22 OR #23 OR #24 OR #25 OR #26 OR #27 OR #28 OR #29 OR #30 OR #31 OR #32 OR #33 OR #34 OR #35 OR #36 OR #37 OR #38 OR #39 OR #40 OR #41
#42. "Treatment Outcome"[Mesh]
#43. Survival [Title/Abstract]
#44. "Tissue Distribution"[Mesh]
#45. Distribut*[Title/Abstract]
#46. Safe*[Title/Abstract]
#47. Toxicity [Subheading]
#48. Toxic*[Title/Abstract]
#49. Effic*[Title/Abstract]
#50. Effec*[Title/Abstract]
#51. #42 OR #43 OR #44 OR #45 OR #46 OR #47 OR #48 OR #49 OR #50
#52. #5 AND #10 AND #18 AND #41 AND #51

EMBASE

#1. 'in vivo study'/exp
#2. 'human'/exp
#3. 'animal'/exp
#4. #1 OR #2 OR #3
#5. 'neoplasm'/exp
#6. cancer:ab,ti
#7. tumo*r:ab,ti
#8. #5 OR #6 OR #7
#9. 'intratumoral drug administration'/exp
#10. intratumo*r*:ab,ti
#11. intralesion*:ab,ti
#12. 'interstitial':ab,ti
#13. 'intra tumo*r*':ab,ti
#14. 'intra lesion*':ab,ti
#15. #9 OR #10 OR #11 OR #12 OR #13 OR #14
#16. 'radiotherapy'/exp
#17. 'radiotherapy':ab,ti
#18. 'radioisotope'/exp
#19. 'radioisotope':ab,ti
#20. 'isotope'/exp
#21. 'isotope':ab,ti
#22. 'gold'/exp
#23. 'gold':ab,ti
#24. 'lutetium'/exp
#25. 'lutetium':ab,ti
#26. 'rhenium':ab,ti
#27. 'rhenium'/exp
#28. 'holmium'/exp
#29. 'holmium':ab,ti
#30. 'iodine':ab,ti
#31. 'iodine'/exp
#32. 'yttrium'/exp
#33. yttrium:ab,ti
#34. 'phosphorus'/exp
#35. 'phosphorus':ab,ti
#36. p32:ab,ti
#37. 'p 32':ab,ti
#38. '32p':ab,ti
#39. '32 p':ab,ti
#40. 'phosphorus 32':ab,ti
#41. #15 OR #16 OR #17 OR #18 OR #19 OR #20 OR #21 OR #22 OR #23 OR #24 OR #25 OR #26 OR #27 OR #28 OR #29 OR #30 OR #31 OR #32 OR #33 OR #34 OR #35 OR #36 OR #37 OR #38 OR #39
#42. 'treatment outcome'/exp
#43. 'survival'/exp
#44. survival:ab,ti
#45. 'toxicity'/exp
#46. tox*:ab,ti
#47. 'safety'/exp
#48. safety:ab,ti
#49. 'tissue distribution'/exp
#50. distribution:ab,ti
#51. effic*:ab,ti
#52. effec*:ab,ti
#53. #42 OR #43 OR #44 OR #45 OR #46 OR #47 OR #48 OR #49 OR #50 OR #51 OR #52
#54. #4 AND #8 AND #15 AND #41 AND #53

Central

#1. MeSH descriptor: [Humans] explode all trees
#2. MeSH descriptor: [Animals] explode all trees
#3. in-vivo:ti,ab,kw or human:ti,ab,kw or animal:ti,ab,kw
#4. #1 or #2 or #3
#5. MeSH descriptor: [Neoplasms] explode all trees
#6. cancer:ti,ab,kw
#7. neoplasia:ti,ab,kw
#8. neoplasm:ti,ab,kw
#9. tumor:ti,ab,kw
#10. tumor:ti,ab,kw
#11. #5 or #6 or #7 or #8 or #9 or #10
#12. intratumor*:ti,ab,kw
#13. intratumor*:ti,ab,kw
#14. intralesion*:ti,ab,kw
#15. intra-tumor*:ti,ab,kw
#16. intra-tumor*:ti,ab,kw
#17. intra-lesion*:ti,ab,kw
#18. interstitial:ti,ab,kw
#19. #12 or #13 or #14 or #15 or #16 or #17 or #18
#20. MeSH descriptor: [Radiotherapy] explode all trees
#21. Radiotherapy:ti,ab,kw
#22. MeSH descriptor: [Radioisotopes] explode all trees
#23. radioisotope*:ti,ab,kw
#24. MeSH descriptor: [Isotopes] explode all trees
#25. phosphorus*:ti,ab,kw
#26. yttrium:ti,ab,kw
#27. Iodine:ti,ab,kw
#28. Holmium:ti,ab,kw
#29. Lutetium:ti,ab,kw
#30. Rhenium:ti,ab,kw
#31. Gold:ti,ab,kw
#32. #20 or #21 or #22 or #23 or #24 or #25 or #26 or #27 or #28 or #29 or #30 or #31
#33. MeSH descriptor: [Treatment Outcome] explode all trees
#34. MeSH descriptor: [Safety] explode all trees
#35. MeSH descriptor: [Tissue Distribution] explode all trees
#36. effic*:ti,ab,kw or effec*:ti,ab,kw or Safety:ti,ab,kw or distribut*:ti,ab,kw or toxic*:ti,ab,kw
#37. survival:ti,ab,kw
#38. #33 or #34 or #35 or #36 or #37
#39. #4 and #11 and #19 and #32 and #38

REFERENCES

1. Lyon SM, Pascoe DM. Percutaneous gastrostomy and gastrojejunostomy. Semin Intervent Radiol 2004;21(3):181–189
2. Loffroy R, Favelier S, Chevallier O, Estivalet L, Genson PY, Pottecher P, et al. Preoperative portal vein embolization in liver cancer: indications, techniques and outcomes. Quant Imaging Med Surg 2015;5(5):730–739
3. de Baere T, Elias D, Dromain C, Din MGE, Kuoch V, Ducreux M, et al. Radiofrequency ablation of 100 hepatic metastaseswith a mean follow-up of more than 1 year. Am J Roentgenol 2000;175(6):1619–1625
4. Bussu F, Tagliaferri L, Mattiucci G, Parrilla C, Dinapoli N, Miccichè F, et al. Comparison of interstitial brachytherapy and surgery as primary treatments for nasal vestibule carcinomas. Laryngoscope 2016;126(2):367–371
5. Bult W, Vente MAD, Vandermeulen E, Gielen I, Seevinck PR, Saunders J, et al. Microbrachytherapy using holmium-166 acetylacetonate microspheres: a pilot study in a spontaneous cancer animal model. Brachytherapy 2013;12(2):171–177
6. Booth A, Clarke M, Dooley G, Ghersi D, Moher D, Petticrew M, et al. The nuts and bolts of PROSPERO:an international prospective register of systematic reviews. Syst Rev Springer Open Ltd 2012;1(1):2
7. Stang A. Critical evaluation of the Newcastle-Ottawa scale for the assessment of the quality of nonrandomized studies in metaanalyses. Eur J Epidemiol 2010;25(9):603–605
8. Zubillaga MB, Boccio JR, Nicolini JO, Ughetti R, Lanari E, Caro RA. Radiochemical and radiopharmacological properties of Pirocarbotrat and other labeled charcoal dispersions: comparative studies in rats with NMU-induced mammary tumors. Nucl Med Biol 1998;25(3):305–311
9. Zubillaga MB, Boccio JR, Nicolini JO, Ughetti R, Lanari E, Caro RA. Pirocarbotrat: a new radiopharmaceutical for the treatment of solid tumors—comparative studies in N-nitrosomethylurea-induced rat mammary tumors. Nucl Med Biol 1997;24(6):559–564
10. Kim YS, Lafave JW, Maclean LD. The use of radiating microspheres in the treatment of experimental and human malignancy. Surgery 1962;52:220–231
11. Blanchard RJ, Lafave JW, Kim YS, Frye CS, RitchieWP, Perry JF. Treatment of patients with advanced cancer utilizing Y90 microspheres. Cancer 1965;18(3):375–380
12. Ariel IM. Cure of an embryonal rhabdomyosarcoma of the nose of an infant by interstitial 90Yttrium microspheres: a case report. Int J Nucl Med Biol 1978;5(1):37–41
13. Tian JH, Xu BX, Zhang JM, Dong BW, Liang P, Wang XD. Ultrasound-guided internal radiotherapy using yttrium-90-glass microspheres for liver malignancies. J Nucl Med 1996;37(6):958–963
14. Goh ASW, Chung AYF, Lo RHG, Lau TN, Yu SWK, Cheng M, et al. A novel approach to brachytherapy in hepatocellular carcinoma using a phosphorus 32 (32P) brachytherapy delivery device-a first-in-man study. Int J Radiat Oncol Biol Phys 2007;67(3):786–792
15. Order SE, Siegel JA, Principato R, Zeiger LE, Johnson E, Lang P, et al. Selective tumor irradiation by infusional brachytherapy in nonresectable pancreatic cancer: a phase I study. Int J Radiat Oncol Biol Phys 1996;Dec 1;36(5):1117-26.
16. Westlin JE, Andersson-Forsman C, Garske U, Linné T, Aas M, Glimelius B, et al. Objective responses after fractionated infusional brachytherapy of unresectable pancreatic adenocarcinomas. Cancer 1997;80(12 SUPPL):2743–2748
17. DeNittis AS, Stambaugh MD, Lang P, Wallner PE, Lustig RA, Dillman RO, et al. Complete remission of nonresectable pancreatic cancer after infusional colloidal phosphorus-32 brachy therapy, external beam radiation therapy, and 5-fluorouracil: a preliminary report. AmJ Clin Oncol Cancer Clin Trials 1999;22(4):355–360
18. Firusian N, Dempke WCM. An early phase II study of intratumoral P-32 chromic phosphate injection therapy for patients with refractory solid tumors and solitary metastases. Cancer 1999;85(4):980–987
19. Montijo IJ, Khurana V, Alazmi WM, Order SE, Barkin JS. Vascular pancreatic gastric fistula: a complication of colloidal 32P injection for nonresectable pancreatic7 cancer. Dig Dis Sci 2003;48(9):1758–1759
20. Alimi KA, Firusian N, Dempke W. Effects of intralesional 32-P chromic phosphate in refractory patients with head and neck tumors. Anticancer Res 2007;27(4 C):2997–3000
21. Rosemurgy A, Luzardo G, Cooper J, Bowers C, Zervos E, Bloomston M, et al. 32P as an adjunct to standard therapy for locally advanced unresectable pancreatic cancer: a randomized trial. J Gastrointest Surg 2008;12(4):682–688
22. Nakhgevany KB, Mobini J, Bassett JG, Miller E. Nonabsorbable radioactive material in the treatment of carcinomas by local injections. Cancer 1988;61(5):931–940
23. Brown RF, Lindesmith LC, Day DE. ^{166}Holmium-containing glass for internal radiotherapy of tumors. Nucl Med Biol 1991;18(7):783–790
24. Wang SJ, Lin WY, Chen MN, Chi CS, Chen JT, Ho WL, et al. Intratumoral injection of rhenium-188 microspheres into an animalmodel of hepatoma. J Nucl Med 1998;39(10):1752–1757

25. Liu L, Jiang Z, Teng GJ, Song JZ, Zhang DS, Guo QM, et al. Clinical and experimental study on regional administration of phosphorus 32 glass microspheres in treating hepatic carcinoma. World J Gastroenterol 1999;5(6):492–505
26. Lin WY, Tsai SC, Hsieh JF, Wang SJ. Effects of 90Y-microspheres on liver tumors: comparison of intratumoral injection method and intra-arterial injectionmethod. JNucl Med 2000;41(11):1892–1897
27. Chen SD, Hsieh JF, Tsai SC, Lin WY, Cheng KY, Wang SJ. Intra-tumoral injection of 90Y microspheres into an animal model of hepatoma. Nucl Med Commun 2001;22(2):121–125
28. Zhang K, Loong SLE, Connor S, Yu SWK, Tan SY, Ng RTH, et al. Complete tumor response following intratumoral 32P BioSilicon on human hepatocellular and pancreatic carcinoma xenografts in nude mice. Clin Cancer Res 2005;11(20):7532–7537
29. Lin YC, Tsai SC, Hung GU, Lee JC, Huang YS, Lin WY. Direct injection of 188Re-microspheres in the treatment of hepato-cellular carcinoma. Comparedwith traditional percutaneous ethanol injection: an animal study. Nuklearmedizin 2005;44(3):76–80
30. Haefeli UO, Pauer GJ, Unnithan J, Prayson RA. Fibrin glue system for adjuvant brachytherapy of brain tumors with 188Re and 186Re-labeled microspheres. Eur J Pharm Biopharm 2007;65(3):282–288
31. Bult W, De Leeuw H, Steinebach OM, Van Der Bom MJ, Wolterbeek HT, Heeren RMA, et al. Radioactive holmiumacetylacetonate microspheres for interstitial microbrachytherapy:an in vitro and in vivo stability study. Pharm Res 2012;29(3):827–836
32. Bult W, Kroeze SGC, Elschot M, Seevinck PR, Beekman FJ, deJong HWAM, et al. Intratumoral administration of holmium-166 acetylacetonate microspheres: antitumor efficacy and feasibility of multimodality imaging in renal cancer. PLoS One 2013;8(1):e52178
33. Li CC, Chi JL, Ma Y, Li JH, Xia CQ, Li L, et al. Interventional therapy for human breast cancer in nude mice with 131I gelatin microspheres (131I–GMSs) following intratumoral injection. Radiat Oncol 2014;Jun 23;9:144
34. Chi JL, Li CC, Xia CQ, Li L, Ma Y, Li JH, et al. Effect of 131I gelatin microspheres on hepatocellular carcinoma in nude mice and its distribution after intratumoral injection. Radiat Res 2014 181(4):416–424
35. Luboldt W, Pinkert J, Matzky C, Wunderlich G, Kotzerke J. Radiopharmaceutical tracking of particles injected into tumors: a model to study clearance kinetics. Curr Drug Deliv 2009;6(3):255–260
36. Lee I. Enhanced tumor targeting by an intratumoral injection of colloidal chromic 32P in two human tumors (AsPC-1 pancreas and Ls174T colon) in nude mice. J Surg Oncol 1999;70(3):161–166
37. Lee I, Lee YH. The effect of various therapeutic solutions including colloidal chromic 32P via an intratumoral injection on the tumor physiological parameters of AsPC-1 human pancreatic tumor xenografts in nudemice. Clin Cancer Res 1999;5(10 SUPPL):3139s–3142s
38. Lee I, Wallner PE. Evaluation of cellular uptake, tumor retention, radiation response, and tumor pathophysiology in experimental solid tumors after an intratumoral infusion of colloidal 32P. Cancer 1997;80(12 SUPPL):2611–2617
39. Nguyen H, Ghanem G, Morandini R, Verbist A, Larsimont D, Fallais C, et al. Tumor type and vascularity: important variables in infusional brachytherapy with colloidal 32P. Int J Radiat Oncol 1997;39(2):481–487
40. Order SE, Siegel JA, Lustig RA, Principato R, Zeiger LS, Johnson E, et al. A new method for delivering radioactive cytotoxic agents in solid cancers. Int J Radiat Oncol Biol Phys 1994;30(3):715–20
41. Junfeng Y, Duanzhi Y, Xiaofeng M, Zili G, Jiong Z, Yongxian W, et al. [188Re]rhenium sulfide suspension: a potential radio-pharmaceutical for tumor treatment following intra-tumor injection. Nucl Med Biol 1999;26(5):573–579
42. Junfeng Y, Ruping Z, Xinlan D, Xiaofeng M, Jianying X,Weiqing H, et al. Intratumoral injection with [(188)re]rhenium sulfide suspension for treatment of transplanted human liver carcinoma in nude mice. Nucl Med Biol 2000;27(4):347–352
43. Watanabe N, Oriuchi N, Igarashi H, Higuchi T, Yukihiro M, Fukushima Y, et al. Preparation of yttrium-90-labeled human macroaggregated albumin for regional radiotherapy.Nucl Med Biol 1997;24(5):465–469
44. Nijsen JFW, Krijger GC, van Het Schip AD. The bright future of radionuclides for cancer therapy. Anti Cancer Agents Med Chem 2007;7(3):271–290
45. Meenan J, Mesenas S, Douglas N, Heatley S, Doig L, Ross P. EUS-delivered therapy for pancreatic cancer: initial experience with targeted injection of 32P Biosilicon™. Gastrointest Endosc 2007;65(5):AB208
46. Flocks RH, Culp D, Elkins HB. Treatment of cancer of prostate by interstitial injection of Au 198: studies in problem of distribution. Trans Am Assoc Genitourin Surg 1956;48(3):188–203
47. Lee JD, Yang WI, Lee MG, Ryu YH, Park JH, Shin KH, et al. Effective local control of malignant melanoma by intratumoral injection of a beta-emitting radionuclide. Eur J Nucl Med Mol Imaging 2002 29(2):221–230
48. Sjoholm H, Ljunggren K, Adeli R, Brun A, Ceberg C, Strand SE, et al.(1995) Necrosis of malignant gliomas after intratumoral injection of 201Tl in vivo in the rat. Anti-Cancer Drugs 1995 Feb;6(1):109-14.
49. Kim JK, Han KH, Lee JT, Paik YH, Ahn SH, Lee JD, et al. Long-term clinical outcome of phase IIb clinical trial of percutaneous injection with holmium-166/chitosan complex (Milican) for the treatment of small hepatocellular carcinoma. Clin Cancer Res 2006;12(2):543–548
50. Ciarrocchi E, Belcari N. Cerenkov luminescence imaging: physics principles and potential applications in biomedical sciences. EJNMMI Physics 2017;4(1):14

51. Ma X, Wang J, Cheng Z. Cerenkov radiation: a multi-functional approach for biological sciences. Front Phys 2014;2:1–14
52. Carpenter CM, Ma X, Liu H, Sun C, Pratx G, Wang J, et al. Cerenkov luminescence endoscopy: improved molecular sensitivity with β-emitting radiotracers. J Nucl Med 2014;55(11):1905–1909
53. Chakraborty S, Sharma KS, Rajeswari A, Vimalnath KV, Sarma HD, Pandey U, et al. Radiolanthanide-loaded agglomerated Fe3O4 nanoparticles for possible use in the treatment of arthritis: formulation, characterization and evaluation in rats. J Mater Chem B 2015;3(27):5455–5460


3

Blood and urine analyses after radioembolization of liver malignancies with [^{166}Ho]Ho-acetylacetonate-poly(L-lactic acid) microspheres

R.C. Bakker

R. de Roos

F.F.T. Ververs

M.G.E.H. Lam

M.K. van der Lee

B.A. Zonnenberg

G.C. Krijger

Nuclear Medicine and Biology

Bakker RC, de Roos R, Ververs FFT, Lam MGEH, van der Lee MK, Zonnenberg BA, Krijger GC. **Blood and urine analyses after radioembolization of liver malignancies with [^{166}Ho]Ho-acetylacetonate-poly(l-lactic acid) microspheres.** Nucl Med Biol 2019;71:11-18.

ABSTRACT

Introduction

[^{166}Ho]Ho-acetylacetonate-poly(L-lactic acid) microspheres were used in radioembolization of liver malignancies by intra-arterial administration. The primary aim of this study was to assess the stability and biodistribution of these microspheres.

Methods

Peripheral blood and urine samples were obtained from two clinical studies. Patient and in vitro experiment samples were analyzed using inductively coupled plasma mass spectrometry (ICP-MS), gamma-ray spectroscopy, light microscopy, Coulter particle counting, and high-performance liquid chromatography (HPLC).

Results

The median percentage holmium compared to the total amount injected into the hepatic artery was 0.19% (range 0.08–2.8%) and 0.32% (range 0.03–1. 8%) in the 1h blood plasma and 24h urine, respectively. Both the blood plasma and urine were correlated with the neutron irradiation exposure required for [^{166}Ho]Ho-AcAc-PLLA microsphere production (ρ=0.616, p=0.002). After a temporary interruption of the phase 2 clinical study, the resuspension medium was replaced to precipitate [^{166}Ho]Ho^{3} pre-administration using phosphate. The in vitro near-maximum neutron irradiation experiments showed significant [^{166}Ho]Ho-AcAc-PLLA microsphere damage.

Conclusion

The amount of holmium in the peripheral blood and urine samples after [^{166}Ho]Ho-AcAc-PLLA microsphere intrahepatic infusion was low. A further decrease was observed after reformulation of the resuspension solution but minimization of production damage is necessary.

INTRODUCTION

Radioembolization using microspheres containing yttrium-90 (^{90}Y) injected directly into the hepatic artery delays the progression of liver malignancies.[1,2] The addition of [^{90}Y]Y-resin radioembolization to fluoropyrimidine-based chemotherapy was found to significantly improve median progression-free survival in the liver by 7.9 months in patients with metastatic colorectal cancer.[3] Furthermore, in patients with primary liver cancer, ^{90}Y-labelled resin radioembolization was better tolerated than targeted therapy with the tyrosine kinase inhibitor sorafenib.[4] However, to date, no survival benefit has been established in phase 3 studies.[3–7]

[^{166}Ho]Ho-acetylacetonate-poly(L-lactic acid) microspheres ([^{166}Ho]Ho-AcAc-PLLA microspheres) have been studied in patients with liver malignancies of various origins as an option for improving the dosimetry for more personalized treatment.[8–13] ^{166}Ho differs in its decay from ^{90}Y. ^{166}Ho emits therapeutic beta-particles of 1.77 MeV and 1.85 MeV and it has a physical half-life of 26.8 hrs. In contrast, ^{90}Y has a longer physical half-life of 64.0 hrs. and it emits higher energy therapeutic beta-particles (2.28 MeV). Holmium distribution can be imaged with magnetic resonance imaging (MRI) or single photon emission computed tomography (SPECT) due to the low energy 81keV gamma emission.[8–10,14] ^{90}Y has no gamma emission, but it can be detected using Bremsstrahlung-emission SPECT and positron emission tomography (PET), because of the low level of positron emission.[15]

The present study, aimed to assess the stability of [^{166}Ho]Ho-AcAc-PLLA microspheres used for radioembolization in a clinical setting. Therefore, blood and urine samples of patients from the Holmium Embolization Particles for Arterial Radiotherapy (HEPAR) phase 1 and phase 2 studies were analyzed. Furthermore, the effect of the changed composition of the resuspension medium on the [^{166}Ho]Ho-AcAc-PLLA microspheres was also analyzed

METHODS

Ho-AcAc-PLLA microspheres preparation

The preparation of Ho-AcAc-PLLA microspheres was previously described.[16–18] In brief, 10 g of $HoCl_3.6H_2O$ (Metall Rare Earth Ltd., Shenzhen, China) was dissolved in 100 mL of sterile water (Fresenius Kabi, Bad Homburg, Germany). This solution was then added to a solution containing 180 g of acetylacetone (Sigma-Aldrich Chemie N.V., Zwijndrecht, The Netherlands) and 1080 mL of sterile water, pH 8.5 (adjusted with NH_4OH, Spruyt Hillen, IJsselstein, the Netherlands) and homogenized by stirring for 1 min. Subsequently, Ho-AcAc crystals were formed after the solution stood at room temperature for 15 hrs. After washing the Ho-AcAc crystals three times with sterile water, they were air-dried at 50 °C for 48 hrs. The Ho-AcAc crystals (10 g) and PLLA (6 g) (Purac Biochem, Gorinchem, the Netherlands) were then

dissolved in chloroform (186 g) (Merck, Darmstadt, Germany) and were added to a 1.0 L of 2% polyvinylalcohol solution (PVA) (Sigma-Aldrich Chemie N.V., Zwijndrecht, The Netherlands). The chloroform of this oil-in-water emulsion was evaporated under continuous stirring (IKA Eurostar power digi-visc stirrer) in baffled beakers using a nitrogen flow at 25 °C for 40–72 hrs. No residual chloroform could be detected in the microspheres after neutron irradiation.[16] The resulting Ho-AcAc-PLLA microspheres were washed three times with 0.1 Mol/L HCl (Merck, Darmstadt, Germany) and three times with sterile water, they were then sieved to obtain the desired size of 15–60 μm using an electronic sieve vibrator (TOPAS EMS755, Dresden, Germany) and an ultrasonic processor (Hielscher UP200S, Teltow, Germany). Finally, the Ho-AcAc-PLLA microspheres were air-dried (50 °C, 24–48 h) and vacuum dried (70 °C, 7 hrs.)."

Neutron irradiation

The Ho-AcAc-PLLA microspheres were neutron irradiated in a nuclear reactor (thermalflux: $1.4–1.8 \times 10^{20}$ neutrons $m^{-2}h^{-1}$, Reactor Institute Delft, Delft, The Netherlands). This resulted in holmium-166 and small amounts of holmium-166^{m} due to the thermal neutron cross sections of 64 barn and 3.1 barn, respectively.[17] A typical neutron irradiation of 540 mg Ho-AcAc-PLLA microspheres with a thermal neutronflux of 1.6×10^{20} neutrons $m^{-2}h^{-1}$ for 4.0 hrs. leads to approximately 10.0 GBq [^{166}Ho]Ho-AcAc-PLLA microspheres and 1.3 kBq [^{166m}Ho]Ho-AcAc-PLLA microspheres at the end of neutron irradiation. The relatively small amount of ^{166m}Ho with a physical half-life of 1200 years was considered negligible both in patients and in waste.

Sterility and apyrogenicity

The equipment used for preparing the Ho-AcAc-PLLA microspheres were steam sterilized at 121 °C for 30 min. at the Central Sterilization Department of the University Medical Center Utrecht. Furthermore, preparation was carried out in a class-D clean room (Ph. Eur., 2002), and it consisted of the following germ-reducing steps: boiling of the PVA solution, flushing with filtered (0.22 m HEPA-filter) nitrogen gas over the stirred water/chloroform mixture, washing the microspheres with 0.1 mol/L HCl, and drying them for 5 hrs. at 70 °C under a vacuum condition.[18]

After preparation of the Ho-AcAc-PLLA microspheres, bioburden and endotoxin tests were conducted for each batch before neutron irradiation to confirm sterility and apyrogenicity using the European Pharmacopoeia 5.0 methods and regulations 2.6.12, 2.6.13 and 2.6.14 (carried out by Bactimm B.V., Nijmegen, The Netherlands).[19] Only the batches that met these requirements were used. During neutron irradiation, the Ho-AcAc-PLLA microsphere samples received an additional excessive gamma dose for final sterilization (>25 kGy) as described previously.[18,20] This samples spiked with Bacillus pumilisspores. Ten samples were neutron irradiated with 0.9×10^{20} thermal neutrons m^{-2} and ten control samples were not neutron irradiated. All samples were tested for bacterial contamination by a certified company and only the neutron irradiated Ho-AcAc-PLLA microspheres were sterile (Bactimm B.V., Nijmegen, The Netherlands).

Quality controls and in vitro experiments

After neutron irradiation [^{166}Ho]Ho-AcAc-PLLA microspheres were resuspended using a medium containing sterile water for injection with ethanol 10% (v/v) and 2% w/v of polyoxyethylene-polyoxypropylene copolymer (Pluronic® F-68, Sigma-Aldrich® Chemie B.V., Zwijndrecht, The Netherlands). The HEPAR 2 study was temporarily halted because of toxicity concerns raised from new animal studies. Clinical outcomes[8,10] and additional SPECT-CT analyses were evaluated and the microspheres were considered to be safe. In addition, brief stability tests using the resuspension medium containing 116 mM phosphate buffer (pH 7.2) and 2% w/v Pluronic® F-68 were performed for these microspheres that are classified as a medical device. The previous, in combination with the desire to provide palliative treatment to these patients, lead to the re-start of the study without extensive and time-consuming new tests.

Batches of both Ho-AcAc-PLLA and [^{166}Ho]Ho-AcAc-PLLA microspheres were visually inspected for irregularities and damage by light microscopy (Eclipse E200 Microscope, Nikon, Japan). In addition, particle size and volume distribution analyses were performed by Coulter counting (Coulter counter III, Beckman, USA). An average diameter of 30 ± 5 μm and a particle volume of >97% between 15 and 60 μm was required.

In additional in vitro experiments the amount ^{166}Ho, Ho and acetylacetonate in the resuspension media was measured at 1, 3, 6 and 24 hrs. to assess the stability. For this, [^{166}Ho]Ho-AcAc-PLLA microspheres were centrifuged for 5 min. at 500 g and the 200 μL taken from the supernatant was centrifuged again for 5 min. at 500g. Subsequently, 150 μL of the supernatant was analyzed for ^{166}Ho, Ho, and AcAc.

Analyses

ICP-MS

All blood plasma and urine samples were digested in twice the sample volume of 65% HNO_3 at room temperature for 3 days and subsequently diluted to 14% (v/v) HNO_3. The Ho content was only determined in the blood plasma, as blood plasma is better digested than whole blood and consequently results in more robust ICP-MS results. Calibration and background samples were digested identically. Blood plasma and urine samples from untreated instead of treated patients were used for standard addition of an ICP-MS holmium standard (Ho_2O_3 in HNO_3 2–3%, Sigma-Aldrich Chemie N.V., Zwijndrecht, The Netherlands). Ho content was determined using a PerkinElmer NEXON 350D ICP-MS (PerkinElmer, Groningen, The Netherlands). A Microflow PFA Nebulizer (PE N8145101) was used for sample introduction into the spray chamber of the ICP-MS. The spray chamber itself was a Quartz Cyclonic spray chamber (PE Revision A, N8145013). Furthermore, the ICP-MS was equipped with a platinum sample cone and a platinum skimmer cone. The NEXION 350D was operating at a forward power of 1600 W and the argon gas flow settings were: plasma gasflow 14L/min., auxiliary gasflow 1.2 L/min. and nebulizer flow 1.1 L/min. Data acquisition was done in standard mode with holmium

measured atm/z 165 and rhodium as an internal standard at m/z 103. The mean difference between calculated standard and ICP-MS measurement in urine and blood plasma was 1.00 ± 0.03% and was used to calculate the final ICP-MS measurements.

Gamma counting

^{166}Ho activity and background were measured using a gamma counter (15 min. per sample, Wizard 3, 1480 automatic Gamma counter, PerkinElmer Life and Analytical Sciences, USA). Calibration was performed using ^{166}Ho samples measured in a validated dose calibrator (VDC-404; Veenstra Instrumenten B.V., Joure, The Netherlands).

High-performance liquid chromatography

High-performance liquid chromatography (HPLC), Thermo Scientific Dionex Ultimate 3000, Thermo Scientific, Waltham, USA) with UV detecting was used to measure acetylacetonate using an Acclaim 120 stainless steel C18 column (120 A, 3 μm, 4.6 × 150 mm). Elution (0.5 mL/min.) was performed using 70% methanol (HPLC grade, VWR International, The Netherlands) and 30% of 0.1% trifluoroacetic acid in H_2O (Biosolve B.V., Valkenswaard, The Netherlands) in 10 min. The retention time of acetylacetonate was 3.7 ± 0.2 min. Calibration samples were prepared 0–1000 mg/L for quantifications (Sigma-Aldrich® Chemie B.V., Zwijndrecht, The Netherlands).

Patient studies

Patients with various liver malignancies were treated by intra-arterial injection of in total 600 mg [^{166}Ho]Ho-AcAc-PLLA microspheres in the HEPAR 1 (NCT01031784) and HEPAR 2 studies (NCT01612325).[8,10] The specific activity of the [^{166}Ho]Ho-AcAc-PLLA microspheres varied because of the dose escalation design HEPAR 1 and the liver size in the HEPAR 2. All patients provided written informed consent. The sample collections were approved also by the Medical Research Ethics Committee of the University Medical Center Utrecht in The Netherlands.

Three intra-arterial injection procedures in the liver were performed per patient. The first two procedures were primarily for safety and treatment optimization reasons, the third one was the actual treatment. First, [^{99m}Tc]Tc-macroaggregates (150 MBq, Technescan LyoMAA, Mallinckrodt Medical B.V, The Netherlands) were injected 1–2 weeks before treatment planning. Secondly, low apparent specific activity [^{166}Ho]Ho-AcAc-PLLA microspheres (250 MBq per 60 mg) were injected prior to the planned treatment the same day. Thirdly, 540 mg therapeutic [^{166}Ho]Ho-AcAc-PLLA microspheres (6.3–24.8 GBq/g) was administrated. After both safety procedures a SPECT-CT was done within 3 hrs., post-treatment SPECT-CT and MRI were carried out within 3–6 days, as described previously.[8,10]

Peripheral blood and urine samples

Blood samples were taken at various timepoints after administration of the therapeutic dose. Urine was cumulatively collected at several time intervals after therapy. 1 mL of whole blood was centrifuged for 10 min. at 500 g to precipitate cells and cell fragments. 0.50 mL of blood plasma was taken for ICP-MS analyses. The ^{166}Ho activity of the blood and urine samples was only measured after the temporary halt of the HEPAR 2 study. In a subgroup of 5 patients, also the ^{166}Ho activity distribution between whole blood and blood plasma was measured in 1, 3, 6 and 24 hrs. samples. The average 64.3% activity in blood plasma of these 20 whole blood samples was used to calculate the blood plasma activities for comparison with ICP-MS measurements.

Statistical analysis

Continuous data are presented as the mean ± standard deviation (SD) if normally distributed and as the median (min–max) if skewed (Shapiro-Wilk test). Categorical data are presented as numbers and proportions. Differences between the treatment characteristics and analytical samples were evaluated by the $\chi 2$ test for categorical data and by the Student's t-test for continuous data if normally distributed. The Mann-Whitney U test was used if the data were skewed. Correlations were evaluated with Pearson (r) if normally distributed or Spearman rank (ϱ) if data were skewed. The data were registered in a dedicated database. The statistical analysis was conducted using IBM SPSS Statistics for Windows, Version 22.0. Armonk, NY: IBM Corp. The significance level was set at $p \leq 0.05$.

RESULTS

In total 23 patients were treated with [^{166}Ho]Ho-AcAc-PLLA microspheres resuspended in 2 mL of 2% Pluronic® F-68 (w/v) in 10% ethanol (v/v). The Ho content of the blood plasma and the urine samples as measured by ICP-MS is presented in Table 3.1 and Figure 3.1. A relatively low amount of Ho was detected in both blood plasma at 1 hr. (median 0.19% of the injected activity; range 0.08–2.8) and cumulative 24 hrs. urine (median 0.32%; range 0.03–1.8). A rapid Ho decrease in both blood plasma and urine was measured over time but Ho remained detectable for up to several months (Table 3.1).

Irradiation of 540 mg Ho-AcAc-PLLA microspheres with a median number of 4.0×10^{20} thermal neutrons/m^2 (range 1.5–8.9) resulted in a median apparent specific activity of 14.4 GBq/g of therapeutic [^{166}Ho]Ho-AcAc-PLLA microspheres at the end of neutron irradiation(range 5.0–28.7). The median time between resuspension and patient administration was 2.0 hrs. (range 0.5–6.0). The median injected activity was 5.2 GBq (range 3.4–11.3). A correlation between the irradiation and the amount of Ho in blood plasma and urine samples

(ϱ=0.57; p<0.01) and (ϱ=0.62; p>0.01), respectively) was detected for up to 24 hrs. (Figure 3.2). In addition, a relation was established between Ho in blood and Ho in urine (ϱ=0.87; p≤0.01).

Table 3.1. Holmium in blood plasma and urine from microspheres resuspended in 10% ethanol

Blood plasma	N	μg/L		%	
	(of total)	Median	(Min–Max)	Median	(Min–Max)
1 hr.	8 (15)	57.0	(33.0–529.8)	0.19	(0.08–2.81)
3 hrs.	21 (23)	63.4	(2.1–935.0)	0.15	(0.00–2.43)
6 hrs.	22 (23)	46.0	(1.3–626.5)	0.14	(0.01–1.63)
24 hrs.	21 (23)	18.8	(0.5–259.8)	0.06	(0.00–0.60)
48 hrs.	13 (15)	7.1	(0.3–59.6)	0.02	(0.00–0.18)
7 weeks	15 (15)	1.4	(0.1–26.5)	0.00	(0.00–0.08)
13 weeks	13 (15)	1.7	(0.3–13.2)	0.01	(0.00–0.04)
Urine	N	μg		%	
	(of total)	Median	(Min – Max)	Median	(Min–Max)
0–3 hrs.	18 (23)	110.7	(12.1–892.4)	0.13	(0.01–1.19)
3–6 hrs.	22 (23)	88.0	(1.4–692.6)	0.08	(0.00–0.72)
6–24 hrs.	23 (23)	67.7	(3.2–469.0)	0.07	(0.00–0.54)
24–48 hrs.	15 (15)	20.1	(0.7–114.4)	0.02	(0.00–0.10)
7 weeks	15 (15)	5.3	(2.6–19.2)	0.01	(0.00–0.02)
13 weeks	15 (15)	4.5	(1.6–18.3)	0.01	(0.00–0.02)
Cumulative 0–24 hrs.	23 (23)	340.5	(25.4–1437)	0.32	(0.03–1.80)

The median percentage of the infused amount of Ho as determined by ICP-MS in blood plasma and urine from patients treated with [^{166}Ho]Ho-AcAc-PLLA microspheres resuspended in 10% ethanol (v/v) 2% Pluronic® F-68. N: number, %: percentage of injected amount.

After substitution of the resuspension medium, a total of 30 patients were treated with [^{166}Ho]Ho-AcAc-PLLA microspheres resuspended in 2 mL of 2% Pluronic® F-68 (w/v) in 116 mM phosphate pH 7.2. The median number of thermal neutrons and resuspension time were 5.4 × 10^{20} neutrons/m^2 (range 3.2–9.1) and 1.8 hr (range 0.2–8.4), respectively, resulting in a median apparent specific activity of 18.7 GBq/g (range 10.9–28.7) at the end of irradiation. The median injected activity was 6.4 GBq (range 5.0–13.2). The median blood plasma values at 1h and cumulative urinary 24h excretion were 0.09% (range 0.00–0.61) and 0.06% (range 0.01–0.40) of the injected activity, respectively (Table 3.2 and Figure 3.1). This was a significant decrease (p<0.05) in comparison with the previously used re-suspension medium.

The ^{166}Ho content was measured in the last 30 patients (Table 3.3). The median blood plasma values at 1 hr. and cumulative urinary 24 hrs. excretion were 0.003% (range 0.000–0.032) and 0.003% (range 0.000–0.022) of the injected activity, respectively. A significant correlation was observed between the injected activity and the percentage of Ho and ^{166}Ho in the 24 hrs. cumulative urine (ϱ=0.38; p=0.04 and ϱ=0.60; p<0.01), respectively. In the blood, a trend was observed between the injected activity and both the Ho and ^{166}Ho content at 1, 3, 6 and 24 hrs. The mean ratio between Ho and ^{166}Ho was 0.03 ± 0.03 in blood and 0.39 ± 0.27 in urine; both ratios were significantly different from 1.0 (p<0.01), so no equilibrium existed between both isotopes.

Table 3.2. Holmium in blood plasma and urine from microspheres resuspended in 116mM phosphate.

Blood plasma	N	µg/L		%	
	(of total)	Median	(Min–Max)	Median	(Min–Max)
1 hrs.	29 (30)	27.8	(0.0–219.8)	0.087	(0.000 –0.606)
3 hrs.	29 (30)	10.8	(0.8–379.8)	0.035	(0.000 –1.220)
6 hrs.	29 (30)	15.8	(0.0–239.8)	0.046	(0.003 –0.609)
24 hrs.	25 (30)	16.8	(0.0–229.8)	0.049	(0.000 –0.571)
Urine	N	µg		%	
	(of total)	Median	(Min–Max)	Median	(Min –Max)
0–3 hrs.	27 (30)	8.0	(0.0–123.9)	0.008	(0.000–0.120)
3–6 hrs.	36 (30)	3.0	(0.1–68.2)	0.004	(0.000–0.066)
6–24 hrs.	30 (30)	15.6	(0.0–129.9)	0.015	(0.000–0.126)
0–24 hrs.	30 (30)	60.1	(12.0–415.4)	0.059	(0.011–0.403)

The median amount of Ho as determined by ICP-MS in blood plasma and urine of patients treated with [^{166}Ho]Ho-AcAc-PLLA microspheres resuspended in 116 mM phosphate 2% Pluronic® F-68 pH 7.2. N: number, %: percentage of injected amount

Quality control analyses of especially the highest neutron irradiated [^{166}Ho]Ho-AcAc-PLLA microspheres for patients showed that the change of resuspension media to phosphate buffered solution altered the microscopic appearance (data not shown). The visual analysis revealed damage consisting of small fragments and, occasionally, dented surfaces. In comparison with the ethanol-containing resuspension medium, the phosphate buffered solution contained additional $HoPO_4$ precipitates both at the [^{166}Ho]Ho-AcAc-PLLA microsphere surface and in the resuspension medium. This was confirmed by the occasionally strongly increased number of small particles, as determined by particle size distribution analysis (Figure 3.3). The maximum small particle volume was within pre-set limitations (0–3% v/v) for use in clinical trials, and subsequently, these therapeutic doses were administrated.

To verify these observations in vitro, [^{166}Ho]Ho-AcAc-PLLA microspheres were analyzed using a previously used near-maximum neutron irradiation of 8.9×10^{20} m^{-2} thermal neutrons and incubation times of 1, 3, 6 and 24 hrs. (Table 3.4). The visual analysis of these [^{166}Ho]Ho-AcAc-PLLA microspheres revealed similar damage to those used for study patients. After near-maximum irradiation, the mean cumulative leakage of ^{166}Ho and Ho at 1 hr. after resuspension in a 2% Pluronic® F-68 (w/v) 10% ethanol (v/v) medium was as high as 15.7 ± 1.7% and 15.0 ± 2.5%, respectively (Table 3.4). Furthermore, the leakage increased with longer incubation time. The use 2% Pluronic® F-68 (w/v) in 116 mM phosphate pH 7.2 medium resulted in the decreased supernatant presence of ^{166}Ho and Ho to 0.09 ± 0.01% and 0.18 ± 0.14%, respectively (Table 3.4). Control experiments showed complete precipitation of [^{166}Ho]Ho^3 in the 116 mM phosphate pH 7.2 resuspension medium, in contrast to its supernatant presence when using 2% Pluronic® F-68(w/v) 10% ethanol (v/v).

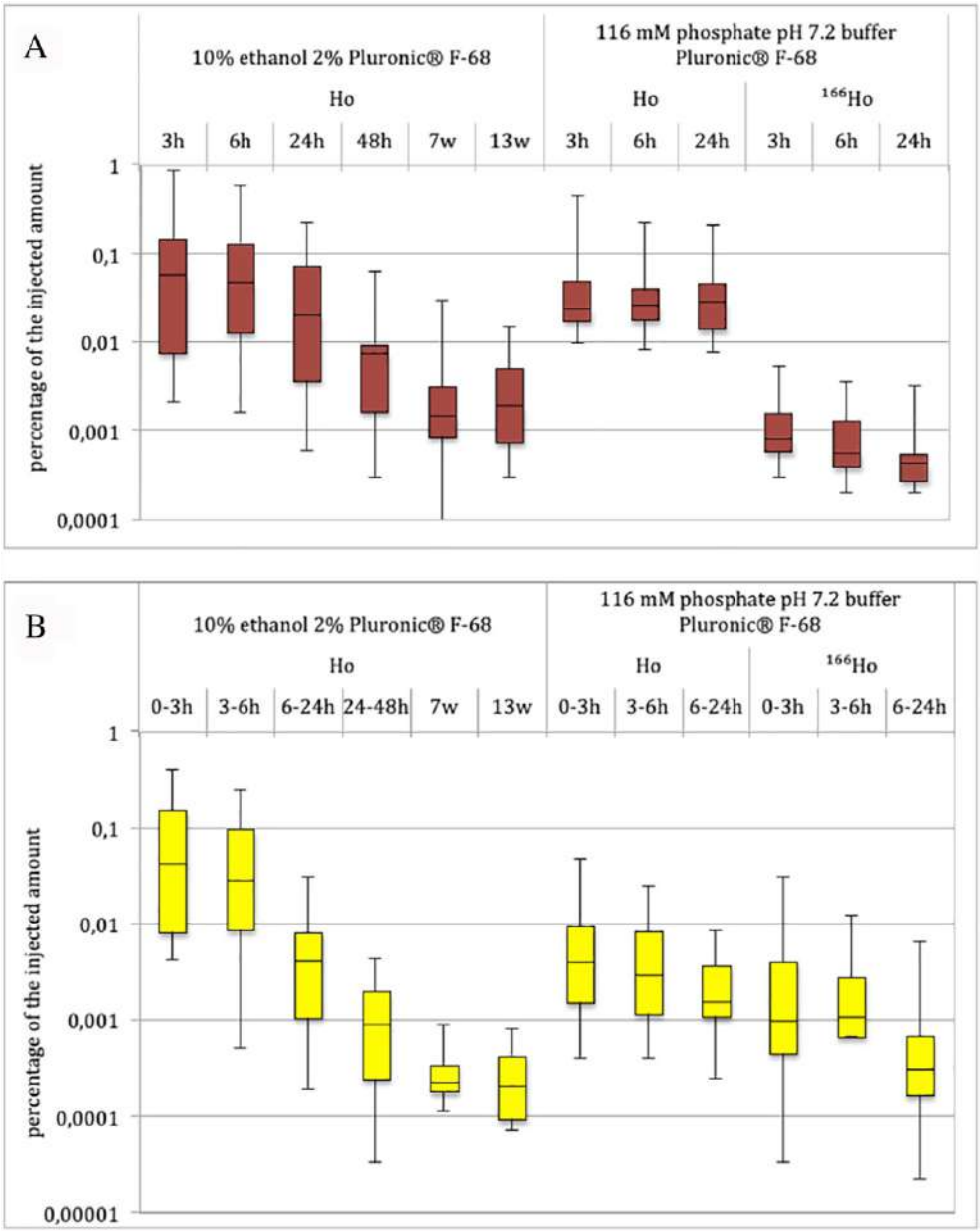

Figure 3.1. *Amounts of Ho and ^{166}Ho in blood plasma (A) and urine (B) of patients treated with [^{166}Ho]Ho-AcAc-PLLA microspheres as the percentage of the injected amount. The number of measurements is represented in Tables 3.1–3.3.*

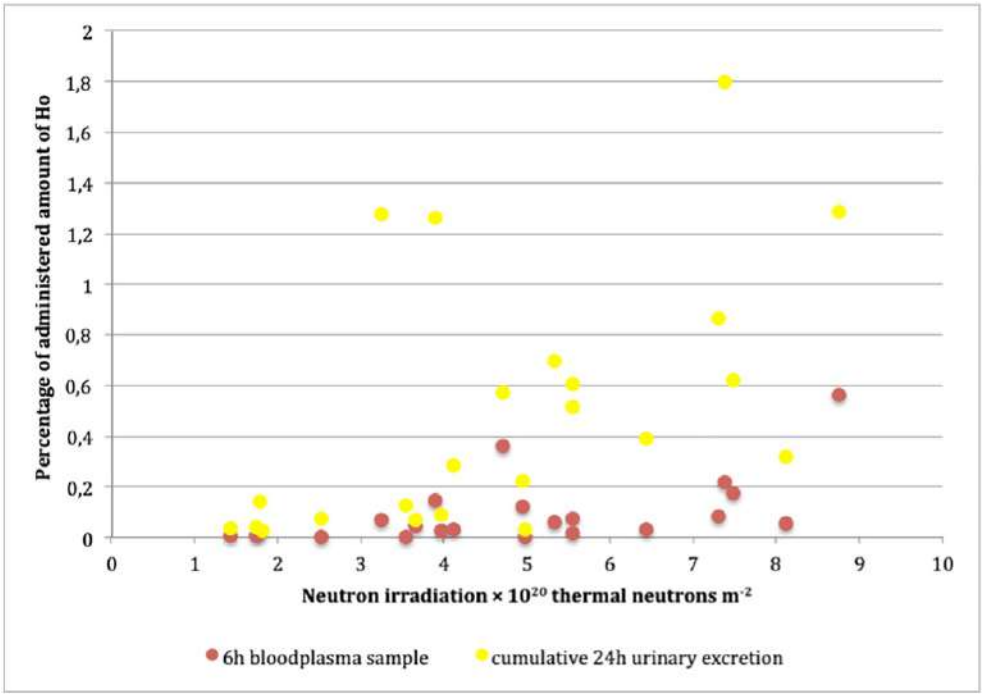

Figure 3.2. *Scatterplot showing the influence of neutron irradiation on the amount of holmium-165 in blood plasma (red dots) and urine (yellow dots) of patients (n=23) treated with [^{166}Ho]Ho-AcAc-PLLA microspheres resuspended in 10% ethanol (v/v) 2% Pluronic® F-68.*

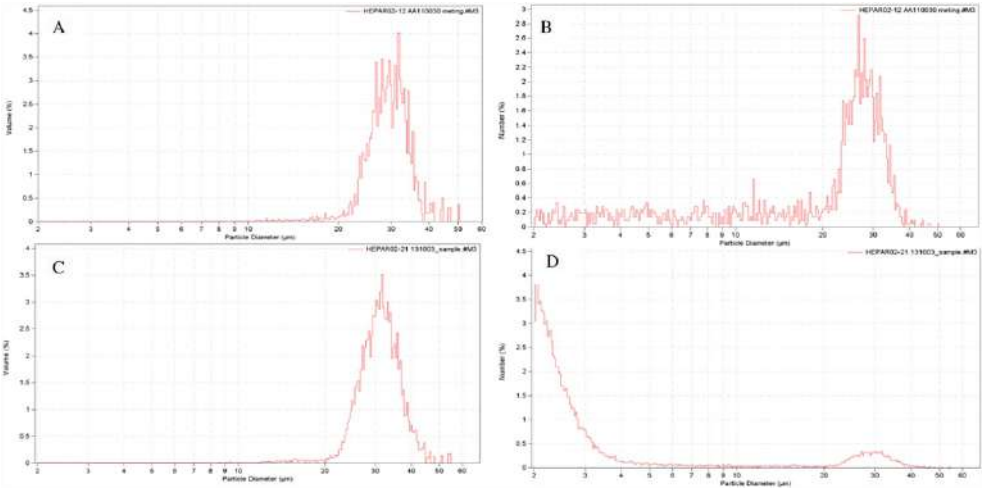

Figure 3.3. *Size distribution plots of [^{166}Ho]Ho-AcAc-PLLA microspheres after irradiation. Size distribution plots of [^{166}Ho]Ho-AcAc-PLLA microspheres after approximately 8.9×10^{20} m^{-2} thermal neutrons and 1 h in suspension showing the difference in size distribution. (A, B) [^{166}Ho]Ho-AcAc-PLLA microspheres in the 10% ethanol and (C, D) 116 mM phosphate pH 7.2 buffered solution. Showing a similar particle volume (A, C) but a difference in particle size distribution with a large amount of small holmium phosphate particles (B, D).*

A yellowish discoloration of both media was already observed within 1h after resuspension. HPLC analysis showed acetylacetonate leakage corresponding to 3.0–10.0% of the total amount initially incorporated in the [^{166}Ho]Ho-AcAc-PLLA microspheres (Table 3.4). In addition, at least one other absorption peak was detected but the probable presence of radiolytic leachables was not investigated in further detail (data not shown).

Table 3.3. Holmium-166 blood plasma and urine from microspheres resuspended in 116mM phosphate

Blood plasma	N	Bq/mL		%	
	(of total)	Median	(Min–Max)	Median	(Min–Max)
1 hr.	25 (30)	34.8	(5.7–573.1)	0.003	(0.000–0.032)
3 hrs.	26 (30)	23.7	(6.7–213.6)	0.003	(0.001–0.017)
6 hrs.	26 (30)	16.0	(4.1–105.5)	0.002	(0.006–0.011)
24 hrs.	23 (30)	9.5	(2.4–30.8)	0.001	(0.006–0.010)
Urine	N	kBq		%	
	(of total)	Median	(Min–Max)	Median	(Min–Max)
0–3 hrs.	25 (30)	175.1	(3.8–6867)	0.003	(0.000–0.090)
3–6 hrs.	23 (30)	156.4	(1.6–2274)	0.003	(0.000–0.036)
6–24 hrs.	25 (30)	171.1	(14.8–1211)	0.005	(0.000–0.024)

The median amount and range of ^{166}Ho as measured by gamma detection in blood plasma and urine of patients treated with [^{166}Ho]Ho-AcAc-PLLA microspheres resuspended in 116 mM phosphate pH 7.2, 2% Pluronic® F-68. N: number, %: percentage of total injected activity calculated to the time of injection.

DISCUSSION

The HEPAR 1 and 2 studies were the first clinical experiences with ^{166}Ho radioembolization. The blood and urine samples were part of the study design to investigate the in vivo stability of [^{166}Ho]Ho-AcAc-PLLA microspheres. The total amount of holmium in the blood plasma and urine samples for both resuspension fluids used was relatively low and declined quickly over time (Tables 3.1–3.3, Figure 3.2). These relatively low blood and urine measurements are consistent with reported results from ^{166}Ho-SPECT, performed three to seven days after therapy.[8,10,14] Up to 13 weeks after treatment, small amounts of Ho were detected in the blood and urine samples (Table 3.2). Therefore, the release appears to be biphasic consisting of a rapid initial phase and a slower phase. The latter phase could be due to slow in vivo biodegradation of the microspheres as previously reported.[20–22]

The neutron irradiation of [^{166}Ho]Ho-AcAc-PLLA microspheres was correlated with the amount of Ho and ^{166}Ho in the collected blood plasma and urine samples (Figure 3.1). This damage is probably caused by gamma heating (free radicals from gamma radiation plus a temperature increase) and fast neutrons.[20,23,24] Concerns about the stability of [^{166}Ho]Ho-AcAc-PLLA microspheres and the absence of a chemical equilibrium between ^{166}Ho and Ho were raised during the clinical HEPAR 2study, resulting in a temporary halt. In other words, thermal neutron capture causes ^{166}Ho recoil that can release from the acetylacetonate complex, and ^{166}Ho decay causes reactive oxygen species during incubation in a resuspension medium.[25–27]

Therefore, ^{166}Ho was also measured after resuming the HEPAR 2 study, because this is more important than Ho from a toxicity point of view, as a median lethal dose of 560 mg/kg for non-radioactive holmium was reported in rodents.[28]

Table 3.4. Release from microspheres in supernatant in two different media

Time	10% ethanol			116 mM phosphate pH 7.2 buffer		
	166Ho	Ho	AcAc	166Ho	Ho	AcAc
1 hr.	15.7 (1.7)	15.0 (2.5)	3.0 (0.2)	0.09 (0.01)	0.18 (0.14)	3.1 (1.2)
3 hrs.	28.6 (5.5)	24.8 (4.4)	6.8 (0.1)	0.11 (0.14)	0.47 (0.21)	4.4 (1.1)
6 hrs.	40.2 (4.0)	30.2 (3.3)	8.1 (3.4)	0.04 (0.05)	0.09 (0.03)	4.1 (0.9)
24 hrs.	50.0 (4.4)	34.0 (1.0)	10.0 (3.3)	0.08 (0.07)	0.18 (0.01)	7.9 (3.9)

Mean (n=3) percentages of ^{166}Ho, Ho and acetylacetonate in the supernatant after centrifugation of [^{166}Ho]-Ho-AcAc-PLLA microspheres in two different media. Mean (SD) amounts of ^{166}Ho, Ho and acetylacetonate in the supernatant after resuspension and two times centrifuging of [^{166}Ho]Ho-AcAc-PLLA microspheres in the resuspension media containing 2% Pluronic® F-68, and 10% ethanol or 116 mM phosphate pH 7.2 buffer after relative long neutron irradiation of 8.9 × 10^{20} thermal neutrons m^{-2}. AcAc: acetylacetonate only, no radiolytic products.

Different ^{166}Ho and Ho amounts in the blood and urine samples suggested no equilibrium and a different biological behavior of their chemical forms (Tables 3.2–3.3). To study this in more detail, in vitro analyses were made after near-maximum neutron irradiation conditions were executed (Table 3.4). The higher amount of ^{166}Ho compared to Ho in the 10% ethanol buffer could be the result of the recoil of ^{166}Ho and the release from the acetylacetonate complex.[25–27] In addition, HPLC showed acetylacetonate release (Table 3.4). The lower detected amount of acetylacetonate in vitro compared to Ho and ^{166}Ho is most likely due to radiolysis, which is extensively described in the literature.[29] At least one other unknown irradiation-induced compound was detected which could be methyl acetonate, monomeric lactate or lactide, which may explain the yellowish discoloration. Similar results were found for neutron irradiated [^{166}Ho]Ho-AcAc microspheres which showed disintegration and high [^{166m}Ho]Ho^3 releases after incubation in water for injection.[30]

In hindsight, the use of the 10% ethanol and 2% Pluronic® F-68 solution was suboptimal. The reason for using this solution was the tendency to aggregation of the hydrophobic [^{166}Ho]Ho-AcAc-PLLA microspheres after neutron irradiation, which could lead to obstructions in the catheter or an undesirable biodistribution. The 10% ethanol and 2% Pluronic® F-68 solution was implemented to improve the solubility and wettability of the [^{166}Ho]Ho-AcAc-PLLA microspheres just before the start of the clinical studies, but after the previous stability studies.[31] The earlier reported stability of [^{166}Ho]Ho-AcAc-PLLA microspheres was studied in vitro using phosphate buffered saline. This probably influenced the interpretation of the results, as discrimination between [^{166}Ho]$HoPO_4$ precipitate and [^{166}Ho]Ho-AcAc-PLLA microspheres was not shown.[21,32,33] Indeed, holmium precipitates after use of the phosphate-containing resuspension medium (Table 3.4). However, separation of the [^{166}Ho]$HoPO_4$ precipitates from [^{166}Ho]Ho-AcAc-PLLA microspheres resuspended in 116 mM phosphate buffered saline could only be distinguished indirectly using size distribution analysis and light microscopy.

Ho^{3} can also form precipitates/nanocolloids with blood components such as phosphate and albumin. A first pass effect/phagocytosis by the reticuloendothelial system (RES) in the liver could be an explanation for the limited detection of holmium in blood and urine and for high, but varying liver detection and distribution on ^{166}Ho-SPECT-CT and Ho-MRI scans, especially after long irradiation times.[14] Other speculations for retention in the liver in such cases are decreased blood flow after embolization and high local concentrations of phosphates in the tumor regions due to necrosis.[34]

Pharmacokinetic analyses in this study were limited by the number and timing of the blood samples and cumulative urine collection. This was done for pragmatic reasons such as multiple administrations and logistics like transport from the intervention room to the ward. Earlier sampling, for example, at 5, 15 and 30 min., as performed in chemoembolization, would be of interest especially, because a fast initial release is suspected.[35] Furthermore, the cancer type and burden of disease could be of influence as it is a known variable in the hepatopulmonary shunt fraction. For example, the [^{99m}Tc]Tc-macroaggregates hepatopulmonary shunt fraction in metastases from colorectal cancer and hepatocellular cancers appears to be higher as compared to breast cancer. Also, patients with compression or tumor thrombosis of a major portal vein branch have higher degrees of shunting than patients with normal portal vein perfusion.[36] The tumor to liver parenchyma ratio could also influence their distribution to the blood.

The quality of the product [^{166}Ho]Ho-AcAc-PLLA microspheres can be improved by minimization of the neutron irradiation damage. The use of additional gamma ray shielding during irradiation or a different neutron irradiation source could be used to decrease the damage, although the sterilization purpose should be kept in mind as well.[37] In addition, other matrices especially inorganic ones, whether or not they are combined with afterloading, could be considered to ease product characterization and to increase the time for transportation and logistics.[18,30,38–42]

Finally, the product characteristics were somewhat different for each patient treatment in the HEPAR 1 and 2 studies. Therefore, a constant number of 6.6×10^{20} neutrons m^{-2} thermal neutrons and fixed logistics were chosen for new patient studies. In conclusion, holmium amounts in peripheral blood and urine samples were low in all patients after intra-arterial injection of [^{166}Ho]Ho-AcAc-PLLA microspheres. A further decline of holmium amounts in blood and urine samples was detected after the reformulation of the re-suspension solution, but neutron irradiation induced production damage should be minimized.

CONFLICT OF INTEREST

M.G.E.H. Lam is trainer and speaker on Quirem/Terumo sponsored events and consultant for BTG.

B.A. Zonnenberg holds patents related to holmium microspheres, which are assigned to University Medical Center Utrecht Holding B.V. He receives honoraria from GSK Netherlands and consulted for, received research funding from and had expenses reimbursed by Novartis pharm Inc.

The department of Radiology and Nuclear Medicine of the UMC Utrecht receives royalties and research funding from Quirem Medical B.V. and Terumo.

ACKNOWLEDGEMENTS

The authors would like to acknowledge Dr. J.F.W. Nijsen and Dr. A.D. van het Schip for their contributions in product management and study designs, and G. van Bemmel and B. Aolad-si Mhammad for their help with analyses and data management. R.C. Bakker is funded by the Dutch Cancer Society research grant: 2014–7075.

REFERENCES

1. Wang EA, Broadwell SR, Bellavia RJ, Stein JP. Selective internal radiation therapy with SIR-spheres in hepatocellular carcinoma and cholangiocarcinoma. J Gastrointest Oncol 2017;8:266–78.
2. Lee EW, Alanis L, Cho SK, Saab S. Yttrium-90 selective internal radiation therapy with glass microspheres for hepatocellular carcinoma: current and updated literature review. Korean J Radiol 2016;17:472–88.
3. Wasan HS, Gibbs P, Sharma NK, Taieb J, Heinemann V, Ricke J, et al. First-line selective internal radiotherapy plus chemotherapy versus chemotherapy alone in patients with liver metastases from colorectal cancer (FOXFIRE, SIRFLOX, and FOXFIRE-global): a combined analysis of three multicentre, randomised, phase 3 trials. Lancet Oncol 2017;1159–71.
4. Vilgrain V, Bouattour M, Sibert A. Selective internal radiation therapy is better toler-ated compared to sorafenib, but does not increase overall survival in patients withHCC. Int Liver Congr 2017;GS0–12:6–8.
5. van Hazel GA, Heinemann V, Sharma NK, Findlay MPN, Ricke J, Peeters M, et al. SIRFLOX: randomized phase III trial comparing first-line mFOLFOX6 (plus orminus bevacizumab) versus mFOLFOX6 (plus or minus bevacizumab) plus selectiveinternal radiation therapy in patients with metastatic colorectal cancer. J Clin Oncol 2016;34:1723–31.
6. Sharma R, Wasan H, Van Hazel G, Heinemann V, Sharma N, Taieb J, et al. Overall survival analysis of the FOXFIRE prospective randomized studies of first-line selectiveinternal radiotherapy (SIRT) in patients with liver metastases from colorectal cancer. J Clin Oncol 2017;35:3507.
7. Chow PHW, Gandhi M. Phase III multi-Centre open-label randomized controlled trial of selective internal radiation therapy (SIRT) versus sorafenib in locally advanced hepatocellular carcinoma: the SIRveNIB study. J Clin Oncol 2017;35:4002.
8. Smits MLJ, Nijsen JFW, van den Bosch MAAJ, Lam MGEH, Vente MAD, Mali WPTM, et al. Holmium-166 radioembolisation in patients with unresectable, chemorefractory liver metastases (HEPAR trial): a phase 1, dose-escalation study. Lancet Oncol 2012;13:1025–34.
9. van den Hoven AF, Prince JF, Bruijnen RCG, Verkooijen HM, Krijger GC, Lam MGEH, et al. Surefire infusion system versus standard microcatheter use during holmium-166 radioembolization: study protocol for a randomized controlled trial. Trials 2016;17:520.
10. Prince JF, van den Bosch MAAJ, Nijsen JFW, Smits MLJ, van den Hoven AF, Nikolakopoulos S, et al. Efficacy of radioembolization with holmium-166 microspheres in salvage patients with liver metastases: a phase 2 study. J Nucl Med 2018;59:582–5888.
11. Kunnen B, van der Velden S, Bastiaannet R, Lam MGEH, Viergever MA, de Jong HWAM. Radioembolization lung shunt estimation based on a ^{90}Y pretreatment procedure: a phantom study. Med Phys 2018;45:4744–53.
12. Garin E, Rolland Y, Pracht M, Le Sourd S, Laffont S, Mesbah H, et al. High impact of macroaggregated albumin-based tumor dose on response and overall survival in hepatocellular carcinoma patients treated with 90Y-loaded glass microsphere radioembolization. Liver Int 2017;37:101–10.
13. Lam MGEH, Goris ML, Iagaru AH, Mittra ES, Louie JD, Sze DY. Prognostic utility of 90Yradioembolization dosimetry based on fusion 99mTc-macroaggregated albumin-99mTc-sulfur colloid SPECT. J Nucl Med 2013;54:2055–61.
14. Smits MLJ, Elschot M, van den Bosch MAAJ, van de Maat GH, van het Schip AD, Zonnenberg BA, et al. In vivo dosimetry based on SPECT and MR imaging of ^{166}Ho-microspheres for treatment of liver malignancies. J Nucl Med 2013; 54:2093–100.
15. Elschot M, Vermolen BJ, Lam MGEH, de Keizer B, van den Bosch MAAJ, de Jong HWAM. Quantitative comparison of PET and Bremsstrahlung SPECT for imagingthe in vivo yttrium-90 microsphere distribution after liver radioembolization. PLoSOne 2013;8:e55742.
16. Zielhuis SW, Nijsen JFW, Dorland L, Krijger GC, van het Schip AD, Hennink WE. Removal of chloroform from biodegradable therapeutic microspheres by radiolysis. Int J Pharm 2006;315:67–74.
17. Squair PL, Pozzo L, Ivanov E. Neutron activation of microspheres containing 165 Ho:theoretical and experimental radionuclidic impurites study. Int Nucl Atl Conf; 2011.
18. de Azevedo MBM, de Melo VHS, Soares CRJ, Miyamoto DM, Katayama RA, Squair PL,et al. Development and characterisation of polymeric microparticle of poly(d,l-lacticacid) loaded with holmium acetylacetonate. J Microencapsul 2018;35:281–91.
19. European Directorate for the Quality of Medicines & HealthCare (EDQM); 2008.
20. Vente MAD, Nijsen JFW, de Roos R, van Steenbergen MJ, Kaaijk CNJ, Koster-Ammerlaan MJJ, et al. Neutron activation of holmium poly(L-lactic acid) microspheres for hepatic arterial radioembolization: a validation study. BiomedMicrodevices 2009;11:763–72.
21. Bult W, De Leeuw H, Steinebach OM, Van Der Bom MJ, Wolterbeek HT, Heeren RMA,et al. Radioactive holmium acetylacetonate microspheres for interstitial microbrachytherapy: an in vitro and in vivo stability study. Pharm Res 2012;29:827–36.

22. Mumper RJ, Ryo UY, Jay M. Neutron-activated holmium-166-Poly(L-lactic acid) microspheres: a potential agent for the internal radiation therapy of hepatic tumors. J Nucl Med 1991;32:2139–43.
23. Nijsen JFW, Zonnenberg BA, Woittiez JRW, Rook DW, Swildens-Van Woudenberg IA,Van Rijk PP, et al. Holmium-166 poly lactic acid microspheres applicable for intra-arterial radionuclide therapy of hepatic malignancies: effects of preparation andneutron activation techniques. Eur J Nucl Med 1999;26:699–704.
24. Mumper RJ, Jay M. Poly(L-lactic acid) microspheres containing neutron-activatable holmium-165: a study of the physical characteristics of microspheres before and after irradiation in a nuclear reactor. Pharm Res 1992;9:149–54.
25. Zeisler SK, Weber K. Szilard-Chalmers effect in holmium complexes. J Radioanal Nucl Chem 1998;227:105–9.
26. Nassan L, Achkar B, Yassine T. Production of ^{166}Ho and ^{153}Sm using hot atom reactions in neutron irradiated tris(cyclopentadienyl) compounds. Nukleonika 2011;56:263–7.
27. Zhernosekov KP, Filosofov DV, Rösch F. The Szilard-Chalmers effect in macrocyclic ligands to increase the specific activity of reactor-produced radiolanthanides: exper-iments and explanations. Radiochim Acta 2012;100:669–74.
28. Haley J, Koste L, Komesu N. Pharmacology and toxicology erbium of chlorides'.Tox App Pharm 1966;8:37–43.
29. Dondi D, Merli D, Pretali L, Buttafava A, Faucitano A. Detailed analytical study of ra-diolysis products of simple organic compounds as a methodological approach to investigate prebiotic chemistry—part 2. Radiat Phys Chem 2011;80:408–13.
30. Arranja AG, Hennink WE, Denkova AG, Hendrikx RWA, Nijsen JFW. Radioactive holmium phosphate microspheres for cancer treatment. Int J Pharm 2018;548:73–81.
31. Zielhuis SW, Nijsen JFW, Figueiredo R, Feddes B, Vredenberg AM, Van Het Schip AD,et al. Surface characteristics of holmium-loaded poly(L-lactic acid) microspheres. Biomaterials 2005;26:925–32.
32. Zielhuis SW, Nijsen JFW, Krijger GC, van het Schip AD, Hennink WE. Holmium-loaded poly(L-lactic acid) microspheres: in vitro degradation study. Biomacromolecules 2006;7:2217–23.
33. Zielhuis SW, Nijsen JFW, De Roos R, Krijger GC, Van Rijk PP, Hennink WE, et al. Production of GMP-grade radioactive holmium loaded poly(L-lactic acid) microspheresfor clinical application. Int J Pharm 2006;311:69–74.
34. Howard S, Jones D, Pui C. The tumor lysis syndrome. N Engl J Med 2011;364:1844–54.
35. Guiu B, Schmitt A, Reinhardt S, Fohlen A, Pohl T, Wendremaire M, et al. Idarubicin-loaded ONCOZENE drug-eluting embolic agents for chemoembolization of hepato-cellular carcinoma: in vitro loading and release and in vivo pharmacokinetics. J Vasc Interv Radiol 2015;26:262–70.
36. Powerski MJ, Erxleben C, Scheurig-Münkler C, Geisel D, Heimann U, Hamm B, et al. Hepatopulmonary shunting in patients with primary and secondary liver tumors scheduled for radioembolization. Eur J Radiol 2015;84:201–7.
37. Burgio N, MacIocco L, Abbas K, Simonelli F,Santagata A, Buono S, et al. Experimental results of an accelerator-driven neutron activator for medical radioisotope production. IEEE Trans Nucl Sci 2011;58:445–50.
38. Brown RF, Lindesmith LC, Day DE. ^{166}Holmium-containing glass for internal radiotherapy of tumors. Nucl Med Biol 1991;18:783–90.
39. Hosseini SH, Enferadi M, Sadeghi M. Dosimetric aspects of ^{166}Ho brachytherapy biodegradable glass seed. Appl Radiat Isot 2013;73:109–15.
40. Costa RF, Azevedo MBM, Nascimento N, Sene FF, Martinelli JR, Osso Junior JA. Production of microspheres labeled with holmium-166 for liver cancer therapy: the preliminary experience at IPEN/CNEN-SP (Ina 2009 Int Nucl Atl Conf Innov NuclTechnol a sustain futur Brazil). 41 (INIS) 2009;1–8.
41. Subramanian S, Vimalnath KV, Dash A. Preparation and preliminary in vivo evaluation of ^{166}Ho-labeled microspheres for possible usein radioembolic therapy of liver cancer. J Label Compd Radiopharm 2018;61:509–14.
42. Marcon L, Gehan H, Khoshnevis M, Marmuse L, Carozzo C, Louis C, et al. Synthesis of highly-loaded holmium-165 siloxane particles for brachytherapy of brain cancer and injectability evaluation in healthy pig. J Nanomed Nanotechnol 2017;8.


4

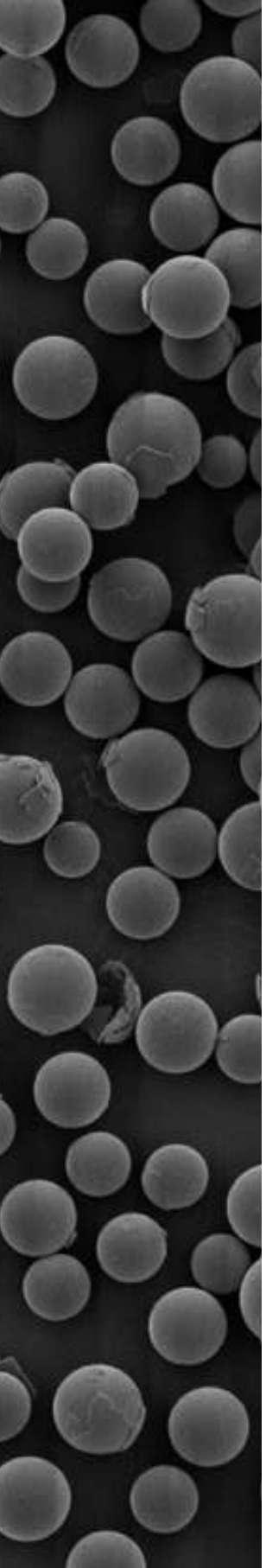

Intra-tumoral injection of radioactive holmium (^{166}Ho) microspheres for treatment of oral squamous cell carcinoma in cats

S.A. van Nimwegen

R.C. Bakker

J. Kirpensteijn

R.J.J. van Es

R. Koole

M.G.E.H. Lam

J.W. Hesselink

J.F.W. Nijsen

Veterinary and Comparative Oncology 2017

Nimwegen SA, Bakker RC, Kirpensteijn J, Es RJJ, Koole R, Lam MGEH, Hesselink JW, Nijsen JFW. **Intratumoral injection of radioactive holmium (^{166}Ho) microspheres for treatment of oral squamous cell carcinoma in cats**. Vet Comp Oncol 2018;16:114–124.

ABSTRACT

Introduction

A "microbrachytherapy" was developed as treatment option for inoperable tumors by direct intra-tumoral injection of radioactive holmium-166 (^{166}Ho) microspheres. ^{166}Ho emits beta-radiation which potentially enables a high, ablative, radioactive-absorbed dose on the tumor tissue while sparing surrounding tissues.

Methods

Safety and efficacy of ^{166}Ho microbrachytherapy were evaluated in a prospective cohort study of 13 cats with inoperable oral squamous cell carcinoma without evidence of distant metastasis.

Results

Local response rate was 55%, including complete response or partial response (down-staging) enabling subsequent marginal resection. Median survival time was 113 days overall, and 296 days for patients with local response. Side effects were minimal. Tumor volume was a significant predictor of response.

Discussion

Response rate may be further improved by optimizing the intra-tumoral spatial distribution of ^{166}Ho-microspheres.

Conclusion

^{166}Ho microbrachytherapy has potential as a minimally invasive, single procedure radio-ablation treatment of unresectable tumors with minimal morbidity.

INTRODUCTION

Oral squamous cell carcinoma (OSCC) is the most common oral malignancy in cats and humans.[1,2] In humans, OSCC accounts for approximately 200,000 (2.7%) of all new cancer cases and 100,000 deaths worldwide annually.[3] The incidence of OSCC has increased with 1.8% per year between 1989 and 2011.[4] This is probably because of the increased prevalence of tobacco abuse, alcohol consumption and slaked lime or betel nut chewing, which are the major risk factors for developing OSCC in humans.[4,5] The etiology of OSCC in felines remains largely unknown. Advanced age, indirect tobacco smoke, poor oral hygiene and papillomavirus exposure are possible risk factors.[5–7] Apart from the resemblance of risk factors, human and feline OSCC also share comparable molecular parameters (eg, overexpression of epidermal growth factor receptor, Vascular Endothelial Growth Factor and p53 mutation). Furthermore, OSCC has comparable biological and histological characteristics (eg, tumor growth and metastasis), as well as their response to therapy.[8] OSCC, is commonly located in the gingiva with invasion of underlying bone. In cats and humans, OSCC is also frequently located in the tongue; ventral in cats and lateral in humans.[9]

Feline OSCC (FOSCC) is, therefore, an optimal and most relevant translational animal model to study various new treatment modalities before their application in humans. The survival of both veterinary and human patients with OSCC mainly depends on the stage of the disease at time of diagnosis. In humans, stage I and II carcinomas, still confined to the primary site, are treated by surgical resection and adjuvant radiotherapy on indication, with a 5-year survival rate of 80–90%. However, only 30–50% of the patients present with this stage. For advanced (stage III–IV) carcinomas, the 5-year survival rate drops to approximately 45%.[10] Despite medical advancements, only limited improvements in survival have been achieved for humans with OSCC over the last decades and curative-intent surgery with ≥1 cm margin remains the most effective therapy for both humans and animals with OSCC. However, morbidity of surgical treatment is high for stage II or higher disease, urging the need for new treatment modalities for OSCC.

Treatment-related loss of tongue functions severely decreases the quality of life in both humans (speech, swallowing) and felines (feeding and grooming). In cats, the diagnosis of OSCC is commonly made in an advanced stage of the disease. Consequently, surgery is considered impossible or unethical in most cases. Surgery is only considered in a very select group of cats with small, localized tumors. Effectiveness of palliative radiation protocols (consisting of 3–6 sessions of 6–10 Gy) and stereotactic radiation is low in felines with response rates of 39% or less and median overall survival (OS) times of 60 to 106 days.[11–13] More recently, several case series of accelerated hypofractionated radiotherapy protocols with or without chemotherapy and/or surgery suggest improved survival outcomes of 86 to 163 days.[14–17] However, these are intensive treatment protocols that require multiple anesthetic interventions and are accompanied by considerable costs and therapy-induced morbidity, with 91% overall complication rate and

up to 78% grade III oral mucositis.[12,14] Chemotherapy, tyrosine kinase inhibitors and immunotherapy alone have not achieved durable responses in macroscopic FOSCC.[18,19]

Holmium-166 (^{166}Ho) loaded microspheres are radioactive microspheres with a diameter of 10 to 30 μm that emit beta-radiation (E_β, max = 1.84MeV, $t_{1/2}$ = 26.8 hours) which has a mean tissue penetration depth of 2.1 mm and a maximum tissue penetration of 8.7 mm. The combination of a localized intra-tumoral microsphere application with the short beta-penetration depth enables a high, tumor-ablative radiation-absorbed dose in a single treatment, without causing extensive collateral damage to surrounding tissues. Furthermore, ^{166}Ho also emits a small fraction of gamma-radiation (6.71%, 80.6 keV) and can be visualized using nuclear Single-photon emission computed tomography (SPECT). In addition, ^{166}Ho can also be observed using Computed Tomography (CT) because of its high density, and with magnetic resonance imaging (MRI) because of its unique paramagnetic properties.[20–23] These qualities provide an excellent opportunity for in vivo multimodality imaging, enabling treatment guidance and monitoring.

In human patients, ^{166}Ho-microspheres are currently used in an intra-arterial transcatheter radio-embolization treatment of metastatic liver cancer.[22] Radio-embolization of small head and neck tumors is technically more demanding with the risk of unintended retrograde flow of particles into the carotid artery and into the brain that may result in serious complications including hemiparesis or even death.[24, 25] To overcome these obstacles, a direct intra-tumoral injection approach has been proposed for FOSCC. This concept of intra-tumoral injection of ^{166}Ho-microspheres, also referred to as ^{166}Ho microbrachytherapy, has been investigated in laboratory animals and veterinary patients with spontaneous cancers. In these in vivo studies, renal cell carcinoma-bearing mice, Vx2 tumor bearing rabbits and feline patients with spontaneous liver tumors were treated with ^{166}Ho microbrachytherapy. In these studies, it was shown that extremely high tumor-absorbed doses could be attained (in excess of 6 times the absorbed dose that can be achieved with external beam radiotherapy) without major associated side effects.[26] ^{166}Ho microbrachytherapy can therefore potentially be a safe and effective treatment option for both human and veterinary patients with head and neck cancer for whom no other treatment options are available.[26–28]

The objective of this study was to prospectively evaluate safety and efficacy of ^{166}Ho microbrachytherapy in cats with spontaneous unresectable FOSCC. Therefore, a pilot study and subsequent dose reduction study were performed in feline patients.

METHODS

Patient selection

All cats with FOSCC referred to the Department of Clinical Sciences of Companion Animals, Utrecht University, The Netherlands, between July 2009 and July 2015 were considered potentially eligible to participate in a prospective cohort study on ^{166}Ho microbrachytherapy. Inclusion criteria were: diagnosis of FOSCC confirmed by histology, a tumor not amenable for surgical therapy with curative-intent because of tumor size and location, localized tumor disease suitable for manual needle injections, no detectable metastasis (locoregional and/or distant), and no life-threatening comorbidities or diseases with a life expectancy of <3 months or a deteriorated state requiring intensive care. The owners were invited to participate in the study after having received detailed information in both oral and written form concerning the treatment protocol, costs associated with work-up and hospital admission, expected risk of complications and restrictions because of radiation safety procedures. The treatments were performed in compliance and under supervision of the radiation safety officer of the Utrecht University radiation protection unit.

Diagnosis and staging

Baseline characteristics including breed, age, weight and tumor location were recorded. Each patient received a standardized staging procedure consisting of oral inspection, tumor inspection, palpation and manual evaluation of tumor size using 3-dimensional caliper measurements under general anesthesia. Contrast-enhanced CT imaging of the primary tumor (head), locoregional lymph nodes (neck), thorax and abdomen was performed to determine tumor size, invasion in surrounding tissues, bone involvement and possible metastasis. The tumor volume was calculated using the 3 longest perpendicular diameters as measured on CT, assuming an ellipsoid shape; tumor volume = π / 6 × Length × Width × height.

Any regional lymph node that was enlarged or abnormal on CT image was examined for metastasis by cytology of an ultrasound guided fine needle aspiration biopsy. Tumor stage was determined according to the World Health Organization Tumor, Node, Metastasis (TNM) system for classification of oral tumors in domestic animals.[29] In addition, a complete blood count, blood biochemistry and urine analysis were performed to screen for subclinical disorders.

Patient preparation

A treatment date was planned within 2 weeks. In case of a large exophytic growing malignancy partial laser debulking was performed with a 1064 nm Nd:YAG laser (Medilas 40 N, MBB-Medizintechnik GmbH, München, Germany) with bare optical fiber (600 μm diameter; Ultraline, Heraeus LaserSonics, Milpitas, California) for immediate reduction of clinical signs of gross tumor. Tumors with a mainly infiltrative growth pattern were not amenable for surgical debulking. Tumor volumes and dosimetry calculations were based on residual tumor volume in case of debulking prior to ^{166}Ho microbrachytherapy.

To ensure maximal patient comfort and reduce radiation dose to nursing personnel the following provisions were made prior to the ^{166}Ho microbrachytherapy. All feline patients received an esophageal feeding tube to ensure adequate food intake in case of anorexia because of pain or discomfort after treatment. The cats received prophylactic antibiotic treatment with a single injection of the long-acting antibiotic, cefovecin sodium (Convenia Zoetis B.V., Louvain-la-Neuve, Belgium). During treatment and hospitalization, all patients received buprenorphine (15 μg/kg 4dd by intramuscular injection, Buprecare, AST Farrma B.V., Oudewater, the Netherlands) and meloxicam (0.05 mg/kg by subcutaneous injection or through feeding tube, after an initial dose of 0.1 mg/kg by subcutaneous injection, Metacam, Boehringer Ingelheim Vetmedica GmbH, Ingelheim/Rhein, Germany) for at least 7 days after ^{166}Ho microbrachytherapy.

Microsphere preparation

The ^{166}Ho-microspheres were prepared as previously described.[28,30] After neutron activation, ^{166}Ho-microspheres were suspended in a solution with Pluronic F-68 (Sigma-Aldrich Chemie B.V., Zwijndrecht, The Netherlands) 2% wt./vol solution. The ^{166}Ho-microspheres were suspended by gentle agitation and repeatedly drawing up and down with a syringe. Subsequently, aliquots of 0.3–0.4 mL were drawn up in 1 mL Luer taper syringes.

The amount of radioactivity present in each syringe was measured in a dose calibrator (VDC-404; Veenstra Instrumenten B.V., Joure, The Netherlands). Each syringe was placed into an acrylic glass cylinder to limit beta-radiation exposure of personnel, especially to the hands, during dose preparation and administration. The treatment was conducted with a fixed quantity of 200 mg of ^{166}Ho-microspheres. The required activity needed for a given tumor treatment was obtained by varying the neutron activation time of the microspheres.

Dosimetry

After selecting the planned tumor-absorbed dose for a certain tumor ("dose cohort", see later), the accompanying ^{166}Ho activity was determined based on tumor volume according to the following equation: $D = A \times 15.87 / W$

In which D = tumor-absorbed dose (in Gray [joules/kilogram]); A= ^{166}Ho activity in MBq; ^{166}Ho-specific tissue dose conversion coefficient = 15.87 mJ/MBq; W = tumor weight in grams. Assumed tumor tissue density was 1.0 g/cm^3.[31] Tumor-absorbed dose is based on a homogeneous distribution of the injected ^{166}Ho-microspheres over the tumor. Furthermore, the tumor margin and its transition to normal surrounding tissue were carefully treated with ^{166}Ho microbrachytherapy. As a result, the "treatment volume" was determined to be 1.5 × the tumor volume as measured on CT images. In addition, extra activity was ordered to account for anticipated losses of ^{166}Ho-microspheres during suspension and syringe preparation, and during the administration procedure (residual ^{166}Ho-microspheres remaining in the syringes after intra-tumoral injections and possible spillage outside of the tumor).[27]

Pilot study

Initially, the treatment was started in a pilot setting (n=5) using a relatively high ^{166}Ho activity, aiming for a tumor-absorbed dose of 400 to 800 Gy. This relatively high-tumor dose was chosen to overcome possible focal low-absorbed dose areas in the tumor because of inhomogeneous ^{166}Ho-microspheres distribution and peritumoral deposition of ^{166}Ho-microspheres. Based on previous pilot experiments,[26, 27] a "loss" of >50% of ^{166}Ho-microspheres was expected during treatment due to possible leakage of ^{166}Ho-microspheres out of the tumor needle tracts and premature settling and accumulation of ^{166}Ho-microspheres in the syringe and needle dead space. A substantial additional loss of ^{166}Ho-microspheres was anticipated during the process of microsphere suspension and preparation of the syringes for treatment. As a result, a double amount of radioactivity needed for the aimed tumor-absorbed dose was ordered for the pilot treatments. Subsequent analysis of the safety and observed efficacy in this pilot indicated that the applied procedures resulted in a higher than anticipated tumor-absorbed dose of >800 Gy. Therefore, the total anticipated loss of activity was adjusted to 50% of the activity needed for the intended treatment dose for further treatments. Furthermore, the study was continued as a minimal effective dose study to comply with the "As Low As Reasonably Achievable" (ALARA) principles of radiation safety guidelines, as described in the next section.

Dose reduction study

A dose reduction study approach was added to obtain data of possible dose-related side effects and minimal effective dose. Subsequent feline patients were randomly placed in 1 of 2 cohorts: a low dose cohort of 200 Gy (n=4) and an intermediate dose cohort of 400 Gy (n=4), to be compared with the initial high-dose cohort of >800 Gy of the pilot study (n=5).

Treatment procedure

The administration procedure was performed under general anesthesia with endotracheal intubation in a dedicated radionuclide facility of our department. Patients were prepared by Povidone Iodine of the tumor location and oral cavity. To aid in a homogenous intra-tumoral absorbed dose distribution and to prevent skipping parts of the tumor, the ^{166}Ho-microspheres injections were orderly divided over predetermined equal tumor segments. The number of syringes was based on tumor volume. The injected volume was 0.3–0.6 mL per 1 mL tumor.

The activity of the prepared syringes was measured before the injection procedure. ^{166}Ho-microspheres suspensions in the prefilled syringes for intra-tumoral injection were gently shaken before administration, to ensure a homogeneous suspension. The ^{166}Ho microbrachytherapy was administered through 22G*1.5" or 22G*2.0" needles under gradual retraction of the needle tip from the center towards the periphery of the tumor segments. Injection positions were separated by ≤6 mm to reduce the chance of inadequate local overlap of dose distributions. After the procedure, the radioactivity of the syringes, needles, and all potentially contaminated disposable materials such as gloves and gauzes were measured in the dose calibrator. The total

injected dose was calculated by subtracting the measured ^{166}Ho activity in materials from the pretreatment syringe measurements, adjusted for decay at the time of measurement.

Directly after the procedure, anterior-posterior and lateral planar scintigraphy images were obtained (Philips SKYLight, Medium-energy General-purpose Collimator) to rule out any unwanted systemic distribution (lungs or intestines) and/or contamination after ^{166}Ho microbrachytherapy.

The patients were housed in a specialized controlled radionuclide ward at the Department of Clinical Sciences of Companion Animals, Utrecht University. Patients were discharged when dose rate was below the local regulatory limit of 1 μSv/hour at 1 m, which corresponds to a maximum total accumulated dose of 40 μSv for the owner. Owners received specific follow-up radiation safety guidelines for the care of their cat for the first week.

Follow-up

A standard follow-up protocol was used for the first 6 months after treatment, consisting of follow-up examinations at 1 week, and at 1, 2, 4 and 6 months after discharge. During these examinations, tumor response was evaluated under general anesthesia by oral examination and taking manual caliper measurements. A physical exam was performed to evaluate general patient condition, signs of tumor progression or metastasis, and possible radiation complications such as radiation ulcers and bone necrosis. If indicated, additional laboratory investigation or imaging was performed. A CT scan was performed at 1 or 2 months if residual tumor could not be accurately measured manually using calipers.

Adverse events were scored according to the Veterinary Radiation Therapy Oncology Group VRTOG.[32] Adverse events were classified by the investigational team according to the suspected relation to the treatment with ^{166}Ho microbrachytherapy into none, unlikely, possible, likely and definitive, based on causal relationship.

In addition to the planned 6-month follow-up protocol, all patients were reviewed until death, at any time in case of suspected side effects or recurrences. Long-term follow-up data of potential side effects, disease recurrence or metastasis, survival and cause of death were recorded for all patients.

Response

Response to therapy was categorized using the following criteria: Local Control, being complete response (CR) or partial response (PR) with sufficient tumor volume reduction enabling subsequent marginal tumor resection (i.e., excision at or just beyond the visual tumor edge; Figure 4.3). Local Failure, in which local tumor control was not achieved, irrespective of initial volume reduction (PR).

OS was defined as the time from first ^{166}Ho microbrachytherapy treatment until subsequent death. Local disease progression free survival (LDPFS) was defined as the time from first ^{166}Ho microbrachytherapy treatment until the first clinical signs of local recurrence or progression.

Statistical analysis

Continuous data are presented as the mean SD if normally distributed and as the median and interquartile range (IQR; Q1−Q3) if skewed (Shapiro-Wilk test). Categorical data are presented as numbers and proportions. Differences between the demographic and treatment characteristics of the patients with response or failure were evaluated by the χ^2 test for categorical data and by the Student's T test for continuous data if normally distributed. The Mann-Whitney U test was used if the continuous data were skewed. The 1-way analysis of variance was used to determine whether there were any statistically significant differences between the dose cohorts. The survival analysis was performed with the Kaplan-Meier method and the baseline characteristic compared by the log-rank tests or Cox hazard for continuous variables. For analyses of treatment efficacy, the periprocedural deaths unrelated to the treatment were excluded. The data were registered in a dedicated database. The statistical analysis was conducted using SPSS 21. A power analysis was not performed. The significance level was set at $p \leq 0.05$.

RESULTS

Patients

Thirteen feline patients with FOSCC were enrolled in the ^{166}Ho microbrachytherapy study between July 2009 and July 2015 with follow-up until February 2016 (Table 4.1). There were 8 male and 5 female patients, with a mean age of 14.3 ± 2.0 years and a mean body weight of 4.6 ± 1.1 kg. The tumors were located ventrally in the tongue/frenulum/sublingual (n=10), the gingiva of the mandible (n=1) or maxilla (n=2). Eleven patients had clinical stage T2 disease, 1 T1 and 1 T3. Bone involvement was seen in 2 patients (Patients 5 and 6) with a tumor located in the maxillary gingiva. Enlarged lymph nodes, cytologically free from tumor, were observed in 5 patients. The mean tumor volume was 3.17 ± 1.70 cm^3 with a range of 0.94 to 6.1 cm^3. Two patients (Patients 7 and 12) with a tumor of the tongue, underwent laser surgery debulking of the tumor before intra-tumoral ^{166}Ho microbrachytherapy. During this laser treatment, the tumor volume was decreased by approximately 80% (patient 7) and 50% (patient 12). Three

patients (Patients 2, 9 and 13) received laser surgery resection after an initial PR of their lingual SCC to the ^{166}Ho microbrachytherapy treatment. Two patients (Patients 1 and 2), received a second ^{166}Ho microbrachytherapy for tumor residue/recurrence after an initial complete and PR (Table 4.1).

Treatment procedure

The ^{166}Ho-microspheres were divided over 3 to 11 aliquots depending on the tumor volume. The fraction of administered activity was 59.8 ± 17.6% of the prepared activity for injection. The administered amount of activity for the High (>800 Gy), Intermediate (400 Gy) and Low (200 Gy) dose group were 377 ± 172 MBq, 135 ± 96 MBq and 63 ± 50 MBq, respectively. The absorbed doses for the High (>800 Gy), Intermediate (400 Gy) and Low (200 Gy) dose group were 1,216 Gy (925–2,725), 440 ± 178 Gy and 168 ± 71 Gy, respectively. Post procedure scintigraphy revealed distant activity of ^{166}Ho-microspheres in the lungs of two patients (Patients 12 and 13). The mean hospital stay was 5.1 ± 1.6 days.

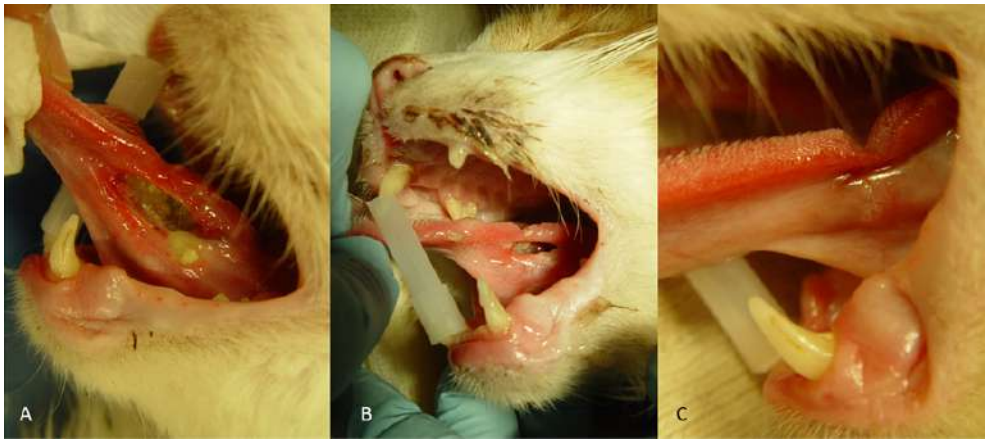

Figure 4.1. *(Patient number 1) A: Tumor at presentation. B: Tumor 4 weeks after first holmium treatment. C: Result after 9 weeks (local control).*

Subsequent treatments

Additional laser ablation was performed in 5 cats: prior to ^{166}Ho microbrachytherapy in 2 cats (Patients 7 and 12) and after a PR in 3 cats (Patients 2, 9 and 13). In total, 2 patients (Patients 1 and 2) received a second treatment with ^{166}Ho microbrachytherapy after 4.5 and 2.5 months, respectively, because of tumor recurrence after an initial complete and PR. These 2 patients had residual tumor volumes of 0.2 and 0.92 cm^3 and received a second dose of 5,400 and 1,088 Gy, respectively. This second treatment resulted in a CR in Patient 1. In Patient 2, the initial ^{166}Ho microbrachytherapy resulted in a 23% tumor volume reduction. The residual lesion was reduced in size by removing approximately 70% of the remaining protruding mass using laser surgery 5 weeks after the initial ^{166}Ho microbrachytherapy. However, local recurrence developed caudal to the initial lesion and a second ^{166}Ho microbrachytherapy treatment was performed 10 weeks

after the first ^{166}Ho microbrachytherapy. This second ^{166}Ho microbrachytherapy did not result in a measurable response. One month later, the tumor was excised by amputation of the rostral 70% of the tongue. The cat became dependent on esophageal tube feeding and intensive grooming care by the owners. It lived free of tumor for another 144 days before the owners decided to let the cat be euthanized because it was still unable to eat or drink without assistance.

Response and survival

Eleven of 13 patients were discharged from the veterinary hospital and followed up for tumor response. Two animals that died within 1 week of ^{166}Ho microbrachytherapy were not included in the response and survival analysis. The maximum tumor response was evaluated approximately 2 weeks after treatment. It often resulted in (temporary) improved quality of life, such as improved eating, drinking and grooming activity and a less inflamed aspect of the lesion. However, if an initial partial tumor response did not lead to a situation of local control (i.e. enabled surgical resection) that case was considered a local failure. For example: Patient 4 had an initial 57% tumor volume reduction 2.5 weeks after ^{166}Ho microbrachytherapy but was still unresectable. This tumor showed a rapid tumor volume increase 2 weeks later.

Local control: CR (n=3) and PR (n=3) with a sufficient size reduction that enabled subsequent marginal laser excision were obtained in 6 of 11 patients (55%) after the initial ^{166}Ho microbrachytherapy. The mean tumor volume decrease was 83 ± 22% in the 6 responders. Three of 11 patients (27%) (Patients 1, 3 and 6) had a CR after a single intra-tumoral ^{166}Ho microbrachytherapy. One patient (Patient 1) had a small local recurrence after 3 months for which a second treatment was curative (Figure 4.1).

A PR was obtained in 3 patients. Subsequent marginal resection was performed in 2 patients with laser surgery and resulted in a LDPFS of 113 and 132 days. Figure 4.3 depicts a typical case of tumor downstaging and subsequent marginal laser excision. The third cat (Patient 2) that underwent laser debulking and a second ^{166}Ho microbrachytherapy, lived despite a near-total glossectomy for 8 months with a relatively good quality of life. Five animals had no objective response (stable disease or progressive disease).

The median OS was 113 (63–341) days. The median LDPFS was 70 (44–123) days. The median OS was better if a local control was achieved: 296 (148–676) vs. 63 (52–72) days ($P<0.01$) (Figure 4.4). In addition, the LDPFS was better if a local control was achieved 123 (87–640) vs. 32 (22–57) days ($P<0.01$). The cause of death after hospital discharge was OSCC-related in 81% (9/11) of the patients. One patient (Patient 3) died after 15 months because of pulmonary metastasis with no evidence of local recurrence. Eight patients had local recurrences or progression of residual disease during follow-up. One cat (patient 1) died of progressive kidney failure after 1 year without signs of local recurrence and 1 patient (Patient 6) is still alive after 1304 days.

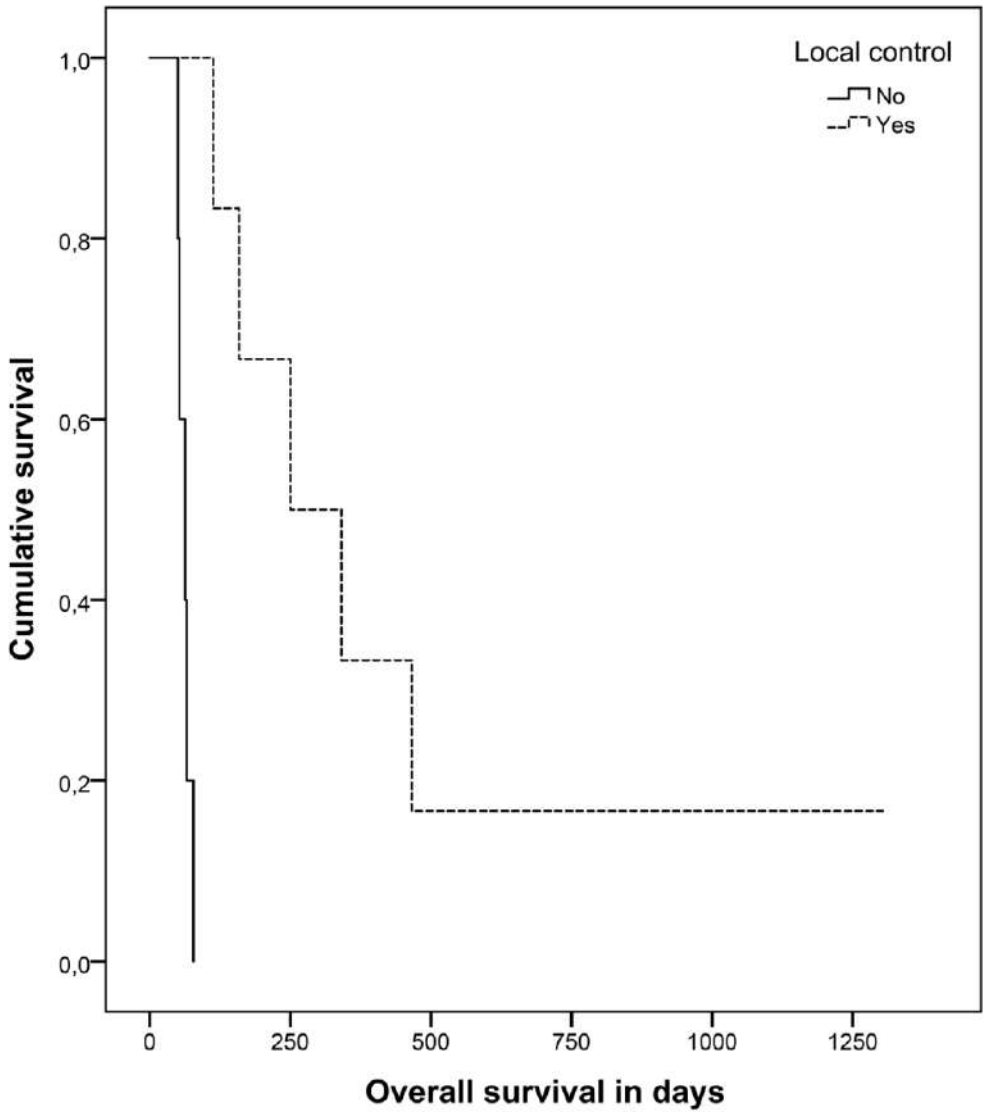

Figure 4.2. *Overall survival. Kaplan-Meier analysis of the overall survival of cats in which local control was obtained (median survival 296 interquartile range (IQR) 148–676 days) vs. cats where no local control was obtained (median survival 63 IQR 52–72 days; p<0.01).*

Tumor volume prior ^{166}Ho microbrachytherapy was significantly smaller in responders compared with non-responders, 1.9 ± 1.0 vs. 4.2 ± 1.7 cm^3 (T-test p=0.028), and was a predictor of LDPFS with a hazard ratio of 1.9, 95% CI (1.0–3.3), p=0.038. No relationship between the absorbed dose and survival could be demonstrated. The median survival for the 200, 400 and >800 Gy cohort was 53, 159 and 250 days, respectively (log-rank p=0.21).

Complications and adverse events

None of the patients was lost to follow-up. During the study, 3 serious adverse events occurred. One was defined as "definitely related" to the ^{166}Ho microbrachytherapy and occurred after treatment of a small superficial tumor in the mandibular gingiva. A localized radiation ulcer developed at the surface of the tongue in the area adjacent to the treated tumor. It healed within 3 weeks with minimal supportive wound care.

Two patients died during the hospitalization period. One cat (Patient 6) developed kidney failure within 1 week after the procedure. This severe adverse event was classified as unlikely related to ^{166}Ho microbrachytherapy. This complication was probably related to a combination of poor physical condition, anesthesia and non-steroidal anti-inflammatory drugs intoxication.

The other cat (Patient 12) died while under anesthesia for the treatment procedure. This severe adverse event was classified as possibly related to ^{166}Ho microbrachytherapy. Post-mortem SPECT imaging of the thorax of this cat revealed the presence of ^{166}Ho activity in the lung region, and at the autopsy, microspheres were detected in the capillaries of the lung. Radiation damage was considered an unlikely cause of morbidity because of the short time frame between the treatment and death. No microspheres were detected in the trachea or bronchi, which argue against inhalation. Acute pulmonary arterial embolization after accidental intravenous injection of ^{166}Ho-microspheres could be a possible explanation for this complication. However, the calculated 99 mg ^{166}Ho-microspheres that was injected during the ^{166}Ho microbrachytherapy procedure in this patient was divided over 5 syringes that were each used to inject 3 to 4 ^{166}Ho-microspheres depots. Therefore, accidental intravenous injection of large amounts of-microspheres was not likely. Furthermore, ^{166}Ho activity was also found in the lung region after ^{166}Ho microbrachytherapy in one other patient in this study (Patient 13) without clinical signs during the follow-up period. Quantitative scintigraphy imaging, using SPECT-CT to enable correction of the scintigraphic images for local radiation attenuation from surrounding tissues, was not performed in this study. However, the fraction of activity in the lungs can be roughly estimated from the available scans using the recorded counts in the lung region and tumor region. This resulted in an estimated deposition of 30% of administered ^{166}Ho-microspheres in the lung region of Patient 13 without complications after treatment. In comparison, an estimated 21% of administered ^{166}Ho-microspheres was detected in the lung region of the cat (Patient 12) that died during the procedure.

A more probable cause for the death of this cat was an anesthetic complication. The cat underwent multiple consecutive procedures in different locations (esophageal feeding tube placement in anesthesia induction room, laser debulking in OR and ^{166}Ho microbrachytherapy in the radionuclide facility) during a single anesthetic period under propofol maintenance and spontaneous breathing. Especially during the ^{166}Ho microbrachytherapy anesthetic monitoring might have been insufficient, resulting in hypoxia from apnea that was not recognized on time.

A laser surgery-related complication occurred in 2 patients: a small unilateral rostral portion of the tongue, several centimeters rostral of the mid-ventral tumor location, became necrotic and was lost (Figure 4.2). This complication developed shortly after laser surgery and was seemingly independent of ^{166}Ho microbrachytherapy in both patients. Loss of a small portion of the tongue was discovered 11 days after laser debulking, prior to ^{166}Ho microbrachytherapy in Patient 6. Acute necrosis with distinct demarcation margin was detected four days after laser surgery of a residual tumor mass in Patient 11. This tumor had decreased 57% in volume after ^{166}Ho microbrachytherapy 16 days earlier without noticeable changes to the tip of the tongue at the time of laser surgery. Therefore, this complication was most likely because of ipsilateral vascular (ie, lingual artery) damage during Nd:YAG laser surgery. The tongue healed within 2 to 3 weeks without apparent functional consequences during follow-up in both cats.

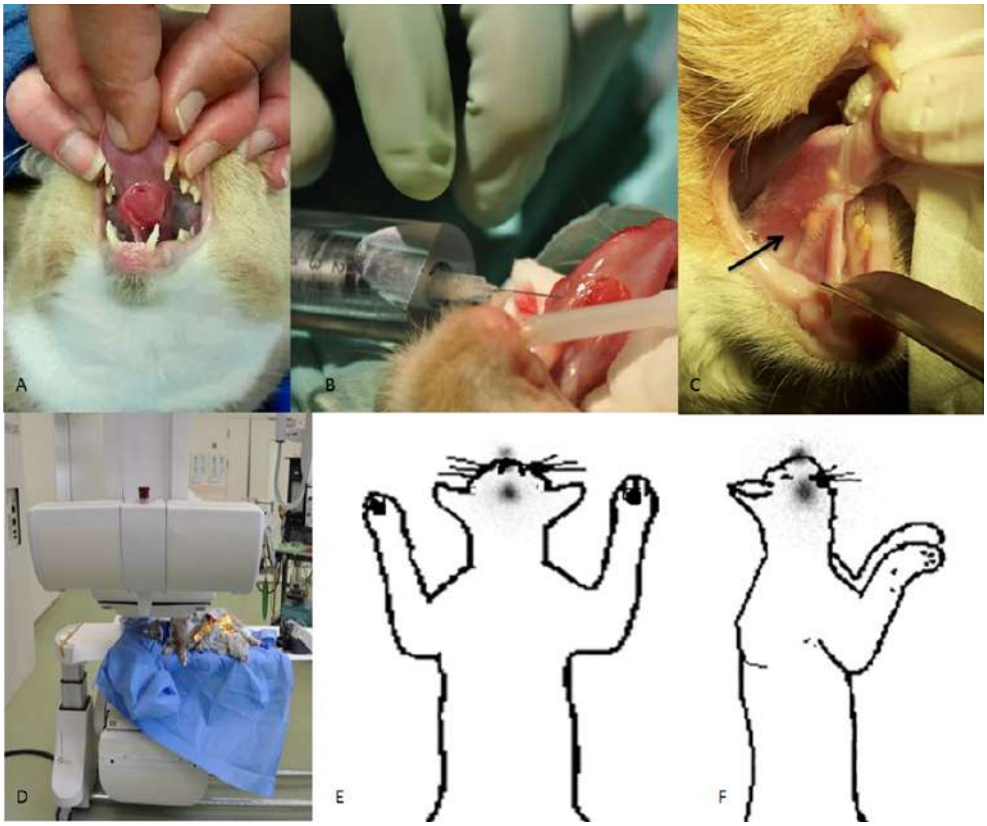

Figure 4.3. *Example of a complete tumor response to ^{166}Ho microbrachytherapy and a typical example for the complication of laser surgery, where the rostral part of the tongue became necrotic after debulking (Patient number 7). A: The tumor at first visit. B: Two weeks after the laser surgery a unilateral rim of the tip of the tongue became necrotic. This was identified prior to the holmium-166 treatment. C: Follow-up visit 2 months after the holmium-166 treatment showing a complete tumor response and loss of a right rostral rim of the tongue edge; holmium depositions are visible (black arrow). D: Set-up of scintigraphy. E and F: Scintigraphy with ^{99m}Tc marker positioned at the nose anteroposterior and lateral view). This animal with a complete response is still under follow-up after 1304 days.*

DISCUSSION

To our knowledge, this is the first study on intra-tumoral treatment with radioactive microparticles in feline patients with OSCC. This study shows that cats with small unresectable OSCC can be curatively treated with a high dose of ^{166}Ho microbrachytherapy. Complete response was obtained in 27%, partial response in 36% and stable disease in 18% of the cats. Treatment-related side effects were mild in most animals; however, some serious adverse events occurred. A possible relation to ^{166}Ho microbrachytherapy will be investigated in further research and potential preventive measures proposed.

The outcome in this study compares favorably with currently available treatments for FOSCC with or without bone involvement in respect of clinical efficacy and complications: Several external beam palliative radiation schemes have been used in cats with 3 to 6 fractions of 6 to 10 Gy with only limited effect.[11–13] Radiation side effects were severe, resulting in a significantly diminished quality of life and early treatment termination: 43% of the patients did not complete the radiation protocol in 1 study.[11]

In a large study of 54 animals, only 3 (6%) animals had a complete response, 30 (61%) had a partial response and 16 (33%) had stable disease at completion of treatment. The majority (49/54 animals, 91%) experienced complications compared with only 1 of 11 (9%) in the present ^{166}Ho microbrachytherapy study.[12] The median OS in these studies was 60, 92 and 111.5 days with a median local progression free survival of 43 days, respectively.[11–13]

Accelerated hypofractionated protocols might be more effective with a median OS of 86 to 174 days with a LDPFS of 91 days in 12 animals.[14,15] However, complications were still present in this twice-a-day radiation scheme resulting in grade III mucositis in 7 of 9 (78%) patients compared with 1 of 11 (9%) local radiation ulcer in the present ^{166}Ho microbrachytherapy study.[14] In the study by Fidel et al., 3 patients experienced a complete response 30 days after completion of the radiation, which resulted in a median OS of 298 days compared with 60 days for the partial responders. This median OS of the partial responders in the study of Fidel et al. is similar to the OS of patients classified as non-responders in the present study. Furthermore, 10 of 11 (91%) of the patients in the present study did not experience any side effects.

Adding a systemic chemotherapeutic/radiosensitizer such as carboplatin or gemcitabine has been described to improve response rates, with 16 of 31 (52%) complete responders with an OS of 163 days.[14] Promising results have also been reported in 6 cats using an intensive multimodal treatment approach consisting of chemotherapy, accelerated hypofractionated radiation and surgery. This resulted in a complete response in 5 of 6 cats, and 3 cats alive with a follow-up of ≥1 year.[17]

Figure 4.4. *Typical presentation of downstaging and subsequent resection showing local tumor control after a partial ^{166}Ho microbrachytherapy treatment response and subsequent laser surgery (Patient number 9). A: Tumor at presentation with a volume of 3.1 cm^3. B: Intra-tumoral injections of ^{166}Ho-microspheres. An acrylic glass cover over the syringe blocks beta-radiation to protect the hand of the operator. C: The result 12 days after ^{166}Ho microbrachytherapy with a 58% tumor volume reduction to 1.3 cm^3. D: Subsequent marginal laser resection of the remaining tumor. E: Result after tumor resection. F: Healing of the tongue at 1 month. G: Final result at 2 months. H: Local recurrence, more diffuse and caudal in the tongue at 4.5 months after initial treatment.*

The OS of feline patients with OSCC treated with ^{166}Ho microbrachytherapy is similar to the OS reported in the studies with best clinical efficacy so far, using hypofractionated radiation protocols alone or in a multimodal approach, as described above (LDPFS of 70 vs. 91 days, OS of 113 days vs. 86–174 days).[14,15] The major advantages of this novel ^{166}Ho microbrachytherapy over other therapies are the single session approach and minimally invasive nature, without the severe side effects that are often seen with external beam radiation and chemotherapy. Especially the local toxic side effects such as mucositis, which are often observed after external beam radiation, are not seen after ^{166}Ho microbrachytherapy.

FOSCC is a locally aggressive malignancy, and most untreated patients die of local disease. In this study, only local treatments were applied: ^{166}Ho microbrachytherapy with or without laser debulking of macroscopic tumors. Despite the 55% local control rate without macroscopic tumor, most patients eventually suffered from a local recurrence after several months. Only 1 patient died of pulmonary metastasis. Recurrent disease often appeared in a more caudal location than the primary tumor site of the tongue (Figure 4.3). This may be related to an insufficient administration of ^{166}Ho-microspheres in the caudal margin of the tumor. However, it could also be related to posterior peri-neural or lymphovascular invasion not detectable on the initial

staging CT scans. These features are associated with a poor prognosis in humans and might implicate the need of a more accurate injection treatment of the caudal peritumoral region. In studies of external beam radiation therapy for OSCC, larger peritumoral treatment margins were used, regional lymph nodes were included in the radiation field, and combinations with multiple chemotherapeutical treatments were often performed. Multimodality treatment with additional systemic or regional treatment for microscopic disease might therefore also further improve the survival time after ^{166}Ho microbrachytherapy.

A local side effect seen in this study was unilateral partial necrosis of the tip of the tongue (Figure 4.2). This complication occurred after laser surgery in 2 cats. Considering the unilateral tongue tip location and a clear demarcation region in the acute phase, it seemed to be the result of vascular compromise during laser surgery, causing ischemic necrosis distal to the tumor site. The fact that this complication occurred before ^{166}Ho microbrachytherapy in 1 patient and 3 weeks after ^{166}Ho microbrachytherapy in the other patient indicates that this was unlikely a complication of the ^{166}Ho microbrachytherapy itself. Absence of a vascular arcade or extensive collateral arterial blood supply of the tongue in cats is the most likely explanation for this complication. In contrast, such unilateral ischemic events are not common after lingual surgery in humans, who have an extensive collateral blood supply of the tongue.

In this study, 3 serious adverse events occurred. One local radiation ulcer and 2 patients died during or shortly after the ^{166}Ho microbrachytherapy treatment procedure. Both deaths were most likely unrelated to the ^{166}Ho microbrachytherapy itself. The local radiation ulcer could be expected if healthy adjacent tissue receives a high absorbed dose. This risk of side effects should be balanced against the chances of an incomplete response or increased risk of local recurrences. More accurate administration, for example with additional imaging, such as ultrasound needle guidance, could aid in preventing this complication.

^{166}Ho activity was detected in the lungs on scintigraphy after the ^{166}Ho microbrachytherapy in two patients. In the patient (nr. 13) with follow-up, an estimated 30% of injected ^{166}Ho-microspheres was detected in the lung region on scintigraphy images without clinical signs during the follow-up period. The other patient (nr. 12) died during the ^{166}Ho microbrachytherapy treatment procedure. Although the cause of death was likely related to the anesthetic procedure with inadequate monitoring, acute pulmonary artery embolization after accidental intravenous injection of ^{166}Ho-microspheres cannot be completely ruled out as cause of death. However, the estimated 21% of administered ^{166}Ho-microspheres that was detected in the lung region of patient 12 on scintigraphy images was less than the 30% detected in patient 13 that did not lead to any side effects. As a comparison, in the arterial ^{166}Ho-microspheres radio-embolization procedure that is commonly performed in humans with liver malignancies, a predetermined safety limit of "shunt-fraction" of microspheres (maximum of 20%) that may pass the liver and lodge in pulmonary vasculature is practiced. Activity in the lungs has been encountered during radio-embolization in humans without clinical signs.[22] Nevertheless, this

unwanted systemic distribution of ^{166}Ho-microspheres should be avoided if possible and monitored. Therefore, during the ^{166}Ho microbrachytherapy treatment procedure, the total amount of ^{166}Ho-microspheres is injected in multiple depots. The number of microspheres per injected location is therefore relatively low. The chance that such a fraction of the total dose of ^{166}Ho-microspheres, when inadvertently injected intravenously, will lead to acute life-threatening pulmonary arteriolar embolization is presumably very small.

One patient died 6 days after ^{166}Ho microbrachytherapy because of kidney failure. Leakage of free holmium from microspheres could, in theory, have caused nephrotoxicity as is described for gadolinium.[33] This is, however, unlikely for ^{166}Ho-microspheres since previous research has shown a high in vivo stability of ^{166}Ho-microspheres for more than 30 days.28 This patient already had abnormal findings during clinical work-up (cardiac murmur, hyperglycemia and low hematocrit) and was unstable during the anesthetic procedure for ^{166}Ho microbrachytherapy, showing ventricular premature complexes. In retrospect, this patient would probably have had benefit of intensive postoperative care and monitoring which was, however, not possible in the current treatment setting in the radionuclide facility and according to radiation safety guidelines. The other patient died during the ^{166}Ho microbrachytherapy procedure, most probably due to anesthetic complications. Especially, when considering that these cats are old, often have low body condition scores because of longer periods of reduced ability to eat and/or drink, periprocedural and anesthetic care and monitoring should be optimally arranged. Considering the experimental nature of the ^{166}Ho microbrachytherapy and the radioactivity involved, anesthesia and post-procedural care are challenging and more complicated compared with high-risk patients undergoing more common procedures. A well-trained team and constant awareness during the whole procedure are essential.

With a median-absorbed dose of 546 Gy, side effects were minimal. This is probably because of the short tissue penetration depth of the ^{166}Ho beta-radiation with a mean of 2.1 mm and a maximum less than 9.0 mm.[34] The present data did not reveal a significant relation between absorbed dose and tumor response or a dose-dependent toxicity. This could be related to the small number of patients, or to the fact that all patients received a relatively high-absorbed dose compared with the 50 to 70 Gy of external beam radiation therapy. However, the spatial distribution of ^{166}Ho microbrachytherapy over and around the tumor and therefore the distribution of the radiation-absorbed dose over the entire tumor is probably more important than the calculated total absorbed dose to a tumor. A suboptimal distribution of radioactive dose is more likely to occur in larger tumors and could, therefore, explain the significantly decreased local response rate in patients with larger tumors. This effect is probably larger than a possible dose-response relation, especially with the relatively low number of patients involved in the current study. Because of the limited tissue range of ^{166}Ho beta-radiation, increasing the ^{166}Ho-microspheres specific activity only has a limited effect on the dose distribution in case of a suboptimal ^{166}Ho-microspheres distribution, stressing the importance of the ^{166}Ho microbrachytherapy strategy. An important limitation of the ^{166}Ho microbrachytherapy

procedure in the present study is the inability to monitor the intra-tumoral-absorbed dose distribution, especially in large tumors. The method of ^{166}Ho microbrachytherapy administration in predetermined tumor segments was aimed to create a proper intra-tumoral dose distribution. The resulting absorbed dose coverage of the entire tumor is, however, not known. The unique imaging properties of ^{166}Ho-microspheres have recently been used to develop an MRI-based dosimetry method that is currently used to monitor dose distribution in humans after radio-embolization of the liver.[23] These developments are promising. A real-time imaging-guided dosimetry technique could enable optimization of intra-tumoral radioactive dose distribution during ^{166}Ho microbrachytherapy, which may result in improved local response rates.

CONCLUSION

The application of ^{166}Ho microbrachytherapy led to promising responses in feline patients with unresectable OSCC. The intra-tumoral microbrachytherapy as conducted in this cohort is an effective, minimally invasive treatment with minimal morbidity and limited side effects. Tumor volume was a significant predictor of response. Optimization of the injection procedure may improve spatial distribution of ^{166}Ho-microspheres inside the tumor after injection, especially in large tumors, and result in an improved tumor response rate in future cases. Advantages of ^{166}Ho microbrachytherapy over current treatments using external beam radiation therapy in Feline OSCC patients warrant further investigation.

Table 4.1. Patient characteristic, treatment details and tumor response

Patient	Breed	Age (yrs)	Tumor (cm^3)	Tumor stage	Tumor location	Dose cohort	Dose (Gy)	Prior Laser
1	DS	13.3	3.30	T2aN0M0	Oral tongue	>800	1216	
2	DS	16.9	1.76	T2aN1aM0	Oral Tongue	>800	939	
3	DS	15.9	0.94	T2aN1aM0	Mandible gingiva	>800	4162	
4	DS	15.0	3.96	T2aN1aM0	Oral tongue	>800	912	
5	MC	1.10	5.23	T3bN0M0	Maxilla/gingiva	>800	1288	
6	DS	14.9	3.37	T2bN1aM0	Maxilla/gingiva	400	635	
7	DS	15.4	0.94	T1aN0M0	Oral Tongue	400	293	X
8	DS	13.4	4.40	T2aN1aM0	Oral tongue	400	546	
9	DS	10.8	3.08	T2aN0M0	Oral tongue	400	285	
10	DS	14.3	6.10	T2aN0M0	Oral tongue	200	165	
11	CB	17.0	1.38	T2aN0M0	Oral tongue	200	81	
12	DS	15.0	4.84	T2aN0M0	Oral tongue	200	253	X
13	DS	13.0	1.90	T2aN0M0	Oral tongue	200	174	

CB, cross breed CR, complete response: DS, domestic shorthair: Gy, Gray: LDFS, local disease free survival: LR, local recurrence: MC, main coon: PD, progressive disease: PR, partial response: SD, stable disease: T1, tumor <2 cm: T2, 2–4 cm: T3, >4 cm: substage Ta, without bone involvement: Tb, with bone involvement: No, no regional lymph node metastasis:

ACKNOWLEDGEMENTS

R.C. Bakker is funded by the Dutch Cancer Society research grant: UU 2014 7075.

We thank the owners and their animals that we were able to treat. Further, we would like to thank Maarten Vente, Remmert de Roos, Nikkie de Wit, Chantal Dekker, Joost Holthof, Jeannette Wolfswinkel, Kees Vos and Angelique Barten for the assistance during the holmium treatments.

Tumor post ^{166}Ho (cm^3)	Response	Post-therapy	Local control	LDFS	Survival (in days)	Complication	Cause of death
0.0	CR	19 wk Second ^{166}Ho	Y	92	341		Chronic kidney failure
1.36	PR	5 wk laser 10 wk second ^{166}Ho	Y	70	250		Tongue amputation→ Inability to feed→ Euthanasia
0.0	CR		Y	466	466	Radiation lesion of adjacent tongue	Lung metastasis
1.69	PR		N	32	63		Local disease and LN metastasis
33.49	PD		N	56	78		Local disease
					6		Kidney failure
0	CR		Y	1304	1304	Necrosis small part of the rostral tongue	Alive
4.27	SD		N	57	66		Local disease
1.32	PR	3 wk laser	Y	132	159		Local recurrence
5.8	SD		N	30	53		Local disease
2.91	PD		N	13	50		Local disease
					0		Anesthesia complication
0.92	PR	3 wk laser	Y	113	113	Necrosis small part of rostral tongue	Local recurrence

N1, movable ipsilateral lymph nodes: substage Na, No evidence of lymph node metastasis: Nb, evidence of lymph node. Tumor stage is according to WHO TNM classification for oral tumors in domestic animals.[29] *, Evaluation of response not available due to limited survival.

CONFLICT OF INTEREST

J.F.W. Nijsen is a co-founder and scientific director of Quirem Medical, and has a minority share in the company Quirem Medical. Furthermore, J.F.W. Nijsen is an inventor on the patents related to the ^{166}Ho-PLLA-microspheres which are assigned to University Medical Center Utrecht Holding B.V. (patent numbers: WO2012060707 A1 and US

2005/0201940 A1). The department of Radiology and Nuclear Medicine of the UMC Utrecht receives royalties from Quirem Medical B.V.

M.G.E.H. Lam is consultant for Sirtex, BTG, Mirada and Bayer Healthcare.

REFERENCES

1. Withrow SJ, MacEwan EG. Small Animal Clinical Oncology: St. Louis,Mo. : Elsevier/Saunders 2001.
2. Howlader N, Noone A, Krapcho M, Miller D, Bishop K, Kosary CL, et al. SEER Cancer Statistics Review. Bethesda, MD: National Cancer; 1975–2013.
3. Ferlay J, Soerjomataram I, Dikshit R, Eser S, Mathers C, Rebelo M, et al. Cancer incidence and mortality worldwide: sources, methods and major patterns in GLOBOCAN 2012. Int J Cancer. 2015;136(5):E359–E386.
4. Braakhuis BJM, Visser O, Leemans RC. Oral and oropharyngeal cancer in The Netherlands between 1989 and 2006: Increasing incidence, but not in young adults. Oral Oncol 2009;45(9):e85–e89.
5. Wypij JM. A naturally occurring feline model of head and neck squamous cell carcinoma. Patholog Res Int. 2013;2013:1–7.
6. Munday JSS, Howe L, French A, Squires RAA, Sugiarto H. Detection of papillomaviral DNA sequences in a feline oral squamous cell carcinoma. Res Vet Sci. 2009;86(2):359–361.
7. Supsavhad W, Dirksen WP, Martin CK, Rosol TJ. Animal models of head and neck squamous cell carcinoma.Vet J. 2015;210:7–16.
8. Yoshikawa H, Ehrhart EJ, Charles JB, Custis JT, Larue SM. Assessment of predictive molecular variables in feline oral squamous cell carcinoma treated with stereotactic radiation therapy. Vet Comp Oncol. 2016;14(1):39–57.
9. Snyder L. Oral squamous cell carcinoma: like owner, like cat.Vet J.2012;193(1):6–7.
10. Sant M, Aareleid T, Berrino F, Bielska Lasota M, Carli PM, Faive J, et al. EUROCARE–3: survival of cancer patients diagnosed 1990–94–results and commentary. Ann Oncol. 2003;14(suppl 5):v61–v118.
11. Bregazzi VS, LaRue SM, Powers BE, Fettman MJ, Ogilvie GK, Withrow SJ. Response of feline oral squamous cell carcinoma to palliative radiation therapy. Vet Radiol Ultrasound. 2001;42(1):77–79.
12. Sabhlok A, Ayl R. Palliative radiation therapy outcomes for cats with oral squamous cell carcinoma (1999–2005).Vet Radiol Ultrasound. 2014;55(5):565–570.
13. Jones PD, de Lorimier LP, Kitchell BE, Losonsky JM. Gemcitabine as a radiosensitizer for nonresectable feline oral squamous cell carcinoma. J Am Anim Hosp Assoc. 2003;39(5):463–467.
14. Fidel JL, Sellon RK, Houston RK, Wheeler BA. A nine–day accelerated radiation protocol for feline squamous cell carcinoma. Vet Radiol Ultrasound. 2007;48(5):482–485.
15. Poirier VJ, Kaser–Hotz B, Vail DM, Straw RC. Efficacy and toxicity of an accelerated hypofractionated radiation therapy protocol in cats with oral squamous cell carcinoma. Vet Radiol Ultrasound. 2013;54(1):81–88.
16. Fidel J, Lyons J, Tripp C, Houston R, Wheeler B, Ruiz A. Treatment of oral squamous cell carcinoma with accelerated radiation therapy and concomitant carboplatin in cats. J Vet Intern Med. 2011;25(3):504–510.
17. Marconato L, Buchholz J, Keller M, Bettini G, Valenti P, Kaser–Hotz B. Multimodal therapeutic approach and interdisciplinary challenge for the treatment of unresectable head and neck squamous cell carcinoma in six cats: a pilot study. Vet Comp Oncol. 2013;11(2):101–112.
18. Wiles V, Hohenhaus A, Lamb K, Zaidi B, Camps–Palau M, Leibman N. Retrospective evaluation of toceranib phosphate (Palladia) in cats with oral squamous cell carcinoma. J Feline Med Surg. 2016;19(2):185–193.
19. Fox LE, Rosenthal RC, King RR, Levine PB, Vail DM, Helfand SC, et al. Use of cis-bis-neodecanoato-trans-R,R-1,2-diaminocyclohexane platinum (II), a liposomal cisplatin analogue, in cats with oral squamous cell carcinoma. Am J Vet Res. 2000;61(7):791–795.
20. Seevinck PR, Seppenwoolde JH, de Wit TC, Nijsen JFW, Beekman FJ, van het Schip AD, et al. Factors affecting the sensitivity and detection limits of MRI, CT, and SPECT for multimodal diagnostic and therapeutic agents. Anticancer Agents Med Chem. 2007;7:317–334.
21. Elschot M, Smits MLJ, Nijsen JFW, Lam MGEH, Zonnenberg BA, van den Bosch MAAJ, et al. Quantitative Monte Carlo-based holmium-166 SPECT reconstruction. Med Phys. 2013;40(11):112502.
22. Smits MLJ, Nijsen JFW, van den Bosch MAAJ, Lam MGEH, Vente MA, Mali WP, et al. Holmium-166 radioembolisation in patients with unresectable, chemorefractory liver metastases (HEPAR trial): a phase 1, dose-escalation study. Lancet Oncol. 2012;13(10):1025–1034.
23. Smits MLJ, Elschot M, van den Bosch MAAJ, van de Maat GH, van het Schip Ad, Zonnenber BA, et al. In vivo dosimetry based on SPECT and MR imaging of ^{166}Ho-microspheres for treatment of liver malignancies. J Nucl Med. 2013;54(12):2093–2100.
24. Blanchard RJ, Lafave JW, Kim YS, Frye CS, Ritchie WP, Perry JF. Treatment of patients with advanced cancer utilizing Y90 microspheres. Cancer. 1965;18(3):375–380.
25. van Es RJJ, Nijsen JFW, van het Schip AD, Dullens HF, Slootweg PJ, Koole R. Intra-arterial embolization of head-and-neck cancer with radioactive holmium-166 poly(L-lactic acid) microspheres: an experimental study in rabbits.Int J Oral Maxillofac Surg. 2001;30(5):407–413.
26. Bult W, Vente MADD, Vandermeulen E, Gielen I, Seevinck PR, Saunders J, et al. Microbrachytherapy using holmium-166 acetylacetonate microspheres: a pilot study in a spontaneous cancer animal model. Brachytherapy. 2013;12(2):171–177

27. Bult W, Kroeze SGC, Elschot M, Seevinck PR, Beekman FJ de Jong HWAM. et al. Intratumoral administration of holmium-166 acetylacetonate microspheres: antitumor efficacy and feasibility of multimodality imaging in renal cancer. PLoS One. 2013;8(1):e52178.
28. Bult W, De Leeuw H, Steinebach OM, van der Bom MJ, Wolterbeek HT, Heeren RM, et al. Radioactive holmium acetylacetonate microspheres for interstitial microbrachytherapy: an in vitro and in vivo stability study. Pharm Res. 2012;29(3):827–836.
29. Owen L. TNM Classification of Tumors in Domestic Animals. World Health Organization; Geneva 1980:46–47.
30. Zielhuis SW, Nijsen JFW, De Roos R, Krijger GC, van Rijk PP, Henning WE, et al. Production of GMP-grade radioactive holmium loaded poly(L-lactic acid) microspheres for clinical application. Int J Pharm. 2006;311(1–2):69–74.
31. Vente MAD, Nijsen JFW, de Wit TC, Seppenwoolde JH, Krijger GC, Seevinck PR, et al. Clinical effects of transcatheter hepatic arterial embolization with holmium-166 poly(L-lactic acid) microspheres in healthy pigs. Eur J Nucl Med Mol Imaging. 2008;35(7):1259–1271.
32. Ladue T, Klein MK. Toxicity criteria of the veterinary radiation therapy oncology group. Vet Radiol Ultrasound. 2001;42(5):475–476.
33. Rose TA, Choi JW. Intravenous imaging contrast media complications: the basics that every clinician needs to know. Am J Med. 2015;128(9):943–949.
34. Nijsen JFW, Krijger GC, van Het Schip AD. The bright future of radio-nuclides for cancer therapy. Anticancer Agents Med Chem. 2007;7(3):271–290.


5

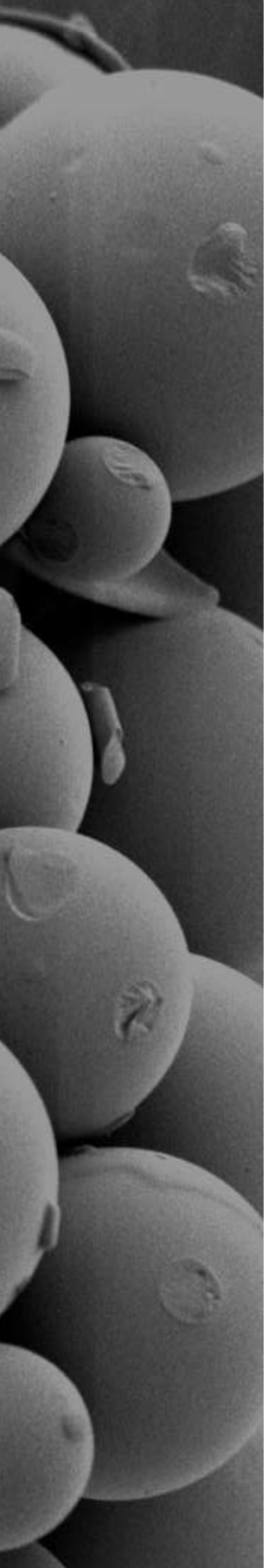

Feasibility of holmium-166 microspheres for selective intra-tumoral treatment in head and neck oncology: a letter to the editor

R.C. Bakker

R.J.J. van Es

J.F.W. Nijsen

M.G.E.H. Lam

Submitted

Radioactive holmium-166 (^{166}Ho) microspheres are CE-approved (QuiremSpheres®, Quirem Medical B.V., Deventer, The Netherlands) and currently used in intra-arterial radioembolization of liver malignancies.[1] In head and neck cancer however, this is technically challenging due to the multiple arterial collaterals, with a high risk of inadvertent activity distribution. Direct intra-tumoral injections may be a good alternative. This was performed in 13 veterinary patients (cats) with oral squamous cell carcinoma of the tongue. A complete remission or sufficient tumor volume reduction for subsequent surgical removal was obtained in 55%, with minimal side effects.[2] It was therefore hypothesized that human patients may also benefit from this innovative microbrachytherapy.

Feasibility was tested in an early clinical phase I study in patients with oral squamous cell carcinoma of the tongue, in a 'treat-and-resect' protocol (NCT02975739). The primary endpoint was the percentage of administered activity retained in the tumor after treatment. Secondary endpoints included biodistribution, safety and efficacy. Unfortunately, the study was prematurely terminated due to the lack of accrual and only one patient completed the protocol.

^{166}Ho loaded poly (L-lactic acid) microspheres were prepared as described earlier. These radioactive microspheres (Ø 10–30 μm) emit β-radiation ($E_{\beta, max}$ = 1.84 MeV, $t_{1/2}$ = 26.8 hours) with a maximum tissue penetration of 8.7 mm, and a small fraction of γ radiation (6.71%, 80.6 KeV) that can be imaged with SPECT. ^{166}Ho can also be imaged with CT because of its high density (8.79 g/cm^3 at room temperature) and atomic number (Z = 67), and with MRI because of its paramagnetic properties.[1,3–5] This provides excellent opportunities for in vivo multimodality imaging, enabling treatment guidance and monitoring.

To obtain a lethal absorbed dose of >100 Gy in 1 mL tumor tissue (i.e. the assumed distribution volume of 1 injection) approximately 6.3 MBq ^{166}Ho was calculated. To account for residual activity in the syringe, 15 MBq was prepared in 0.3 mL suspension. Four intra-tumoral injections were performed under local anesthesia, through a needle (23G*1¼", Becton Dickinson, Madrid, Spain) in the viable tumor edge under ultrasound guidance, followed by SPECT, MRI and CT imaging. The Ethics Committee approved the protocol and the study was conducted according to the principles of the Declaration of Helsinki.

A 77-year-old male with an oral squamous cell carcinoma of the tongue on the left side (25 × 19 × 8 mm) received four intra-tumoral injections. In total, 46.9 ± 14.5% of the prepared activity in the syringes was administered. During the injection, leakage of injection fluid was noted through the ulcerative lesion. After each injection patient was asked to rinse the oral cavity. The rinsing fluid measured 9.8 MBq, 36% of the total injected activity. No activity was detected in blood or urine samples collected three hours post administration. Post-treatment SPECT/CT revealed a clear hotspot in the tongue. Quantitative analysis detected 8.5 MBq (31%). Planar imaging of the thorax did not reveal activity in the lungs, however activity in the intestines was observed (9.1 MBq; 33%). The MRI showed a focal area of decreased signal. (Figure 5.1) Based

on the activity measurements of the SPECT, a total of 1.51 mg of holmium was located inside the tumor. This correlated perfectly with the CT quantification, which detected 1.52 mg. Furthermore, the high resolution of CT was able to identify separate depositions of holmium microspheres suggesting local dose >200 Gy. The patient did not experience any side effects. No macroscopic effect of holmium microspheres was observed 11 days after injections, but histology showed clusters of microspheres surrounded by local necrosis. No wound healing disorder was observed and the patient received radiotherapy after a short recovery.

The injection procedure was relatively easy and clinically tolerable. It resulted in a high local dose of >200 Gy in the tumor, confirmed by necrosis on histology. This high ablative dose may potentially result in radionecrosis of healthy neighboring tissue. However, since 90% of the dose will be absorbed within 2.1 mm, while the surgical resection margin is 10 mm, this risk is expected to be minimal. The retained activity in the tumor was only 31% of the total injected activity. Although the spilled (and partially swallowed) activity is not expected to lead to complications at these low activities, this significant leakage during injection seriously limits the feasibility of intra-tumoral injection in squamous cell carcinoma of the tongue.

The imaging opportunities of ^{166}Ho-microspheres allow for personalized dosimetry and may ultimately lead to optimization of microbrachytherapy with regard to safety and efficacy. This may lead to complete or near-complete tumor reduction, which may result in less extensive surgery, improved functional outcome and improved quality of life. However, more research is needed on feasibility in relation to tumor type and location, administration technique, and biodistribution.

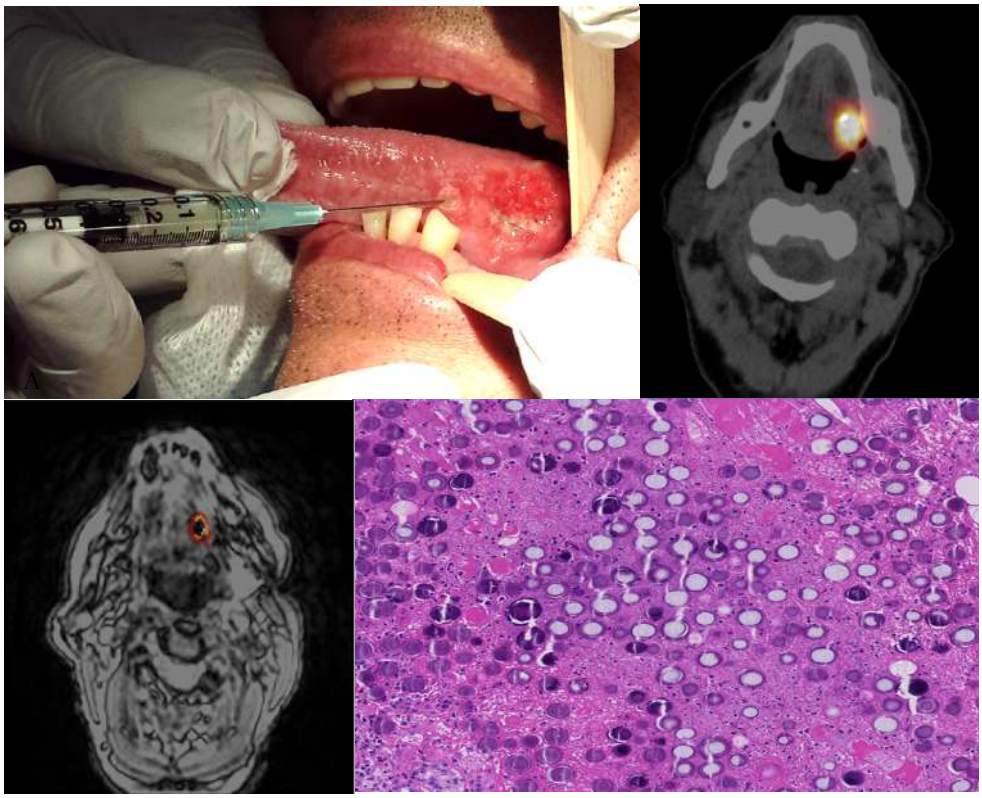

Figure 5.1. *A: Treatment set-up: direct intra-tumoral injection of ^{166}Ho microsphere suspension under local anesthesia in an ulcerative tumor on the border of the tongue, B: Holmium SPECT/CT of the head and neck area, C: MRI with ^{166}Ho dose reconstruction (black center has ^{166}Ho microsphere concentration >10 mg/mL resulting in rapid signal loss and inaccurate quantification), D: Histology, HE staining of clusters of holmium microspheres with localized necrosis surrounding the microspheres, while periphery is unaffected.*

REFERENCE

1. Smits MLJ, Nijsen JFW, van den Bosch MAAJ, Lam MGEH, Vente MAD, Mali WPTM, et al. Holmium-166 radioembolisation in patients with unresectable, chemorefractory liver metastases (HEPAR trial): A phase 1, dose-escalation study. Lancet Oncol. 2012;13(10):1025–34.
2. van Nimwegen SA, Bakker RC, Kirpensteijn J, van Es RJJ, Koole R, Lam MGEH, et al. Intratumoral injection of radioactive holmium (^{166}Ho) microspheres for treatment of oral squamous cell carcinoma in cats. Vet Comp Oncol. 2017;8;0:1–11.
3. Seevinck P, Seppenwoolde J-H, de Wit T, Nijsen JFW, Beekman F, van het Schip AD, et al. Factors Affecting the Sensitivity and Detection Limits of MRI, CT, and SPECT for Multimodal Diagnostic and Therapeutic Agents. Anticancer Agents Med Chem. 2007;1;7(3):317–34.
4. Elschot M, Smits MLJ, Nijsen JFW, Lam MGEH, Zonnenberg BA, van den Bosch MAAJ, et al. Quantitative Monte Carlo-based holmium-166 SPECT reconstruction. Med Phys. 2013;40(11):112502.
5. Smits MLJ, Elschot M, van den Bosch MAAJ, van de Maat GH, van het Schip AD, Zonnenberg BA, et al. In vivo dosimetry based on SPECT and MR imaging of ^{166}Ho-microspheres for treatment of liver malignancies. J Nucl Med. 2013;54(12):2093–100.


6

Intra-tumoral injection of radioactive holmium-166 microspheres in recurrent head and neck squamous cell carcinoma: preliminary results of first use

R.C. Bakker

R.J.J. van Es

A.J.W.P. Rosenberg

S.A. van Nimwegen

R. Bastiaannet

H.W.A.M. de Jong

J.F.W. Nijsen

M.G.E.H. Lam

Nuclear Medicine Communications

Bakker RC, van Es RJJ, Rosenberg AJWP, van Nimwegen SA, Bastiaannet R, de Jong HWAM, Nijsen JFW, Lam MGEH. **Intratumoral injection of radioactive holmium-166 microspheres in recurrent head and neck squamous cell carcinoma: preliminary results of first use.** Nucl Med Commun. 2018;39(3):213–221.

ABSTRACT

Introduction

Limited treatment options exist for patients with locoregional recurrences of head and neck squamous cell carcinoma (HNSCC). In the palliative setting, a single session, minimally invasive, and relatively safe therapy is desirable. This case series illustrates the feasibility of a direct intra-tumoral injection of radioactive holmium-166 microspheres (^{166}Ho-microspheres) in patients as a palliative treatment for recurrent HNSCC.

Methods

In this retrospective analysis, patients with already re-irradiated irresectable recurrent HNSCC, for whom palliative chemotherapy was unsuccessful or impossible, were offered microbrachytherapy with ^{166}Ho-microspheres. The intra-tumoral injection was administered manually under ultrasound guidance. Parameters scored were technical feasibility (i.e. administration, leakage, and distribution), clinical response (response evaluation criteria in solid tumors 1.1), and complications (Common Terminology Criteria for Adverse Events 4.3).

Results

From 2015 to 2017, three patients were treated. None of the patients experienced adverse events; however, therapeutic effects were minimal. Technical difficulties, including precipitating of microspheres and high intra-tumoral pressure, resulted in suboptimal distribution of the microspheres.

Conclusion

Intra-tumoral injections with ^{166}Ho-microspheres are minimally invasive and relatively safe in palliation of HNSCC patients. Careful patient selection and improved administration techniques are required to provide a more effective treatment. Further investigation of this novel treatment modality should be carried out because of the absence of side effects and lack of other treatment options.

INTRODUCTION

Cancer of the head and neck accounts for ~685,000 (4.9%) of all new cancer cases worldwide and over 375,000 deaths annually. The survival of patients with head and neck squamous cell carcinoma (HNSCC) mainly depends on the stage of disease at the time of diagnosis. For advanced (stage III–IV) carcinomas, the survival rate decreases to ~35%. Over the last decades, only limited improvements in survival were achieved, which urges the need for new treatment modalities. Especially for patients with locoregional recurrences, limited options exist.[1–3]

For previously irradiated, irresectable regional recurrences, only two options for palliative treatment remain: palliative reirradiation or chemotherapy. In most cases with recurrent HNSCC, palliative reirradiation can be administered only once. This reirradiation usually consists of accelerated hyper-fractionated schemes of 1.5 Gy twice daily, up to 60 Gy depending on the dose previously administered.[4,5] With new developments such as intensity-modulated radiotherapy and stereotactic body radiation therapy, new schemes of 4–6 fractions of 6 Gy reduce treatment duration in patients with a limited life expectancy.[6] Palliative chemotherapy may provide a meaningful response in some patients. However, many patients are medically unfit for a platinum compound with capecitabine/fluorouracil and/or cetuximab.[7] There are currently some developments with monoclonal antibodies and tyrosine kinase inhibitors such as PI3K/AKT/mTOR that may prove beneficial in the near future.[8] Furthermore, brachytherapy with a high or a pulsed dose rate[9] and bleomycin-electroporation therapy[10,11] are being studied in salvage patients, but these treatment modalities require a good performance status. As a result, only best supportive care remains for patients with severe comorbidities or a poor performance status.

Radioactive holmium-166 microspheres (^{166}Ho-microspheres) and currently used in intra-arterial radioembolization of liver malignancies.[12] These microspheres emit beta-radiation with a maximum penetration depth of 8.7 mm and are also used off-label in veterinary patients with unresectable oral squamous cell carcinomas and other tumors.[13,14] Intra-tumoral injections of ^{166}Ho-microspheres in veterinary patients showed a relevant response without severe morbidity.[13] This article presents the first experience on the feasibility and safety of intra-tumoral injections of ^{166}Ho-microspheres in human patients with recurrent cancer in the head and neck.

METHODS

Patient selection

In this retrospective analysis, patients with confirmed local or regional recurrence of HNSCC with or without distant metastasis, as evidenced by recent imaging, were discussed in the multidisciplinary head and neck oncology team for regular treatment options and/or ongoing trials. If no palliative treatment options were available, and nonetheless a strong wish for treatment existed, patients were amenable for direct intra-tumoral injections of ^{166}Ho-microspheres, with the aim of improving the patients' quality of life. Only tumors accessible for ultrasound (US) guided manual injections with at least more than 5 mm distance to vital anatomical structures, such as the common carotid artery, were selected. Immediately after the injection procedure, a planar scintigraphy of the thorax and abdomen, as well as a single-photon emission computed tomography (SPECT)/computed tomography (CT) of the head and neck region were performed. Patients provided informed consent after receiving detailed information. The Ethical Committee of the University Medical Center Utrecht approved the study.

Holmium-166 microspheres preparation

^{166}Ho-microspheres of 30 μm diameter were prepared in the University Medical Center Utrecht as described previously[15,16] and CE-approved (QuiremSpheres; Quirem Medical B.V., Deventer, The Netherlands). Briefly, nonradioactive ^{165}Ho complexed with acetylacetonate is incorporated into poly(l-lactic acid) by solvent evaporation to form microspheres. Subsequently, the non-radioactive ^{165}Ho-microspheres were made radioactive by neutron activation in a nuclear facility (RID Reactor, Delft University of Technology, Delft, The Netherlands) to form ^{166}Ho-microspheres. After neutron activation, ^{166}Ho-microspheres were suspended in a PBS with 2% weight per volume of polyoxyethylene–polyoxypropylene copolymer (Pluronic F-68; Sigma-Aldrich Chemie B.V., Zwijndrecht, The Netherlands). The ^{166}Ho-microspheres were suspended for 10 min. on a vortex, followed by repeatedly drawing up and down with a syringe.

The amount of radioactivity present in each syringe was measured in a dose calibrator (VDC-404; Veenstra Instruments B.V., Joure, The Netherlands). Each syringe was placed in an acrylic glass cylinder to limit beta-radiation exposure of personnel, especially to the hands, during dose preparation and administration. The treatment was performed with a quantity of 100–250 mg of ^{166}Ho-microspheres, divided over 2–10 syringes, with a volume of 0.2–0.5 mL. The required ^{166}Ho activity was determined on the basis of tumor volume and aimed tumor-absorbed dose according to the following equation: $D = A \times 15.87 / W$, where D is the tumor-absorbed dose [in Gy (J/kg)]; A is the ^{166}Ho activity (MBq); ^{166}Ho-specific tissue dose conversion coefficient = 15.87 mJ/MBq; and W is the tumor weight (g). Assumed tumor tissue density was 1.0 g/cm^3 and beta-radiation was assumed to absorb completely in the treated tissue.[17] The required activity was obtained by varying the neutron activation time of the microspheres.

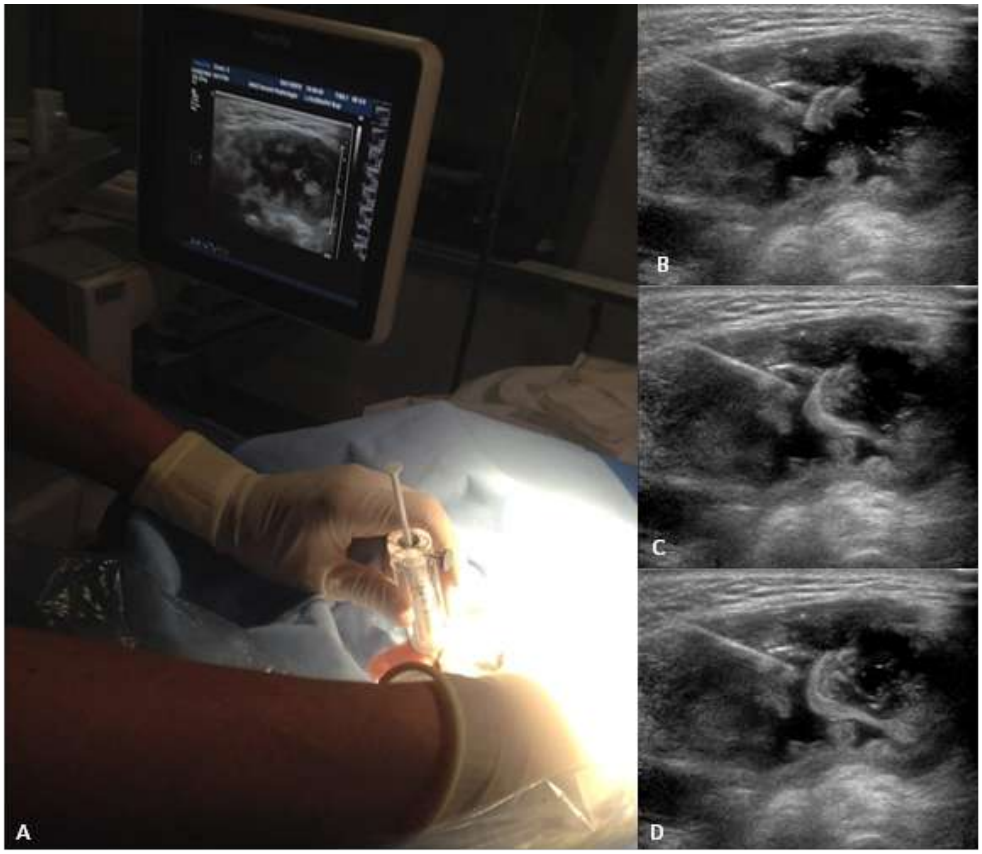

Figure 6.1. *A: Set up of the ultrasound guided injection with the syringe with ^{166}Ho-microspheres shielded with acrylic glass. B, C, D: Ultrasound images of an injection in a large necrotic fluid filled lymph node metastasis, clearly visible flow of microspheres inside the tumor.*

Treatment

Before injection, the ^{166}Ho-microspheres were resuspended in the syringe by gentle agitation. The injections were administered manually under US guidance to prevent accidental intravenous administration. On the basis of the veterinary experience and review of the available literature, the following assumptions were made. The average injection percentage of ^{166}Ho-microspheres in the veterinary experience was ~50%; therefore, the prepared activity was doubled. The injection volume ranged from ~7 to 25% of the tumor volume. Per injection, a 1 cm^3 distribution of microspheres was expected. A 1 mL syringe was used for optimal control during the injection of small volumes with a 'luer lock' tip to reduce the risk of needle dislodgement. 21 G*2" and 23 G*1¼" needles were used depending on the tumor location. The aimed absorbed dose was 70–100 Gy. Immediately after treatment, a SPECT/CT was performed. Follow-up was performed at 1, 2, and at 4 weeks combined with a PET/CT. The following parameters were scored: technical feasibility (i.e. administration, leakage, distribution), response

according to the response evaluation criteria in solid tumors (RECIST 1.1)[18], and complications according to the Common Terminology Criteria for Adverse Events (CTCAE 4.3).[19]

Case series

Three consecutive patients with a locoregional recurrence of HNSCC, who presented to the University Medical Center Utrecht between November 2015 and June 2017, were treated with intra-tumoral ^{166}Ho-microspheres (Tables 5.1 and 5.2).

Patient 1

A 75-year-old man with a history of diabetes, hypertension, a cerebrovascular ischemic accident, coronary artery bypass grafting, and atrial fibrillation was diagnosed with a squamous cell carcinoma of the maxillary gum, staged cT4aN2cM0. A partial maxillectomy was performed, with primary bilateral radiotherapy (70 Gy) of the neck because of his poor general condition. After 1 year, the patient developed a bilateral regional recurrence. US and CT indicated neck nodes with a diameter of 27 and 44 mm on the right and left side, respectively. Because of his poor medical condition, the patient was not amendable for salvage surgery or chemotherapy. The patient refused palliative reirradiation. In consultation with the patient, the largest left sided neck node was treated because of complaints of local compression and pain.

The treatment plan was to inject 200 MBq in 100 mg of ^{166}Ho-microspheres divided over two syringes with a volume of 0.5 mL and a 21 G×2" needle, which would result in an average absorbed dose of 70 Gy. Syringes were filled with 396.3 MBq and 204.1 mg of ^{166}Ho-microspheres to correct for the expected injection percentage of 50%. The injection procedure was not painful (maximum grade I) and particle-reflections could be observed on US during administration (Figure 6.1). In this patient, 366.8 MBq (92.5%) of the prescribed activity could be injected, equivalent to an absorbed dose of 130 Gy. SPECT/CT imaging showed some precipitation of the microspheres, especially in the dorsocaudal part of the tumor. Estimated activity on SPECT/CT was 309.2 MBq or 84.3% of the injected activity (Figure 6.2).

The patient was admitted for observation of unexpected side effects before discharge 24h after treatment. Clinical follow-up was performed at 1 and 2 weeks and did not indicate any toxicity. His complaints of tension in his neck diminished. At 4 weeks, a [^{18}F]Fluorodeoxyglucose PET/CT was performed to evaluate the response. This showed a 37% volume increase of the nontreated right lesion and a 30% volume increase of the treated left lesion. The treated lesion showed a lower maximum standardized uptake value on the [^{18}F]Fluorodeoxyglucose PET/CT of 8.7 compared with 9.5 of the nontreated lesion, respectively. Especially, the uptake of the dorsal and caudal tumor parts was lower. Two months after ^{166}Ho-microspheres treatment, the patient died of respiratory insufficiency caused by aspiration pneumonia and progressive disease.

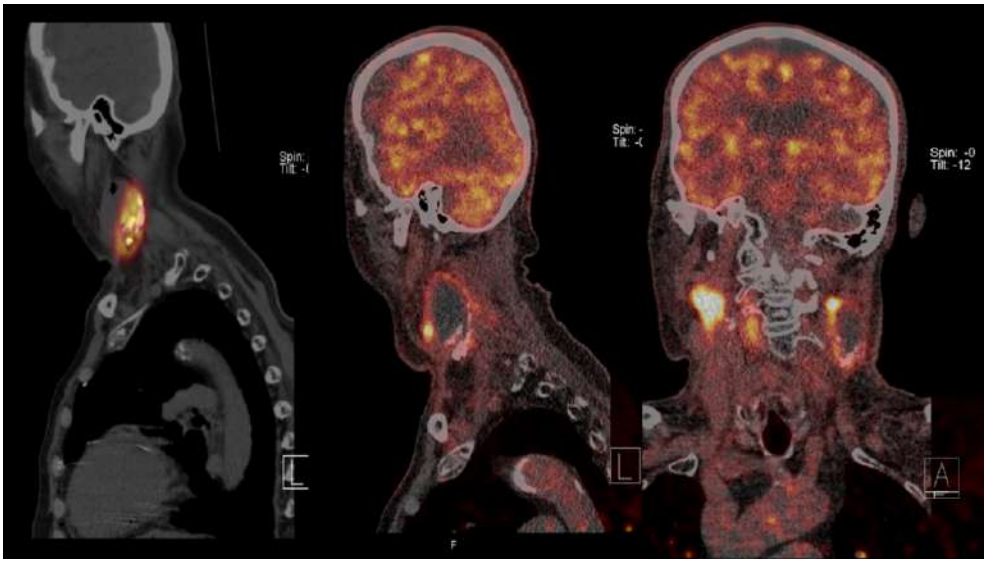

Figure 6.2. *Patient 1 with a large necrotic lymph node metastasis with clearly visible precipitation of the microspheres. A: single-photon emission computed tomography direct post injection in supine position. B, C: sagittal and coronal slices of 18F-fluorodeoxyglucose positron emission tomography, one month after injection.*

Patient 2

A 75-year-old man with a history of hypertension, myocardial infarction, and an out of hospital cardiac arrest was referred with an irradical excision of a left-sided retroauricular cutaneous squamous cell carcinoma. At the initial consultation, a 3×3 cm skin defect with nodules in the parotid gland was found. After surgical resection, which included a left ear amputation, selective neck dissection, and a superficial parotidectomy, the tumor was staged as pT3N2b with extracapsular extension. Subsequently, the patient received 49.5 Gy on the entire surgical field and neck with a simultaneous integrated boost technique: 66 Gy on the tumor bed and lymph nodes in level II. After 8 months, the patient presented with a regional recurrence in the left neck with carotid encasement up to the base of the skull, involvement of the vagal nerve, and tumor infiltration in the skin.

At clinical examination, a massive tumor, infiltrating and ulcerating the skin, was observed. The patient's main complaint was localized pain of the skin just below the mandible, poorly responding to oral morphine. In consultation with the patient, it was decided, despite the poor prognosis, to treat only this superficial area of the recurrence, avoiding the risk of traumatizing the carotid artery, and with the aim to palliate symptoms.

Four syringes with an activity of 13.5–16.5 MBq in 0.3 mL were prepared, which would result in an absorbed dose of 100 Gy for 4 cm^3. However, during the first two injections, an unexplained obstruction of the syringe occurred almost immediately. As a result, the injection procedure was terminated. Post-treatment measurements showed that only 3.3 MBq (9.5%) of the ^{166}Ho-

microspheres was injected. The injection procedure was minimally uncomfortable (i.e. pain: maximum grade I). Unfortunately, the patient was unable to undergo the SPECT/CT imaging because of pre-existing dyspnea. The patient was discharged, but readmitted 2 days later, because of progressive dyspnea. No adverse effects of the ^{166}Ho-microspheres injections were noted and a subjective decline in skin tension and pain was experienced, but no objective response was observed. The clinical condition declined rapidly, and the patient died of respiratory insufficiency 6 days after the treatment.

Patient 3

A 73-year-old woman with a history of alcohol and tobacco abuse was referred with a cT2N0M0 tongue carcinoma. A partial glossectomy, resection of the oral floor, a level I–III neck dissection, and reconstruction with a free radial forearm flap were performed. Simultaneously, a synchronous primary pTis of the floor of the mouth was resected. Six years later, she presented with a third primary T2N2bM0 oropharyngeal carcinoma with a synchronous primary contralateral cT1N2b tonsillar fossa carcinoma. Both tumors were treated with radiotherapy: 69 Gy on both gross tumor volumes and the positive lymph nodes. Level Ib–V left and right received 51 Gy. After 6 months, cutaneous metastases developed on both sides of the neck, causing dyspnea. Additional staging indicated multiple pulmonary nodules suspicious for metastatic disease. The patient received a tracheostomy and palliative carboplatin/capecitabine/cetuximab weekly, which showed a substantial response initially. However, after six cycles of systemic therapy, growth of the cutaneous metastases progressed. The patient's complaints were friction, pain, and the disfiguring sight of the cutaneous metastases.

It was planned to treat multiple nodules; however, in the 3 weeks between consent and treatment, the metastases progressed rapidly (Figure 6.4). Therefore, only two large lateral lesions were treated with five injections of 0.2 mL, with an average of 25 mg and 15 MBq ^{166}Ho-microspheres, respectively. Of the total prescribed activity of 148.7 MBq, 91.2% was injected. Because of the superficial lesions, some backflow of microspheres was observed with needle retraction. In addition, some leakage of ^{166}Ho-microspheres was observed during the injection of the ulcerative tumor on the left side. The cumulative leakage was 3.2 MBq (4.5%) on the right side and 14.7 MBq (21.5%) on the left side, resulting in a total administered activity of 117.7 MBq (79.2%) (Figure 6.3).

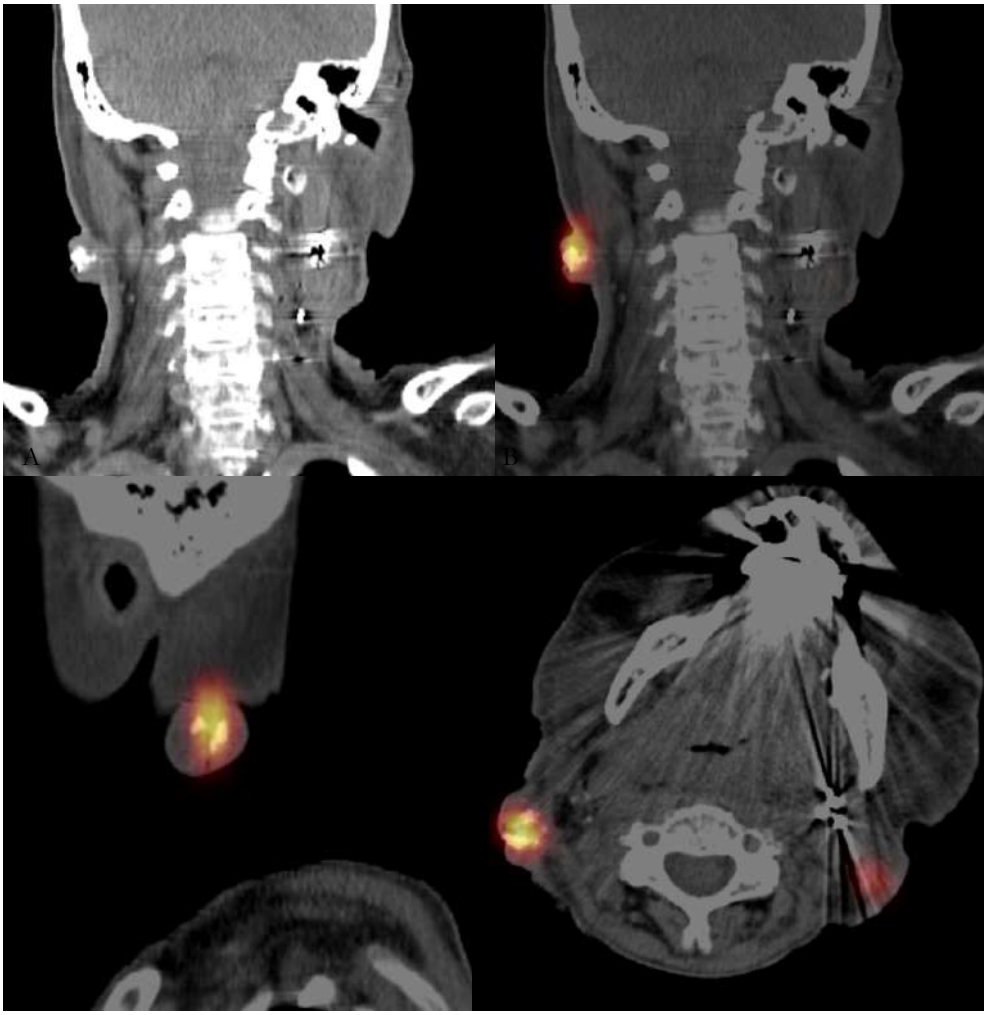

Figure 6.3. *Patient 3 A: Clearly visible accumulations of holmium microspheres as white dots on computed tomography. B, C, D: single-photon emission computed tomography reconstructions in coronal, sagittal and axial directions.*

After the procedure, the patient was discharged. No discomfort was experienced during or after the treatment. The progression of her complaints of friction and the disfiguring sight was halted. Tumor inspection after 1 week showed marked central necrosis of both injected tumors. This remained visible at 2 weeks (Figure 6.4). This was interpreted as treatment effect. The right lesion measured 28×24 mm before treatment and 30×23 mm after 2 weeks, and the left lesion 24×15 and 25×14 mm, respectively. The tumor edge seemed still partially vital 2 weeks after treatment. Progressive dyspnea and growth of nontarget lesions resulted in severe discomfort. The patient asked for and received euthanasia 6 weeks later.

Table 6.1. Patient characteristics

	Patient 1
Sex	Male
Age	75
History	Appendectomy, diabetes + retinopathy, CVA, hypertension, LVH, mild AOS, HNP L5–S1, cognitive impairment, CABG + AF
Origin	Gingiva of the maxilla
TNM classification	cT4aN2cM0
Histopathology	SCC Prior resection specimen G1: well differentiated Infiltrative growth Perineural invasion
Surgical treatment	Subtotal maxillectomy
Radiotherapy	Primary EBRT neck bilateral 35 × 2 = 70 Gy
Chemotherapy	–
Recurrence location	Neck, level II left, Necrotic lymph node
Reason for therapy	Local compression and pain

AF, atrial fibrillation; AOS, aortic valve stenosis; CABG, coronary artery bypass grafting; CVA, cerebrovascular accident; EBRT, external beam radiation therapy; HNP, hernia nuclei pulposi; LN, lymph node; L, left; L5–S1, lumbar 5 sacral 1 disc; LVH, left ventricle hypertrophy; myocardial infarction; ND, neck dissection; R, right; SCC, squamous cell carcinoma; TNM, tumor node metastases; VF, ventricle fibrillation.

DISCUSSION

In this case series, the first experience with a direct intra-tumoral free-hand injection of ^{166}Ho-microspheres in patients with recurrent HNSCC for whom no other palliative retreatment options were available was described. The preparation of syringes with the desired activity and amount of ^{166}Ho-microspheres was accurate, and the resuspension before injection consisted of some gentle agitation of the syringe. The injection procedure went smoothly in patients 1 and 3, with some leakage in superficial and ulcerative lesions. This leakage was easily absorbed in a compress and did not result in contamination of personnel or equipment.

Patient 2	Patient 3
Male	Female
75	73
Hypertension, HNP, cardiac arrest, myocardial infarction	Uterus extirpation, cataract surgery
Skin retroauricular	Oropharynx
pT3N2bM0	cT2N2bM0
SCC Prior resection specimen G2/3: moderately/poorly Differentiated infiltrative growth Perineural invasion + vascular invasion	SCC
Amputation left ear, Selective neck dissection level Ib–III + 5A, Superficial parotidectomy	2010: first T2N0M0 tongue, resection, ND I–III, FRFF-reconstruction + second pTis SCC oral floor right 2016: tracheotomy airway obstruction 2016: third oropharynx + fourth primary tonsil carcinoma cT1N2b
Tumor bed + LN level II right 33 × 2 = 66 Gy Surgical field + LN levels Ib–V left + tract of the nervus facialis till the base of the skull 33 × 1.5 = 49.5 Gy	Gross tumor volume + positive LN 30 × 2.3 = 69 Gy Clinical target volume 30 × 2.2 = 66 Gy Level Ib–V L+R 30 × 1.7 = 51Gy
	Six sessions of carboplatin, capecitabine, cetuximab
Neck, level II left Ulcerative lesion	Neck, multiple cutaneous metastases
Pain of localized skin area	Pain and disfiguring sight

In the palliative setting, a single-session, minimally invasive, and relatively safe treatment is desirable. Intra-tumoral injections with ^{166}Ho-microspheres are minimally invasive and seem to be safe. Only slight discomfort during needle insertion was experienced. No discomfort related to radiation was experienced during follow-up. In addition, no systemic side effects were observed, or expected, as post-treatment imaging did not show activity outside the tumor.

There were some subjective improvements in tension and pain in the tumor region of all patients; however, objective efficacy (i.e. reduction in the size of the targeted metastasis) was not observed. The tissue penetration of the beta-radiation of ^{166}Ho is limited and 90% of the dose is absorbed in the first 2.1 mm.[20] Subsequently, the efficacy is probably strongly related to an appropriate dose distribution. The microspheres distribution therefore needs to be homogeneous for antitumor efficacy and the absorbed radiation dose should sufficiently cover all areas of vital and proliferating tumor tissue. In contrast, however, post-treatment SPECT/CT imaging showed a non-homogenous distribution of^{166}Ho-microspheres after the injections (Figure 6.2). This could explain tumor progression in patient 1, albeit decreased metabolic activity on PET/CT dorsocaudally in the tumor, consistent with the area of higher microsphere density on SPECT/CT. In patient 3, the absorbed dose was high enough and the distribution seemed sufficient for inhibition of tumor growth, although size reduction of targeted metastases was not observed.

An accurate selection of patients for ^{166}Ho-microspheres treatment seems important. Treatment of a large, cyst-like lymph node metastasis with central necrosis resulted in precipitation of microspheres inside the tumor of patient 1. In patient 2, the injection of ^{166}Ho-microspheres proved difficult because of obstruction of the syringes. It was initially hypothesized that precipitation and agglomeration of ^{166}Ho-microspheres could have resulted in obstruction of (smaller) needles. However in patient 2, also the larger 21 G needles seemed obstructed/occluded. With the multisizer (Multisizer 3; Beckman Coulter Life Sciences, Indianapolis, Indiana, USA) (data not shown) and under a microscope, no agglomerations of ^{166}Ho-microspheres were detected in the suspension. Therefore, difficulty in injecting the ^{166}Ho-microspheres suspension was probably caused by a high intra-tumoral pressure in the firm consistency of the tumor in patient 2. As an increased pressure force can result in needle dislodgement, the injection position was sometimes changed in case of high resistance in the veterinary experience.[13] In patient 3, with soft cutaneous metastases without large ulceration, the injection procedure was feasible. However, in the case of a skin ulcer, some precaution is necessary to prevent a potential spill of activity through the skin defect.

On the basis of the current experience, the absence of significant side effects, and lack of other treatment options, an intra-tumoral injection with ^{166}Ho-microspheres deserves further investigation. Therefore, the following considerations are suggested to improve the efficacy of future ^{166}Ho-microspheres treatments. Patients with relatively small, soft, and superficial tumors seem more amenable for ^{166}Ho-microspheres treatment in comparison with patients with large necrotic or indurated tumors. In addition, the focus should be directed toward the vital tumor edge, and peritumoral injections of the tumor bed should be considered. Furthermore, the main advantage of ^{166}Ho over other high-energy beta-emitting radionuclides for local treatment is its visibility on SPECT, CT, and MRI. This should be used for imaging of the ^{166}Ho-microspheres distribution and dosimetry.[21–23] The distribution of ^{166}Ho-microspheres must be a priority in future studies, and the effect of injection volume, the amount of microspheres, and injection locations should be investigated. When image-guided feedback is used, the dose distribution can be improved and treatment efficacy will likely improve. In addition, the aid of robotic administration systems[24] could allow for quicker and more accurate needle placement.

CONCLUSION

Intra-tumoral injections with ^{166}Ho-microspheres seem to be feasible as a single-session, minimally invasive, and relatively safe treatment in the palliative setting for heavily comorbid HNSCC patients. Improving patient selection, administration techniques, and use of real-time high-resolution imaging is necessary to optimize the dose distribution. Considering the suggested improvements and the absence of side effects, this palliative microbrachy treatment may be of additional value in a specific group of HNSCC patients.

ACKNOWLEDGEMENTS

R.C. Bakker is funded by the Dutch Cancer Society research grant: 2014–7075.

CONFLICT OF INTEREST

J.F.W. Nijsen is co-founder and scientific director of Quirem Medical B.V., and has a minority share in the company Quirem Medical B.V. Furthermore, Nijsen is inventor on the patents related to the ^{166}Ho-PLLA-microspheres, which are assigned to University Medical Center Utrecht Holding B.V. (patent numbers: O2012060707 A1 and US 2005/0201940 A1). The Department of Radiology and Nuclear Medicine of the University Medical Center Utrecht receives royalties from Quirem Medical B.V. M.G.E.H. Lam is consultant for Sirtex, BTG, Mirada and Bayer Healthcare. For the remaining authors there are no conflicts of interest.

Table 6.2. Treatment characteristics

	Patient 1			Patient 2		
Number of injections	2			4 (only 2 performed)		
Amount of volume (mL)	0.5			0.5		
Amount of Ho-microspheres (mg)	100			100		
Planned activity (MBq)	200			30		
Tumor						
Injected		Activity	Percentage		Activity	Percentage
Total		366.7	92.5		3.3	9.5
Syringe 1		182.9	92.0		1.4	8.7
Syringe 2		183.8	93.0		1.9	10.3
Syringe 3						
Syringe 4						
Syringe 5						
Leakage						
Administered (MBq)	366.7			3.3		
Tumor volume (cm^3)	44.6			4.0		
Absorbed dose (Gy)	130			13		
SPECT/CT detected		Activity	Percentage			
		309.2	84.3			
Follow-up						
Side effects CTCAE 4.03	Pain: grade I			Pain: grade I		
Efficacy RECIST 1.1	Stable disease at 1 month on ^{18}F-FDG-PET/CT Decreased uptake in the caudal part of the lesion					
Efficacy subjective				Less skin tension		
Observations/remark	Precipitating of microspheres in necrotic/liquid filled lymph node			Solid malignancy, inability to inject		
Survival	2 months			6 days		
Cause of death	PD → aspiration pneumonia → respiratory insufficiency			PD → respiratory insufficiency		

CTCAE: Common Terminology Criteria for Adverse Events, CT: computed tomography; ^{18}F-FDG: fluorine-18-fluorodeoxyglucose, Ho-microspheres: holmium microspheres; MBq: megabecquerel

Patient 3						
10						
0.2						
250						
75						
	Right		Left		Total	
	Activity	Percentage	Activity	Percentage	Activity	Percentage
	67.0	90.8	68.6	91.2	135.6	91.2
	12.7	90.6	14.5	90.9		
	12.6	91.0	14.5	92.0		
	14.3	92.8	13.9	93.2		
	14.0	88.1	13.1	91.4		
	13.5	92.2	14.3	90.1		
	3.2	4.7	14.7	21.4	17.9	13.2
	63.8		53.9		117.7	
	6.1		5.6			
	165		153			
	16.9	26.5	9.6	17.8	26.7	22.7
Pain: grade						
Stable disease at 2 weeks						
Less pain and friction						
External leakage ulcerative lesion						
44 days						
PD → respiratory insufficiency						

Gy: Gray, RECIST: response evaluation criteria in solid tumors, SPECT: single-photon emission computed tomography, PD: progressive disease.

Figure 6.4. *Patient 3. A, B: Tumor 3 weeks prior to treatment, C, D: Tumor 2 days after treatment, E, F: Tumor 8 days after treatment, G, H: Tumor 15 days after treatment.*

REFERENCES

1. Bourhis J, Le Maître A, Baujat B, Audry H, Pignon JP. Individual patients' data meta-analyses in head and neck cancer. Curr Opin Oncol 2007;19:188–194.
2. Brockstein B, Haraf DJ, Rademaker AW, Kies MS, Stenson KM, Rosen F, et al. Patterns of failure, prognostic factors and survival in locoregionally advanced head and neck cancer treated with concomitant chemoradiotherapy: A 9-year, 337-patient, multi-institutional experience. Ann Oncol 2004;15:1179–1186.
3. Posner MR, Hershock DM, Blajman CR, Mickiewicz E, Winquist E, Gorbounova V. Cisplatin and Fluorouracil Alone or with Docetaxel in Head and Neck Cancer, N Engl J Med. 2007;357:1705–1715.
4. Spencer S, Harris J, Wheeler R, Machtay M, Schultz C, Spanos W, et al. Final report of RTOG 9610, a multi-institutional trial of reirradiation and chemotherapy for unresectable recurrent squamous cell carcinoma of the head and neck. Head Neck. 2008:30:281.
5. J. Tortochaux, Y. Tao, E. Tournay, M. Lapeyre, F. Lesaunier, E. Bardet, et al. Randomized phase III trial (GORTEC 98–03) comparing re-irradiation plus chemotherapy versus methotrexate in patients with recurrent or a second primary head and neck squamous cell carcinoma, treated with a palliative intent, Radiother Oncol 2011;100:70–75.
6. Rwigema JC, Heron DE, Ferris RL, Gibson MK, Quinn A, Yang Y, et al. Fractionated Stereotactic Body Radiation Therapy in the Treatment of Previously-Irradiated Recurrent Head and Neck Carcinoma. Am J Clin Oncol. 2010;30:286–93.
7. Colevas AD. Chemotherapy options for patients with metastatic or recurrent squamous cell carcinoma of the head and neck, J Clin Oncol. 2006;24:2644–2652.
8. Sacco AG, Cohen EE. Current treatment options for recurrent or metastatic head and neck squamous cell carcinoma. J Clin Oncol. 2015;33:3305–3315.
9. Bartochowska A, Skowronek J, Wierzbicka M, Leszczynska M, Szyfter W. Is there a place for brachytherapy in the salvage treatment of cervical lymph node metastases of head and neck cancers? Brachytherapy. 2015;14:933–938.
10. Bertino G, Sersa G, De Terlizzi F, Occhini A, Plaschke CC, Groselj A, et al. European Research on Electrochemotherapy in Head and Neck Cancer (EURECA) project: Results of the treatment of skin cancer, Eur J Cancer. 2016;63:41–52.
11. Tijink BM, De Bree R, Van Dongen GAMS, Leemans CR. How we do it: Chemo-electroporation in the head and neck for otherwise untreatable patients. Clin Otolaryngol. 2006;31:447–451.
12. Smits MJL, Nijsen JFW, van den Bosch MAAJ, Lam MGEH, Vente MAD, Mali WPTM, et al. Holmium-166 radioembolisation in patients with unresectable, chemorefractory liver metastases (HEPAR trial): A phase 1, dose-escalation study. Lancet Oncol 2012;13:1025–1034.
13. van Nimwegen SA, Bakker RC, Kirpensteijn J, van Es RJJ, Koole R, Lam MGEH, et al. Intratumoral injection of radioactive holmium (^{166}Ho) microspheres for treatment of oral squamous cell carcinoma in cats. Vet Comp Oncol. 2017;0:1–11.
14. van Es RJJ, Nijsen JWF, van het Schip AD, Dullens HF, Slootweg PJ, Koole R. Intra-arterial embolization of head-and-neck cancer with radioactive holmium-166 poly(L-lactic acid) microspheres: an experimental study in rabbits. Int J Oral Maxillofac Surg 2001;30:407–413.
15. Zielhuis SW, Nijsen JFW, De Roos R, Krijger GD, Van Rijk PP, Hennink WE, et al. Production of GMP-grade radioactive holmium loaded poly(L-lactic acid) microspheres for clinical application, Int J Pharm. 2006;311:69–74.
16. Bult W, De Leeuw H, Steinebach OM, Van Der Bom MJ, Wolterbeek HT, Heeren RMA, et al. Radioactive holmium acetylacetonate microspheres for interstitial microbrachytherapy: An in vitro and in vivo stability study. Pharm. Res. 2012;29:827–836.
17. Vente MAD, Nijsen JFW, de Wit TC, Seppenwoolde JH, Krijger GC, Seevinck PR, et al. Clinical effects of transcatheter hepatic arterial embolization with holmium-166 poly(L-lactic acid) microspheres in healthy pigs. Eur J Nucl Med Mol Imaging. 2008;35;1259–71.
18. Eisenhauer EA, Therasse P, Bogaerts J, Schwartz LH, Sargent D, Ford R, et al. New response evaluation criteria in solid tumors: Revised RECIST guideline (version 1.1). Eur J Cancer 2009;45:228–247.
19. Common Terminology Criteria for Adverse Events v4.0. NCI, NIH, DHHS. (n.d.).
20. Nijsen JFW, Krijger GC, van Het Schip AD. The bright future of radionuclides for cancer therapy. Anticancer Agents Med Chem. 2007;7:271–290.
21. Van De Maat GH, Seevinck PR, Elschot M, Smits MLJ, De Leeuw H, van het Schip AD, et al. MRI-based biodistribution assessment of holmium-166 poly(L-lactic acid) microspheres after radioembolisation. Eur Radiol 2013;23:827–835.
22. Bult W, Kroeze SGC, Elschot M, Seevinck PR, Beekman FJ, de Jong WHAM, et al. Intratumoral administration of holmium-166 acetylacetonate microspheres: antitumor efficacy and feasibility of multimodality imaging in renal cancer. PLoS One. 2013;8:e52178.
23. Smits MLJ, Elschot M, van den Bosch MAAJ, van de Maat GH, van het Schip AD, Zonnenberg BA, et al. In vivo dosimetry based on SPECT and MR imaging of ^{166}Ho-microspheres for treatment of liver malignancies. J. Nucl. Med. 54 (2013) 2093–100.

24. Arnolli MM, Hanumara NC, Franken M, Brouwer DM, Broeders IAMJ. An overview of systems for CT- and MRI-guided percutaneous needle placement in the thorax and abdomen. Int. J. Med. Robot. 11 (2015) 458–75.


7

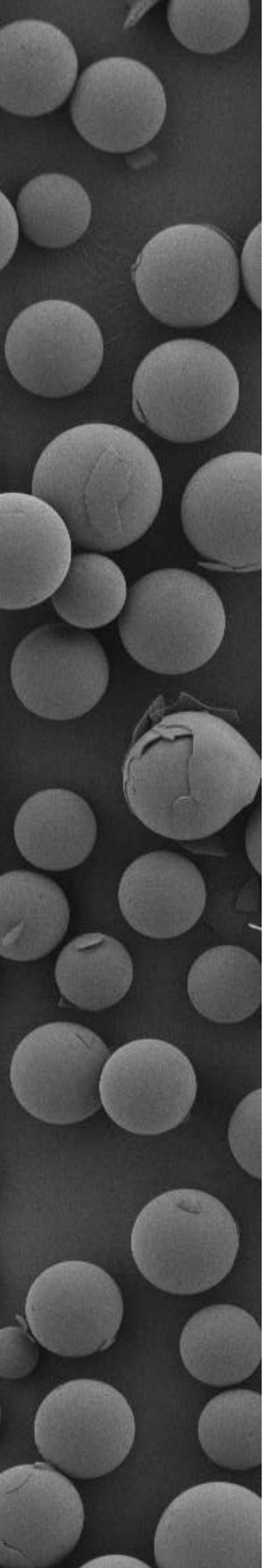

Feasibility of unenhanced CT quantification of holmium microspheres for treatment of local tumors

R.C. Bakker

R. Bastiaannet

S.A. van Nimwegen

A.D. Barten

R.J.J. Van Es

A.J.W.P. Rosenberg

H.W.A.M de Jong

M.G.E.H. Lam

J.F.W. Nijsen

Submitted

ABSTRACT

Introduction

Radioactive holmium-166 (^{166}Ho) loaded microspheres are a novel particle for radioembolization and intra-tumoral treatment. Personalized intra-tumoral treatment of solid malignancies relies on accurate quantitative imaging of the microsphere distribution because of the limited penetration of beta-radiation. Unenhanced CT imaging could provide superior resolution and fast imaging of the distribution of these microspheres, with lower costs and universal availability in comparison with the current standard, SPECT and MRI imaging. This pilot study investigates the feasibility of CT quantification.

Methods

Unenhanced CT quantification was performed on a phantom with various concentrations of holmium chloride and holmium microspheres to calibrate CT-detection and investigate the sensitivity. The holmium microspheres were injected into ex-vivo tissue, in subcutaneous VX-2 tumor-bearing rabbits, and in patients with head-neck cancer to demonstrate the visibility and sensitivity in a clinical set-up. The amount of holmium in tissue was determined by CT using a density-based threshold method and compared with a validated ^{166}Ho SPECT/CT quantification method.

Results

In the phantom, near perfect linearity (least-squares $R^2>0.99$) between Hounsfield Units and concentration of holmium was found. Ex-vivo tissue experiments showed an excellent correlation ($r=0.99$ $p<0.01$) between the dose calibrator, SPECT/CT, and CT imaging. CT recovery was on average 86.4% ex vivo, 76.0% in animals and 99.1% in human patients.

Conclusion

The current study shows that CT-based quantification of holmium microspheres seems feasible and may be a high-resolution alternative to SPECT for local distribution.

INTRODUCTION

A relatively new oncological treatment option is selective internal radiation therapy (SIRT, or radioembolization) with small radioactive particles. Radioactive holmium-166 (^{166}Ho) loaded (poly L-lactic acid) microspheres (^{166}Ho-microspheres) were developed for radioembolization of liver tumors through intra-arterial injection.[1] These ^{166}Ho-microspheres have a mean diameter of 30 μm and emit high-energy beta particles for tumor treatment and also gamma radiation, which allows for quantitative single-photon emission computed tomography (SPECT) imaging.[2,3] In addition, holmium is paramagnetic, which allows for magnetic resonance imaging (MRI). Both imaging modalities are used in radioembolization to investigate the holmium microsphere distribution.[1,3,4]

The intra-tumoral injection of radioactive microparticles might be beneficial for selected patients with local tumors that can be reached with a needle.[5–8] This kind of "microbrachytherapy" might have advantages, including minimally invasive handling, outpatient treatment, and potentially improved (progression-free) survival and quality of life.[5,8,9] In patients with unresectable hepatocellular carcinoma, 12 weeks after intra-tumoral injection of radioactive phosphorus-32 microparticles treatment, all tumors showed response with a complete remission in 25% of the lesions.[7] The first experience with ^{166}Ho-microspheres in recurrent head and neck cancer patients showed the minimally invasive character and relative safety of this treatment but also revealed challenges in obtaining a homogeneous absorbed dose and sufficient tumor coverage.[8] Intra-tumoral treatment with ^{166}Ho-microspheres has also been conducted in several animal studies.[6,10–12] In 13 companion animals (cats) with spontaneous inoperable oral squamous cell carcinomas, a local response rate of 55% was obtained with minimal side effects.[6] The distribution of ^{166}Ho-microspheres in these animals was imaged with planar scintigraphy in the absence of SPECT or MRI. During the follow-up, unenhanced computed tomography (CT) imaging clearly showed the distribution of these microspheres.[6]

CT imaging could offer quicker and higher-resolution feedback on the three-dimensional (3D) distribution of these microspheres compared to SPECT and MRI, apart from being more widely available and relatively low-cost. CT may be used to confirm that a homogeneous absorbed dose and sufficient tumor coverage was achieved, and eventually facilitate an image-guided treatment approach. The purpose of this pilot study was to assess the feasibility of ^{166}Ho-microspheres quantification using CT.

METHODS

Holmium microspheres preparation

Non-radioactive ^{165}Ho-microspheres were prepared as previously described.[13] Neutron activation of the holmium-loaded microspheres was performed via the ^{165}Ho [n,γ] ^{166}Ho reaction in a nuclear reactor with a nominal thermal neutron flux of 5×10^{12} cm^{-2} s^{-1} (Delft University of Technology). Therefore, vials with known amounts of ^{165}Ho-microspheres were irradiated up to two hours. After neutron activation, ^{166}Ho-microspheres emit beta radiation for tumor ablation ($E_{\beta, max}$ = 1.84 MeV), and gamma radiation for imaging (E_{γ} 80.6 keV, 6.71%) and has a half-life time of 26.8 hours. In the preclinical and rabbit experiments a batch of 18.7% (w/w) and in the human patients, a batch of ^{166}Ho-microspheres with a holmium content of 17.6% (w/w) was used, corresponding to approximately 1 mg of holmium per 5.5 mg ^{166}Ho-microspheres.

Phantom for calibration of holmium on CT imaging

To quantify ^{165}Ho-microspheres on CT imaging, series of holmium chloride ($HOCl_3$) and ^{165}Ho-microspheres concentrations were made to create a calibration curve. A serial dilution (n=10) of holmium(III)chloride hexahydrate ($HoCl_3 \bullet 6\ H_2O$ Sigma-Aldrich Chemie N.V.) was made in sterile demineralized water (Versylene, Fresenius Kabi, B.V.) to obtain a homogeneous solution (range 0.0008–0.06 mmol/mL holmium). Therefore, a stock solution was prepared of 0.06 mmol/mL holmium, mixed for 5 minutes, and diluted by adding demineralized water. The concentration of the solutions was corrected for the mass percentage of holmium of the $HoCl_3$ (43.47%).

Two batches of ^{165}Ho-microspheres, mass percentage 18.7 and 17.6%,[14] were weighted (1200 mg) (Mettler Toledo™ NewClassic ME Analytical Balances) and suspended in the injection solution containing 116 mmol phosphate (pH 7.2) buffered saline (PBS) with polyoxyethylene-polyoxypropylene block copolymer (Pluronic F-68, Sigma-Aldrich Chemie N.V.) 2% weight per volume solution, and then diluted to ten concentrations (range 0.25–20.0 mg/mL^{165}Ho-microspheres or 0.0016–0.12 mmol/mL holmium) of ^{165}Ho-microspheres. The ^{165}Ho-microspheres solutions were subsequently mixed 1:1 with a 2% agar (MP Agar, Roche Diagnostics) solution to prevent settling due to the weight of these holmium microspheres (1.4 g/mL). Therefore, the agar powder was dissolved in sterile water (Versylene, Fresenius Kabi, B.V.) and heated to 90°C for 10 minutes, resulting in a transparent fluid. Subsequently, a 5 mL Eppendorf tube was filled with 5 mL of the homogeneously distributed holmium microspheres in agar solution in a series (n=10) with a concentration ranging from 0.125–10.0 mg/mL holmium. Once cooled to room temperature in approximately 5 minutes of continuous rotation to prevent settling, the agar became solid.

Administration of ^{166}Ho-microspheres ex vivo and in vivo

The radioactive ^{166}Ho-microspheres with a known specific activity (Bq/mg) were suspended in a solution of 2% (w/v) Pluronic® F-68 in a 116 mmol phosphate (pH 7.2) buffer by gentle agitation and repeatedly drawing up and down in a 1 mL Luer-lock syringe (Becton Dickinson S.A.). The injections of the ^{166}Ho-microspheres were performed with a 1 mL Luer-lock syringe through a 21G*1½" (0.8 × 40 mm) hypodermic needle (Becton Dickinson S.A.). The activity of the ^{166}Ho-microspheres inside the syringes was measured using a calibrated dose calibrator (VDC-404; Veenstra Instruments). The injection procedures were performed by the intratumoral holmium research team. Ex-vivo, in laboratory animals (and previously in veterinary animal patients) the injections were performed by RCB, FN, BvN. In the human setting the injections were performed under ultrasound guidance by ML (Nuclear Physician) assisted by other members of the team.

Ex-vivo tissue

The feasibility of unenhanced CT quantification was evaluated in five samples of ex-vivo chicken muscle tissue. Syringes with approximately 0.2 mL of ^{166}Ho-microspheres suspension with increasing activity ranging from 15 to 81 MBq (corresponding to concentrations 3.4 to 18.4 mg holmium) were injected into the tissue samples. The actually injected mg of holmium was determined by the injected activity. To determine the injected activity, the syringes (before and after injection), the gauze with potential injection channel leakage, and the tissue sample were measured in the dose calibrator. Based on these measurements, the known specific activity of the ^{166}Ho-microspheres, and the weight and mass percentage of the ^{166}Ho-microspheres, the injected mg of holmium was calculated.

Laboratory Animals

All experiments were performed in agreement with 'The Netherlands Experiments on Animals Act' (1977) and 'The European Convention for the Protection of Vertebrate Animals used for Experimental Purposes' (Strasbourg, 18.III.1986). Approval was obtained from the Utrecht University Animal Experiments Committee (DEC 2011.III.08.080).

The VX-2 tumor model in New Zealand white (NWZ) rabbits was described previously.[15] In short, in one animal, the donor rabbit, a tumor was induced by injection of a suspension of approximately 4.0×10^7 VX-2 carcinoma cells subcutaneously into both flanks of the rabbit. Single tumors were induced in the rabbits by harvesting the tumor from the donor rabbit and subcutaneous injection of three ± 1 mm^3 viable fragments of VX-2 carcinoma with 0.1-0.3 mL PBS into the flank of five adult female NZW rabbits weighing 3–4 kg. All tumor implantations and treatments were performed under analgesia with carprofen 4 mg/kg. During the animal experiments, sedation and analgesia were achieved with a mixture of 0.125 mg/kg dexdomitor and 15 mg/kg ketamine.

After the intra-tumoral injection of 0.2 mL ^{166}Ho-microspheres suspensions, an unenhanced CT was performed according to the clinical protocol described below. In rabbit number five, higher amounts of activity (57.9 MBq) were injected for comparison to quantitative SPECT imaging and depositions outside the tumor. The SPECT/CT analyses were compared to the injected mg holmium, which was determined by the injected activity as described above.

Between 2015 and 2017, four patients with head and neck cancer were referred by their head and neck oncologist. Three patients were treated in a salvage setting. If no palliative treatment options were available, and nonetheless a strong wish for treatment existed, patients were amenable for direct intra-tumoral injections of ^{166}Ho-microspheres, with the aim of improving the patients' quality of life. One patient was part of a prospective clinical pilot study (NCT02975739).[7] All patients provided informed consent before treatment. Immediately after the ultrasound-guided injection procedure, consisting of two to four intra-tumoral injections containing a total of 100 mg of ^{166}Ho-microspheres, a SPECT, high-dose CT and planar scintigraphy of thorax and abdomen (imaging time 300 seconds) were performed. Informed consent was obtained from all patients and the medical ethical committee of the University Medical Center Utrecht approved this study and retrospective analysis of the patients treated in a salvage setting.

CT and SPECT/CT

All CT and SPECT/CT imaging was performed using a Siemens Symbia T16 SPECT/CT system, that combines a dual-headed gamma camera with a 16-slice CT system. The acquisition parameters were identical to a clinical diagnostic high dose CT of the head and neck region: tube voltage 110 kVp, tube current 225 mAs effective; detector configuration, 16 × 0.6 mm; rotation time, 0.6 seconds; helical scan mode; pitch, 1.0. The images were reconstructed with a 1.5 mm slice thickness with a 0.7 mm increment (voxels size 0.56 × 0.56 × 0.7 mm) and a B31s medium smooth reconstruction kernel.

Medium-energy low-penetration collimators were used on both SPECT cameras. Energy windows were set at 80.6 keV (15% window width) for the ^{166}Ho photopeak. A total of 120 projections of 30 seconds were acquired in a 360° non-circular orbit. Quantitative image data were reconstructed to a 128^3 matrix with an isotropic voxel size of 4.8 mm^3. The reconstructions were performed using previously validated Monte-Carlo based reconstruction software[2,16] using an ordered subsets expectation maximization algorithm (10 iterations with 8 subsets) and a quantitatively correct forward model, resulting in an absolute quantitative 3D activity distribution in MBq/voxel.[2] Based on the detected activity and the specific activity of the microspheres, the absolute amount of holmium was calculated.

Data analysis

The CT data were analyzed with ImageJ version 1.50b. In the phantom of both $HoCl_3$ and Ho-microspheres, a circular Region of interest (ROI) with a diameter of 10 mm in the centre of the 5 mL Eppendorf tube was drawn. This ROI was applied over 30 slices to create a 3D ROI of 1.6 cm^3. Subsequently, the mean ± standard deviation (SD) Hounsfield unit (HU) value of this ROI was calculated. A scatterplot of the observed HU against the calculated concentration was made to obtain a calibration curve.

In the chicken muscle tissue experiments, an ROI was drawn in an area without microspheres. From this ROI the mean ± SD and maximum HU were obtained. In the animals and patients, the tumor volume was manually segmented on CT by the investigator (RCB). Based on the literature, it was assumed that all tumor voxels had a HU between -50 and 100,[17] and that all voxels with a HU >100 contained holmium microspheres. The amount of holmium was calculated using the following strategy:

- All voxels with a HU >100 were selected and divided by the HU/concentration calibration curve, to obtain a concentration of mg/mL/voxel.
- This concentration was multiplied by the voxel volume (0.22 mm^3) to calculate the absolute amount of holmium per voxel.
- The total sum of these voxels resulted in the total amount of holmium in mg.

Continuous data are presented as the mean ± standard deviation (SD) if normally distributed and as the median (min–max) if skewed (Shapiro-Wilk test). A Pearson correlation coefficient between the dose calibrator, CT, and SPECT quantification was calculated if normally distributed and spearman rank-order correlation if skewed. Agreement between the measurements was calculated using an intraclass correlation (ICC) ± 95% confidence interval (Two-way mixed effects, absolute agreement) if normally distributed and as relative difference if skewed. SPSS software (SPSS for Windows, version 22.0; SPSS Inc.) was used for all analysis.

RESULTS

Phantom for calibration of holmium on CT imaging

The holmium concentration of the two ^{165}Ho-microspheres solutions and the $HoCl_3$ solution ranged from 0 to approximately 10 mg/mL. Holmium solutions with increasing holmium concentration resulted in increased HU from around zero, up to approximately 370 HU (Table 7.1). The slope of the regression of the three holmium series was 36.9, 37.0 and 37.2 HU per mg/mL of holmium atoms, for the 18.7% and 17.6% ^{165}Ho-microspheres solution and the $HoCl_3$ solution, respectively. (Figure 7.1C). The linear regression between holmium in mg/mL

and the HU showed a good fit (least-squares R^2>0.99) for all series (Figure 7.1), without a significant difference between the three lines.

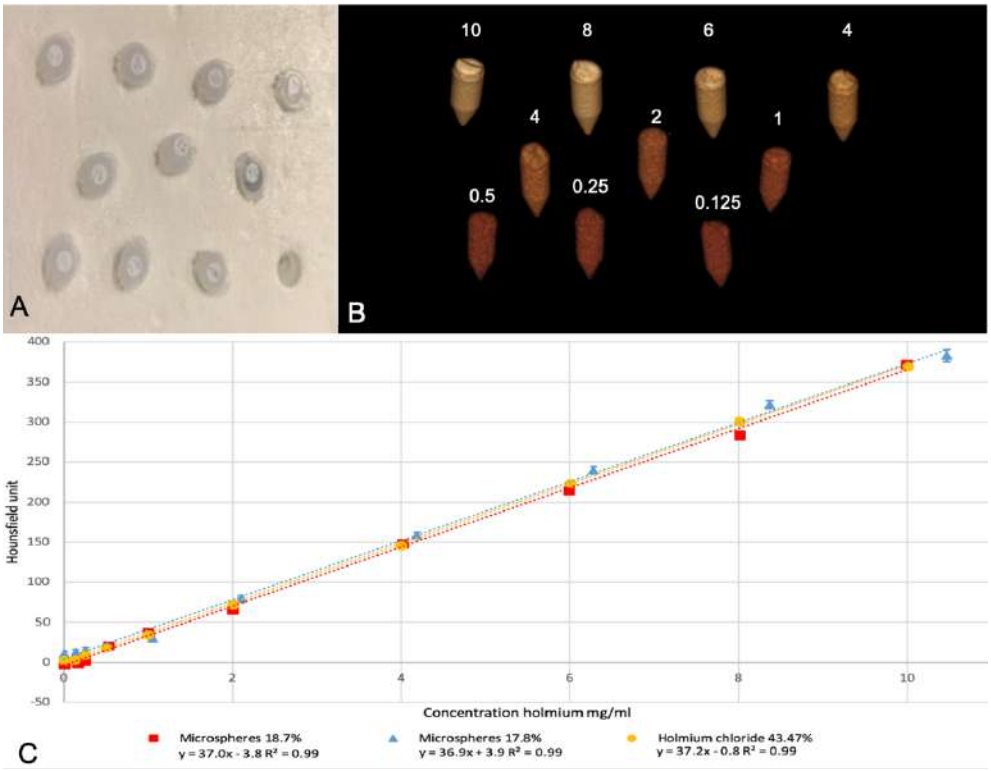

Figure 7.1. *Phantom A: Photo of the phantom setup of ten 5 mL Eppendorf tubes in styrofoam. B: 3D CT-reconstruction of the phantom showing the increasing concentration of HU. C: Regression slopes of obtained HU by the calculated concentration holmium in mg/mL.*

Injections with holmium microspheres

Ex-vivo tissue

The feasibility of unenhanced CT quantification was tested in ex-vivo chicken muscle tissue. Based on the literature, a threshold of 100 HU was used.[17] The ROIs of the chicken muscle tissue without holmium showed a mean HU of 71.2 (SD 6.2–7.9) with a maximum observed HU of 96. The chosen cut-off value of >100 HU was more than the maximum observed HU and more than three times the SD of chicken muscle tissue.

The validated ^{166}Ho-SPECT was tested with 5 mL Eppendorf tubes filled with known activities showing a relative difference of -2.9–1.8%. The SPECT/CT detected 94.6 ± 4.9% of the injected activity in the tissue (Table 7.2). There was a strong positive correlation between the injected activity and the detected activity by SPECT/CT, r=0.99, n=5, p<0.01 with an ICC of 0.99 (0.86–1.0).

After injection, the total volume of voxels with a >100 HU varied between 0.3–1.5 cm^3. A positive correlation was observed between the volume and the amount of injected holmium, r=0.90, n=5, p=0.04. Using the simple method described above, 81.5 ± 6.7% of the holmium was recovered using CT (Table 7.2).

Table 7.1. Concentration of holmium and measured Hounsfield units

Holmium microspheres (18.7%) in agar		Holmium microspheres (17.6%) in agar		Holmium chloride (43.47%) in water	
Holmium (mg/mL)	HU Mean (SD)	Holmium (mg/mL)	HU Mean (SD)	Holmium (mg/mL)	HU Mean (SD)
0.00	-2.6 (8.0)	0.00	10.1 (7.5)	0.00	1.9 (6.6)
0.16	-0.7 (9.9)	0.14	12.5 (7.1)	0.13	3.4 (6.5)
0.25	2.2 (6.9)	0.26	15.3 (6.1)	0.25	9.5 (5.8)
0.53	20.8 (6.8)	0.52	20.9 (7.6)	0.50	18.4 (7.1)
1.00	37.3 (7.1)	1.05	30.3 (8.8)	1.00	34.1 (6.9)
2.00	65.9 (7.1)	2.10	79.9 (7.2)	2.00	72.2 (6.3)
4.02	148.2 (8.2)	4.19	158.4 (8.1)	4.00	145.7 (6.9)
5.99	215.3 (13.4)	6.28	239.7 (9.5)	6.01	223.4 (7.2)
8.01	283.9 (16.8)	8.37	321.4 (9.4)	8.01	301.1 (8.2)
9.99	372.4 (14.1)	10.47	383.1 (14.8)	10.01	370.0 (10.5)

Holmium quantification in a Phantom The observed Hounsfield units for the 5mL Eppendorf tubes with a concentration ranging from approximately 0 to 10 mg/mL holmium microspheres (18.7, 17.6%) and holmium chloride (43.47%) in Styrofoam (as seen in Figure 7.1) measured on a Siemens Symbia T16.

The total volume of voxels with a HU >100 varied between 0.3–1.5 cm^3. A positive correlation was observed between the volume and the amount of injected holmium, r=0.897, n=5, p=0.04. Using this simple method 81.5 ± 6.7% of the holmium was recovered (Table 7.2). There was a strong positive correlation between the injected activity and the detected activity by SPECT/CT, r=0.99, n=5, p<0.01. The SPECT/CT detected 94.6 ± 4.9% of the injected activity (Table 7.2).

Table 7.2. Injected and recovered holmium ex-vivo

	Injected holmium		SPECT recovery		CT recovery	
Tissue	MBq	mg	MBq	%	mg	%
1	81.1	18.0	75.9	93.6	16.1	89.8
2	73.6	16.3	67.6	91.9	13.2	81.0
3	40.3	8.9	36.5	90.6	7.3	81.7
4	24.4	5.4	23.1	94.7	4.4	81.5
5	15.4	3.4	15.6	101.3	2.5	73.8

Holmium recovery with SPECT and CT in ex-vivo tissue. Five samples of chicken muscle tissue were injected with radioactive microspheres ranging from 15.4–81.1 MBq with the corresponding amount of mg holmium. Based on the dose calibrator measurements, SPECT and CT imaging recovered 90.6–101.3% and 73.8–89.9%, respectively.

Laboratory Animals

19 days after VX-2-tumor implantation, five tumors (n=5) reached a diameter of approximately 20 mm in the rabbits (Table 7.3). The mean tumor volume was 4.8 ± 1.9 cm^3, (range 3.2–7.2 cm^3). The mean tumor HU was 31.6 (SD 11.4–16.5) with a maximum of 98 HU.

After the injection of ^{166}Ho-microspheres, areas with high attenuation were seen inside the tumor caused by the accumulation of holmium microspheres (Figure 7.2B). Analysis of the observed HU in the ROI pre and post-injection shows a right-skewed distribution due to voxels containing holmium. Accidental injection of air into rabbit 2 and 5 resulted in voxels with highly negative HU (e.g. -722 HU) observed as the left-skewed distribution. (Figure 7.2D) The volume of voxels with a >100 HU ranged between 0.1–0.5 cm^3 or 3–9% of the total tumor volume.

In these rabbits, 76.0 ± 15.4% (range 59.9–100.0%) of the administered holmium was recovered on CT (Table 7.3). A positive correlation between the injected amount and the recovered amount on CT was found ($r=0.97$, $n=5$, $p<0.03$) with an ICC of 0.89 (-0,15–0.99). The SPECT/CT analysis of rabbit 5, injected with 57.9 MBq of ^{166}Ho-microspheres, showed a clear hotspot at the tumor location. Depositions of activity were not seen outside the tumor (e.g., in the kidney or lung). The retrieved activity on the SPECT/CT was 54.3 MBq, (93.7% of injected activity).

Table 7.3. Laboratory animals

Rabbit	Injected holmium		Tumor volume	Volume >100 HU		Recovery CT		Recovery SPECT	
	MBq	Mg	cm^3	cm^3	%	mg	%	MBq	%
1	0.10	3.6	6.6	0.5	6.9	2.8	77.7	-	
2	0.07	2.2	6.0	0.2	3.5	1.3	59.9*	-	
3	0.04	1.4	7.2	0.2	3.2	1.1	76.9	-	
4	0.01	0.4	3.2	0.1	2.5	0.4	100	-	
5	57.9	2.9	3.4	0.3	9.1	1.9	65.4*	54.3	93.8%

*In vivo recovery in subcutaneous VX-2 tumor-bearing rabbits Five rabbits with subcutaneous VX-2 tumors were injected with decayed or radioactive microspheres with the corresponding amounts of holmium. The tumor volume ranged from 3.2 to 7.2 cm^3, based on de HU< 100 threshold 0.1–0.5 cm^3 or 2.5–9.1% of the tumor volume was filled with holmium after treatment. Recovery with CT was ranged between 59.9–100% (n=5) and SPECT recovery was 93.8% (n=1). *Evident collections of air on CT resulting in decreased detection of holmium due to partial volume effects and voxels with large negative HU.*

Patients

Four patients were treated with intra-tumoral ^{166}Ho-microspheres injections. (Table 7.4) One patient did not have SPECT/CT imaging available due to orthopnoea and was therefore not included in the analysis. Patient 2 was treated on both sides of the neck. The tumor volume of patients ranged from 3.9 to 44.6 cm^3 (Table 7.4). According to the dose calibrator the injected activity ranged between 17.6 and 366.7 MBq, which corresponded with an absorbed dose of 111 to 165 Gy. The total volume of voxels with a >100 HU ranged from 0.5 to 2.7 cm^3 or 6.1 to 23.1% of the tumor volume.

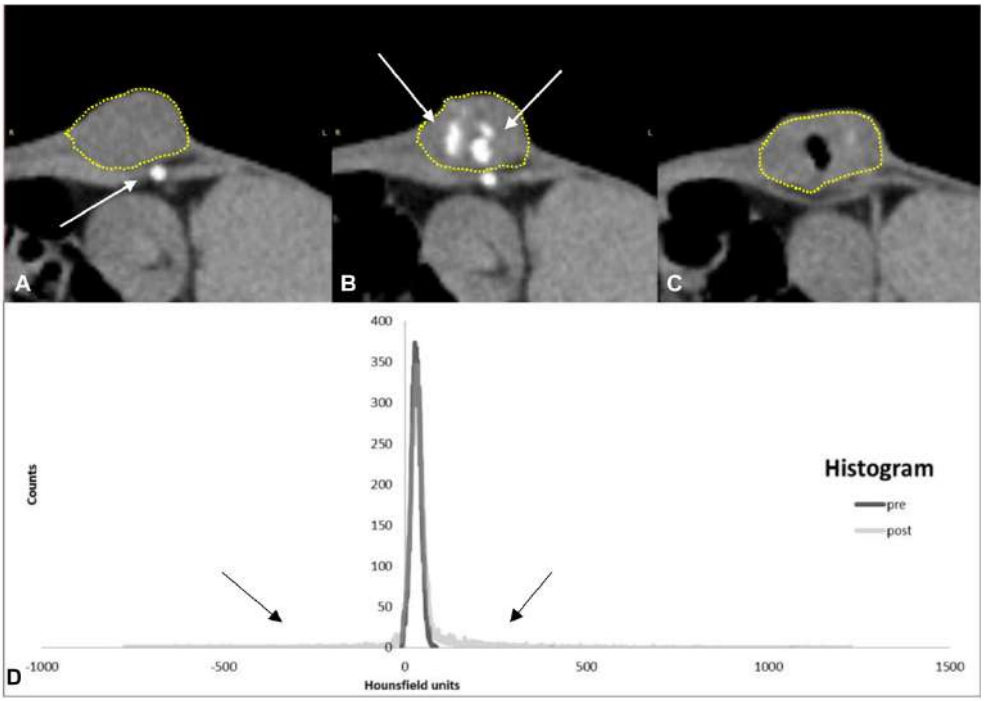

Figure 7.2. *Holmium quantification in a subcutaneous VX-2 bearing rabbit Rabbit 2. A: Tumor pre-injection. The tumor is segmented with a yellow dotted line. (White arrow shows a rib. The rib is also seen in figure 7.2B), B: Tumor post-injection with accumulations of holmium microspheres (seen as white dots, indicated with white arrows), C: Different axial slice showing the effect of inadvertent injection of air (black structure inside the tumor), D: Histogram of HU of the entire tumor pre and post-injection of radioactive holmium microspheres. The large negative (left of peak) and positive tail (right of peak) are caused by a relatively small number of voxels with injected air or holmium, respectively.*

In patient 1, ultrasound guidance showed precipitation of microspheres after injection indicating a liquified tumor centre. Unenhanced CT provided a clear distribution and accumulation of the ^{166}Ho-microspheres after injection as shown in figure 7.3. Compared to SPECT and MRI, the deposition of high concentrations of holmium is more accurately depicted on CT. CT could discriminated two separate distributions which merged on SPECT and MRI, and was able to quantify higher concentrations than MRI (Figure 7.4). The injected ^{166}Ho-microspheres resulted in local tumor necrosis at a microscopic level. (Figure 7.4)

The CT quantification method recovered 88.8% of the injected activity in patient number 1, while 84.3% was recovered by SPECT/CT (Table 7.4). Recovery of injected activity was much lower for patients 2 and 3, because of unknown leakage of activity after intra-tumoral injection. The CT recovery in all patients corresponded well (ϱ=1.0, n=4, $p<0.05$) with the intra-tumoral activity detected on SPECT with a relative difference of -6.3 to +4.5% (Table 7.4).

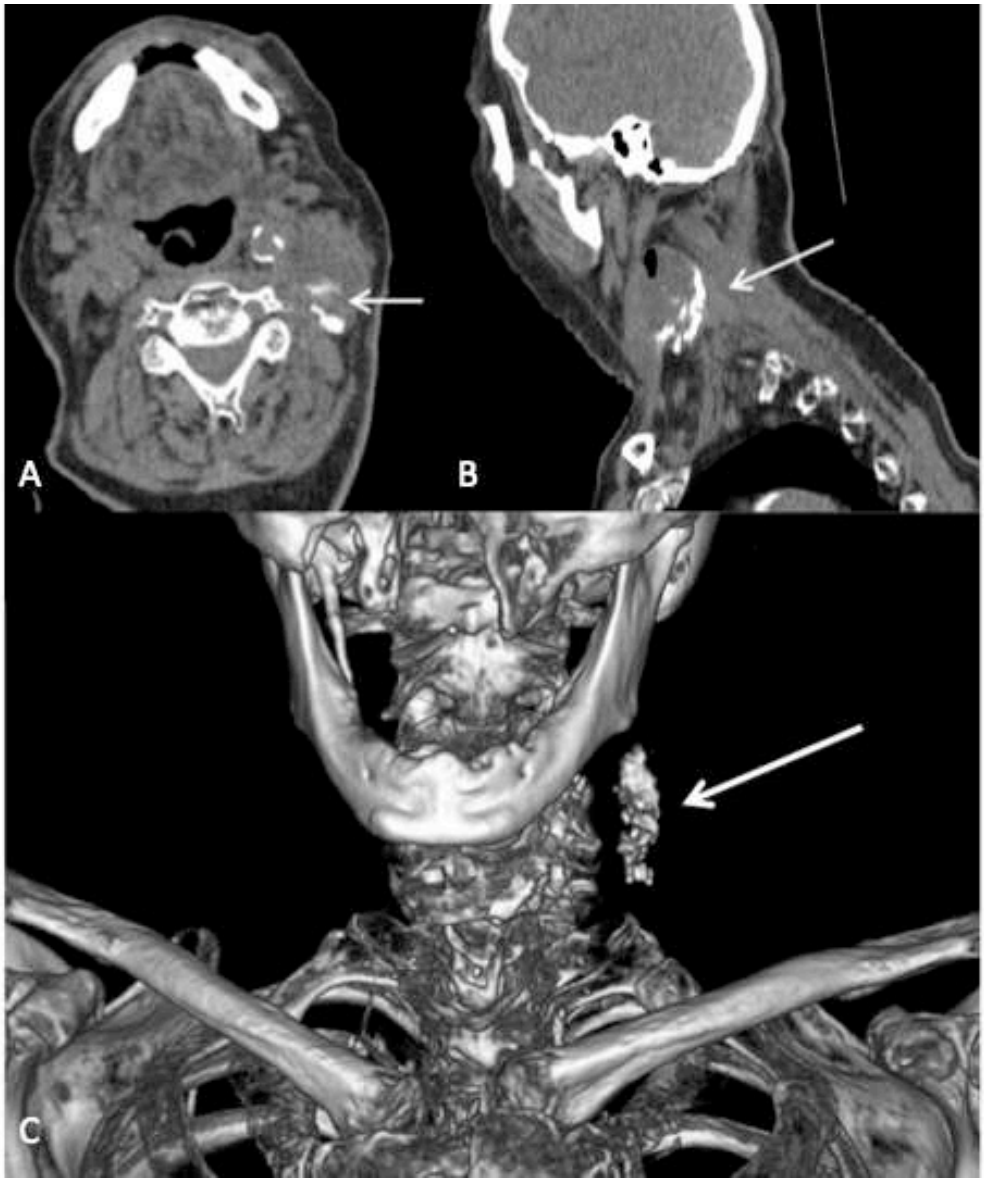

Figure 7.3. *CT images of Patient 1 A, B, C: Axial, sagittal and 3D CT reconstructions of patient 1 with a large necrotic tumor with fluid on the left side of the neck. After injection accumulations of holmium are clearly visible as white dots in the left neck area (see arrows). In addition, precipitating/ accumulation of holmium microspheres dorsocaudally in the tumor in this patient in supine position.*

DISCUSSION

This is the first report investigating the clinical feasibility of quantification of holmium microspheres using computed tomography. Unenhanced CT quantification may be of additional value to the currently used imaging modalities like MRI and SPECT imaging because of its superior resolution, the opportunity to perform real-time imaging, lower costs and universal availability. CT is especially interesting for rapid imaging feedback of the ^{166}Ho-microspheres distribution and to visualise potentially skipped areas during treatment. Based on the CT imaging during treatment the treatment can be optimized by injecting extra microspheres if a lethal absorbed dose is not reached or discontinue further administration if lethal dose is met or if undesired spread of activity is observed. After treatment it is advised to do combined SPECT/CT which allows for imaging of both the distribution but also detect possible minimal leakage outside the treated region.

Holmium has a high attenuation coefficient due to its high electron density (atomic number 67) and a K-edge (56 keV) close to the mean energy of the photons emitted in CT (63 keV at a tube voltage of 120 kV).[18] It has previously been shown that lanthanides like holmium have up to 50% higher X-ray attenuation than iodine in CT.[19] The phantoms with $HoCl_3$ and two batches of Ho-microspheres showed a comparable linear slope of 36.9–37.2 HU per mg/mL of holmium with a good linear fit suggesting that this regression can be used for the entire range of concentrations.

The feasibility of CT quantification was initially tested on ex-vivo muscle tissue. A threshold of 100 HU was used to derive quantification of holmium microspheres. This threshold of 100 HU was selected based on literature research,[17] and on the current data in this article. The maximum HU in ex-vivo muscle tissue was below 100. In addition, this was more than three times the SD of muscle tissue and segmented VX-2 tumors in rabbits. However, recovery of holmium up to 2.7 mg/mL (100 HU / 37.0 HU/mg/mL holmium) may be difficult. A lower threshold would lead to the detection of more holmium but would also result in the quantification of noise, while a higher threshold would result in a higher specificity at the cost of sensitivity. The used >100 HU thresholds remains arguable, nevertheless, using this simple quantification method, 59.9–100% of the injected microspheres were recovered.

There are several advantages of CT-based quantification compared to the current SPECT imaging. Primarily, more accurate assessment of the intra-tumoral distribution of microspheres because of a better spatial resolution of CT. The fact that the beta radiation of ^{166}Ho has an average range of only a few mm, and 90% of the dose is absorbed in 2.1 mm stresses the importance of high-resolution imaging.[20] Additional injections, based on the current microsphere distribution, could provide a more homogeneously absorbed dose, and subsequently a more favourable treatment outcome. CT can provide such high-resolution imaging in seconds, compared with 45 minutes for SPECT, enabling the real-time use of CT for

feedback for subsequent injections. Furthermore, in case of intra-tumoral treatment relative high radiation doses (200–800 Gy)[6] are used with higher concentrations of microspheres, which results in non-quantifiable artefacts on MRI as shown in figure 7.4.

The standard of reference for the quantification of ^{166}Ho-microspheres remains SPECT. First, because of the superior sensitivity at low amounts of activity compared with CT. Primarily in the case of accidental extra-tumoral deposition, voxels with low concentrations of holmium may not be discriminated from normal tissue HU variation on CT. The detection limit under optimal circumstances in a homogeneous solution for holmium with CT (0.057 mg/mL) is higher than that of SPECT (0.00054 mg/mL).[21] Furthermore, SPECT directly quantifies activity, while CT detects holmium metal, which is indirectly used to quantify activity by multiplying the amount of microspheres with the known specific activity.[21] On the other hand, the significantly lower resolution of SPECT has limited sensitivity for intra-tumoral inhomogeneities and provides only limited detail of the actual dose within the treated tumor.

The method presented in this work has several limitations. Foremost, the limited number of images available for analysis in this pilot study. Secondly, CT acquisition protocols, such as tube current, dose, image reconstruction kernels, and equipment, all have an impact on CT-based quantification and could be further optimized. The >100 HU threshold may not be the best threshold in each individual patient. In addition, tissue with high density, like bone, arterial calcification, or foreign bodies such as metallic artefacts and beam-hardening artefact could result in quantification errors on CT. In the presented patients, scatter artefacts were present, however, the effect was minimal at the tumor locations that were injected.

A more specific and sensitive method to determine the content of holmium per voxel is desired. Material decomposition with dual-energy and photon-counting CT may provide more specific and accurate quantification and is currently used for iodine CT quantification.[18,22] Combining the imaging opportunities for treatment planning and evaluation with accurate image-guided and robotic-assisted administration[23,24], may result in "dose painting" in which the planned dose is injected on the desired location within the tumor. This combination of imaging and robotic administration, may ultimately change the treatment paradigm in oncology. In particular for single tumors that may be reached by a needle, including head-neck cancer, brain tumors, and pancreatic tumors that are still associated with a poor prognosis.

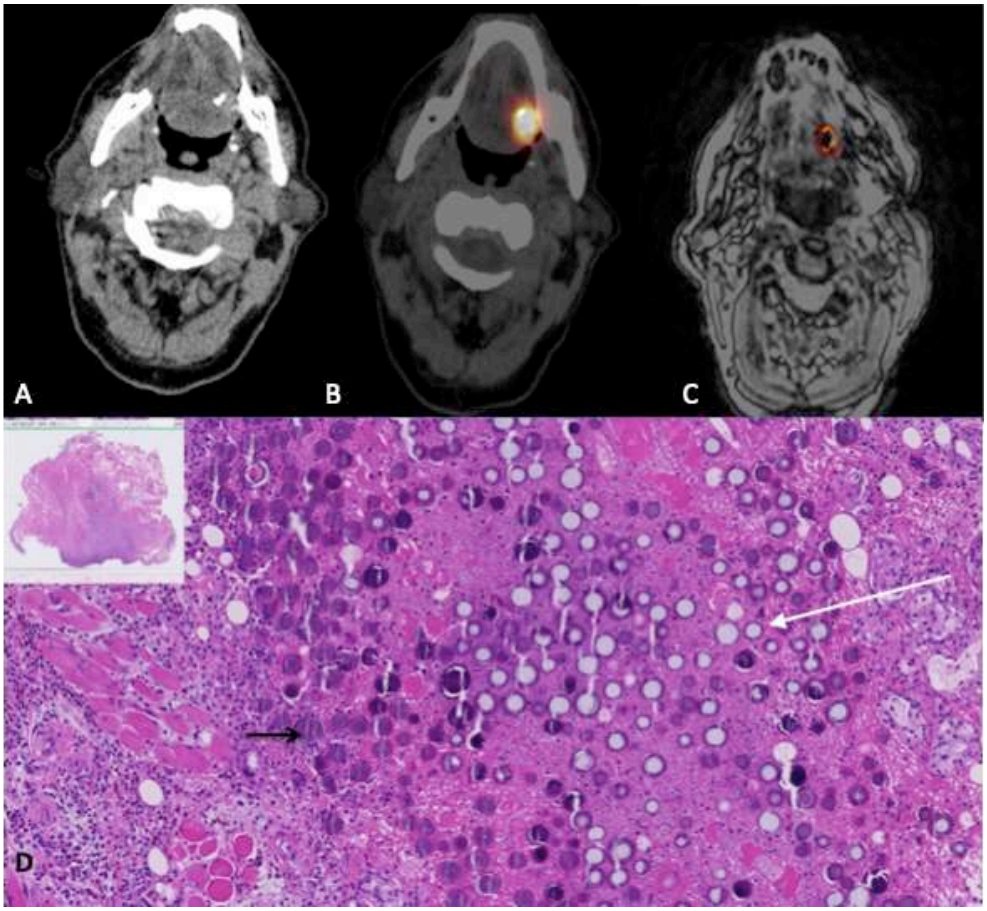

Figure 7.4. *Post-injection imaging op the head and neck area. Multimodality imaging of patient 3 post-injection with A: CT and B: SPECT/CT with ^{166}Ho dose reconstruction and C: MRI with ^{166}Ho dose reconstruction (the black centre has ^{166}Ho microsphere concentration >10mg/mL resulting in a rapid signal loss). D: Histology: HE staining showing a moderately differentiated and partly invasive growing OSCC with clusters of holmium microspheres (see black arrow: purple spherical structure are sliced microspheres and white arrow: white spherical structure are partly or totally removed microspheres by slicing the tissue in 4-micron slices). In the direct environment of the microspheres, necrotic tissue is seen, while the periphery is unaffected by radiation. Infiltration of lymphocytes is most likely not radiation related and often seen in OSCC.*[25]

In conclusion, the metal holmium in radioactive holmium-166 microspheres for local treatment of tumors shows promise in the ability to be quantified on CT and seems to be a true multimodality-imaging isotope with quantitative imaging capabilities using SPECT, MRI and CT. CT provides high resolution imaging of intra-tumoral ^{166}Ho-microspheres distribution and enables quantification of high local ^{166}Ho-microspheres concentrations. Furthermore, CT will especially be interesting for an image-guided treatment approach providing rapid intraprocedural imaging feedback of the ^{166}Ho-microspheres distribution, directing subsequent injections in possible skipped areas. Such a 'dose painting' approach may greatly optimize tumor dose coverage and subsequent clinical outcome.

Table 7.4. Patients with recurrent head and neck cancer

Patient Tumor	Tumor volume	Injected Holmium		Detected SPECT		Detected CT		Volume >100 HU	
	cm^3	MBq	Mg	MBq	%	mg	%	cm^3	%
1	44.6	366.7	36.5	309.2	84.3	32.4	88.8	2.7	6.1
2 Left	5.6	53.9	13.7	10.5	19.5	2.3	16.5	0.5	8.0
2 Right	6.1	63.8	16.2	18.6	29.2	3.8	23.5	0.6	9.3
3	3.9	17.6	3.1	8.5	48.3	1.5	48.6	0.9	23.1

Holmium recovery in patients. Three patients with recurrent head and neck cancer were treated with radioactive holmium microspheres and underwent SPECT/CT imaging. Patient 2 was treated on both sides of the neck. Base on the injected activity, the corresponding amount of mg holmium was calculated. Injected activity compared to SPECT recovery was 17.8–84.3%. CT recovery was in line with SPECT imaging ranging from 16.5–88.8%. Tumor volume was 3.9–44.6 cm^3 based on the >100HU threshold 6.1–23.1% tumor volume filled with holmium microspheres.

ACKNOWLEDGEMENTS

R.C. Bakker is funded by the Dutch Cancer Society research grant: 2014–7075

The QuiremSpheres® were provided by Quirem Medical B.V.

CONFLICT OF INTERESTC

J.F.W. Nijsen is co-founder and scientific director of Quirem Medical, and has a minority share in the company Quirem Medical. Furthermore, Nijsen is inventor on the patents related to the ^{166}Ho-PLLA-microspheres that are assigned to University Medical Center Utrecht Holding B.V. The activities of J.F.W. Nijsen within Quirem Medical are approved and supported by Dirkjan Masman (Director Technology Transfer Office Radboud UMC) and Mathias Prokop (Head of Radiology and Nuclear Medicine at Radboud UMC).

M.G.E.H. Lam is consultant for BTG, Quirem Medical B.V. and Terumo.

The department of Radiology and Nuclear Medicine of the UMC Utrecht receives royalties from Quirem Medical B.V.

REFERENCES

1. Smits MLJ, Nijsen JFW, van den Bosch MAAJ, Lam MGEH, Vente, MADD, Mali WP, et al. Holmium-166 radioembolisation in patients with unresectable, chemorefractory liver metastases (HEPAR trial): A phase 1, dose-escalation study. Lancet Oncol 2012;13:1025–1034.
2. Elschot M, Smits MLJ, Nijsen JFW, Lam MGEH, van den Bosch MAAJ, Viergever MA, et al. Quantitative Monte Carlo-based holmium-166 SPECT reconstruction. Med Phys 2013;40:112502.
3. Smits MLJ, Elschot M, van den Bosch MAAJ, van de Maat GH, van het Schip AD, Zonnenberg BA, et al. In vivo dosimetry based on SPECT and MR imaging of ^{166}Ho-microspheres for treatment of liver malignancies. J Nucl Med 2013;54:2093–100.
4. Prince JF, van den Bosch MAAJ, Nijsen JFW, Smits MLJ, van den Hoven AF, Nikolakopoulos S, et al. Efficacy of radioembolization with holmium-166 microspheres in salvage patients with liver metastases: a phase 2 study. J Nucl Med 2019;117:582–588.
5. Bakker RC, Lam MGEH, van Nimwegen SA, Rosenberg AJWP, van Es RJJ, nijsen JFW. Intratumoral treatment with radioactive beta-emitting microparticles: a systematic review. J Radiat Oncol. 2017;6(4):323–342
6. van Nimwegen SA, Bakker RC, Kirpensteijn J, van Es RJJ, Koole R, Lam MGEH, et al. Intratumoral injection of radioactive holmium (166Ho) microspheres for treatment of oral squamous cell carcinoma in cats. Vet Comp Oncol 2018;16:114–124.
7. Goh AS, Chung AY, Lo RH, Lau TN, Yu SW, Chang M, et al. A novel approach to brachytherapy in hepatocellular carcinoma using a phosphorous32 (32P) brachytherapy delivery device-a first-in-man study. Int J Radiat Oncol Biol Phys 2017;67:786–792.
8. Bakker RC, van Es RJJ, Rosenberg AJWP, van Nimwegen SA, Bastiaannet R, de Jong HWAM, et al. Intratumoral injection of radioactive holmium-166 microspheres in recurrent head and neck squamous cell carcinoma. Nucl Med Commun 2018;39:213-221.
9. Order SE, Siegel JA, Principato R, Zeiger LE, Johnson E, Lang P, et al.(1996) Selective tumor irradiation by infusional brachytherapy in nonresectable pancreatic cancer: A phase I study. Int J Radiat Oncol Biol Phys 1996;36:1117–1126.
10. Bult W, De Leeuw H, Steinebach OM, van der Bom MJ, Wolterbeek HT, Heeren RM, et al. Radioactive holmium acetylacetonate microspheres for interstitial microbrachytherapy: An in vitro and in vivo stability study. Pharm Res 2012;29:827–836.
11. Bult W, Kroeze SGC, Elschot M, Seevinck PR, Beekman FJ, de Jong HWAM, et al. Intratumoral administration of holmium-166 acetylacetonate microspheres: antitumor efficacy and feasibility of multimodality imaging in renal cancer. PLoS One 2013;8:e52178.
12. Bult W, Vente MADD, Vandermeulen E, Gielen I, Seevinck PR, Saunders J, et al. Microbrachytherapy using holmium-166 acetylacetonate microspheres: A pilot study in a spontaneous cancer animal model. Brachytherapy 2013;12:171–177.
13. Zielhuis SW, Nijsen JFW, De Roos R, Krijger GC, van Rijk PP, Hennink We, et al. Production of GMP-grade radioactive holmium loaded poly(L-lactic acid) microspheres for clinical application. Int J Pharm 2006;311:69–74.
14. Zielhuis SW, Nijsen JFW, Figueiredo R, Feddes B, Vredenberg AM, van het schip AD, et al. Surface characteristics of holmium-loaded poly(L-lactic acid) microspheres. Biomaterials 2005;26:925–932.
15. Nijsen JFW, Seppenwoolde J-H, Havenith T, Bos C, Bakker CJ, van het Schip AD. Liver tumors: MR imaging of radioactive holmium microspheres--phantom and rabbit study. Radiology 2004;231:491–499.
16. Beekman FJ, De Jong HWAM, Van Geloven S. Efficient fully 3-D iterative SPECT reconstruction with Monte Carlo-based scatter compensation. IEEE Trans Med Imaging 2002;21:867–877.
17. LeBrun A, Joglekar T, Bieberich C, Ma R, Zhu L. Identification of infusion strategy for achieving repeatable nanoparticle distribution and quantification of thermal dosage using micro-CT Hounsfield unit in magnetic nanoparticle hyperthermia. Int J Hyperth 2016;32:132–143.
18. Nowak T, Hupfer M, Brauweiler R, Eisa F Kalender Wa. Potential of high-Z contrast agents in clinical contrast-enhanced computed tomography. Med Phys 2011;38:6469–6482.
19. Pietsch H, Jost G, Frenzel T, Raschke M, Walter J, Schirmer H, et al. Efficacy and safety of lanthanoids as X-ray contrast agents. Eur J Radiol 2011;80:349–356.
20. Scott LJ, Yanch JC (1991) Absorbed dose profiles for radionuclides of frequent use in radiation synovectomy. Arthritis Rheum 34:1521–1530.
21. Seevinck P, Seppenwoolde J-H, de Wit T, Nijsen JFW, Beekman FJ, van het Schip AD, et al. Factors Affecting the Sensitivity and Detection Limits of MRI, CT, and SPECT for Multimodal Diagnostic and Therapeutic Agents. Anticancer Agents Med Chem 2007;7:317–334.
22. Chandarana H, Megibow AJ, Cohen BA, Srinivasan R, Kim D, Leidecker C, et al. Iodine Quantification With Dual-Energy CT: Phantom Study and Preliminary Experience With Renal Masses. Am J Roentgenol 2011;196:W693–700.

23. Arnolli MM, Buijze M, Franken M, de Jong KP, Brouwer DM, Broeders IAMJ. System for CT-guided needle placement in the thorax and abdomen: A design for clinical acceptability, applicability and usability. Int J Med Robot Comput Assist Surg 2018;14:e1877.
24. Arnolli MM, Hanumara NC, Franken M, Brouwer DM, Broeders IAMJ. An overview of systems for CT- and MRI-guided percutaneous needle placement in the thorax and abdomen. Int J Med Robot 11:458–75.
25. Chen WY, Wu CT, Wang CW, Lan KH, Liang HK, Huang BS, et al. Prognostic significance of tumor-infiltrating lymphocytes in patients with operable tongue cancer. Radiat Oncol 2015;13:157.

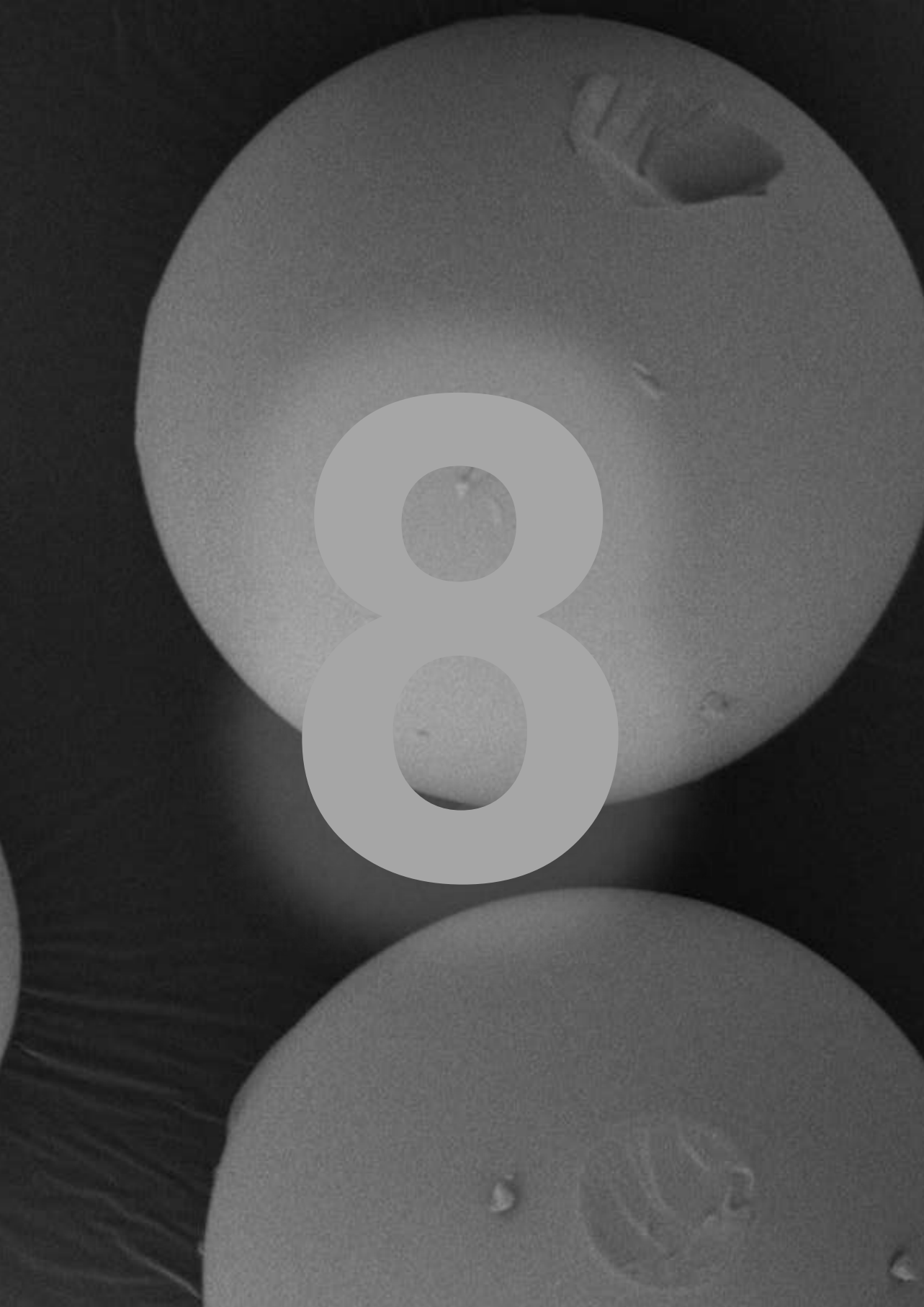
8

Quantitative dual-energy CT imaging of holmium microspheres

R. Gutjahr

R.C. Bakker

F. Tiessens

S.A. Nimwegen

B. Schmidt

J.F.W. Nijsen

Submitted

ABSTRACT

Introduction

The purpose of this study was to assess the feasibility of dual energy CT-based material decomposition using dual X-ray spectra information to determine local concentrations of holmium microspheres in phantoms and in an animal model.

Methods

A spectral calibration phantom with a solution containing 10 mg/mL holmium and various tube setting was scanned using a clinical third-generation dual-energy CT-scanner to depict an energy-dependent and material-dependent enhancement vectors. A serial dilution of holmium microspheres were quantified by spectral material decomposition and compared with known concentrations. Subsequently, the feasibility of the spectral material decomposition was demonstrated in four rabbits with injected holmium microspheres.

Results

The measured CT-values of the holmium series scales linearly to all measured concentrations and tube settings (R^2=1.00). Tube voltage combinations of 80/150 Sn kV and 100/150 Sn kV allow accurate quantifications down to 0.125 mg/mL Ho-microspheres.

Conclusion

Dual Energy CT facilitates image-based material decomposition to detect and quantify holmium microspheres in phantoms and rabbits.

INTRODUCTION

In the 1970s and 1980s dual-energy CT (DECT) technology demonstrated improved tissue characterization, however, the technique was not widely applied due to limitations like noise in low-kilo voltage (kV) images, acquisition time and image registration difficulties.[1–5] Nowadays, DECT technology is clinically applied as a result of fast technological developments, such as detectors with fully integrated electronics minimizing electronic noise, improved spectral separation using optimized beam pre-filtration, increased scan speed and improved post processing techniques.[6–11]

DECT uses two effective X-ray spectra, either generated by a single X-ray tube switching between two different X-ray spectra (kV-switch CT), by using two separated X-ray tubes applying two different voltages (dual source CT, DSCT) or by resolving an incident spectrum at the scanner (dual layer CT or photon counting detector CT). Further image processing enables the quantification of materials by separating their attenuation characteristics into the different contributions of photoelectric absorption and Compton scatter.[8,12–15] Nowadays, DECT is clinically used for diagnostic purposes such as classification of uric acid versus non-uric acid urinary stones or to quantify contrast media (CM) uptake, e.g. the local concentration of iodine in liver tissue.[9,16–19]

A therapy that potentially would benefit from DECT quantification is selective internal radiation therapy (SIRT) with beta-emitting radioactive holmium-166 microspheres (^{166}Ho-microspheres), which are currently used for radioembolization of liver tumors and intratumoral injection in solid malignancies.[20–23] In-vivo dosimetry after therapy application, needed to verify the treatment success, can be performed based on SPECT imaging utilizing the holmium-166 gamma radiation or based on magnetic resonance imaging (MRI) utilizing the paramagnetic properties of holmium. Both modalities have shown their possibilities for application in radioembolization therapy, however for intra tumoral therapy their use might be hampered by resolution limitations or detection limits.[23–26]

In intra-tumoral therapy, high concentrations of microspheres are injected at several locations in the tumor to achieve proper dose levels for the entire tumor. This requires high resolution dosimetry that cannot be achieved by SPECT and quantification of high holmium concentrations which is challenging for MRI.

Conventional CT for quantification of ^{166}Ho-microspheres, utilizing the high attenuation coefficient of holmium, has previously been explored.[24,25] CT in general would allow for fast ^{166}Ho-microspheres quantification of high local concentrations with high spatial resolution and thus accurate local dosimetry at low cost. Although a clear relation was demonstrated between local holmium concentrations and CT signal, discrimination of holmium from e.g., bone, calcified arteries or iodinated CM was found to be difficult.[24]

It is expected that DECT can overcome the previously identified limitations of conventional CT by utilizing the spectral information that DECT offers combined with the presence of a k-edge at 56 keV that holmium expresses, leading to a sudden increase in X-ray attenuation at that energy.

The objective of this study was to demonstrate the feasibility of DECT-based quantification of (radioactive) Ho-microspheres for dosimetry in SIRT by means of phantom and ex-vivo measurements.

METHODS

In this study, the following experiments were performed using. First, a spectral calibration was performed to investigate energy-dependent and material-dependent factors. Second, contrast media quantification measurements were performed to define detection limits and accuracy. Finally, the feasibility of holmium quantification was tested in a pilot study performed in-situ in VX-2 tumour-bearing rabbits. Since only a very small fraction of holmium-165 is converted to holmium-166 after neutron activation during production (approximately 0.001%)[23], no difference is expected in X-ray attenuation between radioactive and non-radioactive microspheres. Therefore, all experiments were performed using ^{165}Ho-microspheres to avoid unnecessary radiation risks.

Spectral Calibration

Spectral calibration is required to depict an energy-dependent and material-dependent material vector.[12] For this purpose a dedicated spectral calibration phantom (QRM GmbH, Möhrendorf, Germany) was scanned using a third-generation dual energy CT-Scanner (SOMATOM Force, Siemens Healthcare GmbH, Forchheim, Germany). The scans were performed using a dual-energy abdomen protocol; collimation 2 × 64 × 0.6 mm with a flying focal spot in the z-direction, rotation time 0.5 s/rot and a pitch 0.6. The images were reconstructed using a weighted filtered backprojection algorithm[27] providing linear handling of contrast, noise, and spatial resolution in order to preserve purely quantitative results. All images were reconstructed with a slice thickness of 1.5 mm, an increment of 1.0 mm, a quantitative medium smooth reconstruction kernel (Qr44f) used for routine reconstruction of DECT images (50% value of the modulation transfer function: ϱ_{50} = 4.62 lp/cm, no edge enhancement), and a reconstruction Field of View (FOV) of 175 mm. The phantom consists of a 10 cm wide cylinder comprised of a synthetic material exhibiting liquid water-equivalent CT-values. Two 2 cm diameter syringes (Omnifix Solo, B. Braun, Melsungen, Germany) were located in the phantom's center and 3 cm horizontally offset, respectively. The centric syringe was filled with holmium (III) chloride hexahydrate (Metal Rare Earth Limited, Shenzhen, China (Holmium content 41.3–45.5% (w/w)) suspended in distilled water (Fresenius SE & Co KGaA, Kabi, Netherland). Titration of

the holmium chloride revealed a 42.0% holmium content resulting in a final concentration of 10.5 mg/mL. The known concentration served as a reference to facilitate quantitative measurements. The offset syringe contained pure water as a reference to the phantom's original material. In the spectral calibration the following effects were investigated using an automatic exposure control (CARE, Dose4D, Siemens Healthcare GmbH); the effect of X-ray tube voltage combinations and size-dependent spectral effects (Table 8.1). Measurements were performed using different X-ray tube voltage combinations: 70/150 Sn kV, 80/150 Sn kV, 100/150 Sn kV, and 80/140 kV, whereas *Sn* denotes the utilization of a 0.6 mm thick tin pre-filtration used for increased spectral separation.[6] In order to evaluate object size-dependent spectral effects, additional extension rings were used to expand the 10 cm wide phantom to 15, 20, 25, 30, or 35 cm (Figure 8.1).[7,26,28]

Table 8.1. Effective tube current time products

Tube voltages kV (system A / system B)	Tube current time products for different phantom sizes (mAs)					
	10 cm	15 cm	20 cm	25 cm	30 cm	35 cm
70/150 Sn	16/16	18/16	37/22	80/36	180/16	410/95
80/150 Sn	16/16	16/16	23/22	45/36	95/60	202/95
100/150 Sn	16/16	20/16	34/22	60/36	109/60	195/95
80/140	16/16	16/16	16/16	30/16	65/16	142/24

Effective tube current time products regarding the different phantom sizes and all tube voltage combinations as investigated in the calibration measurements, kV Kilovolt, mAs: Milliampere/ seconds Sn: Tin filter

Material Decomposition Algorithm

The relationship of the material specific CT-values of corresponding spectral CT acquisitions allows the determination of material vectors unique for the used tube voltages. The used image-based material separation algorithm (syngo.via, VB30A, Siemens Healthcare GmbH, Forchheim, Germany) relies on a base transformation and a projection of every measured set of CT-values to preselected orthogonalized and linearly independent base vectors.[8,29] In our study air (-1000/-1000 HU for the low kV and high kV image, respectively), water (0/0 HU) and ^{165}Ho-microspheres were selected as base materials. Decomposition into these three materials enables the generation of a material images that constitute local concentrations of ^{165}Ho-microspheres, as well as virtual non-contrast images, mimicking a native scan where no CM was applied (Figure 8.1).

Contrast media Quantification Measurements

A serial dilution of Ho-microspheres (0.125–10.0 mg holmium/mL) was examined to test linearity with various concentrations and the detection limit. The concentration inserts were made of a batch of ^{165}Ho-microspheres with a holmium mass percentage of 18.8% (QuiremSpheres, Quirem Medical B.V.). The microspheres were suspended in an injection solution containing 116 mmol phosphate buffered saline (pH 7.2, 77.0 mmol Disodium phosphate dibasic dehydrate, Merck Millipore, and 39.0 mmol Sodium Phosphate monobasic anhydrous, Sigma Aldrich) with polyoxyethylene-polyoxypropylene block copolymer (Pluronic F-68, Sigma-Aldrich Chemie B.V.) 2% weight per volume solution. To prevent precipitation of ^{165}Ho-microspheres due to their weight (1.4 g/mL), an agar solution (MP Agar, Roche Diagnostics) was added. The agar solution was heated to 90°C for 10 minutes, resulting in a transparent fluid. The ^{165}Ho-microspheres suspension and agar were mixed in a rising concentration of ^{165}Ho-microspheres and filled into syringes for the spectral calibration measurements and into 5 mL Eppendorf tubes for the quantitative comparison of measured and known concentration in the CT-images. Once cooled to room temperature, the agar became solid.

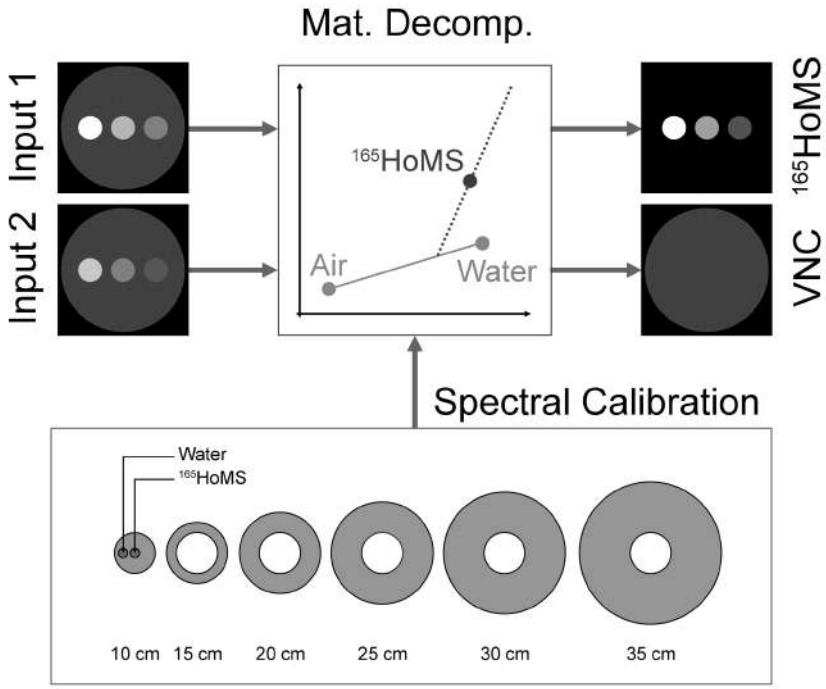

Figure 8.1. *Spectral calibration scans are used to generate energy-dependent and material-dependent material vectors as prerequisite for the image-based material decomposition. Therefore, the X-ray absorption of holmium on the applied X-ray spectra was investigated in the relation of the size of the object (using 10–35cm extension rings). Based on two different energy input images, input 1 and 2, the material decomposition can be calculated and results in material images constituting of local concentrations of ^{165}Ho-microspheres (^{165}HoMS), as well as virtual non-contrast images (VNC).*

The experimental setup consisted of a 20 cm wide (real) water phantom that allowed the positioning of multiple tubes. The solutions were scanned in two groups (0.125–1.0 mg/mL and 2.0–10.0 mg/mL). The inserts were arranged in an equiangular fashion 5 cm distant from the phantom's centerline.

In addition to the clinical dose (CARE Dose4D) measurements a series of high dose measurements were conducted (Table 8.2). With the first mode, the accuracy of ^{165}Ho-microspheres quantification was assessed under clinical conditions, whereas the maximal tube current allows the determination of a contrast agent in a low noise situation. After the image-based material decomposition, the images were quantitatively assessed and ^{165}Ho-microspheres concentrations were compared to the known concentrations.

Equation 1 describes a tolerance term discerning as an estimate error for material quantification.[30] The two terms presume the CT-value stability and spectral stability to be two independent types of errors. The tolerance scales with increased known concentration C_{known}.

$$T = \sqrt{\left(0.5\frac{mg}{mL}\right)^2 + (0.1 \cdot C_{known})^2}$$

Animal preparation

All experiments were performed in conduct with The Netherlands Experiments on Animals Act (1977) and The European Convention for the Protection of Vertebrate Animals used for Experimental Purposes (Strasbourg, 18.III.1986). Approval was obtained from the Utrecht University Animal Experiments Committee (DEC 2011.III.08.080).

Table 8.2. The effective current, Qref and radiation dose

TubevoltagesinkV (systemA/systemB)	Tube Current Determination	Effective Current (mAs)	Qref (mAs)	Dose (CTDI32) (mGy)
70/150 Sn	CARE Dose4D	212 / 55	380 /95	4.36
	High Dose	1083 / 271	-	21.92
80/150 Sn	CARE Dose4D	105 / 54	190 / 95	3.83
	High Dose	1083 / 542	-	38.95
100/150 Sn	CARE Dose4D	60 / 53	190 / 95	4.22
	High Dose	840 / 420	-	48.91
80/140	CARE Dose4D	73 / 18	132 / 24	3.40
	High Dose	997 / 181	-	39.24

Overview of the effective current, Q_{ref} and radiation dose for all applied tube voltage combinations for the quantification measurements

The VX-2 tumor model was described previously.[28] Six tumors were induced by subcutaneous injection of three ± 1 mm^3 viable fragments of VX-2 carcinoma harvested from the donor rabbit. Next, these fragments were injected with 0.1–0.3 mL PBS into three adult female New Zealand White (NZW) rabbits weighting 3–4 kg. All tumor implantations were performed under analgesia with carprofen 4 mg/kg. During the animal experiments, sedation and analgesia were achieved with a mixture of 0.125 mg/kg dexdomitor and 15 mg/kg ketamine.

Subsequently, aliquots with various amounts of ^{166}Ho-microspheres were administered intratumorally. The exact administered amount, regarding holmium mass (mg), was calculated by measuring the radioactivity of the syringes with ^{166}Ho-microspheres before and after injection using a VDC-404 dose calibrator, Veenstra Instruments B.V. Measurements performed on the DECT are primarily based on ^{165}Ho as only a fraction is converted. Animals were sacrificed and frozen for preservation until scanning with the dual energy CT scanner. The average water equivalent diameter of the rabbit-specimen ranged from 15–20 cm, such that the general quantitative detection of the ^{165}Ho-microspheres as from the prior phantom scans can be assumed.

Statistical Analysis

After applying the image-based material decomposition algorithm the quantitative material images were evaluated for ^{165}Ho-microspheres quantification. Descriptive statistics (mean concentration, absolute and relative deviation) of the image-based material decomposition measurements were compared to the known concentrations for all tube voltage combinations and dose settings.

Table 8.3. Injected and detected amounts of ^{166}Ho-microspheres in rabbits

Animal	Injected amount of ^{166}Ho-microspheres (mg)	Detected amount of ^{166}Ho-microspheres (mg)	Relative deviation (%)
1	5.6	6.3	11.4
2	3.3	3.0	-11.7
3	6.0	5.5	-7.7
4	12.6	12.8	1.7

List of injected amounts of ^{165}Ho-microspheres, as well as the detected amounts of ^{165}Ho-microspheres after material decomposition and quantification of the animal measurements. The relative deviations (with reference to the injected amounts) is shown in the fourth column. The measured amounts of the tumor correspond to the injections from figure 86

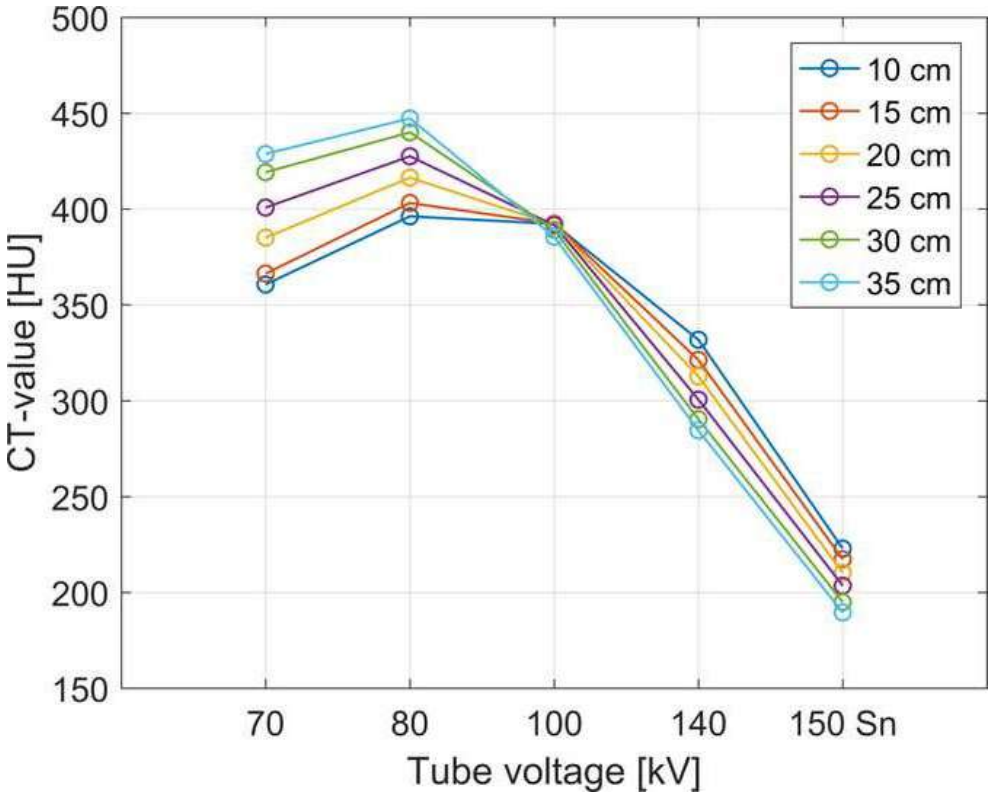

Figure 8.2. *Measured CT-values for 10.0 mg ^{165}Ho-microspheres/mL with regard to different tube voltages and phantom sizes.*

RESULTS

Spectral calibration

Figure 8.2 shows that the X-ray absorption of holmium highly depends on the applied X-ray spectra and the size of the object. With an increased diameter the mean energy of the X-ray spectrum shifts towards higher energies, which for lighter atoms (presuming no K-edge in the applied X-ray spectrum) results in a decrease of X-ray attenuation and therefore lower CT-values. An increased attenuation and an enhanced CT-value are observed when the mean energy of an X-ray spectrum and its spectral barycenter moves closely beyond the K-edge of a material, where the photoelectric effect becomes dominant. The further the energies shift, the more the measured CT-values decreases. For all investigated energies both effects, the decreased X-ray attenuation due to increased object size, as well as the simultaneously mean energy shift towards the K-edge of the material (56 keV for Holmium) results in an increase of total X-ray attenuation at 70 and 80 kV, but eventually to a decrease in absorption at 100–150 Sn kV (Figure 8.2).

Contrast media quantification measurements

The CT-values of the holmium solutions were identical for both dose levels and the image noise level scales square root to the reduction radiation dose (Figure 8.3A, B). Measured concentrations, in the phantom model, using CT quantification were linear ($R^2 = 0.99$ and $R^2 = 1.00$) and slightly lower than the known concentrations (Figure 8.3C, D). Figure 8.3E, F shows the increase of deviation with lower holmium concentrations. With an acceptance of 10% relative measurements error, high dose scans with 80/150Sn kV or 100/150Sn kV tube voltage combinations allows accurate quantification down to 0.125 ^{166}Ho-microspheres mg/mL. Using the automated exposure control allows quantification down to 0.25 ^{166}Ho-microspheres mg/mL for 70/150Sn kV, 80/150Sn kV and 100/150Sn kV.

The measured CT-values decreased with lower holmium concentrations, while the noise level remained the same for a tube voltage. This resulted in a factor 3–4 times lower SNR e.g., from 65.4 to 15.7 for 80 kV with 10 mg/mL holmium (Figure 8.4). The additional value of DECT material decomposition is shown in Figure 8.5, illustrating the output of two separate material decompositions, virtual non-contrast images (Figure 8.5A, B) and the quantitative measured mapping of holmium concentrations (Figure 8.5C, D).

Animal experiment

After the phantom experiment a pilot study was performed on three rabbits. (Figure 8.6) shows rendered 3D models of the animals' bony structures and highlighted tumor findings (using syngo.via Volume Rendering Technique, VB30A, Siemens Healthcare GmbH, Forchheim, Germany). In decomposed material images the tumor injection sites of the rabbits can be evaluated and local holmium concentrations are measured. The injected and detected amount of ^{165}Ho-microspheres, corresponded well with relative deviation ranging between 1 and 11% (Table 8.3).

Spectral calibration

The effective tube current time products for the different phantom sizes and tube voltage combinations are presented in table 8.1. The X-ray absorption of holmium highly depends on the applied X-ray spectra and the size of the object (Figure 8.1). With an increased diameter the mean energy of the X-ray spectrum shifts towards higher energies, which for lighter atoms (presuming no K-edge in the applied X-ray spectrum) results in a decrease of X-ray attenuation and therefore lower CT-values. An increased attenuation and an enhanced CT-value are observed when the mean energy of an X-ray spectrum and its spectral barycenter moves closely beyond the K-edge of a material, where the photoelectric effect becomes dominant. The further the energies shift, the more the measured CT-values decreases. For all investigated energies both effects, the decreased X-ray attenuation due to increased object size, as well as the simultaneously mean energy shift towards the K-edge of the material (56 keV for Holmium) results in an increase of total X-ray attenuation at 70 and 80 kV, but eventually to a decrease in absorption at 100–150 Sn kV (Figure 8.1).

Contrast media quantification measurements

The measured CT-values of the holmium solutions scaled linearly to all measured concentrations and all tube voltages (R^2=1.00). The CT-values of the holmium solutions were identical for both dose levels and the image noise level scales square root to the reduction of radiation dose (Figure 8.2).

In the phantom, the measured ^{166}Ho-microspheres concentrations were systematically lower than the known concentrations. This difference increased for solutions with a lower concentration of holmium (Figure 8.3). Considering a relative measurement error of 10% acceptable, the high dose scans and tube voltage combinations of 80/150 Sn kV or 100/150 Sn kV allowed accurate quantification of concentrations down to 0.125 ^{166}Ho-microspheres mg/mL. Using automated exposure control good accuracy down to 0.25 mg/mL ^{166}Ho-microspheres was obtained with 70/150 Sn kV, 80/150 Sn kV and 100/150 Sn kV. (Figure 8.3)

The measured CT-values decreased with lower ^{166}Ho-microspheres concentrations, while the noise level remained the same for a tube voltage. This resulted in a factor 3–4 times lower SNR e.g., from 36.5 to 15.1 for 70 kV with 10 ^{166}Ho-microspheres mg/mL (Figure 8.4). The additional value of DECT material decomposition is shown in Figure 8.5. This illustrates the output of two separate material decompositions in which the measured ^{166}Ho-microspheres concentration is filtered out or mapped quantitatively.

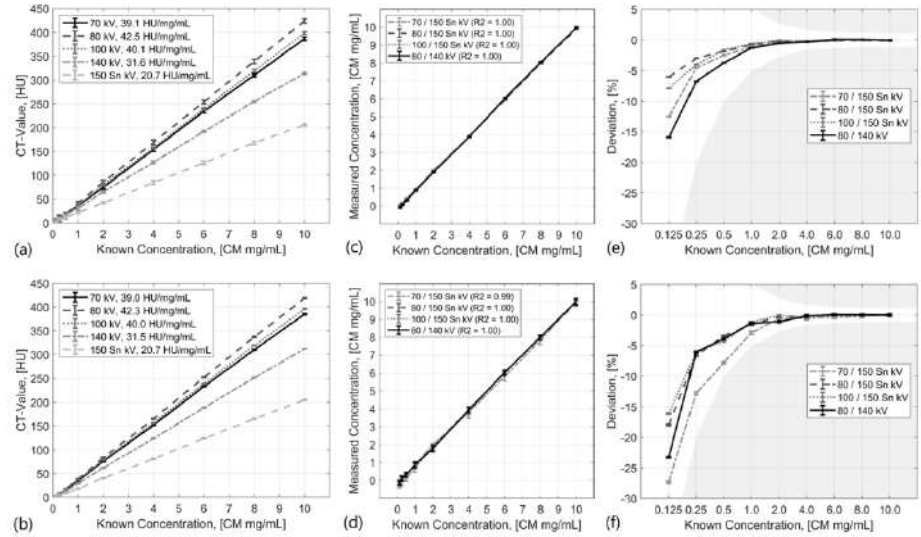

Figure 8.3. *Slope and CT-values for different ^{165}Ho-microspheres mg/mL solutions in a 20 cm wide water-phantom. (a): High dose measurements, (b): Clinical situation with typical clinical radiation dose using automated exposure control. Accuracy of the measured concentrations compared against the known concentrations for high dose measurements (c) and measurements using automated exposure control (d). Relative deviations of the measured concentrations compared against the known concentrations for high dose measurements (e) and measurements using automated exposure control (f). The grey area depicts the area where the given tolerance is exceeded.*

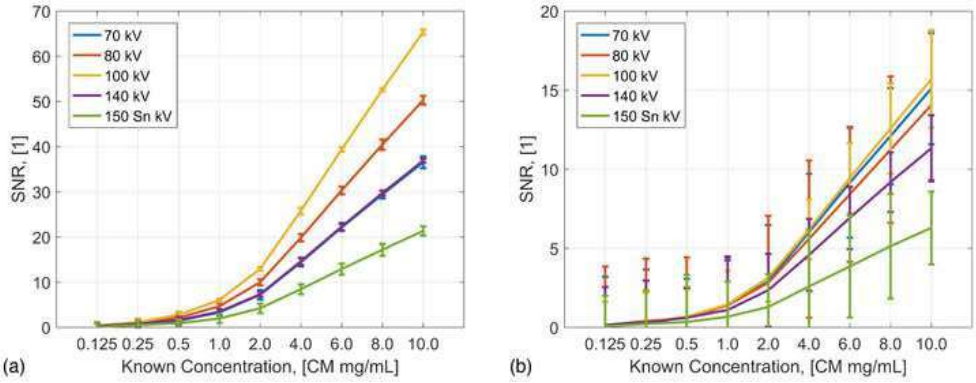

Figure 8.4. *Measured SNRs for all investigated ^{165}Ho-microspheres solutions using high radiation dose (a) and typical clinical radiation dose (b).*

Animal experiment

After the phantom experiment a pilot study was performed on four rabbits. The tumor injection sites of the rabbits were scanned and the measured ^{166}Ho-microspheres concentrations mapped quantitatively. The segmentation of the ^{166}Ho-microspheres and soft tissue shows the exact location of the injected material with respect to the anatomy of the single animals (Figure 8.6). The injected and the detected amount of ^{166}Ho-microspheres, corresponded well with relative measurement error ranging between 1 and 11% (Table 8.3).

DISCUSSION

In this article we presented the first results of DECT-based quantification of holmium microspheres in phantoms and ex-vivo material.

All measurements showed a linear relation between DECT-based holmium concentrations and actual holmium concentrations. This was observed for all investigated X-ray spectra. In the high dose acquisitions, the accuracy per measurement is superior due to the reduced noise level compared to clinical (low) dose acquisitions. In case of low concentrations of holmium, the reduced CT-value can no longer be distinguished from the background signal anymore. This effect propagates through the applied material decomposition algorithm. Ultimately, the quality of the applied material separations based on the image data of the high dose measurements outperformed the quality of the respective low dose measurements.

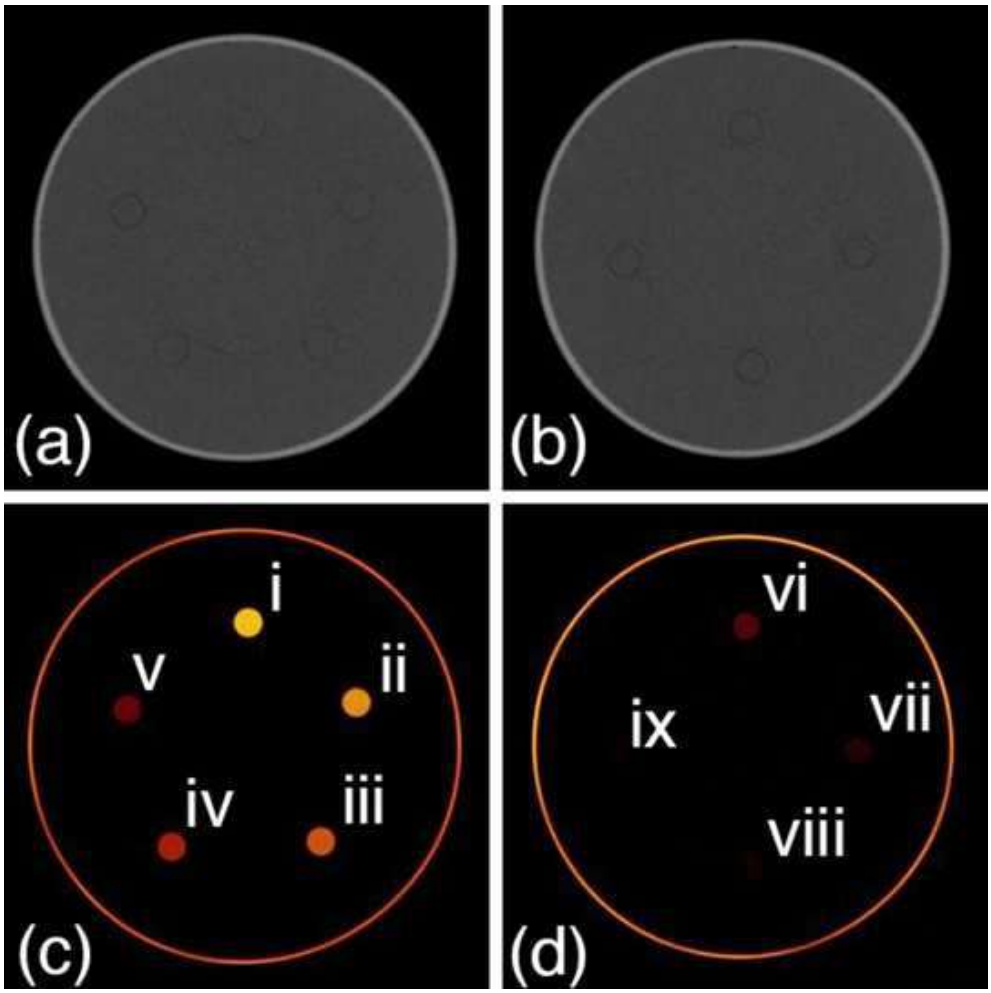

Figure 8.5. *(a) and (b) show virtual non contrast images, i.e. images where the ^{165}Ho-microspheres is virtually removed. The material images (c) and (b) facilitate quantitative readout of the investigated ^{165}Ho-microspheres concentrations: 10.0, 8.0, 6.0, 4.0, 2.0 mg ^{165}Ho-microspheres/mL; vi-ix show the results for 1.0, 0.5, 0.25, 0.125 mg ^{165}Ho-microspheres/mL.*

The measured CT-values of the ^{165}Ho-microspheres solutions depended on the investigated phantom sizes. For lower energetic X-ray spectra (70 kV and 80 kV) the increased phantom size resulted in a shift of the mean X-ray spectra closer to the K-edge of holmium. The suddenly increased proportion of photoelectric absorption causes an increased total mass attenuation and therefore increased CT-values. For higher energetic X-ray spectra (e.g., 140 kV or 150 Sn kV) the mean X-ray energy, as well as the spectral barycenter moves away from the material's K-edge, leading to reduced mass attenuation and decreased CT-values. This effect is different for materials such as iodinated CM, (K-edge at 33 keV) because the mean energies of typical X-ray spectra are already beyond that energy.

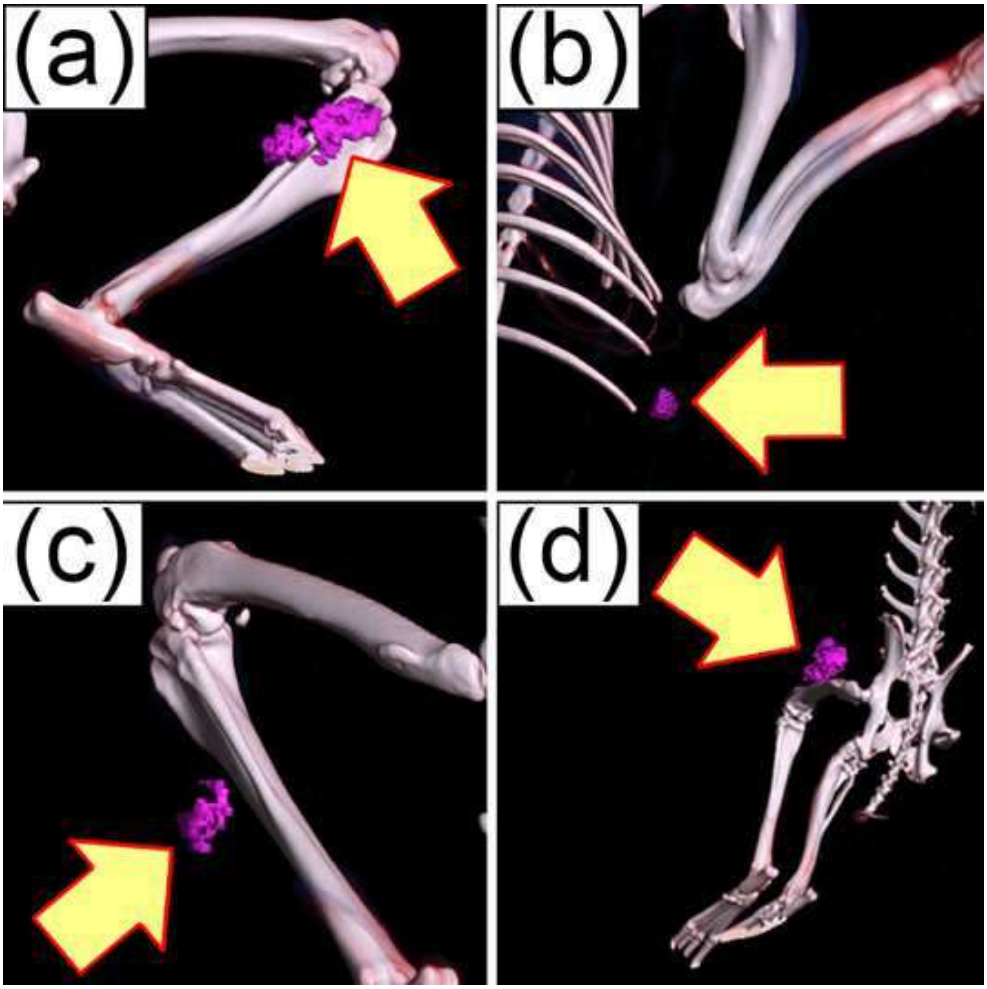

Figure 8.6. *Visually rendered images of four segmented and quantified ^{165}Ho-microspheres injections in different body regions of three single rabbit specimen.*

Material decomposition of high dose acquisitions provided accurate measurements for concentrations down to 0.125 mg/mL holmium when accepting a relative measurement error of 10% with 80/150 Sn kV and 100/150 Sn kV as selected tube voltage combinations. Measurements on three adult female NZW rabbits with subcutaneous VX-2 tumors, which were intratumorally injected with radioactive ^{166}Ho-microspheres and imaged post-mortem, demonstrated DECT-based holmium quantification in a scenario that is much closer to clinical reality. Using parameters identical to the calibration scans, the measured amounts of holmium corresponded well with the known injected amount of holmium with a maximum deviation 11.7%. However, a limitation of this study was the low number of animals and or injections for quantification, which does not allow for a statistical analysis.

The observation of the characteristic mass attenuation behavior with regard to the photon's energies would facilitate K-edge sensitive imaging for either dual or even multi-energetic applications. This could potentially be used for simultaneous imaging of a patient's vascularization and local accumulations of Ho-microspheres in tumorous regions within in a single CT scan by virtually remove or quantify one of the materials as shown in Figure 8.5.

Impaired quality of the material separation that was found is largely a consequence of the experimental setup itself. The axial cross-sections of the investigated rabbits were rather elliptical, and the CT scanner did not correct for this shape with adaptive beam shaping. Additionally, the animals were partially frozen resulting in local changes of tissue densities leading to slightly deficiently determined soft tissue base material vectors. In our example, some tumor parts were not detected because of their proximity to diverse body materials (here: bone and air). In addition, the detection was suboptimal because third base materials are interpreted as a linear combination of the selected two base material vectors. This limitation could be overcome by extending the amount of applied or resolved X-ray spectra and by adding a third material to the equation, as it can be done using alternative spectral CT technologies such as photon counting detectors (PCD).[31,32] Investigating the quantification capability and robustness against clinically realistic artefacts that are per se inherent to a two material separation algorithm using a PCD-CT scanner are considered next steps in holmium microsphere imaging.

In conclusion, the first phantom and ex-vivo holmium DECT data presented in this paper clearly shows the feasibility to detect and quantify concentrations of holmium microspheres. This could be of great clinical value for dose verification during and after holmium microspheres internal radiation therapy.

ACKNOWLEDGEMENTS

The study was supported by Quirem Medical B.V. (Deventer, Netherlands) and Siemens Healthcare GmbH (Forchheim, Germany).

REFERENCES

1. Di Chiro G, Brooks RA, Kessler RM, johnston GS, Jones AE, Herdt JR, et al. Tissue signatures with dual-energy computed tomography. Radiology. 1979;131(2):521–523.
2. Genant HK, Boyd D. Quantitative bone mineral analysis using dual-energy computed tomography. Investigative radiology. 1977;12(6):545–551.
3. McDavid WD, Waggener RG, Dennis MJ, Sank VJ, Payne WH. Estimation of chemical composition and density from computed tomography carried out at a number of energies. Investigative radiology. 1977;12(2):189–194.
4. Millner MR, McDavid WD, Waggener RG, Dennis MJ, Payne WH, Sank VJ. Extraction of information from CT scans at different energies. Medical physics. 1979;6(1):70–71.
5. Rutherford R, Pullan B, Isherwood I. Measurement of effective atomic number and electron density using an EMI scanner. Neuroradiology. 1976;11(1):15–21.
6. Primak AN, Giraldo JCR, Eusemann CD, Schmidt B, Kantor B, Fletcher JG, et al. Dual-source dual-energy CT with additional tin filtration: Dose and image quality evaluation in phantoms and in-vivo. AJR. Am J of roentgenol. 2010;195(5):1164.
7. Kelcz F, Joseph PM, Hilal SK. Noise considerations in dual energy CT scanning. Medical physics. 1979;6(5):418–425.
8. Johnson TRC, Krauss B, Sedlmair M, Grasruck M, Bruder H, Morhard D, et al. Material differentiation by dual energy CT: initial experience. European radiology. 2007;17(6):1510–1517.
9. Pelgrim GJ, van Hamersvelt RW, Willemink MJ, Schmidt BT, Flohr T, Schilham A, et al. Accuracy of iodine quantification using dual-energy CT in latest generation dual source and dual layer CT. Eur radiol. 2017;27(9):3904–3912.
10. Reimann AJ, Rinck D, Birinci-Aydogan A, Scheuering M, Burgstahler C, Schroeder S, et al. Dual-source computed tomography: advances of improved temporal resolution in coronary plaque imaging. Investigative radiology. 2007;42(3):196–203.
11. Yeh BM, Shepherd JA, Wang ZJ, Teh HS, Hartman RP, Prevrhal S. Dual-energy and low kVp CT in the abdomen. AJR. American journal of roentgenology. 2009;193(1):47.
12. Alvarez RE, Macovski A. Energy-selective reconstructions in x-ray computerised tomography. Physics in medicine and biology. 1976;21(5):733.
13. Coursey CA, Nelson RC, Boll DT, Paulson EK, Ho LM, Neville AM, et al. Dual-energy multidetector CT: how does it work, what can it tell us, and when can we use it in abdominopelvic imaging? Radiographics.2010;30(4):1037–1055.
14. Yang C, Zhang S, Jia Y, Yu Y, Duan, HF, Zhang XR, et al. Dual-energy spectral CT imaging for the evaluation of small hepatocellular carcinoma microvascular invasion. Eur J radiol. 2017;95:222–227.
15. Li Y, Shi G, Wang S, Wang S, Wu R. Iodine quantification with dual-energy CT: phantom study and preliminary experience with VX2 residual tumor in rabbits after radiofrequency ablation. Br J radiol. 2013;86(1029):20130143.
16. Primak AN, Fletcher JG, Vrtiska TJ, Dzyubak OP, Lieske JC, Jackson ME, et al. Noninvasive differentiation of uric acid versus non–uric acid kidney stones using dual-energy CT. Acad radiol. 2007;14(12):1441–1447.
17. Graser A, Johnson TR, Bader M, Staehler M, Hasake N, Nikolaou K, et al. Dual energy CT characterization of urinary calculi: initial in vitro and clinical experience. Invest radiol. 2008;43(2):112–119.
18. Fukuda T, Umezawa Y, Asahina A,Nakagawa H, Furuya K, Fukuda K. Dual-energy CT iodine map for delineating inflammation of inflammatory arthritis. Eur radiol. 2017;27(12):5034–5040.
19. Bongartz T, Glazebrook KN, Kavros SJ, Murthy NS, Merry SP, Franz WB, et al. Dual-energy CT for the diagnosis of gout: an accuracy and diagnostic yield study. Ann Rheum Dis. 2015;74(6):1072–1077.
20. Smits MLJ, Elschot M, van den Bosch MAAJ, van de Maat GH, van het Schip AD, Zonnenberg BA, et al. In vivo dosimetry based on SPECT and MR imaging of ^{166}Ho-microspheres for treatment of liver malignancies. J Nucl Med 2013;54:2093–100.
21. van Nimwegen SA, Bakker RC, Kirpensteijn J, van Es RJJ, Koole R, Lam MGEH, et al. Intratumoral injection of radioactive holmium (166Ho) microspheres for treatment of oral squamous cell carcinoma in cats. Vet Comp Oncol 2018;16:114–124.
22. Bakker RC, van Es RJJ, Rosenberg AJWP, van Nimwegen SA, Bastiaannet R, de Jong HWAM, et al. Intratumoral injection of radioactive holmium-166 microspheres in recurrent head and neck squamous cell carcinoma. Nucl Med Commun 2018;39:213–221.
23. Nijsen JFW, Krijger GC, van Het Schip AD. The bright future of radionuclides for cancer therapy. Anticancer Agents Med Chem. 2007;7:271–290.
24. Seevinck PR, Seppenwoolde JH, de Wit TC, Nijsen JFW, Beekman FJ, van het schip AD, et al. Factors affecting the sensitivity and detection limits of MRI, CT, and SPECT for multimodal diagnostic and therapeutic agents. Anticancer Agents Med Chem 2007;7(3):317–334.

25. Seppenwoolde J-H, Nijsen JFW, Bartels LW, Zielhuis SW, van het Schip AD, Bakker CJ. Internal radiation therapy of liver tumors: Qualitative and quantitative magnetic resonance imaging of the biodistribution of holmium–loaded microspheres in animal models. Magn Reson Med. 2005;53(1):76–84.
26. Van de Maat GH, Seevinck PR, Elschot M, Smits MLJ, de Leeuw H van het Schip AD,et al. MRI-based biodistribution assessment of holmium-166 poly (L-lactic acid) microspheres after radioembolisation. Eur Radiol. 2013;23(3):827–835.
27. Stierstorfer K, Rauscher A, Boese J, Bruder H, Schaller S, Flohr T. Weighted FBP—a Simple Approximate 3D FBP Algorithm for Multislice Spiral CT With Good Dose Usage for Arbitrary Pitch. Phys Med biol. 2004;49(11):2209.
28. Nijsen JFW, Seppenwoolde JH, Havenith T, eBos C, Bakker CJ, van het Schip AD. Liver tumors: MR imaging of radioactive holmium microspheres-phantom and rabbit study. Radiology. 2004;231(2):491–499.
29. Liu X, Yu L, Primak AN, McCollough CH. Quantitative imaging of element composition and mass fraction using dual-energy CT: three-material decomposition. Med phys. 2009;36(5):1602–1609.
30. SyngoCT Postprocessing applications - Instructions For Use - syngoCT Workplace syngo CT VB20, 2017
31. Symons R, Cork TE, Lakshmanan MN, Evers R, Davies-Venn C, Rice KA, et al. Dual-contrast agent photon-counting computed tomography of the heart: initial experience. Int J Cardiovasc Imaging. 2017:1–9.
32. Faby S, Maier J, Sawall S, Simons D, Schlemmer HP, LellM, et al. An efficient computational approach to model statistical correlations in photon counting x-ray detectors. Med Phys. 2016;43(7):3945–396


9

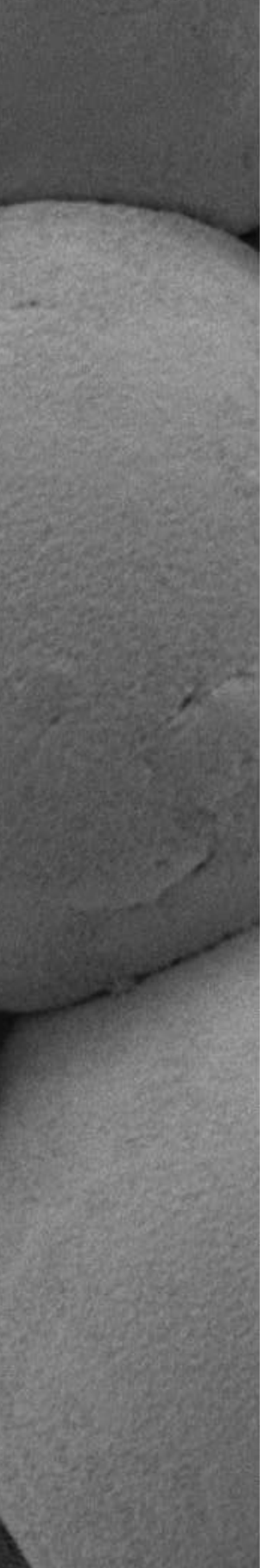

General discussion and future perspectives

INTRODUCTION

Cancer in the head and neck region is the sixth most frequent cancer with 600,000 newly diagnosed patients every year.[1] In addition to this relatively high incidence, head and neck cancer (HNC) is also associated with a poor prognosis, especially in advanced stages of the disease.[2] In the past several decades, the overall 5-year survival rate has only slightly improved.[3] Taking into consideration its poor prognosis and increasing incidence, there is a need for new treatment options.

The increasing collaboration between medical and technical specialties may provide opportunities for the development of new treatments to combat HNC. In the diagnostic setting, improvements have been made in the prediction of lymph node metastasis using prognostic biomarkers, which may be used to individualize the treatment of patients with early oral squamous cell carcinoma (OSCC).[4,5] A joined effort with the Department of Nuclear Medicine resulted in the sentinel node procedure to detect the first echelon of lymph node drainage, which has significantly reduced the number of elective neck dissections.[6] However, these improvements have been primarily focused on better prediction or early detection, and not as much attention has been paid to alternative treatments for patients suffering in the advanced stages of HNC.

Currently, there is an unmet clinical need for patients who cannot employ regular therapies, including cases associated with comorbidities or multiple prior resections, such as oral field cancerization, or for lesions, where surgical resection leads to unaesthetic results or functional deficits. A potential therapeutic option may be intra-tumoral injections with radioactive microparticles.[7] The intra-tumoral injection of radioactive microparticles can be a minimally-invasive option to treat tumors that can be reached by needle. The smaller the size of these particles (μm) compared to brachytherapy seeds (mm) allows these particles to be injected through a regular-sized injection needle. This may aid in reaching difficult to treat locations and makes the procedure less invasive and less painful.[8] A local high dose of radiation could be administered in a single session with minimal risk of systemic side effects. This is especially true in the case of image-guided administration, when the required dose is delivered with a high degree of accuracy. Potentially, intra-tumoral treatment with radioactive microparticles may lead to complete or near-complete tumor reduction, which may result in less extensive surgery, improved functional outcomes, and improved quality of life.

The purpose of this thesis was to assess the feasibility of intra-tumoral treatment with radioactive holmium-166 acetylacetonate-poly(L-lactic acid) microspheres (i.e., ^{166}Ho-microspheres) for HNC patients. In the first part of this study, the characteristics of the microparticle are discussed, including its relationship with radioembolization, the ideal isotope, and the stability of ^{166}Ho-microspheres. The second part describes the clinical experience of intra-tumoral injections of radioactive ^{166}Ho-microspheres in veterinary and human patients. Subsequently, the discussion

concentrates on the technique of intra-tumoral injections with radioactive beta-emitting particles. Next, developments in holmium imaging and tumor response imaging will be discussed, and finally, the lessons learned are summarized, future prospects are discussed, and conclusions are drawn.

Microparticles

Currently, microparticles loaded with radioisotopes are frequently used in radioembolization of the liver. With radioembolization, these particles are injected in the arterial vasculature of the liver through a catheter in the femoral artery. Normal liver parenchyma receives most of its blood supply from the portal system, while liver malignancies depend more on the hepatic arteries. Therefore, when injected intra-arterially, these particles preferentially lodge in the tumor capillaries, resulting in a high local radiation dose. This therapy is routinely performed routinely in the clinical setting, and therefore, most experiences with microparticles are derived from radioembolization.

The 30 μm diameter^{166}Ho-microspheres were developed at the University Medical Center Utrecht together with many research partners.[9,10] In 2014, the microsphere technique was licensed to the UMC Utrecht spin-off company, Quirem Medical, and thereafter, CE-approval was obtained (QuiremSpheres; Quirem Medical B.V., Deventer, The Netherlands). These microspheres were developed as an alternative radioembolization particle and most of the experiences with this product were therefore obtained from this specific treatment method for liver tumors. In this discussion, a comparison to radioembolizations is made, and treatment with ^{166}Ho-microspheres was also investigated in an animal head and neck carcinoma model.[11] Despite promising results, the absence of the unique blood supply to the liver and the risk of neurological complications makes radioembolization of head and neck tumors challenging. Direct intra-tumoral injection of ^{166}Ho-microspheres with a needle may be a promising alternative to radioembolization in these tumors. The main issues considering the actual microparticles are discussed here, including the isotopes used, particle size, and leaching of isotopes from the microspheres.

The isotopes

Currently, multiple radioisotopes are used for microparticles. The ideal radioisotope microparticle combination has the following properties:[12]

- A half-life of several hours for treatment accuracy, acceptable logistics and radiation hygiene;
- High energy for sufficient tumor penetration;
- The abundance of gamma-radiation, or positron emission for imaging;
- Safe decay product;
- Biocompatible or bioresorbable;
- Easy manufacturing at low cost; and
- Minimal release of the isotope (leaching) to prevent systemic exposure.

The isotope ^{166}Ho meets most of these requirements with a half-life of 26.8 hours, a relatively high energy beta-radiation (E_β, max = 1.84 MeV), and a small percentage of gamma-radiation for single photon emission computed tomography (SPECT) imaging. In addition, biocompatibility and low leaching of ^{166}Ho-microspheres were described previously.[13,14] However, the production costs are relatively high because ^{166}Ho-microspheres require neutron activation in a nuclear reactor.

Particle size

There is a relationship between particle size and retention of the microparticles in the tumor after intra-tumoral injection, namely the larger the particle, the higher the retention.[15–19] A higher retention for several days when most of the radiation is emitted results in a higher absorbed dose. Consequently, larger microspheres with a size of 10–90 μm may be preferred over smaller particles of 0.5–5 μm.[20] On the other hand, the microparticles must be small enough to distribute throughout the tumor[20] to deliver an adequate and homogeneous absorbed dose, as the penetration depth of beta-radiation is limited to several mm (depending on beta-radiation energy).[21–23] The ideal particle size of intra-tumoral injection is unknown and warrants further investigation. However, this may be smaller than the ideal particle size for radioembolization (i.e. 30 μm). For example, good results were obtained with 10 μm microspheres in some of the veterinary patients after intra-tumoral injection.

Release of radioisotopes from the microparticles

Leaching of radioisotopes from microspheres depends on the type of microspheres.[24–27] Most knowledge is obtained from microspheres that are used in radioembolization of liver malignancies. The initial patent application for the ^{90}Y-resin microspheres (SIR-Spheres®, Sirtex) indicated that 0.01% to 0.4% of ^{90}Y leached from the microspheres after 20 minutes in water.[28] After radioembolization, 0.0657% and 0.0025% was excreted in the urine after 12 hours with resin and glass microspheres (TheraSphere®, BTG), respectively.[24] Also, rhenium-188

(^{188}Re) glass microspheres are chemically durable in body fluids and release <1.2% of ^{188}Re after being immersed in PBS solution for 32 days at 37°.[29] Release of radioisotopes from human serum albumin is usually larger, in the range of several percent.[30] This has two reasons: release from the microsphere-surface after labeling, and rapid biodegradation in case of a lower degree of crosslinking.[30,31] After ^{188}Re-microspheres radioembolization, an urinary excretion rate of 8.9% of administered activity within 72 hrs. was described.[27]

The leaching of ^{166}Ho from neutron-irradiated ^{166}Ho-microspheres proved to be dependent on several factors. In vitro, leaching of ^{166}Ho from ^{166}Ho-microspheres after maximum irradiation (8.9×10^{20} thermal neutrons m^{-2}) detected in the supernatant, was influenced by the type of injection fluid. After suspension in 10% ethanol 2% Pluronic® F-68 for an hour, 15% free ^{166}Ho was measured in the supernatant, while in 116 mM pH 7.2 buffer with Pluronic® F-68 for injection, <0.2% was found. Free ^{166}Ho precipitates with phosphate on the surface of the microspheres, which reduces the release.

Analysis of urine collections and peripheral blood samples from two prospective clinical studies[32,33] on ^{166}Ho-microspheres radioembolization showed low concentrations of holmium in the blood and urine, 0.15% and 0.13% of the injected amount respectively. These values were comparable to the known ^{90}Y urine excretion after ^{90}Y-microspheres radioembolization. After the initial release, probably caused by neutron activation induced damage, low but persisting levels of ^{165}Ho were detected in peripheral blood (median 0.01%; range 0.00–0.04%) and urine samples (median 0.01%; range 0.00–0.02%) after 13 weeks, indicating continuous slow in vivo microsphere-degradation as described previously.[34–36] Such measurements after weeks were never performed for ^{90}Y.

In accordance with the in-vitro results, the urinary excretion and blood values were significantly lower after the change from a 10% ethanol to a phosphate buffered (Ph. 7.2) suspension fluid. The median amount of ^{165}Ho in the blood sample one hour post-treatment decreased from 0.19% to 0.09%, and cumulative 24h-urine from 0.32% to 0.06%. Therefore, the phosphate buffered (pH 7.2) suspension fluid solution was used for subsequent studies with ^{166}Ho-microspheres.

Furthermore, a positive correlation between holmium release and longer neutron irradiation time was found. It is known that long neutron irradiation results in a decrease in molecular weight[10,37] of the microspheres, and visible damage[38,39] of the microspheres based on concomitant gamma-irradiation.[13] Based on these observations, the stability of ^{166}Ho-microspheres improves by minimization of the neutron irradiation time or the use of additional gamma ray shielding (lead) during irradiation.

Clinical studies with ^{166}Ho-microspheres

Safety and efficacy of ^{166}Ho microbrachytherapy in cats.
The intra-tumoral injection of ^{166}Ho-microspheres was initially performed in a cohort study of 13 cats with spontaneous oral squamous cell carcinoma (OSCC).[40] Feline OSCC (FOSCC) is an optimal and most relevant translational animal model to study various innovative treatment modalities before their application in humans. This is due to the similarities in risk factors[41-43], comparable molecular parameters (e.g., overexpression of epidermal growth factor receptor, vascular endothelial growth factor and p53 mutation), and biological and histological characteristics (e.g., tumor growth and metastasis), as well as their response to treatment.[44]

In this study, a local response rate of 55% was observed, including both complete response and partial response (tumor downstaging), enabling subsequent marginal tongue resection. Median survival time was much longer for patients with a good local response as compared to minimal tumor response or tumor progression (296 days and 113 days, respectively). In general, the side effects were minimal; however, a radiation ulcer developed at the surface of the tongue in a cat treated with >4000 Gy. It healed within 3 weeks with minimal supportive wound care, but in case of treatment near vital structures, caution seems necessary, especially after injection of high doses. Tumor volume was a significant predictor of response, with a better response in smaller lesions. Therefore, the observed response rate may be further improved by optimizing the intra-tumoral spatial distribution of ^{166}Ho-microspheres, as the penetration depth of ^{166}Ho is only a few millimeters. The results also showed that it was difficult to treat feline patients with larger malignancies of the upper jaw and extension to the maxillary sinus. In these cases, the tumor is often more advanced (than based on the CT scan) and the radiation absorbed in this area is usually low because this location is difficult to reach for intra-tumoral injection. This resulted in tumor progression primarily in the maxillary sinus. MRI with its superior soft tissue contrast may provide more information and result in better patient selection in these cases.[45] From this study, it was concluded that microbrachytherapy may have potential application as a minimally invasive, single procedure radio-ablation treatment of small unresectable tumors, with minimal toxicity. However, patient selection and improvements in administration technique are vital for the success of this treatment.

Feasibility in patients with a carcinoma of the tongue in a 'treat and resect' setting.
After the experiences in the veterinary study, this therapy was tried on human patients. A clinical phase I study was designed to determine the feasibility in patients with a squamous cell carcinoma of the tongue in a 'treat and resect' setting. Based on the veterinary experience, the first patients were treated with four intra-tumoral injections of ^{166}Ho-microspheres, followed by surgical resection after a week. A treat and resect study with a novel compound holds a compromise between exposing a patient to potential toxicity and assessing treatment efficacy. For this reason, the HIT (Holmium-166 microspheres Intra-Tumoral) study was performed with a limited number of patients (n=10).

Unfortunately, the HIT study was troubled by low accrual due to the newly introduced sentinel lymph node procedure, where intra-tumoral ^{166}Ho-microspheres hampered the imaging after peri-tumoral ^{99m}Tc-labelled nanocolloid injections. Moreover, patients were not willing to undergo extra injections with a radioactive compound in their tongue. Extending the inclusion criteria and reducing the invasiveness did not result in higher accrual. Therefore, this study was terminated prematurely after only a single patient was treated. This single treatment showed limited distribution in the tumor, again stressing the importance of the administration technique for optimal distribution within the tumor. However, it also showed the multimodal imaging potential of this treatment. Furthermore, tumor efficacy was seen on a microscopic level. Despite the limited results obtained, the observed efficacy encourages further research. The invasiveness of intra-tumoral injection made that most patients were reluctant to participate. Therefore, instead of a treat and resect study, future research should consider patients who may benefit directly from this treatment. This will be discussed in more depth in the next chapter.

Intra-tumoral injection of ^{166}Ho-microspheres in recurrent Head-Neck cancer

For patients with locoregional recurrences of HNC limited treatment options exist. In the palliative setting a minimally invasive single session and safe therapy is desirable. Three patients without regular treatment options were offered intra-tumoral injections with ^{166}Ho-microspheres, as described in **Chapter 5**. None of the patients experienced adverse events. However, technical difficulties were encountered, including precipitation of microspheres in necrotic tissue. This resulted in a relatively small area with a sufficiently high local dose, while the majority of the vital tumor border was left untreated. In another patient, high intra-tumoral pressure resulted in the inability to inject the microspheres. Based on these three patients, and the patient from the HIT study, it was concluded that intra-tumoral injections with ^{166}Ho-microspheres may be safe. However, careful patient selection and improved administration techniques are required to accomplish a more effective treatment, confirming the results found in cats. At this moment, ulcerative, or firm indurated tumors, or large lesions with a necrotic center appear difficult to obtain a sufficient distribution of ^{166}Ho-microspheres. In small lesions, the chance of obtaining a sufficient activity throughout the tumor is higher. In case of future clinical studies, small malignancies, for instance in patients with severe comorbidities or with oral field cancerization after multiple previous resections, may be suitable for this treatment. Other indications may include small lesions on challenging to reconstruct locations, such as the tip of the nose or corner of the eye, or the treatment (for example with holmium skin patches.[22]) of cutaneous malignancies that are currently treated with plesiotherapy[46] or contact radiotherapy.[47] Also malignancies outside the head and neck regions may be considered for intra-tumoral treatment (e.g., pancreas, kidney or brain tumors). [7,48]

Administration of ^{166}Ho-microspheres

The treatment of local tumors by direct intra-tumoral injection of radioactive microparticles may seem relatively straightforward. However, based on the experiences obtained in the preclinical work and the veterinary and human patients, several challenges must be overcome to reach a good tumor distribution in a controlled way.

Safety

Most (pre)clinical studies that were published on intra-tumoral treatment with radioactive particles showed acceptable toxicity, including low grade local redness of the treated area. In addition, increased laboratory values were found as a sign of local damage, which depended on the treated organ, for example, increased amylases and increased blood glucose levels indicating diabetes mellitus in pancreas carcinomas.[20] This is in line with the patients treated with intra-tumoral injection of ^{166}Ho-microspheres. Except for a local radiation ulcer in a cat, side effects were minimal.

The reported systemic side effects in the literature were generally mild, including fever, malaise, and loss of appetite. In addition, hematological side effects like thrombocytopenia and leucopenia occurred, possibly because of treatment of blood pooled organs (i.e. the liver), but also because of leakage of the radioisotopes and/or radioactive microparticles.[49,50] In our studies, no systemic side effects were observed, most likely due to the limited distribution of microspheres and the low activity used. Leakage of radioisotopes can be divided into two separate mechanisms: release or leaching of radioisotopes (e.g. leaching from the microparticles based on the blood and urine measurements after holmium radioembolization), and leakage of microparticles out of the tumor, which is often the result of the injection technique.

Injection technique

The injection of intra-tumoral particles may seem a relatively easy and straightforward procedure. However, the injection procedure of ^{166}Ho-microspheres is currently not predictable enough for controlled administration in a clinical setting. Factors like tumor characteristics, injection volume and technique make that no injection or its distribution of microspheres will be identical. The injected percentage ranged from 9% to 93% in the human and veterinary patients and this wide range must be reduced. First of all, technical solutions are desired to improve the injection procedure with intra-tumoral particles. The density of the microspheres (1.4 g/mL) causes precipitation, and combined with the particle size, a large number of microspheres and limited injection fluid can result in clotting within the needle. Reducing the weight of the particles or increasing the viscosity of the injection fluid could be an option to prevent precipitation.[18,51] Secondly, the ideal particle size for intra-tumoral injection may be smaller than the ideal particle size for radioembolization, for example 10 μm as used in some of the veterinary patients. Smaller particles may improve distribution and reduce clotting, allowing injection through smaller needles. Increasing the specific activity of the microspheres can reduce the total number of microspheres.[52]

Furthermore, tumor related factors like consistency and location result in difficulties during intra-tumoral treatment. Especially if the time from re-suspension to injection is too long (>5 sec), difficulties related to precipitation and clotting seem to appear. This could explain the inability to inject microspheres in the patient described in **Chapter 5** with a firm metastasis in the neck, for whom ultrasound was used to determine the optimal injection location. Improving the injection procedure, and knowing the injected amount instead of measuring and correcting the injected doses after the procedure is necessary. In addition, this allows the change of focus towards imaging and improving the distribution. As described above, in ulcerative, or firmly indurated tumors, or large lesions with a necrotic center it appeared difficult to obtain a sufficient distribution of ^{166}Ho-microspheres.

Leakage of microparticles out of the tumor appears to follow the path of least resistance.[53,54] In most lesions there seemed to be a relative natural barrier between the tumor and its surrounding tissue. However, in the patient with an ulcerous tumor of the tongue leakage occurred, which was partially ingested. Ulcerous or granular tissue must therefore be treated with extra caution. An easy route of leakage after intra-tumoral administration is the so-called injection canal leakage. This leakage was experienced in veterinary patients and the rabbit's experiments and the use of a small needle may reduce this injection canal leakage. However, with small gauge needles settling and clotting of microparticles inside the syringe may block the needle, especially in a firm lesion. A 21G needle seems to be the preferred needle to use. Additional measures to reduce leakage may include low injection volume and slow injection, withdrawal of the needle after a few seconds waiting time as this allows to even out the applied pressure[55], and subsequent injection of obstructing pledged/foam.[56] Other routes of leakage (i.e., intravascular or intra-ductal) may be caused by a wrong injection position, an excessive injection volume, or a too high injection pressure.[56–58] In one of the veterinary patients intravenous leakage may explain the observed microspheres in the lungs at autopsy. Increased permeability of tumor neovascularization may be therefore be considered a risk factor of leakage.[59] Leakage of an entire dose, as described after intra-ductal injection in the pancreas, may happen when a single infusion technique is used in combination with a wrong injection position.[57] This may also occur in the head and neck region in case of treatment of the salivary glands through the ductus Stenoni or ductus Whartoni. A grid-like injection procedure in small volume depots may reduce this risk and enhance the distribution and is therefore preferred over a single infusion.

Efficacy

Previous studies have shown a higher efficacy of beta-radiation in the induction of tumor cell cytotoxicity, apoptosis and necrosis compared to an equivalent dose of gamma-radiation, which may be associated with differential DNA damage and subsequent repair kinetics in tumor cells after these radiations.[60–62] The intra-tumoral injection of beta-emitting microparticles seems to be an effective strategy for administering a high local dose of radiation**.** For example, in hepatocellular cancer patients, the intra-tumoral injection of posphate-32 (^{32}P) microparticles resulted in 25% complete response and 25% partial response at 12 weeks after therapy.[56] Nevertheless, the efficacy in case of intra-tumoral ^{166}Ho-microspheres treatment in humans was limited. The focus in these patients was not curation but quality of life and therefore a safe but relative low activity was used. Nevertheless, microscopically anti-tumor efficacy was seen in the resection specimen. To increase the efficacy of intra-tumoral treatment, the absorbed dose over the total tumor should be high enough.

Absorbed dose

In the performed studies of this thesis, the planned injected dose was 100 Gy in humans, while 200–800 Gy was used in the animals. This may explain the limited efficacy in HNC patients. Increasing the injected activity is a simple strategy to improve the tumor absorbed dose. However, the required dose is unknown. In an ongoing study with intra-tumoral injections of ^{32}P microparticles in pancreas carcinoma also a dose of 100 Gy was injected.[63,64] The used doses in brachytherapy of the prostate depend on the isotope; iodine-125 (140–160 Gy), Palladium-103 (110–125 Gy) or Cesium-131 (115 Gy).[65] The recommended liver absorbed dose for ^{90}Y glass microspheres radioembolization is 80–150 Gy[66], and 60 Gy for ^{166}Ho-microspheres.[32] Part of these differences may be explained by the difference in dose rate and more important, the difference in dose distribution with different internal radiation therapies. Preliminary results from ^{166}Ho-microspheres radioembolization showed that there is a significant effect of tumor absorbed dose on lesion response with a median dose of almost 200 Gy for complete response. This will probably provide more insight in the required absorbed dose in the near future.[67]

Distribution

Finally, the absorbed dose should not only be high enough, but also be sufficient throughout the entire vital tumor tissue, to be effective. However, the exact relationship between the number of particles, the distribution and therefore optimal distance between injection positions is currently unknown. Furthermore, no distribution after intra-tumoral injection is likely to be identical. The heterogeneity in distribution is probably caused by variations in the injection fluid, injection pressure, total volume and number of microspheres, and the heterogeneity in tumor consistency, tumor anatomy, and tissue properties in which the tumor grows as described previously.

The limited tissue penetration of beta-radiation requires an almost perfect distribution of ^{166}Ho-microspheres throughout the tumor. As described above, the majority of the dose is absorbed in the first millimeter, which could easily result in tumor regions with insufficient dose and suboptimal treatment outcomes. In smaller tumors, this is probably less likely to be problematic, which explains the observed correlation between tumor size and efficacy in the veterinary experience. Furthermore, efficacy in the veterinary patients may be explained as the tumor size was much smaller in the animals being 3.17 ± 1.70 cm^3 versus 3.9 to 44.6 cm^3 in humans, respectively.

An option to increase the distribution throughout the tumor, is to use more injection fluid or more force during the injection.[68] Theoretically, more fluid results in more propelling force and a larger distribution of microparticles in the target tumor tissue. The injected volume of the solution with microparticles should range between 7% and 30% of the tumor volume,[56,58,69] to obtain an optimal distribution of the particles throughout the tumor, whereas excessive volume (50–100%) or pressure may result in leakage of microparticles (and radiation) outside the tumor.[68,70] Large injection volumes and forceful injections may lead to an unpredictable distribution and should be avoided. A simple method to increase the distribution may be to increase the number of injections. The number of injections in the human patients was less (2–4) compared to up to 11 in the animals. Combined with the re-suspension and reinjection strategy, often performed in animals in case of visible microspheres in the syringe, the total number of injection locations was even greater. Injecting small depots of a more viscous fluid may be used to obtain more control, and preventing the settling of the microparticles. For example, 25% glucose, fibrin glue, and other formulas were used to improve the injection procedure, or hydrogels such as chitosan.[56,71–73]

Nevertheless, this limited radiation penetration is the case for all beta- and alpha-radiation therapies and yet promising results are obtained.[74] In the case of radioembolization, tumor vasculature aids in the distribution.[75,76] But also systemic immune activation is shown after radioembolization and is likely to play a significant role in the overall tumor response.[77,78] The core mechanism is that ionizing radiation–induced cell death generates a flood of preserved tumor-associated antigens, creating an effective in situ tumor vaccine.[79,80] Among many interactions, radiation improves dendritic cell priming of anti-tumor T cells and increases major histocompatibility complex class-1 expression, thereby facilitating tumor antigen manifestation to T cells.[81,82] This immunologic response to localized irradiation as mediator of systemic effects after localized radiotherapy or abscopal effect may provide some slack in case of suboptimal distribution.[83]

Imaging

Although multiple studies were performed on safety and efficacy previously, relatively little is known of the intra-tumoral distribution after intra-tumoral treatment with microparticles. The experience in the human patients suggests that future studies should take into account the imaging of the particles, to evaluate distribution in vivo, and ideally in real-time.[7] Besides gamma-emission for SPECT imaging, the potential strength of ^{166}Ho-microspheres is the high x-ray attenuation for CT imaging, and paramagnetic properties for visualization by MRI. The multi-modality imaging characteristics of holmium might be advantageous, as no single modality can fulfill the requirements both during treatment and response evaluation. MRI and SPECT/CT quantification are further developed at this stage compared to CT imaging of ^{166}Ho-microspheres. In case of intra-tumoral treatment, CT imaging could be preferred because of its high resolution, and good availability throughout the hospitals.

CT quantification of ^{166}Ho-microspheres

The fact that beta-radiation has limited penetration implies that imaging evaluation of the dose distribution should be performed at high-resolution to account for heterogeneous dose distribution. CT imaging could provide superior resolution (<1 mm) of the distribution of ^{166}Ho-microspheres compared to the currently used SPECT (4.8 mm) and MRI (3 mm). Furthermore, CT imaging may open an entirely new field of CT guided treatment, with the opportunity to perform fast acquisition imaging. In **Chapter 6,** the feasibility of CT imaging of holmium microspheres is presented. The amount of holmium in the tumor was determined by a threshold method, based on the density, and compared with a validated ^{166}Ho-microspheres SPECT/CT quantification method. CT recovered almost identical amounts of holmium compared to the intra-tumoral activity detected on SPECT/CT. Considering some limitations of the currently used SPECT/CT method (e.g. long acquisition times), CT-based quantification for intra-tumoral holmium microspheres injections seems feasible, but more specific detection is necessary.

Advancements with dual-energy CT

New developments for even more advanced analyses and true material decomposition using dual-energy CT imaging were described in **Chapter 7**. The dual-energy CT (DECT) (SOMATOM Force, Siemens Healthcare GmbH, Forchheim, Germany) has two x-ray tubes, instead of one. When using different tube settings, one can discriminate between materials, for example as used in the determination of the composition of kidney stones. Furthermore, DECT quantification could discriminate holmium from bone, arterial calcification and often used iodine contrast agents, which is not possible with conventional CT. In collaboration with Siemens Healthcare, this system was tested on a phantom and in-vivo laboratory animals, to detect and quantify holmium by K-edge imaging. The K-edge (binding energy of the K-shell (innermost) electron of an atom) of holmium (56 keV) is higher than that of commonly used contrast medium such as iodine (33 keV). This facilitates specific holmium K-edge imaging and may be used for simultaneous imaging of a patient's vascularization and local accumulations of ^{165}Ho-microspheres in tumorous regions.

Four adult female rabbits with subcutaneous VX-2 tumors were intra-tumorally injected with neutron activated ^{166}Ho-microspheres. The high dose acquisitions with 80/150 kV, provided excellent accuracy for concentrations down to 0.125 mg/mL. The recovered amount of holmium corresponded well to the injected amount of holmium microspheres with underestimation up to -11.7%. In addition to anatomical and structural information of the treated area, fast, accurate quantification and high-resolution assessment of the (dose) distribution after treatment with holmium microspheres can be made. This feature could be of clinical value for verifying the distribution of holmium microspheres during and after intra-tumoral injection procedures. The long scanning time of 45 minutes of SPECT makes it impossible to check whether the injection procedure provided sufficient distribution of ^{166}Ho-microspheres throughout the tumor. A second or third scan is even less feasible. Furthermore, the resolution of SPECT imaging (>5 mm) is insufficient for imaging intra-tumoral dose distribution. The absorbed dose of holmium declines very rapidly and 70–75% of the dose of holmium is absorbed in the first millimeter. Despite a SPECT showing a homogeneous and sufficient tumor absorbed dose, tumor regions may be left untreated. DECT is becoming more available in the clinical setting and the first experiments are currently being performed in patients after radioembolization.

Imaging of response

A CT scan is usually performed three months after treatment as the only measure of treatment response. In the literature, ^{32}P injections in pancreas carcinomas only caused tumor liquefaction without decreasing tumor size. Possibly, the ^{32}P injections caused central tumor liquefaction, while cancer persisted at the periphery of the injection sites, thus limiting the ability of the ^{32}P injections to cause a decrease in radiologic tumor size.[69] In the patient with a large necrotic metastasis in the neck, the majority of the tumor periphery was insufficiently treated. However, PET/CT showed decreased tumor vitality in the area where the microspheres had precipitated (chapter 6).

Also in radioembolization, lack of tumor size decrease due to tumor liquefaction is observed.[84] Therefore, instead of only imaging the size, the metabolic activity should be investigated, for example with fluor-18 (^{18}F)-fluorodeoxyglucose (FDG) PET/CT or with diffusion-weighted MRI (DW-MRI), as these have shown to be better predictors of survival.[85] Also the chosen time-point for imaging is important. The standard three-months interval currently used after chemo-irradiation, is probably too long in case of beta-emitting particles with a half-life of several hours. For instance, 75% of the radiation of ^{166}Ho is delivered in the first two days, and necrosis/ apoptosis is seen 72 hours and 96 hours after exposure to beta-radiation.[60] Earlier imaging makes sense, especially because previous human studies with intra-tumoral injections performed re-treatments after 2–4 weeks with promising results.[49,57] In the case of imaging the tumor vitality with PET-CT of DW-MRI, the administration locations could be further personalized and should be considered in future studies.

LESSONS LEARNED

This thesis resulted in important new knowledge concerning the injection method, imaging of the particles, and outcomes and treatment of HNC patients. Due to its half-life high energy and imaging characteristics, the isotope ^{166}Ho meets most of the requirements of the ideal radioisotope microparticle combination. Furthermore, leaching of radioisotopes from microparticles does not seem to be a major issue in radioembolization with ^{166}Ho-microspheres. In the case of intra-tumoral treatment, a lower number of ^{166}Ho-microspheres is used and the microspheres are irradiated more briefly, resulting in less damage compared with radioembolization. The ideal particle size for intra-tumoral injection is presumably in the micrometer range, but it may be smaller than the ideal particle size for radioembolization (30 μm; e.g., 10 μm as used in some of the veterinary patients); this should be investigated in more detail in future studies.

In veterinary patients with relatively small tumors, the intra-tumoral injection of microparticles has already shown promising results. This illustrates that intra-tumoral injection may be a potential route for administering an effective lethal tumor dose of beta-radiation. Despite the resemblance of human and feline OSCC,[41,44] intra-tumoral treatment with ^{166}Ho microspheres—as currently performed—does not result in the successful treatment of human patients. In this chapter, multiple explanations for this were discussed. One other important factor is the existence of a learning curve with intra-tumoral injection, similar to other surgical interventions. Efficiency improves with experience.[86] Up to 40 veterinary patients and laboratory animals were treated by a multidisciplinary team, compared to only 4 humans by a newly formed team. Furthermore, the procedure was performed under general anesthesia in animals, whereas local anesthesia was used in the outpatient setting in humans. General anesthesia has the advantage of optimal preparation and probably results in a faster and more accurate injection. Especially in the case of the tongue, obtaining an optimal administration setting was difficult because manipulation of the tongue remained uncomfortable, resulting in movement of the organ. In addition, visualization of the previous injection location and determining the next location is more difficult if the patient swallows between injections, and this is likely to hamper the distribution of the ^{166}Ho-microspheres. In addition, (neo)adjuvant treatments, including re-treatments and laser resection, were performed in cats. Reducing tumor volume before intra-tumoral treatment increases the change of an optimal intra-tumoral dose distribution, while debulking with ^{166}Ho-microspheres sometimes allowed adjuvant treatment. Combinations of therapies in these animals also improved the survival. Another difference was that, in veterinary patients, the primary tumor was treated, whereas most human patients had regional metastases and had previously received chemoradiation or external beam radiation therapy; thus, they were probably relatively radio-resistant. In summary, the easier injection under general anesthesia, more injection locations combined with smaller tumors and higher injected dose resulted in a sufficient distribution of ^{166}Ho-microspheres in animals, but these components were not applied

in the human setting. New developments like CT and DECT in the field of imaging seem promising and may aid in future treatments.

FUTURE PERSPECTIVES

This thesis provided insight into the feasibility and application of intra-tumoral treatment with ^{166}Ho-microspheres in HNC. Based on the first clinical results, ^{166}Ho-microspheres may be an effective anti-tumoral medical device in selected cases, and intra-tumoral injections seem to be relatively safe. As described previously, intra-tumoral treatment with microparticles is not straightforward. Changes in the injection fluid, where during the injection, the microspheres stay homogeneously divided through the fluid; this may simplify the injection resulting in a reduction of injection variance.

The development of high-resolution imaging of the dose distribution may allow for better image guided, personalized treatment. The detection of holmium with CT is the first step, but material decomposition with dual-energy CT—or even next-generation photon-counting CT—permits imaging in even greater detail. Dual-energy CT already reduces the detection limit from approximately 2.5 mg/mL holmium to 0.125 mg/mL. In addition, material decomposition with photon-counting CT allows the use of contrast-enhanced CT necessary for tumor delineation during treatment, and it is routinely performed in HNC. However, the high-resolution imaging and quantification of holmium is not the goal of imaging; rather, it is to produce a three-dimensional map of the absorbed dose. This requires a large amount of computer power. Furthermore, this information should preferably be immediately available during treatment to check the distribution. In future, advances in imaging, such as in (dual-energy) CT, will become more widely available, and the image processing will become faster; this will allow quick analysis of the 3D dose distribution and guide re-injections where necessary.

Solving these issues may result in proper imaging of the treatment, which will allow better prediction of the results. However, for larger tumors in patients with HNC, the final step in intra-tumoral treatment with ^{166}Ho-microspheres is to act in case of suboptimal distribution. Subsequent injections could be performed by experts experienced in image-guided injection. However, more advanced methods are within reach. The combination of the use of a needle placement system and CT imaging was presented in a VX-2 tumor-bearing rabbit. The treatment was performed under general anesthesia under full CT-guidance by four injections of non-radioactive ^{165}Ho-microspheres using a needle placement system, which was developed by DEMCON (DEMCON Advanced Mechatronics, Enschede, Netherlands). (Figure 9.1) The aid of robotic administration systems may allow quicker and more accurate needle placement. In the future, these advanced robotic assisted administration techniques,[87,88] combined with navigation models and steerable needles,[89] may overcome some of the current drawbacks of

intra-tumoral injection. Therefore, further investigation of this novel treatment modality is encouraged in larger tumors, especially because of the absence of side effects, and the lack of other treatment options in case of recurrent HNC.

CONCLUSION

In conclusion, intra-tumoral injection of radioactive microparticles is an innovative and safe treatment approach. Nevertheless, its efficacy must be increased, especially in larger tumors. The combination of an advanced needle position system with steerable needles and real-time imaging of the dose distribution for feedback loops to guide the consecutive injection is needed to reach more control of this technique. The intra-tumoral treatment would then become more convenient and predictable with a small number of microspheres containing a high specific activity in a suspension that prevents settling. In a nutshell, improved injection techniques are needed to mature intra-tumoral microbrachytherapy as a single-session, minimally invasive, safe, effective treatment modality.

Figure 9.1. *A: CT-guided needle placement system by DEMCON mechatronics with customized needle guide for injection of radioactive ^{166}Ho-microspheres. B: 9 mm acrylic glass beta-radiation protection and ruler to measure the injection depth. C: 3D reconstruction rabbit number 4 with 22.3 cm^3 VX-2 tumor after image-guided ^{165}Ho-microspheres injection. D, E, F, and G: zoom in on the segmented tumor after the four sequential injections (Window range HU <100). H: with the segmented tumor translucent.*

REFERENCES

1. Ferlay J, Soerjomataram I, Dikshit R, Eser S, Mathers C, Rebelo M, et al. Cancer incidence and mortality worldwide: Sources, methods and major patterns in GLOBOCAN 2012. Int J Cancer 2015;136:E359–86.
2. Mehanna H, West CML, Nutting C, Paleri V. Head and neck cancer—Part 2: Treatment and prognostic factors. BMJ 2010;341:c4690.
3. Van Dijk BAC, Brands MT, Geurts SME, Merkx MAW, Roodenburg JLN. Trends in oral cavity cancer incidence, mortality, survival and treatment in the Netherlands n.d.
4. Noorlag R. Prognostic biomarker in oral cancer towards more individualized treatment. 2016.
5. Leusink KFJ. Molecular markers of lymph node metastasis in oral cancer. 2016.
6. Demir D. The Role of Sentinel Lymph Node Biopsy in Head and Neck Cancers and Its Application Areas 2016.
7. Bakker RC, Lam MGEH, van Nimwegen SA, Rosenberg AJWP, van Es RJJ, Nijsen JFW. Intratumoral treatment with radioactive beta-emitting microparticles: a systematic review. J Radiat Oncol 2017.
8. Gill HS, Prausnitz MR. Does needle size matter? J Diabetes Sci Technol 2007;1:725–9.
9. Nijsen JFW, Zonnenberg BA, Woittiez JRW, Rook DW, Swildens-Van Woudenberg IA, Van Rijk PP, et al. Holmium-166 poly lactic acid microspheres applicable for intra-arterial radionuclide therapy of hepatic malignancies: Effects of preparation and neutron activation techniques. Eur J Nucl Med 1999;26:699–704.
10. Zielhuis SW, Nijsen JFW, De Roos R, Krijger GC, Van Rijk PP, Hennink WE, et al. Production of GMP-grade radioactive holmium loaded poly(L-lactic acid) microspheres for clinical application. Int J Pharm 2006;311:69–74.
11. van Es RJJ. The rabbit Vx2 auricle carcinoma : an animal model for development of new locoregional treatment strategies against squamous cell carcinoma of the head and neck. universiteit utrecht, 2001.
12. Burrill J, Hafeli U, M Liu D. Advances in Radioembolization - Embolics and Isotopes. J Nucl Med Radiat Ther 2011;01:1–6.
13. Zielhuis SW, Nijsen JFW, Krijger GC, van het Schip AD, Hennink WE. Holmium-loaded poly(L-lactic acid) microspheres: In vitro degradation study. Biomacromolecules 2006;7:2217–23.
14. Zielhuis SW, Nijsen JFW, Dorland L, Krijger GC, van het Schip AD, Hennink WE. Removal of chloroform from biodegradable therapeutic microspheres by radiolysis. Int J Pharm 2006;315:67–74.
15. Junfeng Y, Duanzhi Y, Xiaofeng M, Zili G, Jiong Z, Yongxian W, et al. [188Re]Rhenium sulfide suspension: a potential radiopharmaceutical for tumor treatment following intra-tumor injection. Nucl Med Biol 1999;26:573–9.
16. Zubillaga MB, Boccio JR, Nicolini JO, Ughetti R, Lanari E, Caro RA. Pirocarbotrat(TM): A new radiopharmaceutical for the treatment of solid tumors - Comparative studies in N-nitrosomethylurea-induced rat mammary tumors. Nucl Med Biol 1997;24:559–64.
17. Zubillaga MB, Boccio JR, Nicolini JO, Ughetti R, Lanari E, Caro RA. Radiochemical and radiopharmacological properties of Pirocarbotrat and other labeled charcoal dispersions: Comparative studies in rats with NMU- induced mammary tumors. Nucl Med Biol 1998;25:305–11.
18. Chi JL, Li CC, Xia CQ, Li L, Ma Y, Li JH, et al. Effect of 131I gelatin microspheres on hepatocellular carcinoma in nude mice and its distribution after intratumoral injection. Radiat Res 2014;181:416–24.
19. Luboldt W, Pinkert J, Matzky C, Wunderlich G, Kotzerke J. Radiopharmaceutical tracking of particles injected into tumors: a model to study clearance kinetics. Curr Drug Deliv 2009;6:255–60.
20. Bakker RC, Lam MGEH, van Nimwegen SA, Rosenberg AJWP, van Es RJJ, Nijsen JFW. Intratumoral treatment with radioactive beta-emitting microparticles: a systematic review. J Radiat Oncol 2017;6:323–41.
21. Hosseini SH, Enferadi M, Sadeghi M. Dosimetric aspects of ^{166}Ho brachytherapy biodegradable glass seed. Appl Radiat Isot 2013;73:109–15.
22. Lee J, Park K, Lee M, Kim E, Rhim K, Lee J, et al. Production of Holmium-166 Skin Patch. vol. 38. 1997.
23. Mowlavi AA, Afzalifar A, Afzalifar N, Kashani E. Depth Dose Calculation of Holmium-166 for Different Shape Source by VARSKIN3 Code. n.d.
24. Lambert B, Sturm E, Mertens J, Oltenfreiter R, Smeets P, Troisi R, et al. Intra-arterial treatment with 90Y microspheres for hepatocellular carcinoma: 4 years experience at the Ghent University Hospital. Eur J Nucl Med Mol Imaging 2011;38:2117–24.
25. Grosser OS, Pethe A, Kupitz D, Wissel H, Ulrich G, Ricke J, et al. Release of Yttrium-90 from Resin Based Microspheres used in Radioembolisation of Primary and Secondary Liver Malignancies 1989:39120.
26. Grosser OS, Ruf J, Pethe A, Kupitz D, Wissel H, Benckert C, et al. Urinary Excretion of Yttrium-90 After Radioembolization With Yttrium-90-Labeled Resin-Based Microspheres. Health Phys 2017:1.
27. Liepe K, Brogsitter C, Leonhard J, Wunderlich G, Hliscs R, Pinkert J, et al. Feasibility of High Activity Rhenium-188-Microsphere in Hepatic Radioembolization. Jpn J Clin Oncol 2007;37:942–50.
28. Gray B, inventor; Sirtex Medical Limited, assignee. Polymer based radionuclide containing particulate material. International application number PCT/AU 2001/001370. February 5, 2002., n.d.
29. Conzone SD, Häfeli UO, Day DE, Ehrhardt GJ. Preparation and properties of radioactive rhenium glass microspheres intended for in vivo radioembolization therapy. J Biomed Mater Res 1998;42:617–25.

30. Vranješ-Đurić S, Radović M, Nikolić N, Janković D, Goya GF, Torres TE, et al. Novel multifunctional 90 Y-labelled albumin magnetic microspheres for cancer therapy. n.d.
31. Langer K, Anhorn MG, Steinhauser I, Dreis S, Celebi D, Schrickel N, et al. Human serum albumin (HSA) nanoparticles: Reproducibility of preparation process and kinetics of enzymatic degradation. Int J Pharm 2008;347:109–17.
32. Smits MLJ, Nijsen JFW, van den Bosch MAAJ, Lam MGEH, Vente MAD, Mali WPTM, et al. Holmium-166 radioembolisation in patients with unresectable, chemorefractory liver metastases (HEPAR trial): A phase 1, dose-escalation study. Lancet Oncol 2012;13:1025–34.
33. Prince JF, van den Bosch MAAJ, Nijsen JFW, Smits MLJ, van den Hoven AF, Nikolakopoulos S, et al. Efficacy of radioembolization with holmium-166 microspheres in salvage patients with liver metastases: a phase 2 study. J Nucl Med 2017:jnumed.117.197194.
34. Zielhuis SW, Nijsen JFW, Krijger GC, van het Schip AD, Hennink WE. Holmium-Loaded Poly(l-lactic Acid) Microspheres: In Vitro Degradation Study 2006.
35. Bult W, De Leeuw H, Steinebach OM, Van Der Bom MJ, Wolterbeek HT, Heeren RMA, et al. Radioactive holmium acetylacetonate microspheres for interstitial microbrachytherapy: An in vitro and in vivo stability study. Pharm Res 2012;29:827–36.
36. Vente MAD, Nijsen JFW, de Wit TC, Seppenwoolde JH, Krijger GC, Seevinck PR, et al. Clinical effects of transcatheter hepatic arterial embolization with holmium-166 poly(L-lactic acid) microspheres in healthy pigs. Eur J Nucl Med Mol Imaging 2008;35:1259–71.
37. Nijsen JFW, Van Het Schip AD, Van Steenbergen MJ, Zielhuis SW, Kroon-Batenburg LMJ, Van De Weert M, et al. Influence of neutron irradiation on holmium acetylacetonate loaded poly(L-lactic acid) microspheres. Biomaterials 2002;23:1831–9.
38. Vente MAD, Nijsen JFW, de Roos R, van Steenbergen MJ, Kaaijk CNJ, Koster-Ammerlaan MJJ, et al. Neutron activation of holmium poly(L-lactic acid) microspheres for hepatic arterial radioembolization: A validation study. Biomed Microdevices 2009;11:763–72.
39. Nijsen JF, van Het Schip AD, van Steenbergen MJ, Zielhuis SW, Kroon-Batenburg LMJ, van de Weert M, et al. Influence of neutron irradiation on holmium acetylacetonate loaded poly(L-lactic acid) microspheres. Biomaterials 2002;23:1831–9.
40. van Nimwegen SA, Bakker RC, Kirpensteijn J, van Es RJJ, Koole R, Lam MGEH, et al. Intratumoral injection of radioactive holmium (166 Ho) microspheres for treatment of oral squamous cell carcinoma in cats. Vet Comp Oncol 2017;0:1 – 11.
41. Wypij JM. A Naturally Occurring Feline Model of Head and Neck Squamous Cell Carcinoma. Patholog Res Int 2013;2013:1–7.
42. Munday JSS, Howe L, French A, Squires RAA, Sugiarto H. Detection of papillomaviral DNA sequences in a feline oral squamous cell carcinoma. Res Vet Sci 2009;86:359–61.
43. Supsavhad W, Dirksen WP, Martin CK, Rosol TJ. Animal models of head and neck squamous cell carcinoma. Vet J 2015;210:7–16.
44. Yoshikawa H, Ehrhart EJ, Charles JB, Thamm DH, LaRue SM. Immunohistochemical characterization of feline oral squamous cell carcinoma. Am J Vet Res 2012;73:1801–6.
45. Gomaa MA, Hammad MS, Abdelmoghny A, Elsherif AM, Tawfik HM. Magnetic resonance imaging versus computed tomography and different imaging modalities in evaluation of sinonasal neoplasms diagnosed by histopathology. Clin Med Insights Ear, Nose Throat 2013;6:9–15.
46. Ray A, Basu A, Deb A, Aich RK, Biswas LN, Pal JK. Plesiotherapy for non-melanoma skin cancer: innovating to overcome! Indian J Dermatol 2010;55:363–6.
47. McGregor S, Minni J, Herold D. Superficial Radiation Therapy for the Treatment of Nonmelanoma Skin Cancers. J Clin Aesthet Dermatol 2015;8:12.
48. Klaassen NJM, Arntz MJ, Gil Arranja A, Roosen J, Nijsen JFW. The various therapeutic applications of the medical isotope holmium-166: a narrative review. EJNMMI Radiopharm Chem 2019;4:19.
49. Tian JH, Xu BX, Zhang JM, Dong BW, Liang P, Wang XD. Ultrasound-guided internal radiotherapy using yttrium-90-glass microspheres for liver malignancies. J Nucl Med 1996;37:958–63.
50. Order SE, Siegel JA, Principato R, Zeiger LS, Johnson E, Lang P, et al. Preliminary experience of infusional brachytherapy using colloidal 32P. Ann Acad Med Singapore 1996;25:347–51.
51. Li CC, Chi JL, Ma Y, Li JH, Xia CQ, Li L, et al. Interventional therapy for human breast cancer in nude mice with 131I gelatin microspheres (131I-GMSs) following intratumoral injection. Radiat Oncol 2014;9.
52. Arranja AG, Hennink WE, Denkova AG, Hendrikx RWA, Nijsen JFW. Radioactive Holmium Phosphate Microspheres for Cancer Treatment. Int J Pharm 2018.
53. O ED, Ng KS, Karp JM. Emerging Medical Devices for Minimally Invasive Cell Therapy. Mayo Clin Proc 2014;89:259–73.
54. van Landeghem FKH, Maier-Hauff K, Jordan A, Hoffmann K-T, Gneveckow U, Scholz R, et al. Post-mortem studies in glioblastoma patients treated with thermotherapy using magnetic nanoparticles. Biomaterials 2009;30:52–7.

55. Præstmark KA, Stallknecht B, Jensen ML, Sparre T, Madsen NB, Kildegaard J. Injection Technique and Pen Needle Design Affect Leakage From Skin After Subcutaneous Injections. J Diabetes Sci Technol 2016;10:914.
56. Goh AS, Chung AY, Lo RH, Lau T, Yu SW, Chang M, et al. A novel approach to brachytherapy in hepatocellular carcinoma using a phosphorous32 (32P) brachytherapy delivery device-a first-in-man study. Int J Radiat Oncol Biol Phys 2007;67:786–92.
57. Order SE, Siegel JA, Principato R, Zeiger LE, Johnson E, Lang P, et al. Selective tumor irradiation by infusional brachytherapy in nonresectable pancreatic cancer: a phase I study. Int J Radiat Oncol Biol Phys 1996;36:1117–26.
58. Westlin JE, Andersson-Forsman C, Garske U, Linné T, Aas M, Glimelius B, et al. Objective responses after fractionated infusional brachytherapy of unresectable pancreatic adenocarcinomas. Cancer 1997;80:2743–8.
59. Nguyen H, Ghanem G, Morandini R, Verbist A, Larsimont D, Fallais C, et al. Tumor type and vascularity: Important variables in infusional brachytherapy with colloidal 32P. Int J Radiat Oncol 1997;39:481–7.
60. Murakami D, Suzuki MF, da Silva Dias M, Okazaki K. Genotoxic and cytotoxic effects of 60Co γ-rays and 90Sr/90Y β-rays on Chinese hamster ovary cells (CHO-K1). Radiat Environ Biophys 2004;43:91–9.
61. Kumar C, Jayakumar S, Pandey BN, Samuel G, Venkatesh M. Cellular and molecular effects of beta radiation from I-131 on human tumor cells: a comparison with gamma radiation. Curr Radiopharm 2014;7:138–43.
62. de Oliveira EM, Suzuki MF, do Nascimento PA, da Silva MA, Okazaki K. Evaluation of the effect of 90Sr beta-radiation on human blood cells by chromosome aberration and single cell gel electrophoresis (comet assay) analysis. Mutat Res 2001;476:109–21.
63. Bhutani MS, Cazacu IM, Luzuriaga Chavez AA, Singh BS, Wong FCL, Erwin WD, et al. Novel EUS-guided brachytherapy treatment of pancreatic cancer with phosphorus-32 microparticles: first United States experience. VideoGIE an Off Video J Am Soc Gastrointest Endosc 2019;4:223–5.
64. Harris M, Croagh D, Aghmesheh M, Nagrial A, Nguyen N, Wasan H, et al. P-141PanCO: An open-label, single-arm pilot study of Oncosil™ in patients with unresectable locally advanced pancreatic adenocarcinoma in combination with FOLFIRINOX or gemcitabine+nab-paclitaxel chemotherapies. Ann Oncol 2018;29.
65. Stish BJ, Davis BJ, Mynderse LA, McLaren RH, Deufel CL, Choo R. Low dose rate prostate brachytherapy. Transl Androl Urol 2018;7:341–56.
66. Giammarile F, Bodei L, Giammarile F, Bodei L, Flux G, Forrer F, et al. EANM procedure guideline for the treatment of liver cancer and liver metastases with intra-arterial radioactive compounds. Eur J Nucl Med Mol Imaging n.d.
67. Bastiaannet R, Van Roekel C, Smits MLJ, Bruijnen RCG, Prince JF, De Jong HWAM, et al. First evidence for a dose-response relationship in hepatic holmium-166 radioembolization. n.d.
68. Lee JD, Yang WI, Lee MG, Ryu YH, Park JH, Shin KH, et al. Effective local control of malignant melanoma by intratumoral injection of a beta-emitting radionuclide. Eur J Nucl Med Mol Imaging 2002;29:221–30.
69. Rosemurgy A, Luzardo G, Cooper J, Bowers C, Zervos E, Bloomston M, et al. 32P as an adjunct to standard therapy for locally advanced unresectable pancreatic cancer: a randomized trial. J Gastrointest Surg 2008;12:682–8.
70. Flocks RH, Elkins HB, Culp D. Treatment of cancer of prostate by interstitial injection of Au 198: studies in problem of distribution. J Urol 1957;77:505–20.
71. H??feli UO, Pauer GJ, Unnithan J, Prayson RA. Fibrin glue system for adjuvant brachytherapy of brain tumors with 188Re and 186Re-labeled microspheres. Eur J Pharm Biopharm 2007;65:282–8.
72. Kim JK, Han K-H, Lee JT, Paik YH, Ahn SH, Lee JD, et al. Long-term clinical outcome of phase IIb clinical trial of percutaneous injection with holmium-166/chitosan complex (Milican) for the treatment of small hepatocellular carcinoma. Clin Cancer Res 2006;12:543–8.
73. Suzuki YS, Momose Y, Higashi N, Shigematsu A, Park KB, Kim YM, et al. Biodistribution and kinetics of holmium-166-chitosan complex (DW-166HC) in rats and mice. J Nucl Med 1998;39:2161–6.
74. Emmett L, Willowson K, Violet J, Shin J, Blanksby A, Lee J. Lutetium 177 PSMA radionuclide therapy for men with prostate cancer: a review of the current literature and discussion of practical aspects of therapy. J Med Radiat Sci 2017;64:52.
75. Katsanos K, Kitrou P, Spiliopoulos S, Maroulis I, Petsas T, Karnabatidis D. Comparative effectiveness of different transarterial embolization therapies alone or in combination with local ablative or adjuvant systemic treatments for unresectable hepatocellular carcinoma: A network meta-analysis of randomized controlled trials. PLoS One 2017;12:e0184597.
76. van Es RJJ, Nijsen JFW, van het Schip AD, Dullens HF, Slootweg PJ, Koole R. Intra-arterial embolization of head-and-neck cancer with radioactive holmium-166 poly(L-lactic acid) microspheres: an experimental study in rabbits. Int J Oral Maxillofac Surg 2001;30:407–13.
77. Chew V, Lee YH, Pan L, Nasir NJM, Lim CJ, Chua C, et al. Original article: Immune activation underlies a sustained clinical response to Yttrium-90 radioembolisation in hepatocellular carcinoma. Gut 2019;68:335.
78. Erinjeri JP, Fine GC, Adema GJ, Ahmed M, Chapiro J, den Brok M, et al. Immunotherapy and the Interventional Oncologist: Challenges and Opportunities—A Society of Interventional Oncology White Paper. Radiology 2019;292:25–34.
79. Kepp O, Tesniere A, Zitvogel L, Kroemer G. The immunogenicity of tumor cell death. Curr Opin Oncol 2009;21:71–6.

80. Hacohen N, Fritsch EF, Carter TA, Lander ES, Wu CJ. Getting Personal with Neoantigen-Based Therapeutic Cancer Vaccines. Cancer Immunol Res 2013;1:11–5.
81. Ghiringhelli F, Apetoh L, Tesniere A, Aymeric L, Ma Y, Ortiz C, et al. Activation of the NLRP3 inflammasome in dendritic cells induces IL-1β–dependent adaptive immunity against tumors. Nat Med 2009;15:1170–8.
82. Deng L, Liang H, Xu M, Yang X, Burnette B, Arina A, et al. STING-Dependent Cytosolic DNA Sensing Promotes Radiation-Induced Type I Interferon-Dependent Antitumor Immunity in Immunogenic Tumors. Immunity 2014;41:843–52.
83. Reynders K, Illidge T, Siva S, Chang JY, De Ruysscher D. The abscopal effect of local radiotherapy: using immunotherapy to make a rare event clinically relevant. Cancer Treat Rev 2015;41:503–10.
84. Herba MJ, Thirlwell MP. Radioembolization for hepatic metastases. Semin Oncol 2002;29:152–9.
85. Barabasch A, Heinzel A, Bruners P, Kraemer NA, Kuhl CK. Diffusion-weighted MRI Is Superior to PET/CT in Predicting Survival of Patients Undergoing ^{90}Y Radioembolization of Hepatic Metastases. Radiology 2018;288:764–73.
86. Maruthappu M, Duclos A, Lipsitz SR, Orgill D, Carty MJ. Surgical learning curves and operative efficiency: a cross-specialty observational study. BMJ Open 2015;5:e006679.
87. Arnolli MM, Buijze M, Franken M, de Jong KP, Brouwer DM, Broeders IAMJ. System for CT-guided needle placement in the thorax and abdomen: A design for clinical acceptability, applicability and usability. Int J Med Robot Comput Assist Surg 2017:e1877.
88. Arnolli MM, Hanumara NC, Franken M, Brouwer DM, Broeders IAMJ. An overview of systems for CT- and MRI-guided percutaneous needle placement in the thorax and abdomen. Int J Med Robot 2015;11:458–75.
89. de Jong TL, van de Berg N, Tas L, Moelker A, Dankelman J, van den Dobbelsteen J. Needle placement errors: do we need steerable needles in interventional radiology? Med Devices Evid Res 2018;Volume 11:259–65.


10

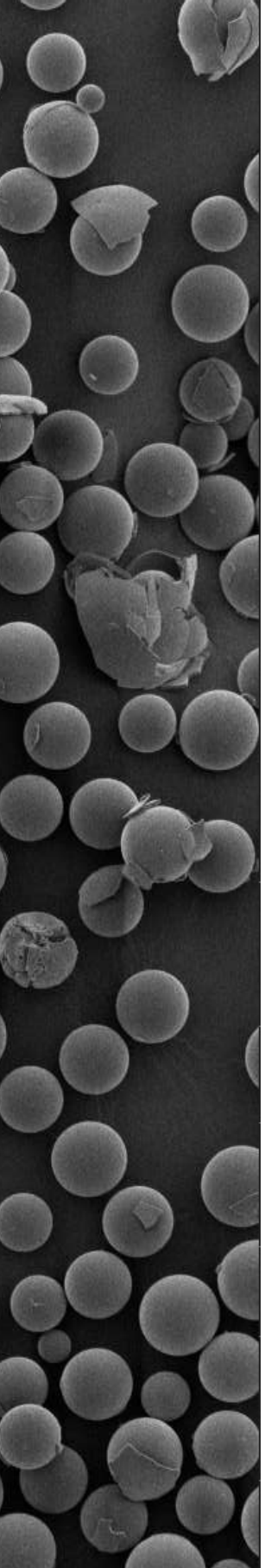

Appendices

SUMMARY

Cancer of the head and neck region is the sixth most frequent cancer. In addition to the high incidence, the prognosis in case of advanced stage disease is poor, and over the past decades, the overall survival rate has only slightly increased. The aim of this thesis, presented in **Chapter 1**, has been to evaluate the feasibility of an alternative treatment modalities against Head and Neck Cancer (HNC). Radioactive holmium-166 (^{166}Ho)-microspheres are frequently used in radioembolization of the liver. The absence of the unique blood supply of the liver and the risk of neurological complications in the head and neck region makes radioembolization in this region challenging. The direct intra-tumoral injection of ^{166}Ho-microspheres seems a promising alternative.

Before testing the clinical feasibility of direct intra-tumoral injection of ^{166}Ho-microspheres, the technique and the ^{166}Ho-microspheres were evaluated. In **Chapter 2** the scientific literature on intra-tumoral injections of radioactive microparticles was reviewed. A large variety of radioactive microparticles; in size, structure and used isotope were injected using different techniques in a variety of tumors in both animals and human patients. This review indicated that intra-tumoral treatment with radioactive beta-emitting microparticles, is relatively safe and effective and may therefore have additional value for patients.

The holmium content in blood and urine after radioembolization of liver malignancies with ^{166}Ho-microspheres was described in **Chapter 3**. This gave an indication what can be expected for other applications with similar ^{166}Ho-microspheres. It was shown that the measured content of ^{166}Ho from ^{166}Ho-microspheres was influenced by the type of injection fluid. In vitro, after suspension in 10% ethanol 2% Pluronic® F-68 for an hour, 15% free ^{166}Ho was measured in the supernatant, while in 116 mM pH 7.2 buffer with Pluronic® F-68 for injection, <0.2% was found. Free ^{166}Ho precipitates with phosphate on the surface of the microspheres, which reduces leaching. In addition, a positive correlation between longer neutron irradiation time and measured holmium in urine and blood was found. Analysis of urine collections and peripheral blood samples from two prospective clinical studies on ^{166}Ho-microspheres radioembolization showed low concentrations of holmium in the blood and urine, 0.15% and 0.13% of the injected amount respectively. This indicates that the microspheres are stable.

This first clinical experience with intra-tumoral injections of ^{166}Ho-microspheres was described in **Chapter 4**. In a cohort study of 13 cats with spontaneous squamous cell carcinoma, a local response rate of 55% was observed. This included both complete response and partial response (tumor downstaging), enabling subsequent marginal tongue resection. Median survival time was much longer for patients with a good local response (113 days versus 296 days respectively). In general, the side effects were minimal. From this study, it was concluded that

microbrachytherapy may have potential as a minimally invasive, single procedure radio-ablation treatment of small unresectable tumors, with minimal toxicity.

After the experiences in the veterinary study, the translation of intra-tumoral injections of ^{166}Ho-microspheres for human patients started. A clinical phase I study was designed to determine the feasibility in patients with a squamous cell carcinoma of the tongue in a 'treat and resect' setting. Unfortunately, the study was troubled by low accrual due to the newly introduced sentinel lymph node procedure, where intra-tumoral ^{166}Ho-microspheres hamper the imaging after peri-tumoral ^{99m}Tc-labelled nanaocolloid injections. Therefore, this study was terminated prematurely after only a single patient was treated. This single treatment, as described in chapter 5, showed limited distribution in the tumor, however, it did show the multimodal imaging potential with SPECT, CT and MRI. Furthermore, tumor necrosis was observed on a microscopic level. Despite the limited results obtained, the observed efficacy encourages further research.

Further evaluation of the feasibility was performed in 3 patients with locoregional recurrences of HNC, as described in chapter 6. For these patients, limited treatment options exist. In the palliative setting, a single session, minimally invasive and safe therapy is desirable. Three patients without treatment options were offered intra-tumoral injections with ^{166}Ho-microspheres. None of the patients experienced adverse events. However, technical difficulties, including precipitation of microspheres in necrotic tissue, resulted in a relatively small treatment area with a sufficiently high local dose, while the majority of the vital tumor border was left untreated. In another patient, high intra-tumoral pressure resulted in the inability to inject the microspheres. These results again stress the importance of the administration technique for optimal distribution within the tumor.

Therefore, the focus of this thesis shifted more towards imaging of the ^{166}Ho-microspheres after intra-tumoral injections. CT imaging provided superior resolution (<1 mm) of the distribution of ^{166}Ho-microspheres compared to the currently used SPECT (4.8 mm) and MRI (3 mm). This was presented in **Chapter 7**. In this chapter, the amount of holmium was determined by a threshold method, based on the density, and compared with a validated ^{166}Ho-microspheres SPECT/CT. In the phantom, a linear relationship between Hounsfield Units and concentration of holmium was found. Ex-vivo tissue experiments showed an excellent correlation ($r=0.99$ $p<0.01$) between the administered dose, SPECT/CT, and CT quantification. CT recovered almost identical amounts of holmium compared to the intra-tumoral activity detected on SPECT/CT. Considering some limitations of the currently used method (e.g. long acquisition times), CT-based quantification for intra-tumoral holmium microspheres injections seems feasible and may open an entirely new field of CT guided treatment.

New developments in imaging like the dual-energy CT (DECT) allows for even more advanced analyses, including material decomposition. DECT imaging uses two x-ray tubes, instead of one. When using different tube settings, one can discriminate between materials. DECT quantification was able to discriminate holmium from bone, arterial calcification etc., which is not possible with conventional CT. In **Chapter 8**, the feasibility of DECT imaging was tested in collaboration with Siemens Healthcare. In four adult female rabbits with subcutaneous VX-2 tumors, after intra-tumoral injection of neutron activated ^{166}Ho-microspheres, the recovered amount of holmium corresponded well with the injected amount of ^{166}Ho-microspheres, with an underestimation up to -11.7%. In addition, the high dose acquisitions with tube settings at 80/150 kV, provided excellent accuracy for concentrations down to 0.125 mg/mL compared to 2.6 mg/mL with conventional CT.

CONCLUSIONS

The most important conclusions that may be drawn from the studies in this thesis are:

- Intra-tumoral injection of radioactive microparticles is an innovative and save treatment approach.
- The isotope ^{166}Ho meets most of the requirements of the ideal isotope with a half-life of 26.8 hours, a relatively high-energy beta-radiation (E_{β}, max = 1.84 MeV) and a small percentage of gamma-radiation for single photon emission computed tomography (SPECT) imaging.
- The release of holmium in blood and urine is low in patients after radioembolization.
- In veterinary patients with small oral squamous cell carcinomas a good local response was observed in 55% of the animals.
- Despite a relatively easy and straightforward procedure, the injection of intra-tumoral particles is technically demanding.
- Treatment of ulcerous or granular tissue must be avoided to prevent leakage of microspheres.
- Further investigation of this novel treatment modality should be encouraged because of the absence of side effects and lack of other treatment options.
- High resolution imaging of ^{166}Ho-microspheres is feasible with CT, based on the density of holmium.
- Dual energy CT improves the detection of ^{166}Ho-microspheres from 2.6 mg/mL down to 0.125 mg/mL compared to conventional CT and discrimination between ^{166}Ho-microspheres, arterial calcifications and bone is feasible with dual energy CT.

NEDERLANDSE SAMENVATTING

Hoofd-halskanker is een relatief veel voorkomende kanker. De prognose is ongunstig vooral als de diagnose in een laat stadium wordt gesteld. Helaas is over de laatste decennia de overleving maar minimaal verbeterd. Het doel van deze studie is het evalueren van de toepasbaarheid van een potentiele nieuwe behandeling voor hoofd-halstumoren zoals beschreven in **Hoofdstuk 1**. Radioactieve holmium-166 (^{166}Ho)-microsferen worden momenteel gebruikt voor radioembolisatie van tumoren van de lever. Hierbij worden deze ^{166}Ho-microsferen in de slagader van de lever gespoten en lopen ze vast in de kleine haarvaatjes van de tumor. Echter, de afwezigheid van de unieke bloedvoorziening van de lever en het risico op neurologisch complicaties maken radioembolisatie minder geschikt voor toepassing in het hoofd-halsgebied. Het direct in de tumor injecteren van deze ^{166}Ho-microsferen is mogelijk een veelbelovend alternatief.

Hoofdstuk 2 geeft een overzicht van de huidige literatuur op het gebied van intra-tumorale injecties met radioactieve micropartikels in solide tumoren. Er zijn meerder studies verricht, vooral in proefdieren, maar ook enkele studies in patiënten. Een grote variatie in deeltjesgrootte, injectievloeistof en volume en de verschillende injectietechnieken worden beschreven. Dit overzicht laat zien dat het direct injecteren van kleine radioactieve deeltjes in een tumor een relatief veilige en effectieve behandeling is en mogelijk van meerwaarde is voor de behandeling van patiënten.

De detectie van vrij holmium in het bloed en de urine van patiënten na radioembolisatie van levertumoren met ^{166}Ho-microsferen is beschreven in **Hoofdstuk 3**. Dit geeft een indicatie van de stabiliteit van de ^{166}Ho-microsferen en wat we mogelijk kunnen verwachten bij het gebruik van de ^{166}Ho-microsferen voor andere toepassingen. De eerste 23 patiënten werden behandeld met ^{166}Ho-microsferen gesuspendeerd in een oplossing van Pluronic® F-68 en 10% alcohol. De volgende groep van 30 patiënten werden behandeld met ^{166}Ho-microsferen holmiumbolletjes gesuspendeerd in een oplossing van Pluronic® F-68 en een fosfaat buffer.

In het laboratorium bleek dat na suspenderen van de microsferen in de 10% alcohol oplossing, na een uur 15% van het ^{166}Ho was vrijgekomen in de vloeistof. Terwijl in de fosfaatbuffer slechts <0.2% werd gemeten. Vrij ^{166}Ho slaat neer met fosfaat op het oppervlak van de microbolletjes, wat de mogelijke lekkage ervan vermindert. Er werd een relatie gevonden tussen langer bestralen van de microsferen en hogere ^{166}Ho waarden in het bloed en in urine. Uit dit onderzoek bleek dat zowel de bloed en urine waardes van beide groepen weinig holmium bevatten, 0.15% en 0.13%, respectievelijk. Dit suggereert dat de microsferen stabiel genoeg zijn.

Hoofdstuk 4 beschrijft de eerste resultaten van de behandeling met intra-tumorale injecties in katten met een spontaan plaveiselcelcarcinoom van de mondholte. Er zijn veel overeenkomsten wat betreft de risicofactoren en het gedrag van deze tumoren in katten en mensen. Daarom is

deze studie met dierpatiënten een goede opstap voor verdere behandelingen in mensen. In totaal werden 13 katten behandeld. Bij 6 katten werd een goed resultaat gezien. Deze 6 katten konden vervolgens chirurgie of een tweede holmium behandeling ondergaan wat resulteerde in een volledige response. Katten waarbij een goed effect van de behandeling werd gezien leefden een stuk langer dan katten waarbij geen tumor controle werd bereikt, 296 dagen versus 113 dagen respectievelijk. De bijwerkingen van de behandeling waren minimaal in deze dierpatiënten die soms in een slechte toestand verkeerden. De tumorgrootte was voorspellend voor de kans op een succesvolle behandeling, waarbij hoe kleiner de tumor des te groter de kans op succes. Om nog betere resultaten te realiseren moet de dosis in de tumor verder verbeterd worden. Deze studie laat zien dat intra-tumorale injecties met radioactieve ^{166}Ho-microsferen mogelijk potentie hebben als een minimaal invasieve behandeling voor kleine niet operabele tumoren, met minimale bijwerkingen.

Na de ervaringen in deze katten werd de translatie van deze intra-tumorale behandeling met ^{166}Ho-microsferen naar de mens ingezet. Een klinische studie werd opgezet om de haalbaarheid te onderzoeken in patiënten met een plaveiselcel tumor van de tong. In deze studie zou na de injecties met ^{166}Ho-microsferen de tumor operatief worden verwijderd. Helaas werd deze studie bemoeilijkt door een laag aantal deelnemers. De recent ingevoerde schildwachtklier procedure, waarbij radioactieve technetium-99m (^{99m}Tc)-nanodeeltjes worden geïnjecteerd rondom de tumor, was waarschijnlijk een belangrijke oorzaak. Deze twee studies konden niet tegelijkertijd worden uitgevoerd vanwege de beeldvorming. Daarbij zagen een tweede behandeling met radioactieve injecties veel patiënten niet zitten. De studie werd daarom beëindigd nadat slechts 1 patiënt was behandeld. Deze behandeling is beschreven in **Hoofdstuk 5** en laat de mogelijkheden zien van de verschillende beeldvormende technieken zoals MRI, CT en SPECT. Daarnaast was er op microscopisch niveau ook anti-tumor effect te zien. Ondanks de beperkte resultaten van deze studie, sporen het geobserveerde anti-tumor effect en de goede mogelijkheid tot beeldvorming van de microsferen aan tot verder onderzoek naar deze nieuwe behandeloptie.

Verdere evaluatie van de toepasbaarheid van deze behandeling werd gedaan in patiënten met recidief tumoren in het hoofd-halsgebied, zoals is beschreven in **hoofdstuk 6**. De behandelopties voor deze patiëntgroep zijn helaas zeer beperkt. Mogelijk is het eenmalig injecteren van radioactieve ^{166}Ho-microsferen een snelle en weinig ingrijpende alternatieve behandeling met als doel de kwaliteit van leven te verbeteren. In de drie behandelde patiënten werd ervaren dat de therapie op het eerste gezicht relatief veilig is. Door technische moeilijkheden, zoals het uitzakken van de ^{166}Ho-microsferen in de tumor en de injectiespuit, en een te hoge intra-tumorale druk werd geen optimale verdeling van microsferen bereikt. Met deze uitkomsten wordt nogmaals het belang van een juiste toedientechniek om een optimale distributie van microsferen in de tumor te realiseren, benadrukt. Ook op basis van dit onderzoek wordt verder onderzoek naar deze nieuwe behandelmethode verder aangemoedigd vanwege de grotendeels afwezigheid van bijwerkingen en het ontbreken van andere behandelopties in deze patiëntengroep.

De focus van het onderzoek verplaatste zich hierdoor meer naar de beeldvorming van ^{166}Ho-microsferen na toediening. CT-beeldvorming kan een veel hogere resolutie bieden (<1 mm) van de distributie van de ^{166}Ho-microsferen dan de momenteel gebruikte SPECT (4.8 mm) of MRI (3 mm) In **Hoofdstuk 7** werd de hoeveelheid holmium bepaald op basis van de doorlaatbaarheid van rontgen gerelateerd aan de concentratie van aanwezig holmium. Op basis van een gekozen afkappunt werd de gemeten concentratie holmium per volume op CT vergeleken met de gevalideerde SPECT-methode.

In een testopstelling werd een lineaire relatie gevonden tussen de concentratie holmium en het aantal op CT gevonden Hounsfield units. Ook met een ex-vivo kippen spierweefsel model werd een perfecte correlatie gevonden ($r=0.99$ $p<0.01$) tussen de toegediende dosis microsferen en de gemeten hoeveelheden volgens , SPECT en CT. In patiënten detecteerde CT een bijna identieke hoeveelheid holmium als SPECT. Omdat de huidige methode SPECT een paar tekortkomingen kent, zoals een lange scantijd, is het verder ontwikkelen van CT-kwantificatie interessant. Daarnaast creëert het mogelijk een geheel nieuwe optie voor CT gestuurde behandeling van tumoren middels intra-tumoral injectie van ^{166}Ho-microsferen.

Nieuwe ontwikkelingen op het gebied van beeldvorming, zoals duale energie CT, maken geavanceerde analyses mogelijk. Door middel van een CT-scan met verschillende energie is het mogelijk om te berekenen waaruit het materiaal bestaat dat wordt gescand, zoals momenteel gedaan wordt bij nierstenen. Deze techniek zou het mogelijk maken om holmium te onderscheiden van andere materialen met een hoge dichtheid, zoals bijvoorbeeld bot, verkalkte bloedvaten of jodium houdend contrastmiddel, hetgeen niet mogelijk is conventionele CT. In **hoofdstuk 8** werd de haalbaarheid van deze techniek getest. In samenwerking met Siemens Healthcare B.V. werd eerst in een fantoom, en vervolgens op enkele laboratoriumdieren, deze techniek getest. Door zowel een scan te maken met een lage stralingsenergie en een hoge stralingsenergie kan de specifieke doorlatendheid van de rontgen stralingsenergie door holmium gedetecteerd worden. Hierdoor is het mogelijk met hoge nauwkeurigheid een concentratie tot 0.125 mg/mL microsferen te detecteren terwijl dit 2.6 mg/mL is met conventionele CT. Ook in de proefdieren lukte het om met een maximale afwijking van 11% de geïnjecteerde hoeveelheid holmium te kunnen inschatten.

CONCLUSIES

De belangrijkste conclusies die kunnen worden getrokken uit de studies in dit proefschrift zijn:

- Intra-tumorale injectie van radioactieve microdeeltjes is een innovatieve en veilige behandelmethode.
- De isotoop ^{166}Ho voldoet aan de meeste eisen van de ideale isotoop met een halfwaardetijd van 26,8 uur, een relatief hoogenergetische bètastraling (E_{β},max = 1,84 MeV) en een klein percentage gammastraling welke kan gebruikt worden voor nucleaire beeldvorming (SPECT).
- De afgifte van holmium in bloed en urine is laag bij patiënten na radio-embolisatie.
- Bij veterinaire patiënten met kleine orale plaveiselcelcarcinomen werd een goede lokale respons waargenomen bij 55% van de dieren.
- Ondanks een relatief eenvoudige procedure is de injectie van intra-tumorale microsferen technisch veeleisend.
- Behandeling van ulcererend of granulatie weefsel moet worden vermeden om lekkage van microsferen te voorkomen.
- Vanwege de afwezigheid van bijwerkingen en het ontbreken van andere behandelingsopties is het belangrijk om deze nieuwe behandelingsmethode verder te onderzoeken.
- Hoge resolutie beeldvorming van ^{166}Ho-microsferen is haalbaar met CT, gebaseerd op de dichtheid van holmium.
- Dual energy CT verbetert de detectie van ^{166}Ho-microsferen van 2,6 mg/mL tot 0,125 mg/mL in vergelijking met conventionele CT en onderscheid holmium gelabelde microsferen, arteriële calcificaties, bot en jodium contrastmiddel.

ACKNOWLEDGEMENTS

Met dit dankwoord is er dan echt een einde gekomen aan mijn promotietraject. Dit traject heeft bloed, zweet en tranen gekost en was waarschijnlijk niet succesvol ten einde gebracht zonder de hulp van velen. In 2015 begon ik vol enthousiasme aan dit traject. Ondanks enige ervaring met onderzoek bleek een promotietraject toch meer, dan het uitvoeren van onderzoek zoals geleerd gedurende mijn master of science. Het delen van meningen, maar zeker soms ook niet is iets wat je vormt als onderzoeker. Hierdoor was het niet altijd de makkelijkste weg maar zoals Shakespeare zei "ik ben niets, als ik niet kritisch ben".

Velen hebben bijgedragen aan de totstandkoming van dit proefschrift. Hieronder wil ik graag de volgende personen in het bijzonder bedanken.

Allereerst wil ik de patiënten bedanken, die in de laatste fase van hun leven, zonder direct gewin deelnamen aan dit wetenschappelijk onderzoek. Met veel respect kijk ik terug naar de manier waarop zij hun ziekte droegen en het hiernaast zagen als een kans voor de wetenschap.

Ook dank aan de eigenaren van de dierpatiënten die we hebben mogen behandelen. Mede door de deelname aan de behandeling van hun huisdieren is het onderzoek weer een stapje verder gebracht.

Geachte **prof. dr. M.G.E.H. Lam**, beste Marnix. Bedankt voor je begeleiding. Het afbakenen van de researchvraag vond ik niet altijd makkelijk. Jij wist koers te houden, helder en daadkrachtig.

Geachte **prof. dr. R. Koole**, beste Ron. Maart 2015 ontving ik per post een uitnodiging van u om te solliciteren voor dit promotietraject. Een brief, die mijn toekomst drastisch heeft veranderd. Ik ben u zeer dankbaar voor het bieden van deze kans die ik met beide handen heb aangepakt. U staat aan het begin en aan het eind van dit promotietraject centraal.

Geachte **prof. dr. A.J.W.P. Rosenberg**, beste Toine. Een nuchtere blik en het doel voor ogen houden zijn kwaliteiten die ik zeer van u waardeer. Ik kijk er naar uit om de komende 4 jaar onder uw supervisie te leren en te werken in het UMCU als MKA-chirurg in opleiding.

Geachte **dr. J.F.W. Nijsen**, beste Frank. Dank voor de dagelijkse begeleiding tijdens mijn promotie traject. Uw onuitputtelijke energie en enorme inzet om de behandeling met holmium (zowel radioembolizatie en intra tumoraal) te laten slagen zijn noemenswaardig. Al decennia zet u zich hiervoor in. Veel succes in het Radboud UMC Nijmegen en met Quirem met de voortzetting van deze werkzaamheden.

Geachte **dr. R.J.J. van Es**, beste Robert. Dank voor uw passie voor het vak, u gedrevenheid en het feit dat bij u de patiënt altijd op nummer 1 staat. Binnen de kortste keren kreeg ik kritische en verhelderende revisies, ook op oudjaars avond. Hartelijk dank voor alle hulp tijdens dit promotietraject.

Beste leden beoordelingscommissie, **prof. dr. de Bree**, **prof. dr. Lagendijk**, **prof. dr. Maal**, **prof. dr. Schiffelers,** en **prof. dr. Terhaard**. Ik ben u dankbaar dat u de tijd hebben genomen mijn proefschrift kritisch te beoordelen.

Geachte **Dr. S.A. van Nimwegen**, Bas. Hartelijk dank voor het mogen mee-behandelen van de veterinaire patiënten. Ik herinner me nog goed een behandeling bij de katten die iets anders liep dan verwacht. Juist dit is onderzoek.

Geachte **Dr. G.C. Krijger**, beste Gerard en **Remmert de Roos**; 'de mannen van het lab'. Onder het genot van een zelf gezette kop koffie keken we samen naar de data. Discussieerde hierover en vormde onze visie. Naast de hulp op het lab wil ik jullie bedanken voor deze waardevolle gesprekken en persoonlijke interesse.

Beste **stafleden, arts-assistenten en onderzoekers MKA**, De ochtend overdrachten waren een goede start van de dag. Sterke verhalen, grappen en no-nonsens confrontaties onder het genot van een sterk bakkie koffie. Met velen van jullie zal ik straks in de kliniek gaan samenwerken ik kijk er naar uit niet alleen de dag met jullie te starten.

Trial bureau, **Tjitske, Shanta**, bedankt voor het mij wegwijs maken in het oerwoud van wet en regelgeving rondom onderzoek en het opsturen van alle amendementen.

Graag wil ik ook alle overige leden van het holmium team bedanken. **Angelique Barten** voor het bijhouden van al het papierwerk rondom de konijnenstudie. **Remco Bastiaannet** vaak vroeg ik jou op het allerlaatste moment je avond vrijmaken om een aantal konijnen te scannen. Nooit was dit een probleem bedankt voor deze inzet. **Gerrit van de Maat**, meerdere malen heb je het geprobeerd uit te leggen, maar nog steeds is de werking van een MRI voor mij een ongrijpbare materie. **Medewerkers GDL** bedankt voor de goede verzorging van mijn konijnen en het me keer op keer te herinneren de tussenschotten te verwijderen.

Studenten en medekamer genoten **Eric, Jeanne**, bedankt de gezelligheid tijdens de periode van jullie afstudeerstage.

Tenslotte iedereen die ik op werkgebied ben vergeten te benoemen, alsnog bedankt!

Lieve **Pa en Ma**, bedankt voor de mogelijkheden die jullie me geboden hebben en nog steeds bieden. Zonder jullie steun had ik nooit de risico's kunnen en durven nemen. Pa nog even geduld en we zijn collega's, al zal ik nooit zo'n goede tandarts worden als jij. Nu sta je, als paranimf aan

mijn zijde, zoals je dit ook deed als getuige. Ma de basis van ons gezin, bedankt voor dit onvoorwaardelijke thuis. **Jessica**, collega dokter en grote zus. Een kritische blik hebben we gemeen. **Chris** we waren onafscheidelijk als kind. Nu zijn we allebei gevorderde vaders. Fijn om je ook nu als paranimf dichtbij te hebben. **Eva** altijd mijn kleine zusje. Ook de 'koude' kant; **Jurre**, **Julian** en **Sanne**. Door jullie aanwezigheid extra veel gezelligheid in de familie, bedankt hiervoor. Mijn schoonmoeder, **Marry**, bedankt voor je prachtige dochter en het zijn van een lieve oma. Lieve **Nore**, **Jip** en **toekomstige kleine apenkop**, graag wil ik nog lang genieten jullie. De onbevangenheid waarop jullie de wereld ontdekken is erg aandoenlijk.

Liefste **Rosanne,** Ik ben een man van weinig woorden maar, jij bent het beste dat me ooit is overkomen. Graag wil ik je ontzettend bedanken voor al je steun en onvoorwaardelijke liefde. Ik bewonder je energie en enthousiasme, maar ook je geduld met mij en de kids. Ik hou van jou!

BIOGRAPHY

Robbert Christiaan Bakker was born on the 5th of March 1987 in Graafstroom, the Netherlands. After obtaining his VWO diploma at the Willem de Zwijger College in Papendrecht, he started medical school at the Erasmus University Rotterdam in 2005. In 2007, he was selected to participate in a special program for medical students organized by the Netherlands' Institute of Health Sciences (NIHES). This program enabled him to combine Medical school with the Master of Science in Clinical Research program. Part of this program was completed at the Harvard School of Public Health in Boston, Massachusetts, the USA. He completed his research internship at the Cardiovascular Research School Erasmus MC Rotterdam (Coeur) with publications in international journals and went for a clinical internship to Auckland City Hospital, New Zealand. After obtaining his medical degree he worked as a resident at several hospitals in the Netherlands.

In 2015 he started his PhD. project "Holmium microbrachytherapy; an innovative intratumoral treatment modality in head and neck cancer" under the supervision of Prof. dr. Marnix Lam, Prof. dr. Ron Koole, prof. dr. Toine Rosenberg, dr. Frank Nijsen and dr. Robert van Es and dr. Bas van Nimwegen at the University Medical Center Utrecht, a collaboration between the departments of Radiology and Nuclear Medicine and Oral and Maxillofacial Surgery. In 2017 he started with dentistry school for Medical Doctors at Radboud University in Nijmegen and in May 2020 he will start as a resident in the department of Oral and Maxillofacial Surgery in the University Medical Center Utrecht.

LIST OF PUBLICATIONS

Bakker RC, van Es RJJ, Rosenberg AJWP, van Nimwegen SA, Bastiaannet R, de Jong HWAM, Nijsen JFW, Lam MGEH. Intratumoral injection of radioactive holmium-166 microspheres in recurrent head and neck squamous cell carcinoma: preliminary results of first use. Nucl Med Commun. 2018 Mar;39(3):213-221.

van Nimwegen SA, **Bakker RC**, Kirpensteijn J, van Es RJJ, Koole R, Lam MGEH, Hesselink JW, Nijsen JFW. Intratumoral injection of radioactive holmium (^{166}Ho) microspheres for treatment of oral squamous cell carcinoma in cats. Vet Comp Oncol. 2018 Mar;16(1):114-124.

Bakker RC, Lam MGEH, van Nimwegen SA, Rosenberg AJWP, van Es RJJ, Nijsen JFW. Intratumoral treatment with radioactive beta-emitting microparticles: a systematic review. J Radiat Oncol. 2017;6(4):323-341.

Bakker RC, de Roos R, Ververs FFT, Lam MGEH, van der Lee MK, Zonnenberg BA, Krijger GC. Blood and urine analyses after radioembolization of liver malignancies with [^{166}Ho]Ho-acetylacetonate-poly(l-lactic acid) microspheres. Nucl Med Biol. 2019 Apr 15;71:11-18.

Bakker RC, Bouma W, Wijdh-den Hamer IJ, Natour E, Mariani MA. Mitral valve repair in a patient with an anomalous left coronary artery. J Card Surg. 2014 Nov;29(6):782-4. **Bakker RC**, Osse RJ, Tulen JH, Kappetein AP, Bogers AJ. Preoperative and operative predictors of delirium after cardiac surgery in elderly patients. Eur J Cardiothorac Surg. 2012 Mar;41(3):544-9.

Bakker RC, Akin S, Rizopoulos D, Kik C, Takkenberg JJ, Bogers AJ. Results of clinical application of the modified maze procedure as concomitant surgery. Interact Cardiovasc Thorac Surg. 2013 Feb;16(2):151-6.